Cellular trafficking and functional characterisation of the human glucagon like peptide-1 receptor.

Thompson, Aiysha

Cellular Trafficking and Functional Characterisation of the Human Glucagon Like Peptide-1 Receptor

Aiysha Thompson

Submitted to Swansea University in fulfilment of the requirements for the Degree of Doctor of Philosophy

Swansea University

2014

Abstract

The binding of glucagon like peptide-1 (GLP-1) to its receptor, the GLP-1 receptor (GLP-1R), results in insulin secretion from pancreatic β-cells. This makes the receptor an important drug target for type 2 diabetes. The GLP-1R is a family B G-protein coupled receptor (GPCR) and functions at the cell surface by coupling to $G\alpha_s$ and $G\alpha_q$ pathways and causing ERK phosphorylation. The objective of this study was to analyse trafficking, activity and internalisation of GLP-1R at the cellular and molecular level.

The human GLP-1R (hGLP-1R) N-terminus is required for trafficking and maturation. This study demonstrated the importance of signal peptide (SP) cleavage, *N*-linked glycosylation and the hydrophobic region after the SP (HRASP) within the N-terminus of the hGLP-1R for cell surface expression.

Due to difficulties in peptide drugs, orally active small molecule agonists of the GLP-1R are of high importance. Small molecule allosteric agonists, compounds 2 and B, were found to cause cAMP production similar to orthosteric GLP-1, but not intracellular Ca^{2+} accumulation, ERK phosphorylation or internalisation of the receptor. Compounds 2 and B binding to the GLP-1R inhibits GLP-1 internalisation, intracellular Ca^{2+} accumulation and ERK phosphorylation of the receptor.

Agonist induced hGLP-1R internalisation is important for insulin secretion. Inhibition of the $G\alpha_q$ pathway but not the $G\alpha_s$ pathway reduced hGLP-1R internalisation. Consistent with this, the hGLP-1R T149M mutant and compounds 2 and B, which activate only the $G\alpha_s$ pathway, failed to induce hGLP-1R internalisation. Chemical inhibitors of the $G\alpha_q$ pathway significantly reduced agonist induced hGLP-1R internalisation and suppressed ERK phosphorylation demonstrating phosphorylated ERK acts downstream of the $G\alpha_q$ pathway in hGLP-1R internalisation.

Finally, distinct regions within the C-terminus of hGLP-1R required for its cell surface expression, activity and internalisation were identified. Residues 411-418, 419-430 and 431-450 are essential for hGLP-1R cell surface expression, activity and internalisation, respectively.

Declaration and Statements

Declaration

This work has not previously been accepted in substance for any degree and is not being concurrently submitted in candidature for any degree.

Signed.....(candidate)
Date...10/12/2014.....

Statement 1

This thesis is the result of my own investigations, except where otherwise stated. Where correction services have been used, the extent and nature of the correction is clearly marked in a footnote(s).

Other sources are acknowledged by footnotes giving explicit references. A bibliography is appended.

Signed.. ..(candidate)
Date...10/12/2014.....

Statement 2

I herby give consent for my thesis, if accepted, to be available for photocopying and for inter-library loan, and for the title and summary to be made available to outside organisations.

Signed ....(candidate)
Date.....10/12/2014.....

Contents

Acknowledgements

The last four years have not been the easiest and I have had a lot of ups and downs. From the excitement of publishing my first paper to stressing after a new batch of transfection reagent halted experiments for six months, it has definitely been a rollercoaster. After experiencing a jumble of joy and torment, I can finally say 'I've done it! Woohoo!'

First and foremost I would like to thank my supervisor, Professor Venkateswarlu Kanamarlapudi. This thesis would not have been possible without his help, support and knowledge over the past four years. I am forever indebted to Dr Sian Owens for all of her western blot and bug work help, all that multi tasking would not have been possible without you. I also thank Professor Jeffrey Stephens and Professor Steve Bain for their supervision too. Not forgetting Professor Catherine Thornton who helped me with all the flow cytometry work.

The saying goes 'all work and no play makes Jack a dull boy', well that is why I would like to thank Rachel Smith, Lleucu Davies, Aled Bryant and Riaz Jannoo. They have been with me for almost the whole journey and I think we kept each other going. I will never forget squeezing into popup tents for free stuff, cup towers, office Frisbee, blow up daffodil fights, homemade tomato ketchup, and the shenanigans involved in egg free/nut free/wheat free/gluten free meals out and birthday cakes! Thank you for being there.

Finally, a million and seven thank you's to my amazing fiancé, Darren, I love you so much. All those times you cooked, cleaned, made me cups of tea and generally kept me alive because I was too busy writing, you have been awesome. I would like to thank my Dad who could probably sit my viva for me after proofreading everything. Also to my Mum, Nan Mum, Da and my brother, Shane, who weren't directly involved in my PhD but have supported me and are very important to me.

Without everyone mentioned, this thesis would not have been possible. I look forward to what the future holds.

Thank you again :o)

List of Figures

List of Tables

Abbreviations

Δ	Deletion
Φ	Hydrophobic amino acid
Δ31-40	SP-VSVG-hGLP-1RΔN23 Δ31-40-GFP
ΔN24	SP-VSVG-hGLP-1RΔN24-GFP
ΔN30	SP-VSVG-hGLP-1RΔN30-GFP
ΔN35	SP-VSVG-hGLP-1RΔN35-GFP
ΔN40	SP-VSVG-hGLP-1RΔN40-GFP
ΔN145	SP-VSVG-hGLP-1RΔN145-GFP
ΔSP	VSVG-hGLP-1RΔN23-GFP
Δ411-418	SP-VSVG-hGLP-1RΔN23 Δ411-418-GFP
Δ419-430	SP-VSVG-hGLP-1RΔN23 Δ419-430-GFP
Δ431-450	SP-VSVG-hGLP-1RΔN23 Δ431-450-GFP
2-APB	2-Aminoethoxydiphenylborane
5-HT_{2A}	5-hydroxytryptamine receptor 2a
7-AAD	7-aminoactinomycin D
A	Absorbance
A21R	VSVG-hGLP-1R A21R-GFP
aa	Amino acid
AC	Adenylate cyclase
ANOVA	Analysis of variance
AP-2	Activating protein-2
APS	Ammonium persulphate
AR	Adrenergic receptor
ARF	ADP-ribosylation factor
ARNO	ARF nucleotide-binding site opener
AT_2R	Angiotensin II receptor
ATG	Start codon
BAPTA-AM	1,2-*bis*(2-aminophenoxy)ethane-*N,N,N',N'*-tetraacetic acid tetrakis (acetoxymethyl ester)
BCA	Bicinchoninic acid

BMI	Body mass index
BSA	Bovine serum albumin
Ca^{2+}	Calcium
$CaCl_2$	Calcium chloride
cAMP	Cyclic adenosine monophosphate
CAV-1-P132L	CAV-1-P132L-pcDNA$_3$
CD26	Cluster of differentiation 26
Chlorpromazine	2-chloro-10-(3-dimethylaminopropyl)phenothiazine hydrochloride
CM	$CaCl_2$ and $MgCl_2$
Compound 1	2-(2'methyl)thiadiazolylsulfanyl-3-trifluoromethyl-6,7-dichloroquinoxaline
Compound 2	6,7-dichloro-2-methylsulfonyl-3-*N-tert*-butylaminoquinoxaline
Compound A	4-(3,4-dichlorophenyl)-2-(ethanesulfonyl)-6-(trifluoromethyl)pyrimidine
Compound B	4-(3-(benzyloxy)phenyl)-2-(ethylsulfinyl)-6-(trifluoromethyl)
COOH	Carboxyl
CREB	cAMP response element binding protein
CRF	Corticotropin-releasing factor
CST	Cytometer setup and tracking
CT	C-terminal domain
D1R	Dopamine D1 receptor
DABCO	1,4 Diazabicyclo (2.2.2) octane
DAG	Diacylglycerol
DAPI	4′,6-Diamidino-2-phenylindole dihydrochloride
ddH_2O	Double distilled water
DMSO	Dimethyl sulfoxide
DMEM	Dulbecco's modified Eagle medium
DN	Dominant negative
DPP-IV	Dipeptidyl peptidase-IV
DTT	Dithiothreitol

Dynasore	3-hydroxy-naphthalene-2-carboxylic acid (3,4-dihydroxy-benzylidene)-hydrazide hydrate
E408A,V409A,Q410A	SP-VSVG-hGLP-1RΔN23 E408A,V409A,Q410A -GFP
ECL	Extracellular loop
E. coli	*Escherichia coli*
EDTA	Ethylenediaminetetraacetic acid
ELISA	Enzyme linked immunosorbent assay
EPAC	Exchange protein activated by cAMP
ER	Endoplasmic reticulum
ERK	Extracellular signal-regulated kinase
ET_BR	Endothelin B receptor
EVH	Enabled/VASP homology
FACS	Fluorescence-activated cell sorting
FCS	Fetal calf serum
Fillipin	$C_{35}H_{58}O_{11}$
FITC	Flourescein
FL	Full length
FSM	Full serum medium
Fuc	Fructose
Gal	Galactose
GAPs	GTPase-activating proteins
G-CRSR,	G-CSF receptor
GDP	Guanosine diphosphate
GEF	Guanine nucleotide exchange factor
Genistein	5,7-dihydroxy-3-(4-hydroxyphenyl)-4*H*-1-benzopyran-4-one
GFP	Green fluorescent protein
GIP	Glucose-dependent insulinotropic polypeptide
GIT protein	GPCR interacting protein
GlcNAc	*N*-acetylglucosamine
GLP-1	Glucagon like peptide-1
GLP-2	Glucagon like peptide-2
GLP-1R	GLP-1 receptor

Go6976	5,6,7,13-tetrahydro-13-methyl-5-oxo-12*H*-indolo[2,3-*a*]pyrrolo[3,4-*c*]carbazole-12-propanenitrile
GPCR	G-protein coupled receptor
GRK	GPCR kinases
GRPP	Glicentin-related pancreatic C-peptide
GRPR	Gastrin-releasing peptide receptor
GTP	Guanosine triphosphate
h	Hour
H	Human
H_2SO_4	Sulphuric acid
HbA1c	Glycosylation of haemoglobin
HCAR	Hydroxycarboxylic acid receptor
HCl	Hydrogen chloride
HEK293	Human embryonic kidney 293
hGLP-1	Human GLP-1
hGLP-1R	Human GLP-1R
HRASP	Hydrophobic region after SP
HRP	Horseradish peroxidase
ICL	Intracellular loop
IgG	Immunoglobulin
IP_3	Inositol-1,4,5-triphosphate
IP_3R	Inositol-1,4,5-triphosphate receptor
IP	Intervening peptide
IRS-1	Insulin receptor substrate-1
K334A	SP-VSVG-hGLP-1RΔN23 K334A-GFP
kbp	Kilo base pair
KCl	Potassium chloride
KLD	Oligonucleotide kinase, T4 DNA ligase and *Dpn*I
LB	Luria-Bertani
LL	Dileucine
M_3R	M_3 muscarinic receptor
Man	Mannose

MAPK	Mitogen-activated protein kinase
MDC	Monodansylcadaverine; *N*-(5-aminopentyl)-5-di-methylaminonaphthalene-1-sulfonamide, *N*-(dimethylaminonaphthalenesulfonyl)-1,5-pentane-diamine
MGC	Mammalian gene collection
$MgCl_2$	Magnesium chloride
mGluR	Metabotropic glutamate receptor
$MgSO_4$	Magnesium sulphate
Min	Minute
$MnCl_2$	Manganese chloride
MPGF	Major proglucagon fragment
MTT	Methylthiazol tetrazolium, 3-(4,5-dimethlthiazol-2-yl)-2,5-diphenyltetrazolium bromide
N410	SP-VSVG-hGLP-1RΔN23 N410
N430	SP-VSVG-hGLP-1RΔN23 N430
N440	SP-VSVG-hGLP-1RΔN23 N440
N443	SP-VSVG-hGLP-1RΔN23 N443
N450	SP-VSVG-hGLP-1RΔN23 N450
N63,82,115L	SP-VSVG-hGLP-1RΔN23 N63,82,115L-GFP
NaCl	Sodium chloride
NaOH	Sodium hydroxide
NH_2	Amide
NHS	National Health Service
NMR	Nuclear magnetic resonance
NP40	Nonyl phenoxypolyethoxylethanol
NRTFD	Asn^{63}-Arg^{64}-Thr^{65}-Phe^{66}-Asp^{67}
NT	N-terminal domain
OGTT	Oral glucose tolerance test
PC	Prohormone convertase
PBP10	Rhodamine B-Gln-Arg-Leu-Phe-Gln-Val-Lys-Gly-Arg-Arg
PBS	Phosphate buffered saline

PBS-T	PBS-0.1% triton
PCR	Polymerase chain reaction
PD98059	2-(2-amino-3-methoxyphenyl)-4*H*-1-benzopyran-4-one
PE	Phycoerythrin
pEGFP-N1	Plasmid enhanced green fluorescent protein-N1
PFA	Paraformaldehyde
pGL4.29-CRE Luc	cAMP response element containing the luciferase reporter gene luc2P
PI3K	Phosphoinositide-3 kinase
PIP_2	Phosphatidylinositol-4,5-bisphophate
PKA	Protein kinase A
PKC	Protein kinase C
PLC	Phospholipase C
PLD	Phospholipase D
PMSF	Phenylmethanesulfonylfluoride
PVDF	Polyvinylidene fluoride
rbs6	Ribosomal protein S6
RFP	Red fluorescent protein
RIPA	Radioimmunoprecipitation assay
RLU	Relative light units
Ro318820	3-[3-[2,5-Dihydro-4-(1-methyl-1*H*-indol-3-yl)-2,5-dioxo-1*H*-pyrrol-3-yl]-1*H*-indol-1-yl]propyl carbamimidothioic acid ester mesylate
RT	Room temperature
SDS	Sodium dodecyl sulphate
SDS-PAGE	SDS-polyacrylamide gel electrophoresis
s	Second
SEM	Standard error of the mean
SFM	Serum free medium
SOB	Super optimal broth
SP	Signal peptide
SP-VSVG	SP-VSVG-hGLP-1RΔN23-GFP

SP-VSVG-GFP	SP-VSVG-hGLP-1RΔN23-GFP
SP-VSVG-hGLP-1R-EGFP	N-terminal SP and VSVG tagged hGLP-1R with a C-terminal tagged EGFP
SRP	Signal recognition particle
T149M	SP-VSVG-hGLP-1RΔN23 T149M-GFP
TAG	Stop codon
TB	Transformation buffer
TBS	Tris-buffered saline
TBS-T	TBS-0.1% tween20
TBS-Tween20	200 mM Tris (pH 7.5), 3 M NaCl, 0.1% (v/v) tween20
TEMED	N, N, N', N'-tetramethylethylenediamine
TORC2	Transducer of regulated CREB activity 2
TM	Transmembrane
TR	Thyrotropin receptor
Tris HCl	Tris hydrogen chloride
Tunicamycin	n=10, $C_{39}H_{64}N_4O_{16}$
U73122	1-[6-[[(17β)-3-methoxyestra-1,3,5(10)-trien-17-yl]amino]hexyl]-1*H*-pyrrole-2,5-dione
U73343	1-[6-[[(17β)-3-methoxyestra-1,3,5(10)-trien-17-yl]amino]hexyl]-2,5-pyrrolidinedione
V	Volts
V36A	SP-VSVG-hGLP-1RΔN23 V36A-GFP
VPAC	Vasoactive intestinal peptide
VSP-ΔSP	VSVG-VSP-hGLP-1RΔN23-GFP
VSVG	Vesicular stomatitis virus glycoprotein
VSVG-SP	VSVG-hGLP-1R-GFP
W39A	SP-VSVG-hGLP-1RΔN23 W39A-GFP
WDN	Trp^{48}-Asp^{49}-Asn^{50}
WT	Wild type
X	Any amino acid
Y69A	SP-VSVG-hGLP-1RΔN23 Y69A-GFP
Y88A	SP-VSVG-hGLP-1RΔN23 Y88A-GFP

Amino Acid Abbreviations

Neutral (Nonpolar)

Amino Acid	3 Letter Abbreviation	1 Letter Abbreviation
Alanine	Ala	A
Glycine	Gly	G
Isoleucine	Ile	I
Leucine	Leu	L
Methionine	Met	M
Phenylalanine	Phe	F
Proline	Pro	P
Tryptophan	Trp	W
Valine	Val	V

Neutral (Polar)

Amino Acid	3 Letter Abbreviation	1 Letter Abbreviation
Asparagine	Asn	N
Cysteine	Cys	C
Glutamine	Gln	Q
Serine	Ser	S
Threonine	Thr	T
Tyrosine	Tyr	Y

Basic

Amino Acid	3 Letter Abbreviation	1 Letter Abbreviation
Arginine	Arg	R
Histidine	His	H
Lysine	Lys	K

Acidic

Amino Acid	3 Letter Abbreviation	1 Letter Abbreviation
Aspartic Acid	Asp	D
Glutamic Acid	Glu	E

Conference Presentations

Thompson A, Stephens J, Bain S and Kanamarlapudi V. Agonist Induced Internalisation of the Glucagon Like Peptide-1 Receptor. College of Medicine Postgraduate Research Conference, 19-23rd May 2014, Swansea. Poster Presentation.

Thompson A and Kanamarlapudi V. The N-terminal Region of GLP-1R Regulates the Receptor Cell Surface Expression. 5th British Pharmacological Society Focused Meeting on Cell Signalling, 28-29th April 2014, Leicester. Poster presentation.

Thompson A, Stephens J, Bain S, Thornton C and Kanamarlapudi V. Role of the N-Terminal and C-Terminal Epitope Tags on Glucagon Like Peptide-1 Receptor Internalisation. College of Medicine Postgraduate Research Conference, 13-17th May 2013, Swansea. Poster Presentation. **Awarded the John White Award.**

Thompson A, Stephens J, Bain S, Owens S and Kanamarlapudi V. Agonist Induced Internalisation of the GLP-1R. College of Medicine Postgraduate Research Conference, 17-18th May 2012, Swansea. Oral Presentation.

Thompson A, Stephens J, Bain S and Kanamarlapudi V. Glucagon Like Peptide-1 Receptor Trafficking and Agonist Mediated Internalisation. College of Medicine Postgraduate Research Conference, 27-28th May 2011, Swansea. Poster Presentation.

Publications

Thompson A and Kanamarlapudi V (2014) The Region After the Signal Peptide is Critical for Human Glucagon Like Peptide-1 Receptor Cell Surface Expression. *Sci. Rep.* (DOI: 10.1038/srep07410)

Thompson A and Kanamarlapudi V (2014) Agonist Induced Internalisation of the Glucagon Like Peptide-1 Receptor is Mediated by the Gαq Pathway. *Biochem Pharmacol.* (DOI: 10.1016/j.bcp.2014.10.015)

Thompson A and Kanamarlapudi V (2013) Type 2 Diabetes Mellitus and Glucagon Like Peptide-1 Receptor Signalling. *Clin Exp Pharmacol.* **138** (DOI: 2161-1459.1000138)

1. General Introduction

1.1. Introduction

The actions of glucagon like peptide-1 (GLP-1) have been greatly examined over the last twenty years, due to the hormones effectiveness at lowering blood glucose levels and increasing insulin secretion in type 2 diabetic patients (Doyle & Egan, 2007; Holz et al, 1999). GLP-1 exerts its actions through the GLP-1 receptor (GLP-1R), a family B G-protein coupled receptor (GPCR), which mediates its effects through the $G\alpha_s$ subunit, which in turn activates adenylyl cyclase (AC). The involvement of $G\alpha_s$ and the subsequent accumulation of cyclic adenosine monophosphate (cAMP) in glucose induced insulin secretion is well established (Drucker et al, 1987).

1.2. Type 2 diabetes

1.2.1. Background

The World Health Organization describes diabetes mellitus as a "metabolic disorder of multiple actiology characterised by chronic hyperglycaemia with disturbances of carbohydrate, fat and protein metabolism resulting from defects in insulin secretion, insulin action, or both" (Alberti & Zimmet, 1998; World Health Organisation, 1999). It was estimated that 382 million people (approximately 9% of the world's adult population) lived with diabetes in 2013. This number will continue to rise and has been estimated to reach 439 million by 2030 and 592 million by 2035 (Guariguata et al, 2014; Whiting et al, 2011). Diabetes remains the leading cause of blindness, end stage renal disease, lower limb amputation and cardiovascular disease (Schwarz et al, 2007; Zimmet et al,

2001). Diabetes mellitus is classified into four categories, type 1, type 2, other specific types and gestational diabetes (Table 1.1), of which, type 2 is the most common form (Alberti & Zimmet, 1998; Kuzuya & Matsuda, 1997; World Health Organisation, 1999).

Table 1.1. Aetiological classification of disorders of glycaemia

Types	Description and Subtypes
Type 1	β-cell destruction, usually leading to absolute insulin deficiency Autoimmune Idiopathic
Type 2	Ranging from predominantly insulin resistant with relative insulin deficiency to a predominantly secretory defect with or without insulin resistance
Other Specific Types	Genetic defects of β-cell function Genetic defects in insulin action Diseases of the exocrine pancreas Endocrinopathies Drug or chemical induced Infections Uncommon form of immune mediated diabetes Other genetic syndromes sometimes associated with diabetes
Gestational Diabetes	Carbohydrate intolerance resulting in hyperglycaemia of variable severity with onset or first recognition during pregnancy

Table showing description and subtype of type 1, type 2, other specific types and gestational diabetes. Adapted from (Alberti & Zimmet, 1998).

1.2.2. Pathophysiology and causes

Insulin is a hormone that is secreted in response to food intake to maintain glucose homeostasis. It is produced by the β-cells in the islets of Langerhans in the pancreas (Rhodes & White, 2002). Synthesis occurs on the rough endoplasmic reticulum (ER) as preproinsulin, containing a signal peptide (SP) that is cleaved to form proinsulin (Figure 1.1). Proinsulin then traffics through the trans Golgi network and is packaged into secretory vesicles until required (Nelson et al, 2008). The hydrolysis of dietary carbohydrates such as starch or sucrose within the small intestines results in the production of glucose, which is then absorbed into the blood. An increase in glucose concentrations in the blood stimulates the release of insulin. Insulin has different effects depending on the target tissue; it either facilitates the entry of glucose into adipose and muscle tissue or stimulates the liver to store glucose as glycogen. If insulin is absent or in low concentrations within the body, insulin sensitive cells are unable to absorb glucose and therefore use other fuel sources such as fatty acids for energy, which can lead to ketoacidosis. When blood glucose levels are low, insulin is not produced and instead glucagon is secreted, broken down and released as glucose (Berg et al, 2002; Sadava et al, 2006).

In normal individuals, glucose homeostasis keeps glucose levels under control and within the normal range of 80-120 mg/100 ml (4.4-6.7 mM). For patients with diabetes, insufficient insulin release results in hyperglycaemia and high blood glucose levels (Bansal & Wang, 2008; Berg et al, 2002). An absolute lack of insulin producing β-cells in the pancreas results in the development of type 1 diabetes (Alberti & Zimmet, 1998; World Health Organisation, 1999; Yoon & Jun, 2005). In contrast, type 2 diabetes is a result of insulin dependent cells not being able to respond to insulin effectively, also known as insulin resistance (Alberti & Zimmet, 1998; World Health Organisation, 1999). Individuals who are obese and have a genetic predisposition to both insulin resistance and β-cell dysfunction are at high risk of developing type 2 diabetes. Overtime, the β-cell is unable to compensate for insulin resistance and causes a decline in β-cell function (Prentki & Nolan, 2006).

It is estimated that 60-90% of patients with type 2 diabetes are obese and obesity itself can cause insulin resistance (Muoio & Newgard, 2008). There is a greater than 90-fold possibility of developing type 2 diabetes if you are obese compared to non-obese individuals (Anderson et al, 2003). Body mass index (BMI) is defined as the individual's body weight divided by the square of their height (kg/m^2). A BMI greater than 25 is overweight and above 30 is obese (Eknoyan, 2008). It is suggested that type 2 diabetic patients should aim for a BMI of 25 or below (Hollander, 2007). However, there is still a 2.4-fold increased risk of developing type 2 diabetes in those who are of normal BMI (between 18.5 and 24.9) but have an increased percentage of body fat distributed in the abdominal region (Cassano et al, 1992; Tuomilehto et al, 2011; Venables & Jeukendrup, 2009).

Diet, genetics and sedentary lifestyle all play a role in the development of type 2 diabetes (Bazzano et al, 2005; Diabetes UK, 2014; Hu, 2011). The dietary intake of saturated fat, trans fatty acids and total fats were considered risk factors in the development of type 2 diabetes. In contrast dietary fibres or non-starch polysaccharides were considered protective factors (Bazzano et al, 2005). Low-fat vegetarian and vegan diets have the potential to be used for the management of type 2 diabetes because they are associated with weight loss, improved cardiovascular health and increased insulin sensitivity (Barnard et al, 2009; Riserus et al, 2009). A cohort study evaluated the association of multiple lifestyle factors, including diet, physical activity, alcohol use, smoking habits and adiposity measures, with the risk of developing type 2 diabetes. This risk was approximately 50% lower in individuals whose physical activity and dietary habits indicated low risk and approximately 80% lower in those whose diet, physical activity, alcohol use and smoking habits all indicated low risk (Mozaffarian et al, 2009; Tuomilehto et al, 2011). In addition, having relatives with type 2 diabetes substantially increases an individual's chance of developing type 2 diabetes. The insulin receptor substrate-1 (IRS-1) gene has been associated with type 2 diabetes, insulin resistance and hyperinsulinemia in a large scale study, which studied 14,000 people all around the world (Rung et al, 2009).

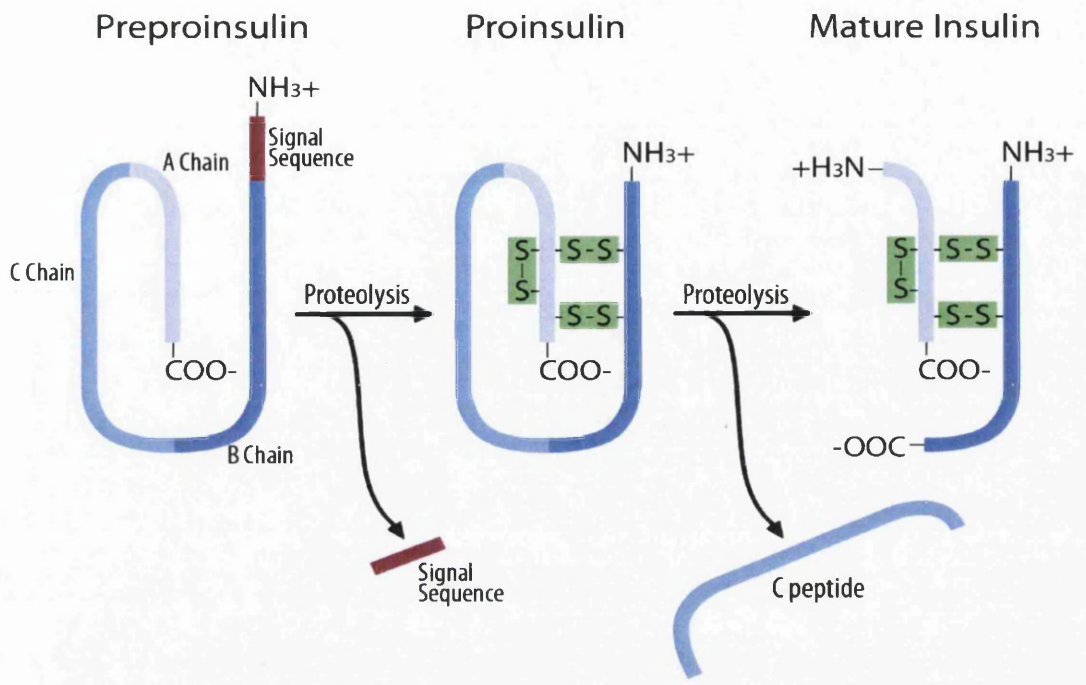

Figure 1.1. Processing of preproinsulin. The SP sequence (23 amino acids) is removed from the N-terminus of preproinsulin by proteases. This forms three disulphide bonds producing proinsulin. Further proteolytic cleavage of proinsulin removes the C-peptide producing mature insulin. Redrawn from (Nelson et al, 2008).

1.2.3. Signs and symptoms

Type 2 diabetes often develops slowly from pre-diabetes and symptoms may not be obvious for years (Diabetes UK, 2014). The characteristic symptoms of type 2 diabetes include blurred vision, dehydration, excessive thirst, polydipsia (increased fluid intake) and polyuria (excessive urine production), which develop as a result of hyperglycaemia. In diabetes, insulin producing β-cells are either partially or completely unable to use glucose as a fuel and therefore switch to using fats, carbohydrates and protein metabolism as a fuel source instead. This requires more energy and leads to polyphagia (excessive eating), weight loss and lethargy (Alberti & Zimmet, 1998; Cooke & Plotnick, 2008;

World Health Organisation, 1999). Additionally, hyperglycaemia can lead to skin infection as a result of open and slow healing sores because it is more difficult for the body to heal itself (Alba-Loureiro et al, 2007).

Serious long-term complications of type 2 diabetes include nerve dysfunction, cardiovascular disease, microvascular damage, renal failure, blindness, impotence and poor healing, and are a result of prolonged hyperglycaemia (Alberti & Zimmet, 1998; Blonde, 2009; World Health Organisation, 1999). These complications may also occur if the disease is not controlled correctly. Hypoglycaemia is caused by inaccurately administered insulin. A shortage of insulin causes the body to switch to metabolising fatty acids and as a result produces ketone bodies. This response results in ketoacidosis and causes dehydration in addition to many of the symptoms and complications already described (Kitabchi & Nyenwe, 2006). Another metabolic complication is known as hyperglycaemia hyperosmolar state and is the end result of sustained osmotic diuresis. It is characterised by severe hyperglycaemia, hyperosmolarity and dehydration, but without ketoacidosis (Kitabchi & Nyenwe, 2006; Stoner, 2005).

1.2.4. Diagnosis

Diabetes is diagnosed by recurrent or persistent hyperglycaemia. This can be demonstrated by any of the following criteria: a fasting plasma glucose level of 7.0 mM; a single plasma glucose reading in excess of 11.1 mM; and an oral glucose tolerance test (OGTT) administered 2 hours after 75 g oral glucose with fasting plasma glucose concentrations in excess of 11.1 mM (Alberti & Zimmet, 1998; World Health Organisation, 1999).

Glycosylation of haemoglobin (HbA1c) is primarily used as a treatment-tracking test and reflects average glucose levels over 8-12 weeks (Rahbar et al, 1969; World Health Organisation, 2011). Measurements can be performed at any time and there is no need for fasting. It is recommended that HbA1c be used to measure blood glucose control in both pre-diabetics and patients with diabetes.

A reading of 6.5% HbA1c or above is used to diagnose diabetes (World Health Organisation, 2011). OGTT or intravenous glucose tolerance tests are used to determine the pancreatic insulin response and degree of insulin resistance. However, it was noted that glucose administered orally promoted a significantly greater insulin response than glucose administered intravenously (Figure 1.2), although plasma glucose levels were the same (Creutzfeldt & Ebert, 1985; Nauck et al, 1986; Perley & Kipnis, 1967). Further, cross reactivity with partially degraded proinsulin and insulin may occur and as a result insulin measurement may be problematic. It is especially problematic in patients who have developed anti-insulin antibodies through administering animal insulin. As a result, C-peptide concentration has been used as a semi quantitative measure of β-cell secretory activity instead of insulin itself. C-peptide has a half-life 2.5 times longer than insulin and therefore higher concentrations exist in the peripheral circulation and levels fluctuate less (Vezzosi et al, 2007).

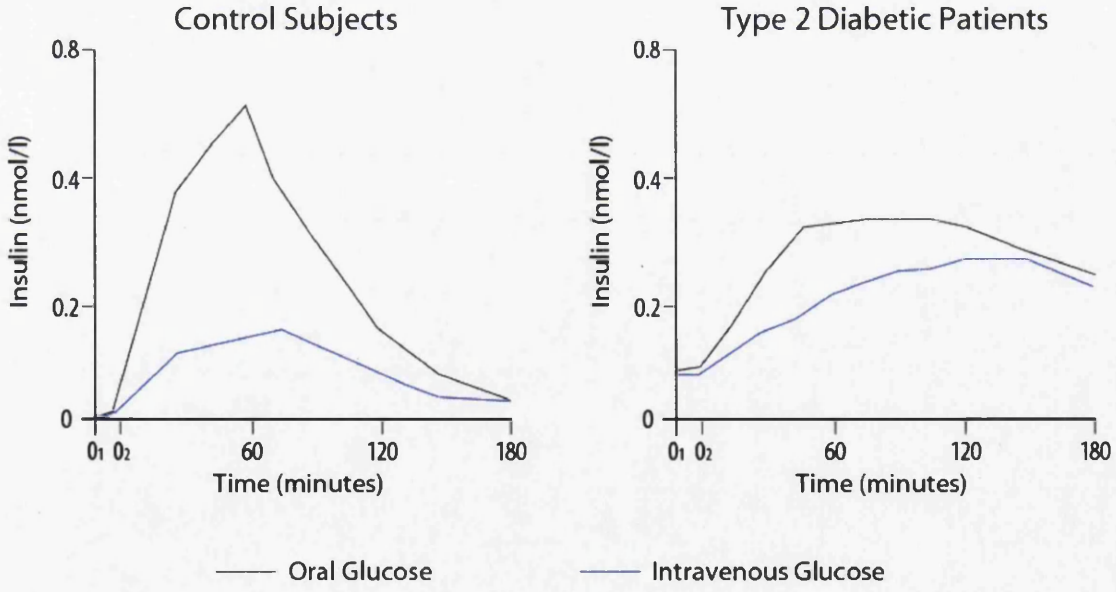

Figure 1.2. The incretin effect in healthy subjects and type 2 diabetic patients. Venous insulin levels after oral glucose load (50 g/400 ml, black) and during intravenous glucose (blue) in healthy subjects and type 2 diabetic patients. Redrawn from (Nauck et al, 1986).

1.2.5. Treatment

More intensive glucose control, mainly determined by HbA1c levels, can delay or prevent the development and progression of serious complications in type 2 diabetics (Blonde, 2009). Initial treatment of type 2 diabetes generally begins with non-pharmacological interventions such as diet, lifestyle and exercise. These interventions combined with antihyperglycaemic agents (such as metformin) are used to improve blood glucose control (Table 1.2). If a HbA1c level greater than 7% is not achieved within 2-3 months, then the recommended second stage is the addition of hypoglycaemic agents (such as sulfonylureas) or insulin injections to the treatment (Table 1.2). Hypoglycaemic agents reduce plasma glucose levels by increasing insulin secretion, reducing insulin resistance and/or delaying glucose absorption in the gut (Nathan et al, 2008; Nathan et al, 2009; Wright, 2009).

In many cases treatment with either antihyperglycaemic or hypoglycaemic agents is not usually enough to achieve adequate blood glucose control and therefore insulin therapy is intensified (Meneghini, 2009; Swinnen et al, 2009; Wright, 2009). However, insulin therapy has a number of risks associated with it including hypoglycaemia, weight gain and increased risk of colorectal cancer (Chiasson, 2009). These risk factors, together with the route of administration (usually subcutaneous injection), contribute to many patients being reluctant to maintain intensive insulin therapy (Hamnvik & McMahon, 2009).

Consequently, these classic treatments are often unsatisfactory, which is why there is a crucial need for new classes of glucose lowering agents. Recently, incretin-based therapies have been used in the treatment of type 2 diabetes, namely Exenatide and Liraglutide (Table 1.2). These drugs have the ability to improve glycaemic control by preserving normal physiological responses to food intake.

Table 1.2. Summary of glucose lowering drugs

Drug	Mechanism of Action	Adverse Effects
Metformin	Suppresses glucose produced by the liver	Gastrointestinal side effects, renal insufficiency
Insulin	Lowers blood glucose levels	1-4 injections daily, monitoring, weight gain, hypoglycaemia, colorectal cancer
Sulfonylurea	Enhances insulin secretion	Weight gain, hypoglycaemia
Thiazolidine or glitazone	Increases sensitivity of muscles, fat and liver to insulin	Fluid retention, weight gain, bone fractures, congestive heart failure, increase in myocardial infarction
GLP-1R agonists (Liraglutide and Exenatide)	Potentiates glucose stimulated insulin secretion	2 injections daily, frequent gastrointestinal side effects, papillary thyroid cancer, pancreatitis, long-term safety not established
α-glucosidase inhibitor	Prevent digestion of carbohydrates	3 times daily dosing, frequent gastrointestinal side effects, hypoglycaemia
Glinide	Enhances insulin secretion	3 times daily dosing, hypoglycaemia, weight gain
Amylin agonist	Inhibits glucagon secretion	3 injections daily, frequent gastrointestinal side effects, long-term safety not established
DPP-4 inhibitor	Enhances the effects of GLP-1 and GIP, increasing glucose mediated insulin secretion	Long-term safety not established

Summary of currently available glucose lowering drugs, their mechanisms of action and adverse effects (Drucker et al, 2010; Nathan et al, 2009).

1.3. GLP-1 in type 2 diabetes

1.3.1. Incretin hormones

Incretins are gastrointestinal hormones that contribute to postprandial insulin release (Nauck et al, 2011; Perley & Kipnis, 1967). GLP-1 and glucose-dependent insulinotropic polypeptide (GIP) are two major incretins and are thought to be responsible for up to 70% of insulin secreted from the β-cells of the pancreas following food intake. This increase in insulin is called the 'incretin effect' and maintains glucose concentrations at low levels irrespective of the amount of glucose ingested. This is achieved by increasing the sensitivity of β-cells to glucose (Holst et al, 2008). The 'incretin effect' is either reduced or absent in type 2 diabetic patients and is due to the loss of insulinotropic action of GLP-1 and GIP. However, more recently it has been suggested that the secretion of GIP and GLP-1 is normal in type 2 diabetic patients (Meier & Nauck, 2010). In opposition to this latter suggestion, evidence strongly suggests a role for incretin hormones or their actions in the treatment of type 2 diabetes (Haluzik, 2014; Knop et al, 2007; Nauck et al, 1986; Nauck et al, 1993; Toft-Nielsen, 2001; Zander et al, 2002).

The GIP gene is mainly expressed in K-cells and enterochromaffin cells of the proximal small intestine. GIP secretion is stimulated by enteral glucose, lipids and products of meal digestion in a concentration dependent manner (Schirra et al, 1996). In patients with type 2 diabetes, GIP concentrations after food intake are either normal or slightly elevated. GIP infusion does not reduce plasma glucose concentrations in type 2 diabetics. As a result GIP has not been thought of as a suitable candidate for therapeutic development (Holst & Gromada, 2004; Vilsboll et al, 2002). In contrast, type 2 diabetic patients have decreased GLP-1 activity (Kjems et al, 2003; Knop et al, 2007; Toft-Nielsen, 2001). It is currently unknown whether reduced GLP-1 activity is a cause or consequence of diabetes. In response to glucose, normal GLP-1 secretion is seen in first degree relatives of type 2 diabetic patients, which suggests that a reduction in GLP-1 secretion seen in type 2 diabetic patients is more likely acquired (Nauck et al, 2004;

Nyholm et al, 1999). Additionally, glucose dependent insulin secretion is induced by GLP-1 in type 2 diabetic patients under hyperglycaemic conditions (Holst et al, 2009; Nauck et al, 1993; Salehi et al, 2010). Furthermore, administration of exogenous GLP-1 to type 2 diabetic patients causes near-normalisation of hyperglycaemic conditions (Nauck et al, 1993; Nauck et al, 2009; Ratner et al, 2010). As a result, GLP-1 based strategies appear a more suitable target for the treatment of type 2 diabetes (Gallwitz, 2010).

The insulinotropic effects of GLP-1 and GIP is reduced or absent in patients with type 2 diabetes (Meier & Nauck, 2010). Glucotoxicity has been suggested as the cause for this diminished effect because normalisation of blood glucose levels restores incretin levels and efficiency (Hojberg et al, 2009; Poitout, 2013). Interestingly, lipotoxicity has recently been demonstrated to also have an effect on GLP-1 and GIP receptor expression and signalling (Kang et al, 2013). It was demonstrated that GLP-1R expression was inhibited with prolonged exposure to palmitate in isolated mouse islets and insulin secreting cells, reducing glucose stimulated insulin secretion and abolishing GLP-1 signalling. In *db/db* mice islets, both GLP-1 and GIP receptor expression was inhibited and restored with the addition of lipid lowering drug bezafibrate. Glucose tolerance, islet morphology and β-cell mass improved in *db/db* mice with bezafibrate and dipeptidyl peptidase-IV (DPP-IV, see section 1.3.2) inhibitor des-fluoro-sitagliptin in combination. The administration of bezafibrate with GLP-1 agonist exendin-4 enhanced these effects (Muscelli et al, 2008). This links obesity with a reduced incretin effect, independent of glucose tolerance. Additionally, GLP-1 and GIP receptor expression is reduced in islets isolated from type 2 diabetic patients (Shu et al, 2009), suggesting the mechanisms observed in mice are also highly likely to occur in humans.

1.3.2. Synthesis and secretion of GLP-1

GLP-1 is 42 amino acids in length and is synthesised from the post-translational modification of proglucagon, by prohormone convertase (PC) 1 within the intestinal L-cells. PC1 is specific to GLP-1 production in the L-cells (Dhanvantari

et al, 2001; Mojsov et al, 1986). The proglucagon gene (Figure 1.3A) is expressed in both the pancreatic α-cells and in the intestinal L-cells, but post-translational processing differs in these two tissues (Holst, 2007; Orskov et al, 1986; Orskov et al, 1987). In the pancreatic α-cells (Figure 1.3B), proglucagon is processed to glucagon, intervening peptide (IP)-1, major proglucagon fragment (MPGF) and glicentin-related pancreatic peptide (GRPP) by PC2 (Mojsov et al, 1986; Rouille et al, 1994). In the intestinal L-cells (Figure 1.3C), proglucagon is cleaved to GLP-1, glucagon like peptide-2 (GLP-2), IP-2, oxyntomodulin and glicentin by PC1 (Baggio & Drucker, 2004; Orskov et al, 1989; Thomas et al, 1991). However, it has been suggested that recombinant expression of PC2 can cause pancreatic α-cells to also produce GLP-1 (Wideman et al, 2007; Wideman et al, 2009; Wideman et al, 2006).

In secretory vesicles, the first six amino acids of GLP-1 are cleaved from the N-terminus forming the bioactive peptides. Approximately 80% of truncated GLP-1 forms the predominantly secreted GLP-1 (7-36)-NH_2 and the remaining 20% is released as GLP-1 (7-37) (Figure 1.4) (Vahl et al, 2003). Both GLP-1 (7-36)-NH_2 and GLP-1 (7-37) bind to the GLP-1R with similar affinity and show similar potency (Orskov et al, 1993). GLP-1 is produced in response to food intake, in particular glucose and triacylglycerols, and lowers blood glucose levels (Nauck et al, 2011; Nystrom, 2008). In times of fasting, GLP-1 plasma concentrations are very low and can be lowered even further with the administration of somatostatin in humans, suggesting there are some basal rates of secretion (Holst, 2007). Typically, 'total' GLP-1 concentrations are about 5-15 pmol/l in basal state, rising to about 20-60 pmol/l after food intake (Nauck et al, 2011). The secretion of GLP-1 from L-cells increases within about 10 minutes of food intake, which is later than the 'cephalic phase' stimulation of insulin secretion. This suggests that neuronal signals generating insulin release does not influence GLP-1 secretion. Evidence suggests that the presence of nutrients in the gut and the interaction with the microvilli of L-cells are responsible for GLP-1 secretion (Holst, 2007).

In vivo, GLP-1 has a very short half-life of ~1.5 minutes due to the rapid proteolytic degradation of GLP-1 by enzyme DPP-IV (Hansen et al, 1999; Larsen et al, 2001; Mentlein, 2009; Vilsboll et al, 2003). This enzyme cleaves the active GLP-1 (7-36)-NH_2/(7-37) to its inactive GLP-1 (9-36)-NH_2/(9-37) form by removing two amino acids at the N-terminus of the peptide (Kieffer et al, 1995; López de Maturana & Donnelly, 2002; Montrose-Rafizadeh et al, 1997). GLP-1 (9-36)-NH_2 and GLP-1 (9-37) (Figure 1.4) have both been identified as products of GLP-1 cleavage by DPP-IV action *in vitro* and *in vivo* (Mentlein, 2009). The degradation occurs so quickly that less than 25% of the active GLP-1 secreted enters the portal vein prior to reaching the liver (Reimann, 2010). As a result, it is estimated that approximately 85% of circulating postprandial GLP-1 is either GLP-1 (9-36)-NH_2 or GLP-1 (9-37) (Abu-Hamdah et al, 2009).

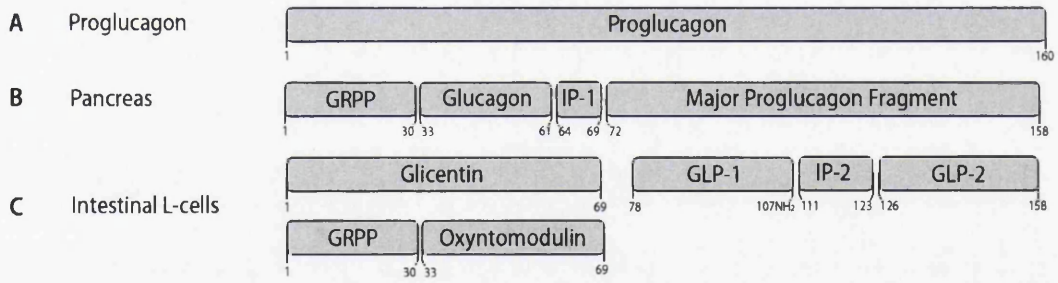

Figure 1.3. The post-translational processing of proglucagon. In the pancreas, proglucagon (A) is cleaved to glucagon, GRPP, IP1 and MPGF by PC2, respectively (B). (C) In the intestinal L-cells proglucagon is processed by PC1 to GLP-1, GLP-2, IP2, oxyntomodulin and glicentin, respectively.

Figure 1.4. The post-translational processing of GLP-1. DPP-IV cleaves the active GLP-1 (7-36)-NH_2/(7-37) to its inactive GLP-1 (9-36)-NH_2/(9-37) form. The cleavage site is indicated by the arrow.

1.3.3. Biological activities of GLP-1

GLP-1 has several actions in various tissues and exerts its effects through its cell surface receptor, the GLP-1R (Figure 1.5). Other members of the glucagon family of peptides such as GLP-2, glucagon and GIP do not bind the GLP-1R at physiologically relevant concentrations (Holst, 2007). The human GLP-1R (hGLP-1R) gene is transcribed in pancreatic islet, brain, heart, intestine, kidney, liver, lung and stomach. However, the actions of GLP-1 in fat and muscle most likely occur through indirect mechanisms and do not occur in many species (Bullock et al, 1996; De Leon et al, 2006; Gupta et al, 2010; Wei & Mojsov, 1995). The expression of the GLP-1R is consistent with the roles of GLP-1 in glucose homeostasis, β-cell proliferation, heart rate, food intake and appetite and even learning (De Leon et al, 2006).

In the pancreas, GLP-1 increases insulin secretion from islet β-cells and suppresses glucagon secretion from islet α-cells, in a glucose dependent manner (De Marinis et al, 2010; Rayner et al, 2001). Additionally, GLP-1 has been shown

to promote β-cell proliferation and prevent apoptosis (Cunha et al, 2009; Li et al, 2005; Quoyer et al, 2010). Additionally, GLP-1 delays gastric emptying in the gastro intestinal tract and also plays a role in supressing appetite by acting as a postprandial satiety signal to the brain (Kim et al, 2009; Schirra et al, 1996). Furthermore, GLP-1 plays an important role in the enteric and central nervous system. The release of GLP-1 is tightly regulated and involves the gut-to-brain and the brain-to-periphery axis (Burcelin et al, 2009; Hayes, 2012; Hayes et al, 2009; van Bloemendaal et al, 2014). Pharmacological applications of GLP-1 have demonstrated a number of positive effects in the cardiovascular system, suggesting GLP-1 may play an important role in that system (Angeli & Shannon, 2014; Grieve et al, 2009). Additionally, evidence suggests GLP-1 and its receptor may modulate components of the insulin signalling pathway and decrease hepatic steatosis *in vitro* (Gupta et al, 2010).

Interestingly, evidence is emerging to suggest GLP-1 (9-36)-NH_2 and GLP-1 (9-37), the inactive forms of GLP-1, strongly reduce GLP-1R activity within pancreatic β-cells and have insulin-like actions on heart, liver and vasculature. It has therefore been proposed that they may act through a novel signalling pathway by binding to a different cell surface receptor (Tomas & Habener, 2010).

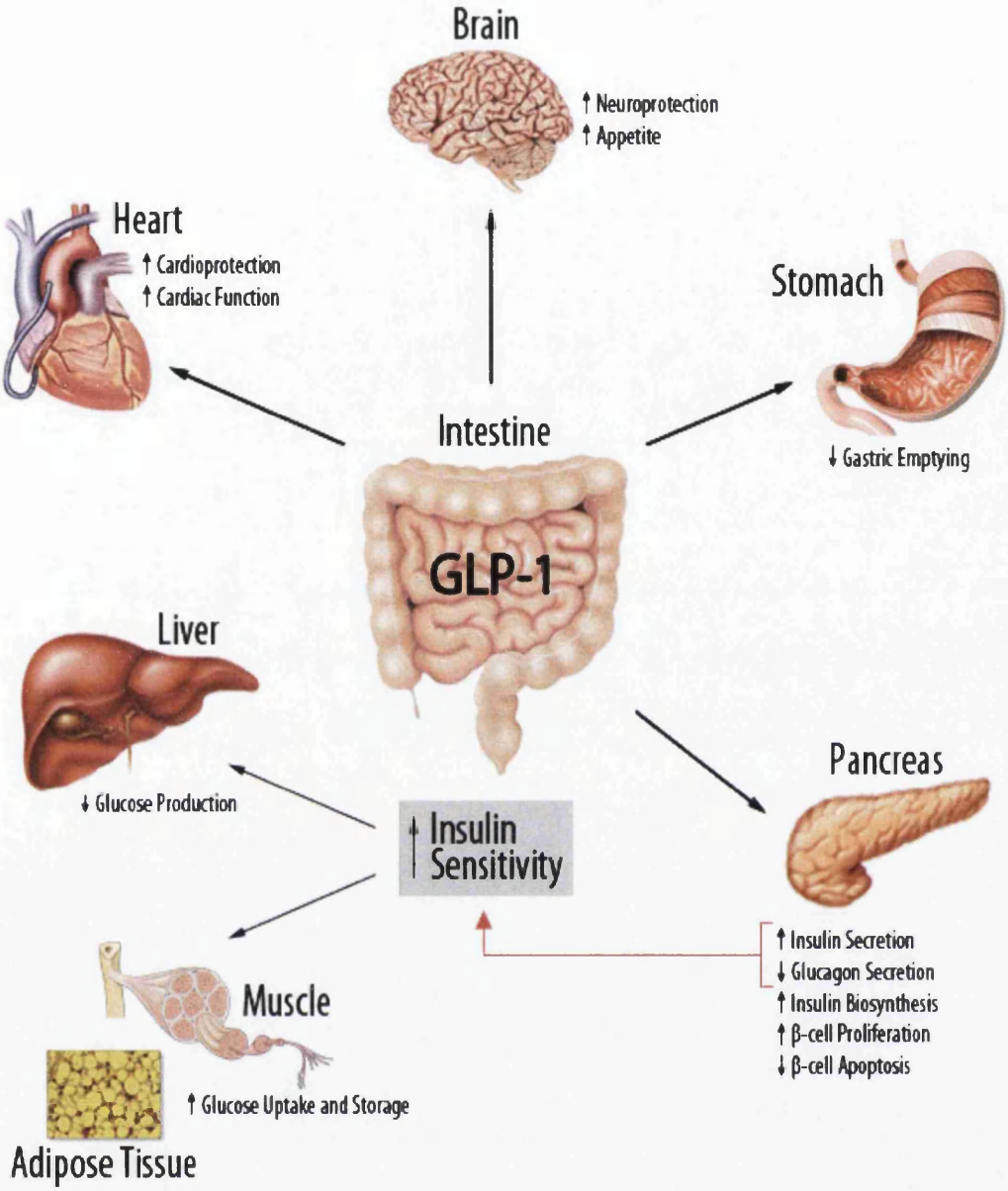

Figure 1.5. Biological activities of GLP-1. GLP-1 increases insulin sensitivity, decreases appetite, slows gastric emptying, increases β-cell proliferation, increases cardiac function as well as other physiological actions as indicated in the diagram. Redrawn from (Baggio & Drucker, 2007; De Leon et al, 2006).

1.3.4. GLP-1 based therapies in the treatment of type 2 diabetes

The binding of GLP-1 to the GLP-1R results in insulin secretion from pancreatic β-cells, making them important targets in the treatment of type 2 diabetes. The biological and pharmacological activities of GLP-1 have been the basis for two type 2 diabetic therapies. The first therapy is based on using DPP-IV inhibitors to prevent the breakdown of GLP-1 from its active to inactive form (Gallwitz, 2010). The second therapy is based on using DPP-IV resistant GLP-1 mimetics, which replicate the physiological actions of the GLP-1 peptide but with a longer half-life.

DPP-IV, also named adenosine deaminase complexin G-protein or cluster of differentiation 26 (CD26), is an antigenic enzyme. It is associated with signal transduction, immune regulation and apoptosis and therefore is expressed on the surface of most cell types. DPP-IV is highly specific and cleaves between X-proline and X-alanine dipeptides (where X is any amino acid) at the N-terminus, but is unable to cleave peptides with a third proline (for example glycine-proline-proline) (Mentlein, 2009). DPP-IV inhibitors increase GLP-1 levels by 2-3-fold over 24 hours by inhibiting 90% of plasma DPP-IV activity *in vivo*. They also have an additional advantage of oral administration (Charbonnel et al, 2006). There are currently three DPP-IV inhibitors, saxagliptin, sitagliptin and vildagliptin, used in the treatment of type 2 diabetes in Europe (Khunti & Davies, 2010). These inhibitors significantly decrease postprandial glucose levels and HbA1c by 0.5-1.0% (Gallwitz, 2010; Gilbert & Pratley, 2009). Sitagliptin and vildagliptin have been shown to improve β-cell function and reduce systolic blood pressure (Deacon & Holst, 2006). However, the long-term inhibition of DPP-IV may have adverse effects as this enzyme is expressed in many types of tissues and has many functions (Lamont & Andrikopoulos, 2014; Yu et al, 2010). Experimental evidence has demonstrated an increase in infection and some tumours, supporting adverse immunological and oncological effects after prolonged use of DPP-IV inhibitors (Stulc & Sedo, 2010).

The main limitation of GLP-1 is its very short half-life (~1.5 minutes) due to the rapid proteolytic degradation of GLP-1 by DPP-IV, cleaving the active GLP-1 (7-

36)-NH_2 to the inactive GLP-1 (9-36)-NH_2 form (Hansen et al, 1999; Larsen et al, 2001; Vilsboll et al, 2003). DPP-IV cleaves GLP-1 between alanine and glutamic acid at positions 8 and 9. A substitution at position 8 from alanine to valine (Ala^8Val) stabilises the peptide without affecting its activity and prevents peptide degradation. However, the half-life of the modified peptide is still too short (~4-5 minutes) to be used as a drug (Deacon et al, 1998). As a result, therapeutic strategies that activate GLP-1R and improve GLP-1 actions have been extensively studied and developed because of its short half life. This has lead to the development of two DPP-IV resistant GLP-1R agonists, Liraglutide and Exenatide. Liraglutide is a long-acting GLP-1 analogue with 97% sequence homology to human GLP-1 (hGLP-1) (Edavalath & Stephens, 2010). It is chemically similar to hGLP-1 but with structural modifications resulting in resistance to GLP-1 inactivation by DPP-IV and prolonged duration of action (Gonzalez et al, 2006). Liraglutide has a half-life of approximately 11-13 hours and is administered once a day irrespective of meal times (Pinkney et al, 2010). Exenatide is a peptide found within the salivary glands of the Gila monster lizard and has 52% sequence homology to hGLP-1 (Eng et al, 1992). It is also not enzymatically degraded by DPP-IV and therefore has a prolonged *in vivo* half-life of 3.4-4 hours compared with hGLP-1. As a result it is administered twice daily within 60 minutes of a meal (Gallwitz, 2006). Both GLP-1R agonists are currently in use as drugs for the treatment of patients with type 2 diabetes, as they are effective insulinotropic agents, regulating blood glucose levels by increasing insulin secretion and supressing glucagon secretion in a glucose dependent manner (Bond, 2006; Kim Chung le et al, 2009). Liraglutide and Exenatide significantly reduce both fasting and postprandial glucose levels and HbA1c levels by 0.8-1.5% (Edavalath & Stephens, 2010). The most common side effects of GLP-1 strategies are dyspepsia or nausea, which may lead to delayed gastric emptying. However, the effects seem to subside with continuous administration (Buse et al, 2009; Gallwitz, 2010). Acute pancreatitis and papillary thyroid cancer has been reported in a few rare cases but their clinical significance remains unclear (Drucker et al, 2010). The side effects associated with the long-term administration of these peptides have necessitated the search for orally active small molecule agonists of the GLP-1R (Coopman et al,

2010). Interestingly, GLP-1 mimetics have recently been shown to cross the blood-brain barrier and have impressive neuroprotective effects in neurodegenerative disorders such as strokes, Parkinson's disease and Alzheimer's disease (Campbell & Drucker, 2013; Holscher, 2014; Hunter & Holscher, 2012).

A series of eleven-amino acid peptide agonists of the GLP-1R, have been reported to have excellent potency and *in vivo* activity in *ob/ob* mouse models of diabetes (Haque et al, 2010; Mapelli et al, 2009). These peptides are closely related structurally to nine C-terminal residues of GLP-1 but are substituted with several unnatural amino acids at position 11, such as homohomophenylalanine. This gives rise to the opportunity of increasing stability against proteolytic degradation by DPP-IV. However, the activity of these peptides can be blocked with inactive exendin (9-39) (exendin antagonist) (Mapelli et al, 2009).

1.4. G-protein coupled receptors (GPCRs)

1.4.1. GPCRs in drug discovery

GPCRs, also named seven transmembrane receptors, are the largest family of cell surface receptors. GPCRs are the most common target for medical therapeutics due to their involvement in many physiological and pathological processes. Over 50% of drugs available on the market act on GPCRs (Millar & Newton, 2010). Therefore, a need for a greater understanding of these targets and interaction with drugs is required to allow for novel drug discovery.

1.4.2. Classification and structure

All GPCRs are made up of a single polypeptide chain of up to 1100 amino acids, which pass through the plasma membrane seven times. This membrane topology results in an extracellular N-terminal domain, seven transmembrane

(TM) α-helices joined by three extracellular loops (ECL) and three intracellular loops (ICL) followed by an intracellular C-terminal domain that interacts with G-proteins (Figure 1.6). GPCRs are classically divided into three families: A, B and C based on their sequence homology and functional similarities (Kristiansen, 2004).

Family A GPCRs, also called the rhodopsin-like family, is the largest subfamily (Figure 1.6A). It consists of 672 members and accounts for approximately 85% of all GPCR genes (Heilker et al, 2009; Millar & Newton, 2010). A short N-terminal domain and a disulphide bridge, which join ECL1 and ECL2 is characteristic to this family. Additionally, highly conserved residues in the transmembrane bundle and a C-terminal palmitoylated cysteine residue is present (Jacoby et al, 2006). The crystal structure of rhodopsin demonstrated the transmembrane domains of family A GPCRs 'kink' and 'tilt' (Palczewski, 2000). This was further supported by solving the crystal structures of the β_2- and β_1-adrenergic receptors (AR) and the A_{2A}-adenosine receptor (Millar & Newton, 2010). Comparisons between these structures revealed the transmembrane domains to be extremely similar and small molecule agonists would occupy the same space within the transmembrane pocket (Hanson & Stevens, 2009).

Family B GPCRs, also known as the secretin receptor family, is a small family made up of only 15 members (Kristiansen, 2004; Parthier et al, 2009). This family is distinguishable from the other two families by the large N-terminal extracellular domain, which is 100-160 amino acids in length and has an important role in agonist binding (Figure 1.6B). Additionally, this family contains several conserved disulphide bonds in the N-terminus of the receptor, which stabilises the large N-terminal structure (Parthier et al, 2009). This study has concentrated on the GLP-1R within this family.

Family C GPCRs, also named the glutamate family, form another small family consisting of 24 members. It is characterised by large N-terminal and C-terminal domains. Furthermore, a conserved disulphide bridge links ECL1 to ECL2, in

addition to a short and highly conserved ICL3 (Figure 1.6C). The N-terminal domain of family C GPCRs is usually described as a 'venus fly trap' (Kristiansen, 2004; Urwyler, 2011). This agonist binding site is a characteristic of all family C GPCRs except the $GABA_B$ receptor which contains nine conserved cysteine residues linking the 'venus fly trap' to the transmembrane bundle (Brauner-Osborne et al, 2007).

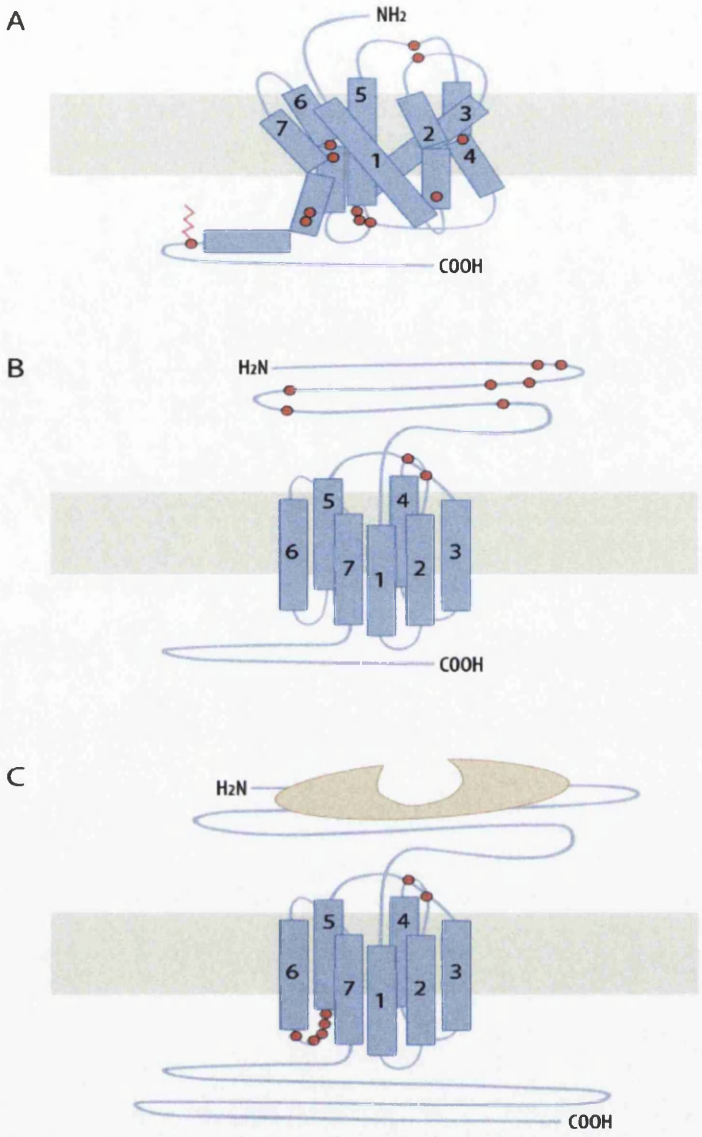

Figure 1.6. Structure of GPCRs. All GPCRs share a common membrane topology consisting of a NH_2-terminal extracellular domain, seven transmembrane α helices joined by three ECL and ICL and an intracellular COOH-terminal domain. Red circles denotes conserved residues. (A) Family A GPCRs contain a disulphide bridge, which connects ECL1 and ECL2 causing the receptor to 'kink' and 'tilt'. The C-terminal domain contains a conserved palmitoylated cysteine residue. (B) Family B GPCRs are characterised by a long N-terminal tail consisting of many conserved disulphide bonds. (C) Family C GPCRs have very large N- and C-terminal domains with an agonist binding domain described as a 'venus fly trap' located at the N-terminus. Additionally, a conserved disulphide bridge connects ECL1 and ECL2 and a short and conserved ICL3 also define family C GPCRs. Redrawn from (George et al, 2002).

1.4.3. The N-terminal signal peptide (SP)

Approximately 15% of GPCRs show evidence of a signal peptide (SP) sequence, which is often critical for synthesis and processing of the receptor (Kochl et al, 2002). This SP sequence is usually located in the N-terminal domain of the protein and is highly structured. It is about 20 amino acids in length and contains a run of hydrophobic residues (Huang et al, 2010). The first stage of protein targeting is insertion into the ER by binding to the signal recognition particle (SRP). This is usually mediated by a SP sequence within the N-terminal domain of the protein (Hegde & Lingappa, 1997). Two types of SP sequences can be observed. One group contains a SP sequence, which is cleaved by a signal peptidase and is required for ER targeting and insertion. The second group possess a non-cleavable anchor sequence within the first transmembrane domain for ER targeting and insertion. Interestingly, the ER targeting and insertion of GPCRs can occur in either manner but the majority have a non-cleavable anchor sequence. Subsequently, the mature receptor is subjected to further post-translational modifications in the Golgi prior to translocation and insertion to the plasma membrane (Wallin & Vonheijne, 1995).

It is unclear why some GPCRs require a cleavable signal sequence and other do not. It has been suggested that the SP may be required for cell surface expression. Enhanced translocation was demonstrated with the addition of the influenza SP sequence to the β_2-AR, which ordinarily contains a non-cleavable anchor sequence (Guan et al, 1992). Additionally, the SP of the vasoactive intestinal peptide (VPAC) 1 receptor was found to play a critical role in receptor expression and functionality. It was suggested that the SP was cleaved during translocation to the plasma membrane, most likely in the ER (Couvineau et al, 2004). Statistical analysis suggests that the length of the N-terminal domain and the number of positively charged residues it contains denotes the presence of a cleavable SP sequence (Wallin & Vonheijne, 1995). Cleavage of the SP sequence is not essential for all GPCRs that contain them. Deleting the SP sequence of the thyrotropin receptor (TR) abolished functionality (Akamizu et al, 1990; Ban et al, 1992). However, the SP of the corticotropin-releasing factor (CRF) receptor 2a (also known as the corticotropin-releasing hormone receptor), although

present, was found to be incapable of mediating ER targeting (Rutz et al, 2006; Schulz et al, 2010). Further, the SP of the CRF_1 receptor was required for its expression but not its function (Alken et al, 2005).

The mechanisms for the initial steps of cleavable SP and ER targeting and insertion are based on secretory proteins, which must be translocated across the ER membrane. Proteins are usually integrated (membrane proteins) into or translocated (secretory proteins) across the ER by ribosomes. This process begins by synthesising the N-terminal domain of the protein in the cytosol. Translation continues until the cleavable SP sequence is synthesised after which the SRP binds and translation halts. The SRP-protein complex is targeted to the SRP receptor on the ER membrane. Translation continues when the SRP-protein complex is transferred to the translocase complex. Membrane proteins are integrated in the ER bilayer and secretory proteins are translocated across the ER membrane (Brodsky, 1998; Hegde & Lingappa, 1997). However, this mechanism contains differences between GPCRs, which contain a cleavable SP sequence or a non-cleavable anchor sequence. For receptors with a non-cleavable anchor sequence, translation halts once the anchor sequence appears (usually in TM1) and therefore the N-terminal domain is synthesised in the cytoplasm. As a result, the N-terminal domain is post-translationally translocated across the ER membrane through the translocase complex (Figure 1.7) (Brodsky, 1998; Kochl et al, 2002).

It is difficult to experimentally verify whether the SP sequence of some GPCRs is cleaved or not and as a result their presence is usually predicted. A total of 270 secreted proteins, which had previously been experimentally shown to have their SP sequence cleaved were predicted with less than 80% accuracy (Zhang & Henzel, 2004). This difficulty in predicting whether a SP is cleaved is shown by the CRF_1 and CRF_{2a} receptors. Both receptors were predicted to have a greater than 98% probability of a cleavable N-terminal SP. However, only the type 1 receptor indicated this experimentally (Alken et al, 2005). However, the CRF_{2a} receptor demonstrated a pseudo SP, which forms part of the mature protein. A mutation at position Asn^{13} resulted in a fully functioning SP, which is

cleaved (Rutz et al, 2006). Although this result was unexpected, it highlights the importance of experimental verification to assess the role of the SP for GPCR synthesis, trafficking and function.

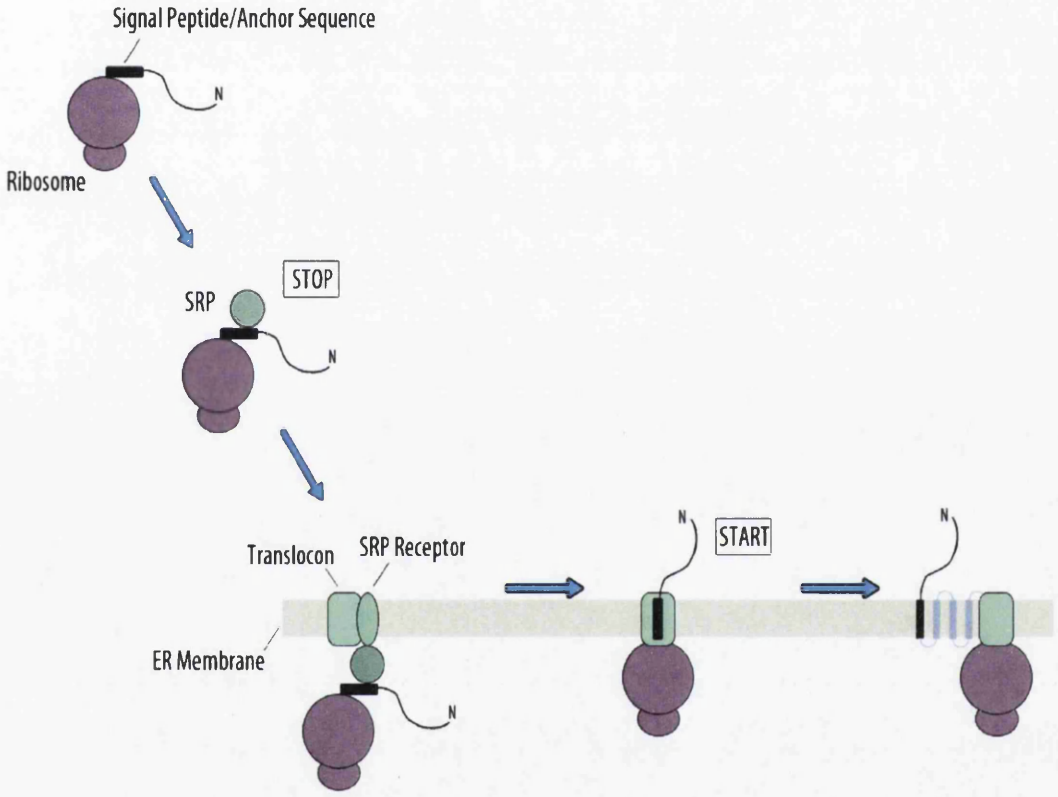

Figure 1.7. Targeting and insertion of GPCRs to the ER. The translation of the N-terminal tail is stopped once the signal anchor sequence appears and SRP binds. The SRP-protein complex is targeted to the SRP receptor on the ER membrane. The SRP-protein complex is transferred to the translocase complex and translation starts once more.

1.4.4. *N*-linked glycosylation of GPCRs

GPCRs are synthesised in the ER and require translocation to the Golgi. In this trafficking process, GPCRs undergo post- or co-translational modifications including glycosylation, methylation, phosphorylation, sulfation and lipid addition. It is likely that glycosylation plays an important role in cell surface trafficking and maturation of the receptor (Achour et al, 2008; Duvernay et al, 2005).

N-linked glycosylation usually occurs in the ER, which adds a glycan core unit (glucose$_3$-mannose$_9$-*N*-acetylglucosamine$_2$) to an asparagine residue within a sequence of asparagine-X-serine/threonine, where X can be any amino acid but proline (Balzarini, 2007; Elbein, 1987; Marshall, 1974). Terminal glucose residues are cleaved by glucosidases and oligomannoses are formed (Figure 1.8A) (Helenius & Aebi, 2001). During trafficking of glycoproteins from the ER to the Golgi, glycans can be extensively modified to form either complex or hybrid *N*-glycans (Figure 1.8B-C) (Balzarini, 2007; Varki et al, 2009). Hybrid *N*-glycans are formed in the medial Golgi and are due to the incomplete actions of α-mannosidase II. Hybrid *N*-glycans are unable to be processed to complex *N*-glycans (Varki et al, 2009). *O*-linked glycosylation that occurs within the Golgi is not very well understood. This process involves the addition of *N*-acetyl-galactosamine to serine or threonine residues and may occur at any residue with no sequence protein (An et al, 2009; Brooks, 2009). Glycans can be cleaved with the use of enzymes. PNGase F cleaves between asparagine and *N*-acetylglucosamine residues on oligomannoses and both hybrid and complex *N*-glycans. Endo H cleaves between *N*-acetylglucosamine residues on oligomannoses and some hybrid glycans (Figure 1.8) (Maley et al, 1989).

O-linked glycosylation has been shown to occur in the V2 vasopressin receptor (Sadeghi & Birnbaumer, 1999) and δ-opioid receptor (Petaja-Repo et al, 2000). However, most GPCRs undergo *N*-linked glycosylation but the role varies between receptors. *N*-linked glycosylation is important for cell surface expression of angiotensin II receptor subtype I (Deslauriers et al, 1999), follicle-stimulating hormone receptor (Davis et al, 1995), gastrin-releasing peptide

receptor (GRPR) (Benya et al, 2000), GLP-1R (Chen et al, 2010; Whitaker et al, 2012), melanocortin 2 receptor (Roy et al, 2010), relaxin receptor (Kern et al, 2007), VPAC1 (Couvineau et al, 1994) and μ-opioid receptor (Ge et al, 2009). However, *N*-linked glycosylation is not essential for cell surface expression in neuropeptide S receptor (Clark et al, 2010), histamine H_2 receptor (Fukushima et al, 1995) and the muscarinic M_2 acetylcholine receptor (van Koppen & Nathanson, 1990). Therefore, the role of *N*-linked glycosylation on mature GPCRs is varied and unpredictable.

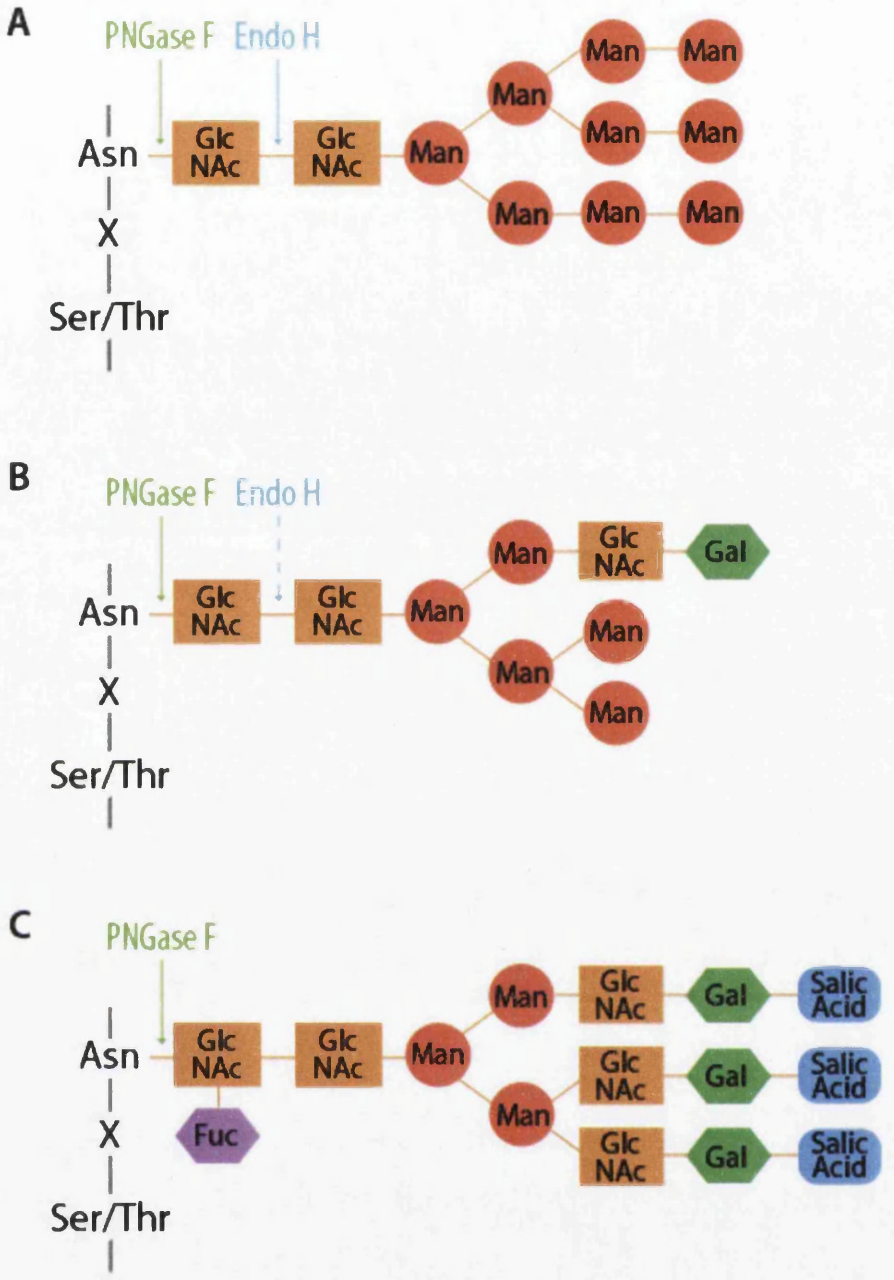

Figure 1.8. Structure of common *N*-glycans. *N*-linked glycosylation at the ER involves the addition of oligosaccharides to asparagine residues within a sequence of asparagine-X-serine/threonine. (A) Terminal glucose residues are cleaved by glucosidases and oligomannoses are generated. During trafficking of glycoproteins from the ER to the Golgi, glycans can be extensively modified to form either hybrid (B) or complex (C) *N*-glycans. The cleavage sites of glycosidase enzymes PNGase F and Endo H are indicated. Asn, asparagine; Fuc, fructose; Gal, galactose; GlcNAc, *N*-acetylglucosamine; Man, mannose; Ser, serine; Thr, threonine; X, any amino acid except proline.

1.4.5. The C-terminal domain

The C-terminal domain of GPCRs is known to interact with intracellular proteins involved in the internalisation desensitisation, down regulation and arrestin signalling of the receptor (McArdle et al, 2002). There are three regions involved, which include: a region just downstream of TM7; the very end of the C-terminus; and the region in between (Figure 1.9) (Kuramasu et al, 2006).

The region located just downstream of TM7 is called the helix-8. It is an α-helix, which terminates with palmitoylated cysteine residues and associates with a number of proteins (Figure 1.9) (Kuramasu et al, 2006). In the metabotropic glutamate receptor (mGluR) type 7a and 7b, the βγ subunit of the G-protein and calcium (Ca^{2+})/calmodulin bind to this domain and regulate P and Q type Ca^{2+} channels (O'Connor et al, 1999). Further, the dopamine receptor interacting protein 78 binds to a conserved sequence located in the helix-8 domain of the dopamine D1 receptor and is responsible for receptor trafficking to the plasma membrane (Bermak et al, 2001). At the very end of the C-terminal domain, many GPCRs possess a PDZ binding domain, which plays a role in targeting, internalisation, recycling and signalling of the receptor (Figure 1.9) (Bockaert et al, 2003). The PDZ binding domains are grouped into three classes based on their amino acid sequences (Table 1.3) (Harris & Lim, 2001; Hung & Sheng, 2002). GPCRs without a PDZ binding domain have been shown to interact with other proteins through the very end of the C-terminus. For example, Tctex-1 interacts with the C-terminal end of the rhodopsin receptor. A mutation at the C-terminal end of the receptor inhibited this interaction and prevented the transport of rhodopsin in vesicles to the rod (Tai et al, 1999). The C-terminus of the rhodopsin receptor was also reported to interact with ADP-ribosylation factor (ARF) 4 (Deretic et al, 2005). The region between helix-8 and the very end of the C-terminus is referred to as 'binding sites with GPCR interacting proteins' (Figure 1.9) (Kuramasu et al, 2006). The mGluR (types 1a, 5a and 5b) contains a PPXXFR motif, which is known as the homer ligand or enabled/VASP homology (EVH)-binding domain. This region interacts with EVH-like domain of homer proteins 1, 2 and 3. This interaction plays a role in targeting and regulating the mGluR to dendritic synapse sites (Ango et al, 2000; Ango et al,

2001; Ango et al, 2002). The β_3-AR is another example of protein interactions in this region. A PXXP motif interacts with the Src homology 3 domain of Src and results in the activation of extracellular signal-regulated kinase (ERK) (Cao et al, 2000). In addition, the extreme of TM7 close to the C-terminal domain is also known to interact with other proteins. A NPXXY motif within the serotonin 5-hydroxytryptamine receptor 2a (5-HT_{2A}) interacts with ARF1 and couples to phospholipase D (PLD) in a G-protein independent manner (Robertson et al, 2003).

GPCRs regulate intracellular effector proteins such as phospholipase C (PLC) and AC via heterotrimeric G-proteins (see section 1.4.6). Upon high levels or sustained levels of agonist stimulation, G-protein mediated responses typically desensitise (Ferguson, 2001). Desensitisation occurs by either an agonist specific response (homologous desensitisation) or activation of a different receptor (heterologous desensitisation) (see section 1.4.7). GPCR phosphorylation and arrestins mediate the receptor's desensitisation and cause uncoupling from G-proteins (Bohm et al, 1997a). Typically, GPCRs are phosphorylated at regions of the C-terminal domain in response to agonist binding (Tobin, 2008). For many GPCRs, phosphorylation facilitates interaction with arrestin. This sterically hinders G-protein association and prevents activation of the receptor (Ferguson, 2001; Zhang et al, 1997). Arrestin is also involved in targeting desensitised GPCRs for internalisation via activating protein (AP)-2, clathrin, Src and mitogen-activated protein kinase (MAPK) (Ferguson, 2001; Goodman et al, 1996). This is interesting because it now appears that GPCRs desensitised by G-protein activation may instead be due to arrestin mediated MAPK activation. It is the C-terminal domain of the receptor, which is phosphorylated to bind and activate arrestin (McArdle et al, 2002).

GPCRs are internalised via both clathrin-coated pits and caveolae mediated endocytosis (Vazquez et al, 2005a). Clathrin interacts with motifs present at the C-terminal domain of the receptor (Clague, 1998; Trowbridge et al, 1993). The C-terminal domain of GPCRs is also required for targeting to endosomes, Golgi and the plasma membrane. These motifs are four to six amino acids in length

and contain a critical tyrosine residue and follow a general consensus of YXXΦ, where Y is a tyrosine residue, X denotes any amino acid and Φ is a hydrophobic residue (Ohno et al, 1995; Sandoval & Bakke, 1994; Trowbridge et al, 1993). Previous studies have shown this tyrosine based motif associates with clathrin, however, a common binding motif has not yet been identified (Chang et al, 1993; Glickman et al, 1989; Pearse, 1988; Sorkin & Carpenter, 1993; Sorkin et al, 1995). For some GPCRs such as the β_2-AR, GRPR and the GLP-1R, serine and threonine rich amino acid sequences are required in TM3 or the cytoplasmic domain for internalisation of the receptor (Benya et al, 1993; Hausdorff et al, 1991; Widmann, 1997). Some other GPCRs require aromatic residues, for example the neurokinin 1 receptor or the angiotensin II receptor (Bohm et al, 1997b; Thomas et al, 1995). Dileucine sequences have also been shown to promote GPCR internalisation by binding to adapter proteins (Ferguson, 2001).

Table 1.3. Classification of PDZ domains

Class	Harris & Lim (2001)	Hung & Sheng (2002)
I	-S/T-X-Φ	-X-S/T-X-Φ
II	-Φ-X-Φ	-X-Φ-X-Φ
III	-X-X-C	-X-D/E-X-Φ

The PDZ domains are classified by their amino acid sequence into three classes by two research groups (Harris & Lim, 2001; Hung & Sheng, 2002). X denotes an unspecified amino acid and Φ denotes a hydrophobic amino acid.

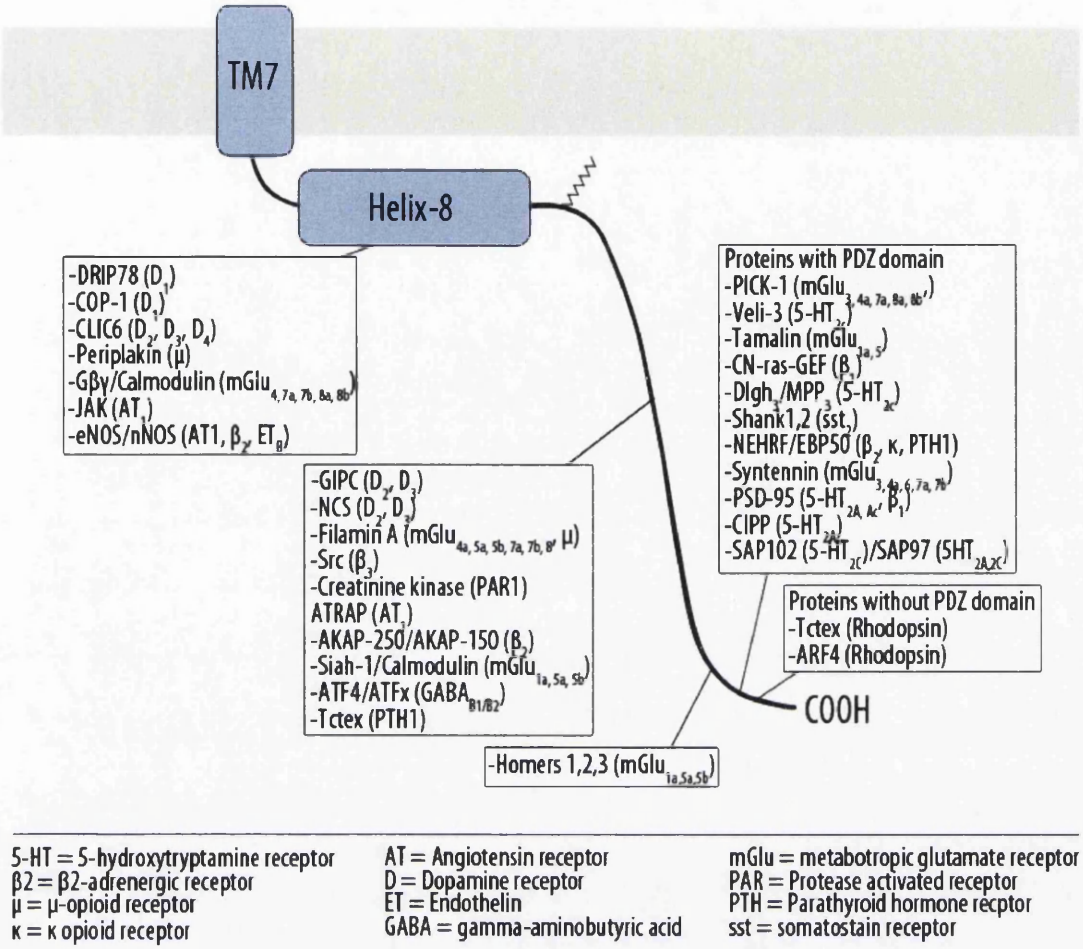

Figure 1.9. Interacting proteins of the C-terminus of GPCRs. Diagram representing the three regions of the C-terminal domain known to interact with intracellular proteins. The first region is called the helix-8, which is an α-helix that terminates with palmitoylated cysteine residues. The second includes the PDZ domain and is located at the very end of the C-terminal domain. The region in between is known as 'binding sites with GPCR interacting proteins'. Redrawn from (Kuramasu et al, 2006).

1.4.6. Heterotrimeric G-protein activation and regulation

Upon agonist binding, GPCRs undergo a conformational change and transmits extracellular signals through heterotrimeric G-proteins. The α and βγ subunits of the activated G-protein promote the actions of a series of membrane-bound

or cytosolic signalling molecules, triggering signalling cascades and producing specific cellular responses. However, more G-protein independent signalling pathways have been described. GPCRs may activate signalling pathways by adaptor molecules or direct signalling (Claing et al, 2002; Hall & Lefkowitz, 2002; Tuteja, 2009). The G-proteins are so called because they interact with guanosine diphosphate (GDP) and guanosine triphosphate (GTP). There are two main types of G-proteins, monomeric or heterotrimeric, both of which are involved in signal transduction pathways. Monomeric G-proteins include ARF, Rab, Ran, Ras and Rho families. Heterotrimeric G-proteins are of most interest due to their involvement in physical interactions with GPCRs (Cabrera-Vera et al, 2003).

Heterotrimeric G-proteins are made up of α, β and γ subunits. The α subunit (Gα) consists of an α-helical domain, which binds guanine nucleotides and a GTPase domain, which binds and hydrolyses GTP. The Gα subunit has been categorised into four families based on similarities within their primary sequence: $G\alpha_s$, $G\alpha_{i/o}$, $G\alpha_{q/11}$ and $G\alpha_{12/13}$. The β and γ subunits are bound in a complex (Gβγ) through an N-terminal coil on the Gγ subunit to the base of the Gβ subunit. The Gβγ subunit binds to the hydrophobic pocket in the Gα subunit in the inactive state (Cabrera-Vera et al, 2003). The Gα subunit is bound to the Gβγ subunit when GDP is bound, to form an inactive αβγ trimer (Figure 1.10A). Upon agonist binding, the receptor becomes active and undergoes a conformational change. This conformational change increases the receptor's affinity for the G-protein. The receptor functions as a guanine nucleotide exchange factor (GEF) once bound to Gα-GDP, exchanging GDP for GTP. The binding of GTP leads to a reduced affinity of the Gα subunit for the Gβγ complex and the dissociation of the heterotrimer. Gα-GTP is released from the heterotrimer, activating the G-protein and initiating signal transduction events (Figure 1.10B). After signal transduction, the Gα subunit is hydrolysed from GTP to GDP by Gα-GTPase and as a result the Gα subunit associates with the Gβγ complex and is inactivated (Figure 1.10C) (Cabrera-Vera et al, 2003; Tuteja, 2009).

The activated heterotrimeric G-protein can activate or inhibit a number of effectors. Members of the $G\alpha_s$ family activate AC, increasing cAMP levels and in turn activate both exchange protein activated by cAMP (EPAC) and protein kinase A (PKA) (Bos, 2003). Activating members of the $G\alpha_{i/o}$ family inhibit AC activity and regulate inward rectifier potassium channels (Vilardaga et al, 2009). $G\alpha_{q/11}$ family members activates PLC, which in turn hydrolyses phosphatidylinositol-4,5-bisphophate (PIP_2) to inositol-1,4,5-triphosphate ($Ins(1,4,5)P_3$; IP_3) and diacylglycerol (DAG). DAG activates protein kinase C (PKC) and IP_3 activates Ca^{2+} signalling (Werry et al, 2003). $G\alpha_{12/13}$ family members regulate intracellular actin through Rho GTPase activity (Heasman & Ridley, 2008). The $G\beta\gamma$ complex can also activate a number of intracellular signalling molecules and pathways including phospholipases, phosphatidylinositol 3-kinase, Ras, Raf, ERK and ion channels (Jacoby et al, 2006). The specific function of the $G\beta\gamma$ complex in various receptors is not fully known but these complexes often play a significant role in $G\alpha_{i/o}$ coupled GPCRs (Vilardaga et al, 2009).

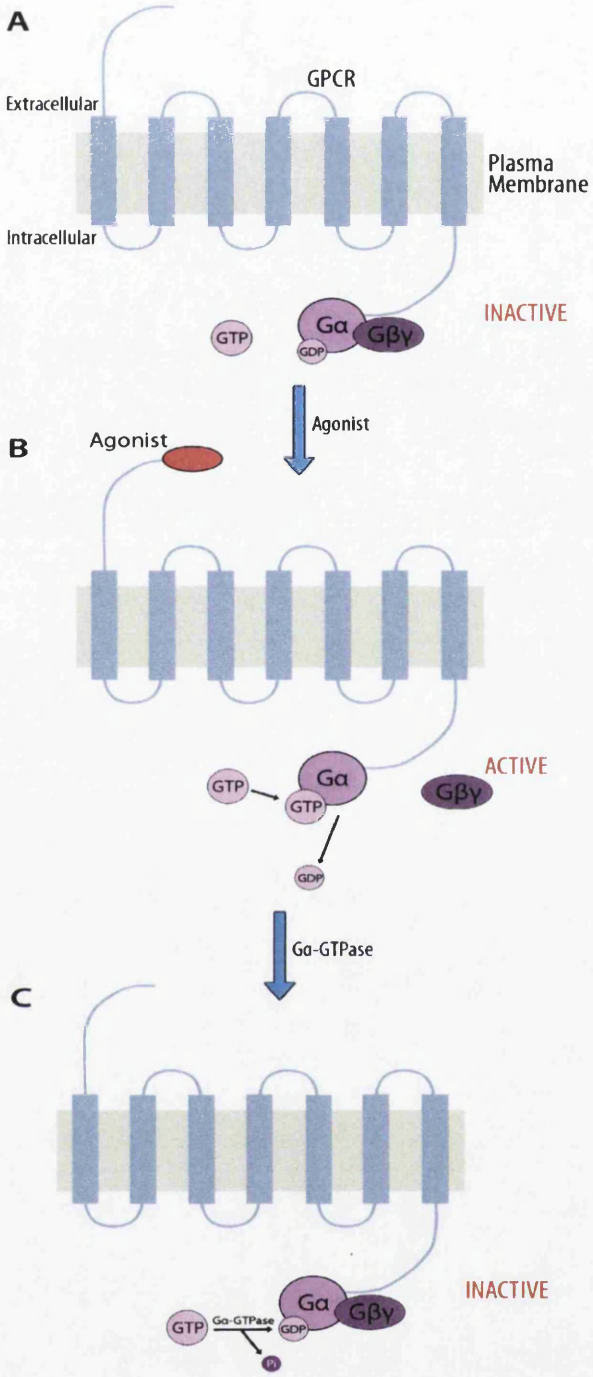

Figure 1.10. Activation and inactivation of heterotrimeric G-Proteins through GPCRs. (A) Prior to agonist binding, the Gαβγ complex are associated with each other. GDP is bound to the Gα subunit rendering it inactive. (B) Upon agonist binding, the Gα subunit dissociates from the Gβγ complex and GTP binds the Gα subunit, initiating signalling events. (C) After signal transduction, GTP is hydrolysed back to GDP by Gα-GTPase and the Gα subunit associates with the Gβγ complex.

1.4.7. GPCR internalisation and desensitisation

After stimulation with agonist, most GPCRs internalise from the cell surface to dampen the biological response, for resensitisation of the system or propagation of the signal through novel transduction pathways. Agonist induced GPCR internalisation typically occurs in a clathrin dependent fashion via GPCR kinases (GRKs), β-arrestins and ARF proteins (Figure 1.11) (Kanamarlapudi et al, 2012; Luttrell & Lefkowitz, 2002). Agonist stimulation causes the receptor to undergo a conformational change, promoting GRKs to translocate to the plasma membrane and to phosphorylate the receptor (Premont et al, 1995). GRKs interact with phosphoinositide-3 kinase (PI3K) and GPCR interacting (GIT) proteins (Claing, 2004). At the plasma membrane they interact with the βγ subunits of the activated G-protein (Daaka et al, 1997). When GRKs are in proximity to the receptor they phosphorylate specific residues on the C-terminal domain and ICL of the GPCR. Additionally, phosphorylation can occur by protein kinases, and the nature of phosphorylation (GRK or protein kinases) can characterise which endocytic pathway the GPCR uses (Claing, 2004; Rapacciuolo et al, 2003). Phosphorylation creates a binding site for arrestin proteins on the receptor. Arrestin interacts with ARF nucleotide-binding site opener (ARNO) promoting the activation of ARF6. The activation of ARF6 may promote actin organisation, clathrin and AP-2 recruitment. Inactivation of ARF6 by GIT proteins or ARF GTPase-activating proteins (GAPs) allows the assembly of clathrin-coated pits (Claing, 2004). Dynamin then polymerises around the neck of the vesicle, is phosphorylated and a conformational change causes the vesicle to 'pinch off' from the plasma membrane and traffic to intracellular compartments (Doherty & McMahon, 2009).

After targeting to endosomal compartments, adapter proteins and clathrin dissociate from the receptor. GPCRs are desensitised in a number of different ways including rapid phosphorylation, targeted to lysosomes for degradation or recycled back to the membrane (Gray & Roth, 2002). Agonist induced receptor phosphorylation is the most rapid and common type of desensitisation. Here, conformational changes lead to phosphorylation of serine or threonine residues

by GRKs (Tobin, 2008). Phosphorylation promotes arrestin binding and inactivation of heterotrimeric G-proteins (Jalink & Moolenaar, 2010; Marchese et al, 2008; Moore et al, 2007). Additionally, desensitisation can also occur in a GRK independent mechanism by phosphorylating different serine or threonine residues by protein kinases (Benovic et al, 1985; Ferguson, 2001). Therefore, GPCR internalisation controls the number of receptors at the cell surface, signal activation and termination, in addition to resensitisation (Wolfe & Trejo, 2007).

However, some receptors localise and internalise via clathrin independent endocytosis pathways, for example via caveolin-1 (Figure 1.12)(Pelkmans et al, 2001). GPCRs that internalise in a caveolae dependent manner include the endothelin A, somatostatin and angiotensin II type 1 receptors (Chini & Parenti, 2004). Several factors must control the pathway by which the receptor is internalised because the role and interaction of the receptor with caveolin varies. For example, the endothelin A receptor resides in lipid rafts and enters the cell via caveolae (Chun et al, 1994). Interestingly, cholesterol depletion of the endothelin A receptor can switch caveolae mediated endocytosis to clathrin mediated endocytosis (Okamoto et al, 2000). In contrast, the β_2-AR leave lipid rafts and internalise via clathrin-coated pits after agonist binding (Rybin et al, 2000; Schwencke et al, 1999).

A feature of GPCRs that are endocytosed via caveolae is their ability to bind caveolin-1, a protein weighing approximately 21-24 kDa. Caveolin-1 is the principle component of caveolae and can interact with a number of signalling molecules including receptor tyrosine kinases, G-proteins and GPCRs. This occurs via a common caveolin-binding motif, ΦXΦXXXXΦ and ΦXXXXΦXXΦ, where Φ is an aromatic residue and X is any amino acid (Couet et al, 1997; Okamoto et al, 1998). Caveolae are cholesterol rich, flasked shaped vesicles with a diameter of approximately 55-56 nm and contain a number of different signalling molecules (Nabi & Le, 2003; Parton & Richards, 2003). Endocytosis in this manner can lead to fission of caveolae enriched vesicles and then fusion with caveosomes, large intermediate intracellular organelles (Pelkmans et al, 2001).

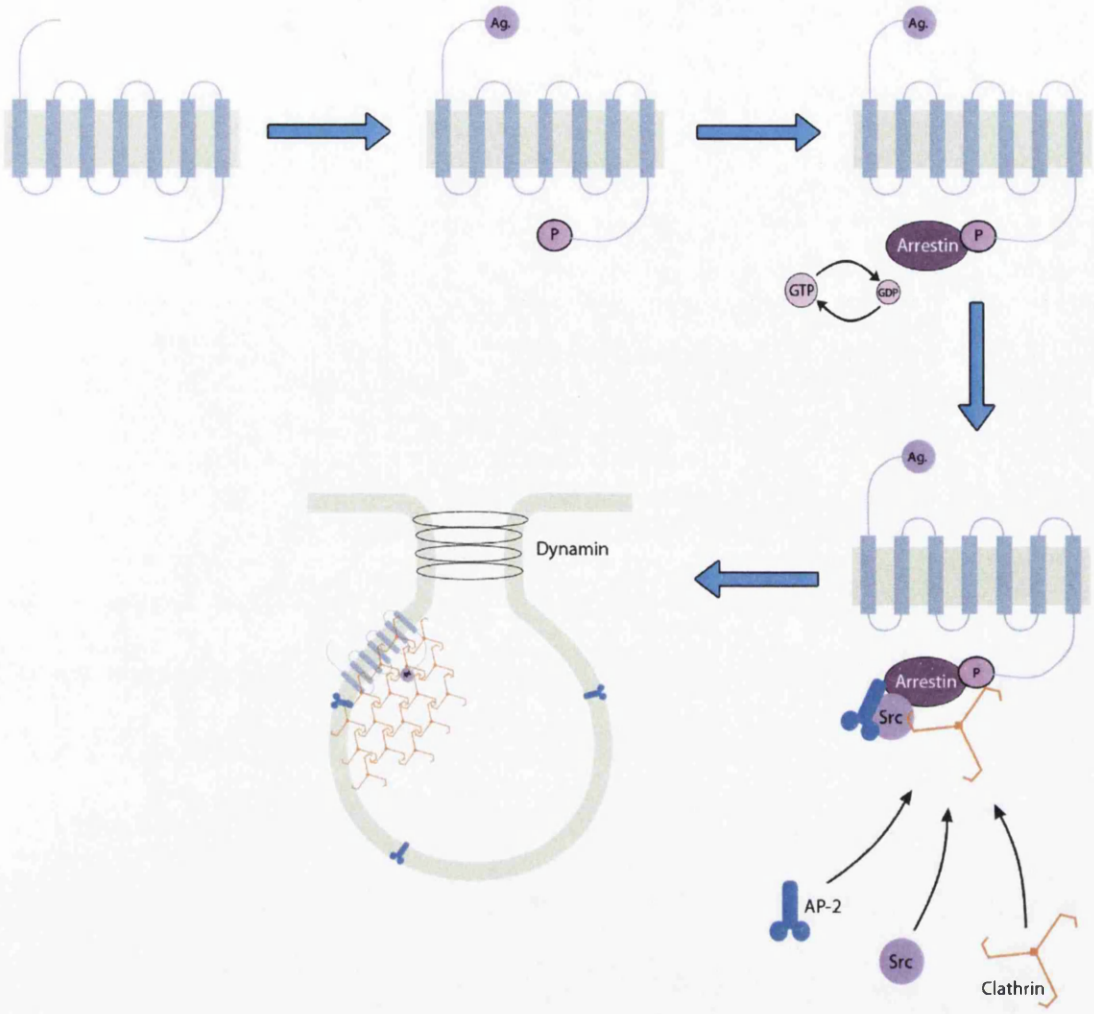

Figure 1.11. Clathrin dependent internalisation of GPCRs. The proposed model for GPCR internalisation is based on the β_2-AR. Upon agonist binding, GPCRs are phosphorylated by GRKs, this leads to the recruitment of arrestin and subsequent ARF6 activation. The activation of ARF6 results in the promotion of clathrin, AP-2 and Src to form clathrin-coated pits. Finally, dynamin causes the 'pinching off' of vesicles from the plasma membrane into the cytosol.

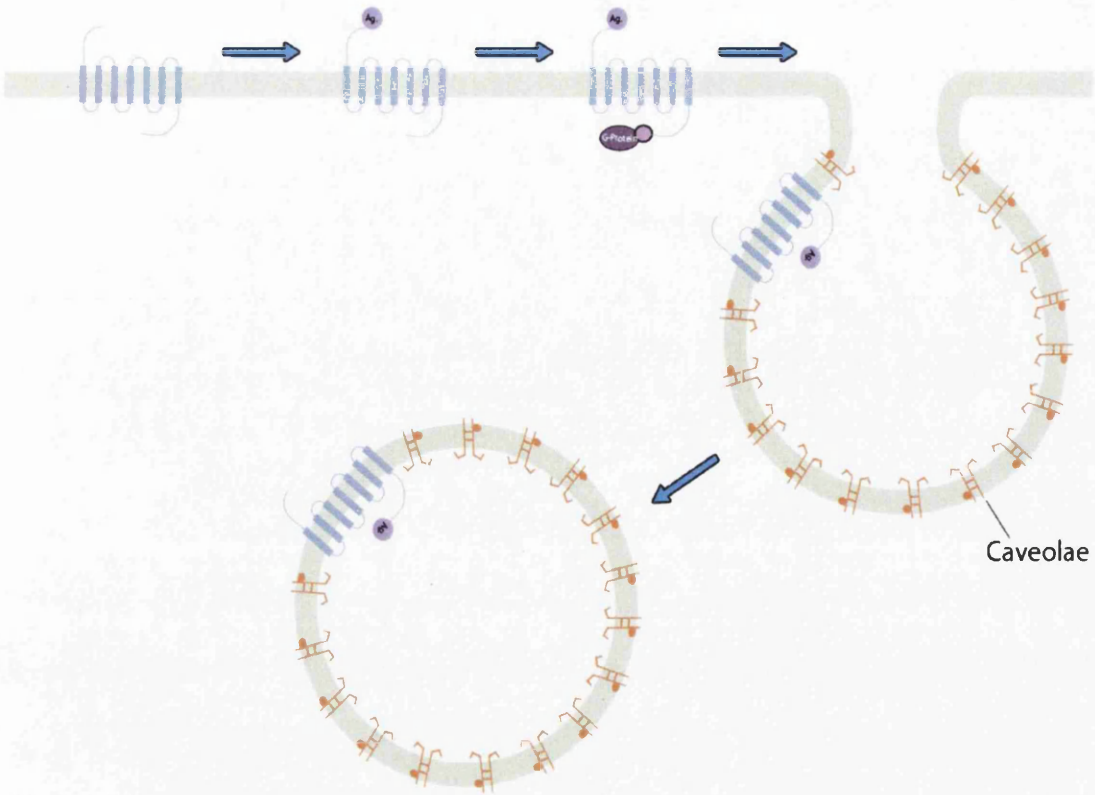

Figure 1.12. Caveolae dependent internalisation of GPCRs. The proposed model for caveolae mediated endocytosis. Upon agonist binding a number of signalling pathways are activated. This results in the recruitment of caveolin, forming a flask-shaped vesicle from the plasma membrane, which enters into the cytosol.

1.4.8. Allosteric modulation of GPCRs

Many GPCRs have been shown to have allosteric binding sites (Figure 1.13B), which are spatially and often functionally distinct to the primary agonist (orthosteric) binding site (Figure 1.13A) (Schwartz & Holst, 2007; Wang et al, 2009). Small molecule allosteric agonists can either increase or decrease the binding efficiency of an orthosteric agonist. Such agonists are generally termed positive allosteric modulators or negative allosteric modulators depending on what effects they have on the receptor (De Amici et al, 2010). Allosteric sites may provide novel therapeutic targets as well as a number of advantages

compared to classical orthosteric agonists. This is beneficial where selective orthosteric therapy has been difficult, for example, where the orthosteric site is highly conserved. Targeting the allosteric site allows for greater selectivity to be obtained (Kenakin, 2009; Urban et al, 2007). Additionally, allosteric agonists may provide a second advantage in that they can be selectively regulated by endogenous agonists (Kenakin, 2009). Finally, low molecular weight agonists that have the potential for oral administration can be used to target allosteric binding sites (Schwartz & Holst, 2007).

Some small molecule agonists, named ago-allosteric agonists, can bind to GPCRs and act as both agonists and allosteric modulators in the absence of orthosteric agonists. It is unknown how these agonists affect the binding or efficiency of compounds acting at the orthosteric site. Compounds with allosteric or ago-allosteric properties increase the potential for GPCR subtype selectivity. This allows for more improved, targeted and novel therapeutics (Bridges & Lindsley, 2008). GPCR internalisation and signalling mediated by ago-allosteric agonism may provide further information into the activation and regulation of the receptor.

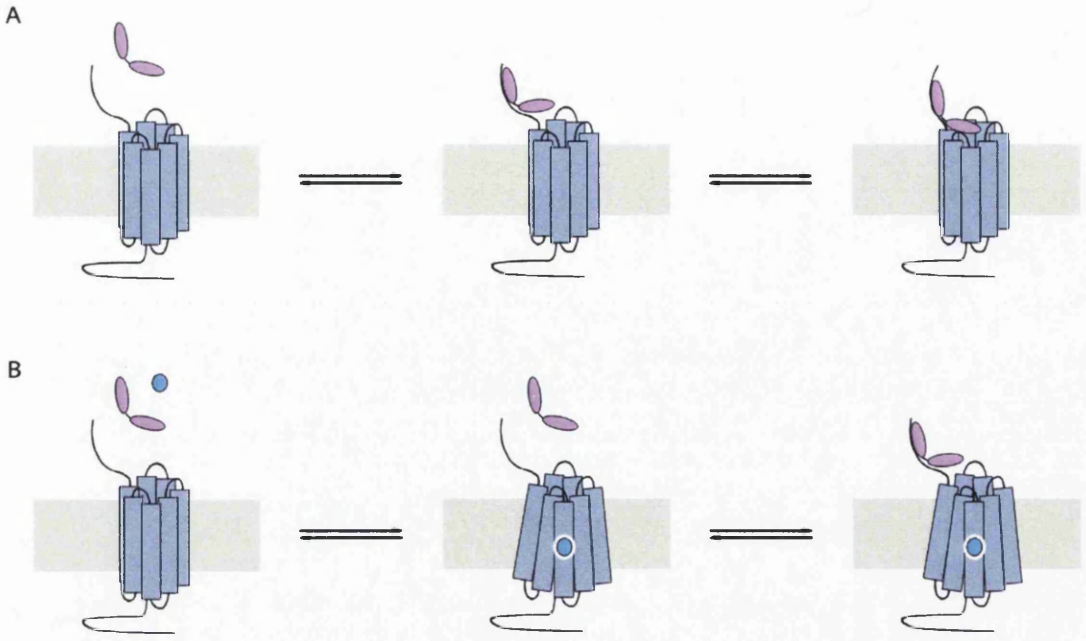

Figure 1.13. Binding models of orthosteric and allosteric agonists of family B GPCRs. (A) The general peptide (orthosteric) binding model for family B GPCRs is shown. The C-terminal region of the orthosteric peptide binds to the N-terminal region of the GPCR. This results in a weak interaction and consequently causes the formation of a bi-tethered confirmation. (B) Non-peptide (allosteric) binding and antagonist model for family B GPCRs. Non-peptide/antagonist (blue circle) binds the receptor and causes a conformational change, which prevents peptide binding. This non-peptide interaction can either block peptide stimulated receptor signalling or may not affect peptide binding to the N-terminal domain of the GPCR. Redrawn from (Hoare, 2005).

1.4.9. An alternative model for agonist induced activation

An alternative model for agonist induced activation of family B GPCRs has been proposed. It has been suggested that upon binding of an orthosteric agonist to the receptor, the N-terminal domain of the receptor undergoes a conformational change and interacts with another region of the receptor, which results in GPCR activation (agonism) (Beinborn, 2006). This hypothesis originally arose from

observations with the CRF_{2b} receptor, another family B GPCR. Nuclear magnetic resonance analysis of the CRF_{2b} receptor showed agonist induced conformational changes where the C-terminal region of the agonist binds the N-terminal domain of the receptor, which in turn causes the N-terminus to dock with the transmembrane bundle (Grace et al, 2004). Additionally, similar conformational changes were noticed with the secretin receptor where secretin peptides with minor modifications to the N-terminus were no longer able to interact with the receptor, but still resulted in full agonism (Dong et al, 2005). These findings could not be explained by current agonist binding models of family B GPCRs. Further, it was shown that the synthetic peptide corresponding to a conserved sequence in the N-terminal region of the secretin receptor, Trp^{48}-Asp^{49}-Asn^{50} (WDN), acts as a full agonist and docks where the top of TM6 continued onto ICL3 in the secretin receptor (Dong et al, 2006). This suggests that the N-terminal domain of the secretin receptor folded to allow a 'built in agonist' to interact with the transmembrane bundle (Gether, 2000). More recently, a synthetic peptide encoding an N-terminal sequence of the GLP-1R, Asn^{63}-Arg^{64}-Thr^{65}-Phe^{66}-Asp^{67} (NRTFD), was shown to have full agonist activity. Further, this peptide was also able to activate the secretin and VPAC1 receptors because it was able to form an intradomain salt bridge between side chains of arginine and aspartate in ECL3 above TM6 like the WDN peptide. Moreover, GLP-1 (9-37) antagonist failed to block the actions of the NRTFD peptide, confirming that the site of action of NRTFD peptide is different from that of endogenous GLP-1 agonist (Dong et al, 2008).

1.4.10. Dimerisation of GPCRs

Recently, there has been increasing interest in the stoichiometry of GPCRs and how this impacts the receptor's function (Casado et al, 2009; Milligan, 2009). For family B GPCRs, homodimerisation has been shown to occur with the calcitonin receptor (Harikumar et al, 2010), secretin receptor (Harikumar et al, 2007), GLP-1R (Harikumar et al, 2012) and parathyroid receptor (Pioszak et al, 2010). There has also been interest in the development of allosteric agonists and whether they interact with a single receptor (*in cis*) or across dimers (*in*

trans). Currently, most drug development is dependent on an *in cis* conformation and mechanism of action (Harikumar et al, 2012; Hoare, 2007). Heterodimerisation of GPCRs, such as GLP-1R dimerisation with GLP-1, also has physiological significance (see section 1.5.3) (Harikumar et al, 2012).

1.5. The GLP-1R

1.5.1. Characterisation of the GLP-1R

The gene encoding the GLP-1R is located on the short arm of chromosome 6 (6p21) and encodes a 463 amino acid long protein (Figure 1.14) (Brubaker & Drucker, 2002; Stoffel et al, 1993; van Eyll et al, 1994). The GLP-1R contains a large hydrophilic N-terminal domain (122 amino acids in length) with a putative SP, seven hydrophobic transmembrane domains (TM1-TM7) joined by three hydrophilic ICL (ICL1, ICL2, ICL3) and three ECL (ECL1, ECL2, ECL3), ending in an intracellular C-terminal domain (Table 1.4) (Palczewski, 2000). The GLP-1R is a family B GPCR, characterised by a large N-terminal extracellular domain, which contains between 100 and 150 amino acids (Doyle & Egan, 2007).

The GLP-1R has been shown to contain a cleavable N-terminal SP, which is essential for processing and trafficking of the receptor to the cell surface (Figure 1.14). A mutation to the SP cleavage site ($Ala^{21}Arg$) still allowed GLP-1R synthesis but prevented cleavage and resulted in retention of the receptor within the ER (Huang et al, 2010). The rat GLP-1R has previously been demonstrated to undergo *N*-linked glycosylation (Goke et al, 1994; Widmann et al, 1995). Further, the N-terminal domain of the hGLP-1R contains three *N*-linked glycosylation sites at positions Asn^{63}, Asn^{82} and Asn^{115}. Tunicamycin, an inhibitor of *N*-linked glycosylation interfered with GLP-1R biosynthesis and trafficking, abolishing agonist binding. Individual mutations to Asn^{63}, Asn^{82} and Asn^{115} with leucine did not affect cell surface expression of the receptor and

agonist binding. However, combination mutations of two or three residues resulted in complete loss of GLP-1 binding. Immunofluorescence staining of cells transfected with the mutant receptors demonstrated that these mutant receptors were still synthesised but were localised to the ER or Golgi (Chen et al, 2010; Whitaker et al, 2012).

The ICLs of GPCRs are known to interact with G-proteins and play a role in the activation of the receptor (Strader et al, 1995). For the GLP-1R, ICL3 has been shown to mediate signalling via G-proteins. However, ICL1 and ICL2 have demonstrated an importance in discriminating between different types of G-proteins. ICL1 and ICL3 specifically mediates $G\alpha_s$, whereas ICL2 activates $G\alpha_s$, $G\alpha_{i/o}$ and $G\alpha_{q/11}$ (Bavec, 2003). Additionally, different domains of ICL3 have been shown to be responsible for the $G\alpha_s$ and $G\alpha_{i/o}$ activation in the GLP-1R. The entire ICL3 (amino acids 329-351) has been shown to prefer $G\alpha_s$ over $G\alpha_{i/o}$. However, the C-terminal end of ICL3 (amino acids 329-341) stimulated both $G\alpha_s$ and $G\alpha_{i/o}$ subtypes. Further, the N-terminal end of ICL3 (amino acids 341-351) stimulated both subtypes with higher EC_{50} but also favours $G\alpha_s$ over $G\alpha_{i/o}$ (Hallbrink et al, 2001).

The ECLs of GPCRs have shown importance in agonist binding and trafficking of the receptor. A disulphide bridge between ECL1 and ECL2 is conserved across all GPCRs, which has been suggested to be involved in stabilising the receptor during agonist binding (Knudsen et al, 2007). Residues within TM2 and ECL1 appear to be more important in GLP-1 binding than exendin-4 binding (López de Maturana & Donnelly, 2002; Lopez de Maturana et al, 2004). Mutations within ECL1 of the receptor have been shown to decrease agonist binding (see section 1.5.3) (López de Maturana & Donnelly, 2002; Lopez de Maturana et al, 2004; Xiao et al, 2000). ECL2 of the GLP-1R has been shown to play a critical role in agonist binding and activation of the receptor. Alanine substitutions within ECL2 have been shown to affect GLP-1 binding and efficacy but had varying effects on the receptor's function depending on the signalling pathway, agonist and mutations position. This indicates that ECL2 plays an important role in GLP-1R activation as some mutations resulted in a distinct signal bias of

pathway responses (see section 1.5.4) (Koole et al, 2012a). Further, ECL2 was also found to be critical for GLP-1 peptide mediated signalling but not allosteric agonist signalling. For example, an alanine substitution at positions Asp^{293}, Arg^{299}, Try^{305} and Leu^{307} abolished exendin-4 mediated Ca^{2+} response, whereas GLP-1 signalling was reduced but still measurable, highlighting the subtle differences these peptides have on activation of the receptor. However, stimulation with small molecule agonist, compound 2, showed very little effect on GLP-1R signalling, providing further evidence that this agonist signals through a distinct mechanism (see section 1.5.3) (Koole et al, 2012b). ECL3 of the GLP-1R was originally hypothesised to act as an endogenous agonist (Dong et al, 2006). However, this was disproven when it was recognised that ECL3 could not establish the necessary spatial approximation with the agonist binding region of the GLP-1R (Dong et al, 2010). The GLP-1R has recently been shown to bind an agonist peptide (NRTFD), corresponding to the sequence of the GLP-1R, Asn^{63}-Asp^{67}, at the N-terminal region of ECL3 (see section 1.4.9) (Dong et al, 2012; Dong et al, 2008). Furthermore, ECL3 has been shown to be important for endogenous agonist action of several members of family B GPCRs, suggesting that this region is likely to be important for drug binding (Bisello et al, 1998; Dong et al, 2004a; Dong et al, 2004b).

The C-terminal domain of GPCRs is known to interact with intracellular proteins involved in the internalisation desensitisation, down regulation and arrestin signalling of the receptor (McArdle et al, 2002). GPCRs, including the GLP-1R, regulate intracellular effector proteins such as PLC and AC via heterotrimeric G-proteins, at the C-terminus.

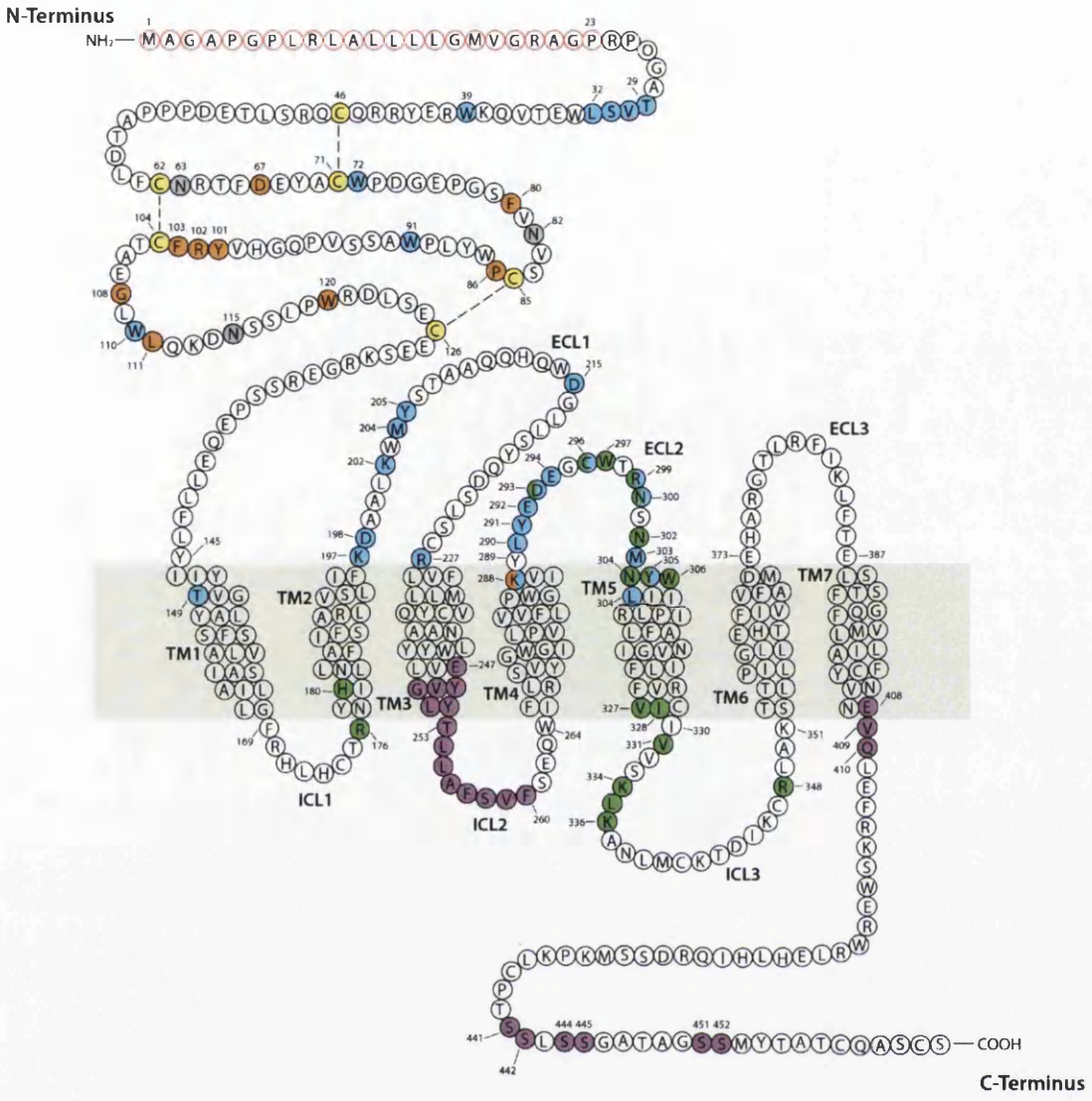

Figure 1.14. Amino acid sequence of the hGLP-1R. The SP is highlighted in red circles (1-23). Residues in yellow highlight conserved cysteine residues, which form disulphide bonds. Residues in blue show amino acids important in agonist binding. Amino acids that have a structural role are highlighted in orange. Glycosylation sites are shown in grey. Residues important in receptor internalisation are shown in purple and for activation and function are in green. Adapted from (Doyle & Egan, 2007).

Table 1.4. The amino acid sequence of the GLP-1R domains

Amino Acids Length (from-to)	Description	Amino Acids Length (from-to)	Description
23 (1-23)	Putative SP	122 (24-145)	NT
23 (146-168)	TM1	8 (169-176)	ICL1
20 (177-196)	TM2	31 (197-227)	ECL1
25 (228-252)	TM3	12 (253-264)	ICL2
24 (265-288)	TM4	15 (289-303)	ECL2
26 (304-329)	TM5	22 (330-351)	ICL3
21 (352-372)	TM6	15 (373-387)	ECL3
21 (388-408)	TM7	55 (409-463)	CT

SP, signal peptide; TM, transmembrane domain; NT, N-terminal domain; CT, C-terminal domain; ICL, intracellular loop; ECL, extracellular loop (Uniprot).

1.5.2. Allosteric modulation of the GLP-1R

A small molecule GLP-1R agonist, compound 1 (2-(2'methyl) thiadiazolylsulfanyl-3-trifluoromethyl-6,7-dichloroquinoxaline) (Figure 1.15A), has demonstrated low affinity, low potency allosteric agonism to the GLP-1R. In an effort to produce a more potent agonist, compound 2 (6,7-dichloro-2-methylsulfonyl-3-*N-tert*-butylaminoquinoxaline) was developed (Figure 1.15B). Compound 2 is an ago-allosteric agonist, which not only increased the affinity of GLP-1 for its receptor, but also acted as an agonist. Additionally, exendin (9-39) antagonist did not inhibit compound 2 binding, showing a second binding site on the GLP-1R distinct from the orthosteric binding site (Knudsen et al, 2007). The effectiveness of compound 2 to stimulate insulin secretion has also been assessed *in vivo*. Although, compound 2 was able to stimulate insulin secretion it was unable to do so as effectively as GLP-1, Liraglutide or Exenatide. Further, combining compound 2 with either GLP-1, Liraglutide or Exenatide did not

show a substantial improvement in insulin secretion response in mice (Irwin et al, 2010).

Two additional small molecule agonists of the GLP-1R, compound A (4-(3,4-dichlorophenyl)-2-(ethanesulfonyl)-6-(trifluoromethyl)pyrimidine) and compound B (4-(3-(benzyloxy)phenyl)-2-(ethylsulfinyl)-6-(trifluoromethyl)), have also demonstrated ago-allosteric properties (Figure 1.15C-D). Like compound 2, these compounds induced cAMP signalling and increased insulin secretion in rodent islets and animal studies. Further studies showed treatment with compound B to near-normalise insulin secretion in human islets isolated from a donor with type 2 diabetes (Sloop et al, 2010). These small molecule agonists indicate a useful starting point for the identification and design of orally active allosteric GLP-1R compounds.

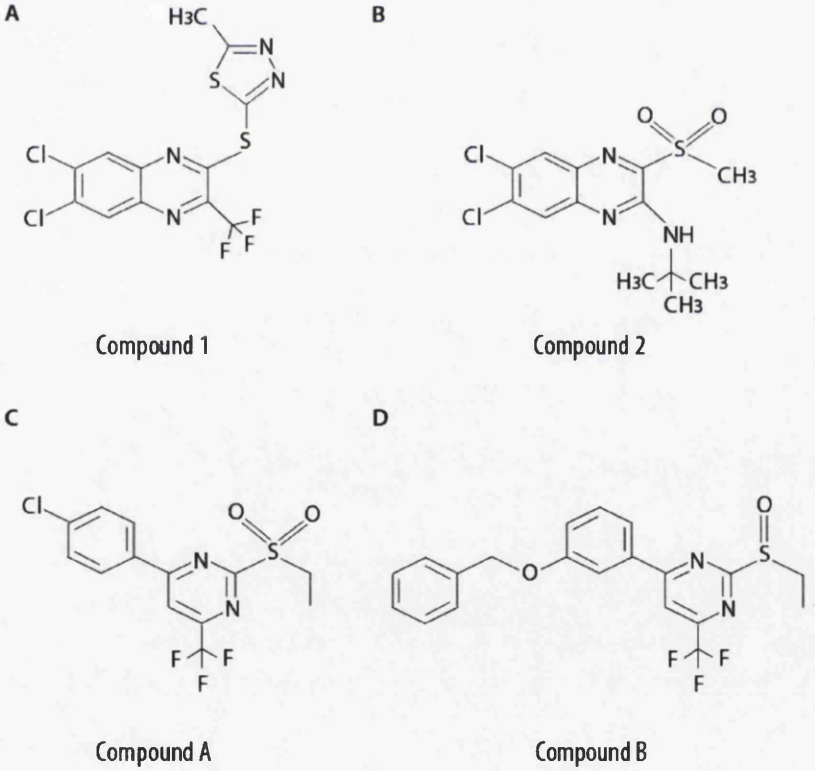

Figure 1.15. Small molecule allosteric agonists of the GLP-1R. The chemical structures of compound 1 (A), compound 2 (B), compound A (C) and compound B (D) are depicted.

1.5.3. Residues important for GLP-1R structure and agonist binding

The GLP-1R has six highly conserved cysteine residues at the N-terminal region, highlighting their structural importance. These cysteine residues form disulphide bonds between Cys^{46} and Cys^{71}, Cys^{62} and Cys^{104}, and between Cys^{85} and Cys^{126} (Bazarsuren et al, 2002) (Figure 1.14). Additionally, Asp^{67}, Trp^{72}, Pro^{86}, Arg^{102}, Gly^{108} and Trp^{110} are six other residues, which are highly conserved across family B GPCRs, of which Trp^{72} and Trp^{110} have been shown to be important in agonist binding (Doyle & Egan, 2007; Wilmen et al, 1997; Xiao et al, 2000). The crystal structure of the GLP-1R extracellular domain has shown these conserved residues to be positioned centrally. For example, Asp^{67} is centrally located and forms intermolecular interactions directly with Trp^{72} and Arg^{121} and indirectly interacts with Arg^{102} via a water molecule. Asp^{67} interacts with Tyr^{69} and Ala^{70}. Arg^{102} is sandwiched between the side chains of Trp^{72} and Trp^{110}. These interactions and Gly^{108}, stabilise the receptor's N-terminal domain. Pro^{86} plays a critical role in forming the agonist binding site (Figure 1.14) (Runge et al, 2008). Additionally, an alanine mutation to Val^{36} significantly reduced GLP-1 binding, demonstrating a vital role within the GLP-1R agonist binding site (Underwood et al, 2010).

In addition to the highly conserved tryptophan residues, Trp^{72} and Trp^{110}, already mentioned. Substitution of Trp^{39}, Trp^{72}, Trp^{91}, Trp^{110}, or Trp^{120} by alanine in the full-length rat GLP-1R abolished GLP-1 binding. Whereas, substitution of Trp^{87} had no effect on agonist binding (Wilmen et al, 1997). The role of Trp^{33} still remains unclear. Trp^{120} has no role in agonist binding but instead plays a structural role by forming a hydrophobic cluster with Phe^{80}, Tyr^{101}, Phe^{103} and Leu^{111} (Figure 1.14) (Runge et al, 2008).

Residues Thr^{29}-Val^{30}-Ser^{31}-Lys^{32} have been shown to confer peptide specificity. A mutation to this region of the GLP-1R resulted in a 7-fold decrease in GLP-1 affinity showing its importance in agonist binding (Figure 1.14) (Graziano et al, 1993). The NRTFD, corresponding to the sequence of GLP-1R (Asn^{63}-Asp^{67}), was shown to have full agonist activity when compared to GLP-1. Moreover, GLP-1 (9-37) antagonist failed to block the NRTFD action, confirming that the site of

action of the NRTFD peptide is different from that of the endogenous GLP-1 agonist. As a result this sequence may also be involved in agonist binding (Dong et al, 2008).

In addition to the N-terminal domain, residues of TM1 through to TM3 are also important for agonist binding. For example, a missense mutation of Thr^{149} in TM1 of the GLP-1R reduced agonist binding (Beinborn et al, 2005). Additionally, Lys^{197}, Asp^{198}, Lys^{202}, Met^{204}, Tyr^{205}, Asp^{215} or Arg^{227} mutations within ECL1 of the receptor also decreased agonist binding affinity (López de Maturana & Donnelly, 2002; Lopez de Maturana et al, 2004; Xiao et al, 2000).

The GLP-1R has been shown to form a homodimer through an interface along TM4 and is required for signalling of the receptor. Alanine substitutions to Leu^{256}, Val^{259} or Gly^{252}, Leu^{256}, Val^{259} abolished GLP-1 binding, reduced cAMP and ERK signalling and abolished Ca^{2+} signalling. Dimerisation of the GLP-1R was important for signal bias and discriminated between peptide and non-peptide activation. Additionally, dimerisation was not required for allosteric modulation by compound 2 (see section 1.5.2) demonstrating that this small molecule agonist acted in *cis* (Harikumar et al, 2012).

A positively charged Lys^{288} in TM4 is highly conserved in all family B GPCRs and has been demonstrated to be important for the interaction of GLP-1 to its receptor (Figure 1.14). Substitution of Lys^{288} by neutral leucine or alanine reduced the affinity of GLP-1 for its receptor. However, substitution with a positively charged arginine had very little effect, demonstrating a positive charge was essential at this particular location (Al-Sabah, 2003). Additionally, mutating at Lys^{288} resulted in a reduced binding affinity of GLP-1 compared to exendin-4 (Al-Sabah, 2003; Koole et al, 2012b).

Scanning alanine substitutions were made on ECL2 of the GLP-1R and the effect of GLP-1, exendin-4 and oxyntomodulin was assessed (Figure 1.14). Mutations at positions Glu^{292}, Cys^{296} and Asn^{300} resulted in a greater potency of exendin-4 but reduced oxyntomodulin efficacy, possibly because the receptor was unable

to form an active ternary complex. Met^{303} appeared to play a role in cAMP signalling and was more important for exendin-4 and oxyntomodulin than GLP-1. When positions Lys^{290}, Tyr^{291} and Glu^{294} were mutated, a significant loss in GLP-1 Ca^{2+} signalling was witnessed but no effect was seen when stimulated with oxyntomodulin. In cAMP stimulation, Arg^{299} and Lys^{307} mutations had a reduced potency for GLP-1 compared to exendin-4 suggesting exendin-4 cAMP signalling required the distal portion of ECL2. Exendin-4 mediated Ca^{2+} responses were abolished in mutations at Asp^{293}, Arg^{299}, Tyr^{305} and Lys^{307} yet reduced but measurable responses were observed with GLP-1 suggesting subtle differences in Ca^{2+} signalling mechanisms. Cys^{296}, Arg^{299} and Tyr^{305} mutants demonstrated no detectable Ca^{2+} signalling and increased ERK signalling. Collectively, these mutations have suggested that GLP-1, exendin-4 and oxyntomodulin activate the GLP-1R using different mechanisms (Koole et al, 2012b).

1.5.4. Residues important in GLP-1R activation and internalisation

Residues important in coupling to heterotrimeric G-proteins are mainly located in ICL3 and where TM5 meets ICL3 (Takhar et al, 1996). Alanine substitutions to Val^{327}, Ile^{328} or Val^{331}, where TM5 meets ICL3, caused significantly lowered cAMP production but had no effect on cell surface expression of the GLP-1R (Figure 1.14). These residues and Lys^{334} (Figure 1.14) form a hydrophobic face, which interacts directly with the G-protein (Mathi, 1997). Additionally, different regions of ICL3 are responsible for specific G-protein interactions. For example, half of ICL3 closest to the N-terminal end of the receptor couples and stimulates $G\alpha_s$ G-proteins, to generate cAMP (Hallbrink et al, 2001). A single block deletion of Lys^{334}-Leu^{335}-Lys^{336} within the N-terminal half of ICL3 caused a significant decrease in cAMP production in response to GLP-1, of which Lys^{334} showed most significance with no effect on the expression of the receptor (Figure 1.14). This indicated that this region was required to couple $G\alpha_s$ and stimulate AC (Takhar et al, 1996). The second half of ICL3 closest to the C-terminal end of the receptor couples and stimulates $G\alpha_i/G\alpha_o$ G-proteins (Hallbrink et al, 2001). A glycine substitution to Arg^{348}, near the C-terminal end of ICL3, nearly abolished

cAMP production and decreased the affinity of the receptor in response to GLP-1 (Figure 1.14) (Heller et al, 1996).

The GLP-1R has a number of conserved amino acids within ECL2 including Lys^{288}, Asp^{293}, Cys^{296}, Trp^{297} and Trp^{306}. These residues have been demonstrated to be essential for the receptor's function because alanine mutations resulted in a significant loss of GLP-1 binding and attenuation of the receptor's signalling (Koole et al, 2012a; Koole et al, 2012b). Mutations within ECL2 have been shown to affect GLP-1 binding and efficiency, indicating an important role in GLP-1R activation. Interestingly, some mutations resulted in distinct changes in pathway responses. For example alanine substitutions to Cys^{296}, Trp^{297}, Arg^{299}, Asn^{300}, Asn^{302}, Tyr^{305} and Leu^{307} resulted in increased signal bias towards ERK activation. However, an alanine mutation at Trp^{306} abolished all biological activity. Further, a mutation to Lys^{288} has been hypothesised to be important in stabilising the top of TM4 (Figure 1.14) (Koole et al, 2012a).

An alanine substitution at Arg^{176} within ICL1, caused a reduction in GLP-1 mediated stimulation of cAMP but had no effect on the internalisation of the receptor (Figure 1.14) (Mathi, 1997). Additionally, substitution of His^{180} by arginine within TM2 of the GLP-1R resulted in a reduction in both the potency of cAMP production and affinity of the receptor for GLP-1 (Figure 1.14) (Heller et al, 1996).

Currently, there is some confusion over which pathway is used for GLP-1R internalisation. It has been reported that clathrin-coated vesicles mediate GLP-1R internalisation and three PKC phosphorylation sites play an important role for this to occur. Removal of these phosphorylation sites ($Ser^{441,442}$, $Ser^{444,445}$ and $Ser^{451,452}$) prevented phosphorylation and inhibited internalisation of the receptor (Figure 1.14) (Widmann, 1997). In addition, deletion of the last 33 amino acids from the C-terminal domain containing these phosphorylation sites, were required for efficient GLP-1R activation and therefore internalisation (Widmann et al, 1996a). Interestingly, internalisation of the receptor was more rapid when amino acids $^{408}EVQ^{410}$ were substituted with alanine at the C-

terminal domain of the GLP-1R (Vazquez et al, 2005a). However, more recently it has been shown that the GLP-1R is internalised by caveolae mediated endocytosis upon agonist stimulation. The GLP-1R was reported to contain a classical caveolin-1 binding motif, ^{247}EGVYLYTLLAFSVF^{260}, within ICL2 (Figure 1.14) (Syme et al, 2006).

Three *N*-linked glycosylation sites, Asn^{63}, Asn^{82} and Asn^{115}, are present within the N-terminal domain of the GLP-1R (Figure 1.14). Inhibition of these glycosylation sites in RINm5F cells resulted in a concentration dependent reduction in the association of the cells with GLP-1 due to a decrease in GLP-1 binding sites at the membrane (Goke et al, 1994). Substitution of the putative *N*-glycosylation sites with glutamine reduced cell surface expression of the receptor (Whitaker et al, 2012).

1.5.5. GLP-1R signal transduction in pancreatic β-cells

In β-cells, the main action of GLP-1 through the GLP-1R is the formation of cAMP and its insulinotropic activity (Holst, 2007). Upon agonist binding, the $G\alpha_s$ subunit dissociates from the receptor, couples to AC and generates cAMP (Coopman et al, 2010; Thorens, 1992). When blood glucose levels rise, glucose enters the β-cell through GLUT1 and GLUT2 transporters (Figure 1.16). Glucose is phosphorylated by glucokinase to glucose-6-phosphate, which results in the ATP/ADP ratio in the cytosol increasing and the plasma membrane depolarising by closing K_{ATP} channels. The closure of K_{ATP} channels, in turn opens Ca^{2+} channels, releasing intracellular stores of Ca^{2+}. The increase of cytosolic Ca^{2+} causes secretory vesicles containing insulin to fuse to the plasma membrane and insulin is exocytosed (De Vos et al, 1995; Holz, 2004). There is a strong likelihood that human glucokinase activity is more important in glucose-induce insulin secretion than the rate at which glucose enters the β-cell (Matschinsky, 2002).

GLP-1 has been shown to increase the quantity of insulin secreted per cell and cause β-cells to become more sensitive to increased glucose levels by GLP-1

modulated K_{ATP} channels (Holz et al, 1993; Montrose-Rafizadeh et al, 1994). Activation of GLP-1 can also increase Ca^{2+} concentration by partial activation of L-type voltage dependent Ca^{2+} channel and/or increase Ca^{2+}-induced Ca^{2+} release from intracellular stores and is mediated by PKA phosphorylation in an ADP-dependent manner (Holst, 2007). The release of intracellular stores of Ca^{2+} is achieved by either PKA activation or EPAC activation (Kashima et al, 2001; Ozaki et al, 2000). It has been suggested that GLP-1 induced PKA activation results in Ca^{2+} release through the IP_3 receptor (IP_3R, PKA dependent) and EPAC activation results in Ca^{2+} release through ryanodine receptors (PKA independent) (Kang et al, 2003; Tsuboi et al, 2003).

The increase in Ca^{2+} levels cause an exocytotic response and is potentiated by elevated cAMP levels due to an increase in the amount of vesicles available for release (Holst & Gromada, 2004). In pancreatic β-cells, there are three different pools of insulin secretory vesicles (Figure 1.16). A reserve pool is situated in the cytoplasm; a readily release pool and an immediate release pool are situated close to the membrane. GLP-1 increases the amount of insulin secretory vesicles in the readily release pool. GLP-1 depolarises the cell membrane closing K_{ATP} channels and therefore the current is inactivated before the cell can begin repolarising. Consequently, the cell does not reach its resting membrane potential and starts to depolarise before it has recovered from inactivation (Bratanova-Tochkova et al, 2002; Kasai, 2005).

Additionally, a sustained increase in cAMP induced nuclear translocation leads to the activation of cAMP response element binding-protein (CREB) and cell proliferation. The phosphorylation of PKA is said to activate CREB, interact with transducer of regulated CREB activity (TORC2), increase insulin receptor substrate-1 expression and cause activation of a serine-threonine protein kinase, Akt (Jhala et al, 2003). Akt has been described to link GLP-1 signalling to β-cell growth and survival (Wang et al, 2004). Furthermore, the activation of ribosomal protein S6 (rbS6) in animal models has been reported as a key regulator of glucose homeostasis and β-cell mass (Ruvinsky et al, 2005).

Two mutations within the GLP-1R have been shown to alter insulin secretion. In a Japanese study, one patient diagnosed with type 2 diabetes had a missense mutation, which resulted in the substitution of Thr^{149} with methionine (Tokuyama et al, 2004). The patient exhibited impaired glucose tolerance, insulin secretion and sensitivity. The mutated receptor had reduced affinity *in vitro* for GLP-1 and peptide specificity (Beinborn et al, 2005). A second mutation deleting Lys^{334}-Leu^{335}-Lys^{336} of ICL3 in the HIT-T15 insulinoma cell line showed an absence of GLP-1 induced cAMP production, Ca^{2+} channel activation and insulin secretion (Salapatek, 1999).

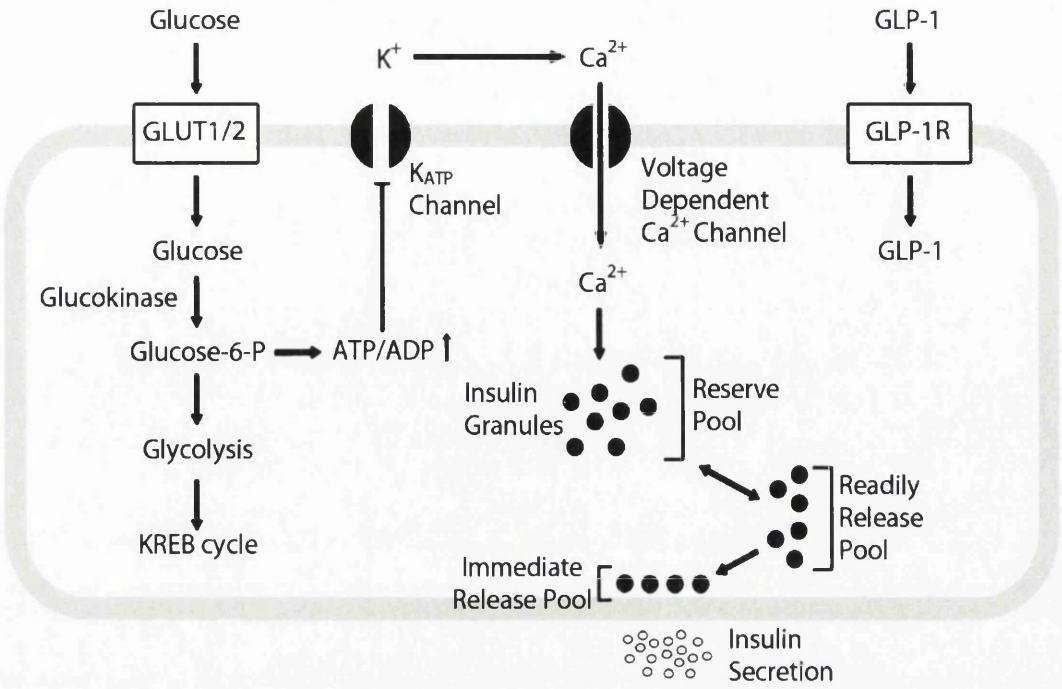

Figure 1.16. Glucose dependent insulin secretion in the β-cell. Glucose enters the cell through GLUT1 and 2 transporters. Glucose is phosphorylated to glucose-6-phosphate, which increases the cytosolic ATP/ADP ratio and in turn closes K_{ATP} channels. The closure of K_{ATP} channels depolarises the membrane and opens voltage dependent Ca^{2+} channels, releasing intracellular Ca^{2+} stores. The increase in intracellular Ca^{2+} causes the transport of insulin granules to the membrane and insulin is exocytosed. The opening of K^+ channels terminates Ca^{2+} influx by repolarising the membrane. GLP-1 potentiates insulin secretion by effecting glucose dependent ATP production, K_{ATP} channels, voltage dependent Ca^{2+} channels, intracellular Ca^{2+} release and the transport of insulin granule (Bratanova-Tochkova et al, 2002; Holz, 2004).

1.6. Aims and objectives

The ability of GLP-1 to lower postprandial hyperglycaemia by increasing insulin secretion and inhibiting glucagon secretion makes this peptide an ideal candidate for the treatment of type 2 diabetes. Additionally, as GLP-1 is able to retain its glucose lowering activity in patients with type 2 diabetes, it is also of significant clinical relevance (Haluzik, 2014). The main limitation of GLP-1 is its very short half-life and as a result therapeutic strategies, which activate the GLP-1R and improve GLP-1 actions have been extensively studied and developed.

GLP-1R activation by GLP-1 has many beneficial effects, most likely due to the activation of a number of signalling pathways upon agonist binding. But, the precise signalling pathway, which is activated and is critical for GLP-1 to exert its effects on the β-cell it still unknown. Therefore, agonists that act through the GLP-1R would be ideal for the treatment of type 2 diabetes, but only Liraglutide and Exenatide are currently available. These drugs are injectable and their long-term use may lead to a number of side effects including pancreatitis and papillary thyroid cancer. As a result, there is a need for small molecule agonists, which have a longer half-life and are orally active. It is also important to note that receptor-agonist interactions are more complex than was previously believed. Some GPCRs do not function as monomers and can be regulated by more than one agonist and can also 'self activate'. This knowledge is important for further agonist development of GPCRs.

After activation by agonist, most GPCRs internalise from the cell surface to dampen the biological response, to resensitise the desensitised receptor by recycling, or to propagate signals through novel transduction pathways (Hanyaloglu & von Zastrow, 2008). In agonist stimulated pancreatic β-cells, the internalised GLP-1R colocalises with AC within endosomes and stimulates insulin secretion (Kuna et al, 2013). Therefore, a better understanding of the GLP-1R internalisation pathway is essential for introducing novel agonists that activate the GLP-1R in the treatment of type 2 diabetes.

The GLP-1R is a major therapeutic target in the treatment of type 2 diabetes, but little is known about its plasma membrane trafficking. A better understanding of its membrane trafficking is of high importance because there is evidence demonstrating that reduced GLP-1R expression in β-cells contributes to the impaired incretin effect in type 2 diabetes (Shu et al, 2009; Xu et al, 2007). This is consistent with observations of reduced GLP-1 responses on β-cells in type 2 diabetes (Fritsche et al, 2000; Kjems et al, 2003). The N-terminal domain of family B GPCRs has been shown to be important for membrane trafficking and maturation of the receptor (Doyle & Egan, 2007; Thompson & Kanamarlapudi, 2013). However, the importance of specific regions and residues within the N-terminal domain of the GLP-1R has yet to be studied.

The C-terminal domain of GPCRs plays a critical role in agonist induced internalisation, desensitisation, down regulation and arrestin signalling (Kuramasu et al, 2006; McArdle et al, 2002). Further, the C-terminal region is also required for GPCR trafficking to the plasma membrane (Ohno et al, 1995; Sandoval & Bakke, 1994; Trowbridge et al, 1993). Unlike other GPCRs, the GLP-1R does not contain motifs within the C-terminal domain for trafficking, interactions with intracellular proteins and internalisation of the receptor. Therefore, the importance of the C-terminal domain for cell surface expression, activity and internalisation is unknown.

Overall, a lot still remains to be determined in GLP-1R plasma membrane trafficking, cell surface expression, internalisation and drug development for the treatment of type 2 diabetes. The focus of this study is to assess cellular trafficking and functional characterisation of the hGLP-1R.

The objectives of this study are to:

1. Assess the importance of the N-terminal domain for cell surface expression of the hGLP-1R.
2. Examine the effect of two small molecule agonists on hGLP-1R internalisation and activation.

3. Determine the downstream signalling pathway for internalisation of the hGLP-1R after agonist activation.
4. Identify distinct regions within the C-terminal domain required for hGLP-1R cell surface expression, agonist induced cAMP production and internalisation.

2. Materials and Methods

2.1. Materials

2.1.1. Water

Water used to make solutions was double distilled (ddH_2O) with purity of 18 MΩ.cm and obtained through the Milli-Q® Synthesis System (Millipore (U.K.) Ltd, Nottingham, UK).

2.1.2. Standard laboratory chemicals, reagents and consumables

All chemicals and mammalian cell culture reagents were purchased from Sigma Aldrich (Dorset, UK) unless otherwise stated. Glass coverslips (13 mm, 1.5 mm), cell culture universals and plasticware were purchased from VWR International (Leistershire, UK) unless mentioned specifically. Cell culture plates, bacterial culture plates and cAMP 1x8 flat well strips were obtained from Greiner-Bio One (Gloucestershire, UK).

2.1.3. Peptides, chemical inhibitors, antibodies, primers and enzymes

Peptide agonists and antagonists of the hGLP-1R, GLP-1 (7-36) amide and Exendin (9-39) were supplied by Tocris (Bristol, UK). The small molecule agonists, compound 2 and compound B, were purchased from Calbiochem (Nottingham, UK). Antagonist JANT-4 was obtained from Prof. Richard DiMarchi, Indiana University (IN, USA). GLP-1 (Liraglutide) and Exendin-4 (Exenatide) were from Novo Nordisk (Sussex, UK) and Eli Lilly and Company Limited (Liverpool, UK), respectively.

Chemical inhibitors 2-APB (2-aminoethoxydiphenylborane), BAPTA-AM (1,2-*bis*(2-aminophenoxy)ethane-*N,N,N',N'*-tetraacetic acid tetrakis (acetoxymethyl ester)), chlorpromazine hydrochloride (2-chloro-10-(3-

dimethylaminopropyl)phenothiazine hydrochloride), filipin complex (*streptomyces filipinensis,* $C_{35}H_{58}O_{11}$), genistein (5,7-dihydroxy-3-(4-hydroxyphenyl)-4*H*-1-benzopyran-4-one), monodansylcadaverine (MDC, *N*-(5-aminopentyl) -5-dimethylaminonaphthalene-1-sulfonamide,*N*- (dimethylamino-naphthalenesulfonyl)-1,5-pentanediamine), and tunicamycin (n=10, $C_{39}H_{64}N_4O_{16}$) were purchased from Sigma Aldrich (Dorset, UK). Dynasore (3-hydroxy-naphthalene-2-carboxylic acid (3,4-dihydroxy-benzylidene)-hydrazide hydrate) was purchased from Abcam Biochemicals (Cambridge, UK). Go6976 (5,6,7,13-tetrahydro-13-methyl-5-oxo-12*H*-indolo [2,3-*a*] pyrrolo [3,4-*c*] carbazole-12-propanenitrile), PD98059 (2-(2-amino-3-methoxyphenyl)-4*H*-1-benzopyran-4-one), Ro318820 (3-[3-[2,5-Dihydro-4-(1-methyl-1*H*-indol-3-yl)-2,5-dioxo-1*H*-pyrrol-3-yl]-1*H*-indol-1-yl]propyl carbamimidothioic acid ester mesylate), U73122 (1-[6-[[(17β)-3-methoxyestra-1,3,5(10)-trien-17-yl]amino]hexyl]-1*H*-pyrrole-2,5-dione, and U73343 (1-[6-[[(17β)-3-methoxyestra-1,3,5(10)-trien-17-yl]amino]hexyl]-2,5-pyrrolidinedione) were all obtained from Tocris (Bristol, UK). PBP10 (Rhodamine B-Gln-Arg-Leu-Phe-Gln-Val-Lys-Gly-Arg-Arg) was from Millipore (U.K.) Ltd (Nottingham, UK) and penetratin peptide was from Thermo Scientific (Northumberland, UK).

Endoglycosidase enzymes PNGase F and Endo H were bought from New England Biolabs (Hertfordshire, UK). The antibiotics, ampicillin and kanamycin were both obtained from Sigma Aldrich (Poole, UK).

Monoclonal mouse anti-hGLP-1R antibody (MAB2814) for enzyme linked immunosorbent assay ELISA, immunofluorescence and flow cytometry was purchased from R&D Systems (Abington, UK). Monoclonal mouse anti-hGLP-1R antibody (sc390774) for immunoblotting and monoclonal mouse anti-CAV-1 antibody (sc894) for coimmunoprecipitation was obtained from Santa Cruz Biotechnology (Heidelberg, Germany). Cy™3-conjugated AffiniPure anti-mouse immunoglobulin (IgG) (from donkey) secondary antibody (715-165-150) for immunofluorescence experiments was purchased from Jackson ImmunoResearch (Suffolk, UK). Polyclonal rabbit anti-phospho p44/42 MAPK (mitogen-activated protein kinase) (Thr^{202}/Try^{204}) antibody (9101) and anti-

p44/42 MAPK antibody (9102) for immunoblotting were obtained from New England Biolabs (Hertfordshire, UK). Polyclonal rabbit anti-vesicular stomatitis virus glycoprotein (VSVG) tag (Biotin) antibody (ab34774) for immunoblotting and polyclonal rabbit anti-red fluorescent protein (RFP) tag (Biotin) antibody (ab34771) was purchased from Abcam Biochemicals (Cambridge, UK). Monoclonal mouse anti-green fluorescent protein (GFP) antibody (11814460001) for immunoblotting was purchased from Roche (West Sussex, UK). ECL™ (enhanced chemiluminescence) anti-rabbit IgG, horseradish peroxidase (HRP)-linked whole antibody (from donkey, NA934) and ECL™ anti-mouse IgG, HRP-linked whole antibody (from sheep, NA933) was supplied by GE Healthcare (Hertfordshire, UK). DAPI (4′,6-diamidino-2-phenylindole dihydrochloride, 1 mg/ml, D8417) to stain nuclei in immunofluorescence was also obtained from Sigma Aldrich (Dorset, UK).

Standard cAMP was purchased from Sigma Aldrich (Dorset, UK). 1 mg/ml unconjugated goat-anti rabbit (A00131) for coating cAMP plates, cAMP polyclonal antibody (A00614) and cAMP-HRP antibody (M01059) were both from Genscript (NJ, USA).

Primers used to produce the hGLP-1R constructs were supplied by Sigma (Dorset, UK) and sequenced by Dundee University DNA sequencing services (Scotland, UK). High fidelity Taq Polymerase, dNTPs and 10x high fidelity buffer with 15 μM magnesium chloride ($MgCl_2$) for cloning by polymerase chain reaction (PCR) were purchased from Roche (West Sussex, UK). Restriction enzymes (RE) including the relevant buffers for restriction digestion were also obtained from Roche (West Sussex, UK). T4 deoxyribonucleic (DNA) ligase and 2x ligation buffer (for ligation of hGLP-1R to pEGFP-N1 [plasmid enhanced green fluorescent protein-N1]) was obtained from Promega (Southampton, UK).

2.1.4. Specific reagents and kits

50x Tris/acetic acid/ethylenediaminetetraacetic acid (EDTA) (TAE) buffer was purchased from BioRad (Herts, UK). Agarose tablets and HyperLadder™ I molecular weight marker was obtained from Bioline (London, UK).

QIAquick® Gel Extraction Kit and QIAprep Spin Miniprep Kit purchased from QIAGEN (West Sussex, UK) were used for plasmid DNA preparation. GenElute™ HP Plasmid Midiprep Kit purchased from Sigma Aldrich (Dorset, UK) was used for large scale plasmid preparation. The QuikChange Site-Directed Mutagenesis kit was obtained from Stratagene (Leicestershire, UK). The Q5® Site-Directed Mutagenesis Kit was obtained from Thermo Scientific (Northumberland, UK).

Polyplus JetPrime® transfection reagent was obtained from VWR International (Leistershire, UK) or Source Bioscience (Nottingham, UK). 1-Step™ Ultra TMB ELISA substrate was from Thermo Scientific (Northumberland, UK). ONE-Glo™ lysis buffer to detect luminescence activity was purchased from Promega (Southampton, UK).

Precision Plus Protein All Blue Standard was obtained from BioRad (Herts, UK). Acrylamide stock solution (30%, w/v) was purchased from National Diagnostics (Hull, UK). Polyvinylidene fluoride (PVDF) transfer membrane was purchased from Millipore (U.K.) Ltd (Nottingham, UK). Low sensitivity Pierce® ECL Western Blotting Substrate and normal sensitivity Supersignal® West Pico Chemiluminescence Substrate were obtained from Thermo Scientific (Northumberland, UK). High sensitivity Amersham ECL Select immunoblotting Detection Reagent was purchased from GE Healthcare Ltd (Buckinghamshire, UK) or VWR International (Leistershire, UK) for the visualisation of proteins by immunoblotting.

2.1.5. Bacterial strains

Escherichia coli (*E. coli*) strain XL1-Blue was used as a host to amplify plasmid DNA and for gene cloning. XL1-Blue ultracompetent cells were used for plasmid

DNA transformation in the generation of hGLP-1R constructs. XL1-Blue competent cells were used for routine plasmid DNA transformation. NEB 5-alpha *E. coli* (supplied by Q5® Site-Directed Mutagenesis Kit) was used for deletion mutation plasmid DNA transformation.

2.1.6. Plasmid DNA constructs

A series of plasmid DNA constructs were used in this study, which included both vectors and constructs. See Table 2.1, Table 2.2 and Table 2.3.

Table 2.1. Series of plasmid DNA constructs used in this study.

Construct	Epi-tope	Vector	Antibiotic Resistance	Source
SP-VSVG-hGLP-1RΔN23-pEGFP-N1	VSVG	pEGFP-N1	Kanamycin	Made in Lab
VSVG-hGLP-1R-pEGFP-N1	VSVG	pEGFP-N1	Kanamycin	Made in Lab
VSVG-hGLP-1R	VSVG	pEGFP-N1	Kanamycin	Made in Lab
hGLP-1R-pEGFP-N1	-	pEGFP-N1	Kanamycin	Made in Lab
hGLP-1R	-	pEGFP-N1	Kanamycin	Made in Lab
hGLP-1RΔN23	-	pEGFP-N1	Kanamycin	Made in Lab
VSVG-VSP-hGLP-1R ΔN23-pEGFP-N1	VSVG	pEGFP-N1	Kanamycin	Made in Lab
VSVG-hGLP-1RΔN23-pEGFP-N1	VSVG	pEGFP-N1	Kanamycin	Made in Lab
VSVG-hGLP-1RΔN24-pEGFP-N1	VSVG	pEGFP-N1	Kanamycin	Made in Lab
VSVG-hGLP-1RΔN30-pEGFP-N1	VSVG	pEGFP-N1	Kanamycin	Made in Lab
VSVG-hGLP-1RΔN35-pEGFP-N1	VSVG	pEGFP-N1	Kanamycin	Made in Lab
VSVG-hGLP-1RΔN40-pEGFP-N1	VSVG	pEGFP-N1	Kanamycin	Made in Lab
VSVG-hGLP-1RΔN145-pEGFP-N1	VSVG	pEGFP-N1	Kanamycin	Made in Lab
SP-VSVG-hGLP-1RΔN23 Δ450	VSVG	pEGFP-N1	Kanamycin	Made in Lab
SP-VSVG-hGLP-1RΔN23 Δ443	VSVG	pEGFP-N1	Kanamycin	Made in Lab

SP-VSVG-hGLP-1RΔN23 Δ440	VSVG	pEGFP-N1	Kanamycin	Made in Lab
SP-VSVG-hGLP-1RΔN23 Δ430	VSVG	pEGFP-N1	Kanamycin	Made in Lab
SP-VSVG-hGLP-1RΔN23 Δ410	VSVG	pEGFP-N1	Kanamycin	Made in Lab
pEGFP-N1	-	pEGFP-N1	Kanamycin	Available in Lab
pGL4.29 CRE Luc	-	pGL4.27	Ampicillin	Bought from Promega
pGL4.30 NFAT Luc	-	pGL4.27	Ampicillin	Bought from Promega
pGL4.33 SRE Luc	-	pGL4.27	Ampicillin	Made in Lab
$pcDNA_3$	-	$pcDNA_3$	Ampicillin	Available in Lab
β-Arrestin1 (319-418) Dominant Negative (DN)	-	$pcDNA_3$	Ampicillin	Available in Lab
EPS15Δ DN	-	pEGFP-C1	Kanamycin	Available in Lab
Dynamin (K44A) DN	-	$pcDNA_3$	Ampicillin	Available in Lab
CAV-1-P132L-Cherry DN	-	pmCherry -N1	Kanamycin	Addgene (MA, USA)
$G\alpha_q$ G188S $pcDNA_3$ DN	-	$pcDNA_3$	Ampicillin	Prof. Karnam S. Murthy (Virginia Commonwealth University, USA)

The table shows the construct, epitope tag, vector and source of all plasmid DNA constructs used in this study. Constructs "made in lab" were with the help of Prof. Venkateswarlu Kanamarlapudi.

Table 2.2. Primer for generating mutated hGLP-1R constructs.

Muta-tion	DNA Sequence		Primer (from 5'to 3')
	Wild Type	Mutant	
E63L, N82L, N115L	AAC AAT AAC	CTA CTA CTA	5': CTGCCACAGACTTGTTCTGCCTACGGACCTTCGATGAATAC 5': CCAGGCTCGTTCGTGCTAGTCAGCTGCCCCTGG 5': CTGGCTGCAGAAGGACCTATCCAGCCTGCCCTGGA
A21R	GCC	CGC	5': GGTGGGCAGGCGCGGCCCCCGC 3': GCGGGGGCCGCGCCTGCCCACC
E34K	GAG	AAG	5': CACTGTGTCCCTCTGGAAGACGGTGCAGAAATG 3': CATTTCTGCACCGTCTTCCAGAGGGACACAGTG
V36A	GTG	GCG	5': CCTCTGGGAGACGGCGCAGAAATGGCGAGAATACCG 3': CTCGCCATTTCTGCGCCGTCTCCCAGAGGGACAC
W39A	TGG	GCG	5': TCTGGGAGACGGTGCAGAAAGCGCGAGAATACCG 3': CGGTATTCTCGCGCTTTCTGCACCGTCTCCCAGA
Y69A	TAC	GCC	5': TGCAACCGGACCTTCGATGAAGCCGCCTGCTGGC 3': GCCAGCAGGCGGCTTCATCGAAGGTCCGGTTGCA
Y88A	TAC	GCC	5': GGCCCAGGGCAGGGCCCAGGGGCAGCTG 3': CAGCTGCCCCTGGGCCCTGCCCTGGGCC
T149M	ACG	ATG	5': CCTGTTCCTCTACATCATCTACATGGTGGGCTACGC 3': GCGTAGCCCACCATGTAGATGATGTAGAGGAACAGG
K334A	AAA	GCA	5': CATCTGCATCGTGGTATCCGCACTGAAGGCCAATCTCATG 3': CATGAGATTGGCCTTCAGTGCGGATACCACGATGCAGATG
E408A, V409A, Q410A	GAG GTC CAG	GCG GCC GCG	5': TTATACTGCTTTGTCAACAATGCGGCCGCGCTGGAATTTCGG AAGAGC 3': CAGCTCTTCCGAAATTCCAGCGCGGCCGCATTGTTGACAAAG CAGTATAA

The table shows the mutations used in this study and the primer required to make these mutations. Constructs were generated with the help of Prof. Venkateswarlu Kanamarlapudi.

Table 2.3. Primers for generating hGLP-1R deletion mutation constructs.

Deletion	Primer (from 5'to 3')
hGLP1R Δ31-40	5': CACAGTGGCACCCTGGGG 3': GAATACCGACGCCAGTGCCAGCGC
hGLP-1R Δ411-418	5': CTGGACCTCATTGTTGACAAAGCAG 3': CGCTGGCGCCTTGAGCACTTG
hGLP-1R Δ419-430	5': CTCCCAGCTCTTCCGAAATTC 3': AGCAGCATGAAGCCCCTC
hGLP-1R Δ431-450	5': GTCCCTCTGGATGTGCAAGTG 3': AGCAGCATGTACACAGCCAC

The table shows the deletions used in this study and the primers required to make these deletions. Constructs were generated with the help of Prof. Venkateswarlu Kanamarlapudi.

2.1.7. Mammalian cell line

Human embryonic kidney 293 (HEK293) cells obtained from ATCC® (CRL-1573, Middlesex, UK) were used for transient expression of plasmid DNA between passages 15 and 30. HEK293 cells are relatively easy to both culture and transfect and have been used extensively as a model cell line to study GPCR function and trafficking.

2.2. Bacterial cell culture

2.2.1. *E. coli* stock

To make glycerol stocks of *E. coli*, 1 ml of fresh overnight culture and 0.5 ml of 50% glycerol (VWR International, Leistershire, UK) in ddH_2O (v/v) were added

to sterile 2 ml cryovials (Greiner-Bio One, Gloucestershire, UK) and vortexed using a vortex genie 2 (Scientific Industries, NY, USA). Vials were then stored at -80°C. To grow cells from frozen, cells were scraped from the cryovial using a sterile pipette tip and streaked onto a fresh 10 cm Luria-Bertani (LB) agar plate (Greiner-Bio One, Gloucestershire, UK) containing the appropriate antibiotic for selection. The plate was then incubated inverted at 37°C (Genlab incubator, Cheshire, UK) overnight for approximately 16 hours (h).

2.2.2. Preparation of XL1-Blue competent cells

XL1-Blue competent cells were prepared by soaking the cells in cold calcium chloride ($CaCl_2$) (Salehi et al, 2010). Using aseptic techniques, 5 ml of LB medium was inoculated with a single colony of *E. coli* and incubated overnight at 37°C/250 rpm in an orbital incubator SI500 (Stuart, Staffordshire, UK). 1 ml of overnight culture was then grown up at 37°C/250 rpm in 100 ml of fresh LB medium until the A_{600} (absorbance at 600 nm) reached 0.5 (~2.5-3 h). The bacterial culture was then centrifuged at 6000 xg using a Beckman Coulter Avanti J-26 XP centrifuge (High Wycombe, UK) for 20 minutes (min) at 4°C. The supernatant was removed and the pellet resuspended in 20 ml ice cold 0.1 M $CaCl_2$ and incubated on ice for 10 min. This was again centrifuged (6000 xg, 10 min, 4°C) and the supernatant decanted. This time the pellet was resuspended in 2 ml ice cold 0.1 M $CaCl_2$ and 70 µl dimethyl sulfoxide (DMSO) was added to the resuspended cells and mixed gently prior to incubation on ice for 15 min. An additional 70 µl DMSO was added, mixed and immediately dispensed into 50 µl aliquots. Aliquots were quickly snap frozen in liquid nitrogen and stored at -80°C.

2.2.3. Preparation of XL1-Blue ultracompetent cells

Using aseptic techniques, 1 ml of LB medium containing 12.5 µg/ml tetracycline was inoculated with a single colony of *E. coli* and incubated overnight at 37°C/250 rpm in an orbital incubator. 0.1 ml of this culture was added to 60 ml LB containing 12.5 µg/ml tetracycline and again grown overnight at 37°C/250 rpm. 5% inoculation was made by adding 25 ml of culture to 2x 500 ml of super

optimal broth (SOB, 2% [w/v] bacto tryptone, 0.5% [w/v] yeast extract, 10 mM sodium chloride [NaCl], 2.5 mM potassium chloride [KCl], 10 mM $MgCl_2$, 10 mM magnesium sulphate [$MgSO_4$], pH 6.7-7.0) in a 2L conical flask and incubated at 18°C/250 rpm (multitron standard incubator, Infor HT, Surrey, UK) until the A_{600} reached 0.6 (~18 h). Cultures were then left on ice for 10 min and centrifuged at 6000 xg using a Beckman Coulter Avanti J-26 XP centrifuge (Beckman JLA-8.1 rotor) for 10 min at 4°C. The bacterial pellet was then gently resuspended in 380 ml of ice cold transformation buffer (TB; 10 mM pipes, 55 mM manganese chloride [$MnCl_2$], 15 mM $CaCl_2$, 250 mM KCl, pH 6.7) and incubated on ice for 10 min. This was again centrifuged (6000 xg, 10 min, 4°C) and the bacterial pellet resuspended in 10 ml of ice cold TB. 700 µl of DMSO was added to a final concentration of 7% and then placed on ice for a further 10 min. This was then dispensed into 100 µl aliquots, snap frozen in liquid nitrogen and then stored at -80°C.

2.3. Transformation and purification of plasmid DNA

2.3.1. Transformation of plasmid DNA

A 50-100 µl aliquot of XL1-Blue or NEB 5-alpha *E. coli* was thawed on ice. 1 µg plasmid DNA or 5 µl of ligation mixture (see section 2.8) was added to the *E. coli* cells and then incubated on ice for 30 min. The *E. coli* cells/plasmid DNA mixture was then heat shocked at 42°C for 45 seconds (s) in a Grant GD100 water bath (Cambridgeshire, UK) and then immediately placed on ice for 2 min. 0.5-1 ml of LB medium was added to the transformed cells and incubated at 37°C/250 rpm in an orbital incubator. The cells transformed with ligation mixture was centrifuged at 16000 xg for 1 min, 0.4-0.9 ml medium (supernatant) was removed and the cell pellet resuspended in the remaining 100 µl of medium. 100 µl of transformed cells was spread onto an LB agar plate containing the appropriate antibiotic for selection and incubated inverted overnight at 37°C in a Genlab incubator. The plates were then sealed with parafilm and stored inverted at 4°C.

2.3.2. Purification of plasmid DNA

Plasmid DNA for transfection was purified from bacteria using either the miniprep kit for 5 ml volumes or the midiprep kit for 100 ml volumes. Manufacturer's protocols were followed when using plasmid mini or midiprep kits.

QIAprep Spin Miniprep Kit was used to produce small volumes of plasmid DNA and was sufficient to select for DNA clones containing an expected insert. Here, a single colony of bacteria transformed with plasmid DNA was grown up overnight in 5 ml LB medium containing antibiotic in a 30 ml universal, at 37°C/250 rpm in an orbital incubator, and harvested for plasmid DNA purification. Just before harvesting, a small volume of culture was streaked on LB agar plates containing the appropriate antibiotic for selection and incubated inverted overnight at 37°C in a Genlab incubator. The plates were then sealed with parafilm and stored inverted at 4°C, so bacteria could be used for plasmid midipreps if required. Briefly, 5 ml of overnight culture was harvested by centrifugation at 3000 xg for 5 min using an Eppendorf 5810R centrifuge. The bacterial pellet was resuspended in 250 µl buffer P1 and transferred to a microcentrifuge tube. 250 µl buffer P2 was added and inverted to lyse bacteria. The solution was then neutralised with the addition of 350 µl buffer N3 by inversion. The supernatant was applied to a QIAprep spin column, centrifuged for 1 min at 16000 xg in a table top Eppendorf 5415D centrifuge (Stevenage, UK) and the flow through discarded. 750 µl buffer PE was added to wash the QIAprep spin column, centrifuged (16000 xg, 1 min) and the flow through discarded. The QIAprep spin column was centrifuged (16000 xg) for an additional 1 min and transferred to a clean 1.5 ml microcentrifuge tube. 100 µl (kanamycin resistance vectors) or 50 µl (ampicillin resistance vectors) of buffer EB (100 mM Tris hydrogen chloride (Tris HCl), pH 8.5) was placed in the centre of each QIAprep spin column, left to stand for 1 min and then centrifuged for 1 min (16000 xg).

In addition to this, GenElute™ HP Plasmid Midiprep Kit was used to purify plasmid DNA for transfection from larger volumes of bacterial culture. A single

colony of transformed plasmid DNA was first grown up overnight in 1.5 ml LB medium containing antibiotic at 37°C/250 rpm. 1 ml of bacterial culture was then grown up in 100 ml LB medium containing antibiotic, overnight at 37°C/250 rpm multitron standard incubator. Prior to harvesting, glycerol stocks were made by adding 1 ml of overnight culture and 0.5 ml 50% glycerol (v/v) in ddH_2O to sterile 2 ml cryovials. Cryovials were vortexed and stored at -80°C. The remaining culture was harvested by centrifugation at 3000 xg using an Eppendorf 5810R centrifuge for 20 min and the supernatant discarded. 4 ml of resuspension/RNAase A solution was added to the bacterial pellet and resuspended. Cells were lysed with the addition of 4 ml lysis solution, immediately mixed by inversion and left to sit for 3-5 min until the solution was clear and viscose. 4 ml chilled neutralisation solution was added to neutralise the solution and mixed by inversion. 3 ml of binding solution was added to the neutralised lysate and inverted 1-2 times. This was immediately poured into the barrel of the filter syringe and allowed to sit for 5 min. As the lysate was left to sit, 4 ml of column preparation solution was added to the column, centrifuged at 3000 xg for 2 min in a rotanta 460R centrifuge (Buckinghamshire, UK) and the flow through discarded. The clear lysate was passed through the filter syringe into the column, centrifuged (3000 xg, 2 min) and the flow through discarded. The column was washed with 4 ml wash solution 1, centrifuged (3000 xg, 2 min) and the flow through discarded. The column was washed again with 4 ml wash solution 2 and centrifuged (3000 xg, 5 min). The column was transferred to a new collection tube, 1 ml elution buffer added and then centrifuged at 3000 xg for 5 min.

After plasmid DNA preparations, the concentration and quality of DNA was determined by measuring absorbance at 260 nm using a BioPhotometer (Eppendorf, Stevenage, UK). Here, 10 µl of plasmid DNA was diluted in 1 ml ddH_2O. The ratio of the absorbance at 260/280 nm and 260/230 nm was also noted and the ratio of the absorbance at 260/280 nm greater than 1.5 was assumed to be satisfactory for use in transfection experiments. The concentration (mg/ml) was calculated using the equation below and the plasmid DNA was stored at -20°C.

Concentration (mg/ml) = $\frac{A_{260} \text{ reading x dilution factor}}{20}$

2.4. Generating hGLP-1R constructs

2.4.1. Design of primers

The primers used to produce the SP-VSVG-hGLP-1RΔN23-GFP plasmid, are shown in Figure 2.1. HGLP-1RΔN23 cDNA was amplified from mammalian gene collection (MGC) clone 142053 (Source Bioscience) by PCR using High Fidelity Taq DNA polymerase (Roche Applied Science) and sequence specific primers containing *Eco*RI RE site and VSVG-tag coding sequence (5' primer), and *Sal*I restriction site and no stop codon (3' primer). The full length SP-VSVG-hGLP-1RΔN23 cDNA was amplified by overlap PCR using VSVG-hGLP-1RΔN23 cDNA as the template, the sense primer, containing *Eco*RI restriction site, the SP (1-23 amino acids) coding sequence followed by VSVG coding sequence and 3' primer. The cDNA was digested with *Eco*RI and *Sal*I, and cloned in frame into the same sites of pEGFP-N1 vector (Clontech) for expression as the N-terminus VSVG-tagged and the C-terminus GFP-tagged fusion protein in mammalian cells (SP-VSVG-hGLP-1RΔN23-GFP). The SP-VSVG-hGLP-1RΔN23 with no GFP-tag and its C-terminal deletion constructs were generated by PCR using sequence specific primers containing *Eco*RI restriction site (5' primer), *Sal*I restriction site and stop codon (3' primer), which prevents GFP-tagging at the C-terminus and SP-VSVG-hGLP-1RΔN23-GFP plasmid as the template.

The VSVG tag sequence was included in each primer used for generating the N-terminal deletion constructs of the hGLP-1R. The sequence primers included *Eco*RI RE site and the start codon (ATG) in the 5' primer and *Sal*I RE site and no stop codon (TAG) in the 3' primer. A Kozak sequence (GCCACC) was also

inserted before the start codon to increase the translation efficiency and expression of the DNA product (Nauck et al, 2009).

A. 5' primer

EcoRI Kozak Start hGLP-1R – Signal Peptide

5'- CGC GAA TTC *GCCACC* **ATG** GCC GGC GCC CCC GGC CCG CTG CGC CTT GCG CTG CTG

CTG CTC GGG GTG GGC AGG GCC GGC CCC ATG TAC ACC GAT ATA GAG ATG AAC -3'

hGLP-1R – Signal Peptide VSVG

B. 3' primer

Sal I hGLP-1R (1389-1365)

5'- CG CGT CGA CTG GCT GCA GGA GGC CTG GCA AGT GGC -3'

Figure 2.1. Primers for cloning the SP-VSVG-hGLP-1RΔN23-GFP plasmid. Bases underlined once show the RE digest sites. Bases in italics represent the Kodak sequence and in bold is the start codon. The coding sequence of the hGLP-1R is on a waved underline. The double underline highlights the VSVG tag.

2.4.2. Amplification of DNA by PCR

A 100 µl PCR mixture was made up in a PCR tube, which contained 86.5 µl ddH_2O, 10 µl high fidelity buffer (10x) with 15 µM $MgCl_2$, 1 µl 100 mM dNTPs, 1.5 µl high fidelity Taq polymerase (3.5 U/µl), 0.5 µl of 100 µM 5' primer and 0.5 µl of 100 µM 3' primers and a template DNA. However, a 20 µl reaction mixture

containing Red Taq polymerase (Sigma) and bacterial colony as a template was used for colony PCR, which was useful in identifying bacterial colonies harbouring recombinant plasmids with gene inserts.

PCR amplification for cloning proceeded with initial denaturation, 30 cycles of denaturation, annealing and elongation, and a final extension using the thermal cycler (GeneAmp PCR System 2400, Perkin Elmer, Cambridgeshire, UK). Initial denaturation was carried out at 95°C for 2 min. The denaturation in each cycle was at 95°C for 30 s. The annealing was performed at 60°C for 30 s in each cycle. The elongation temperature was for 1 min per kilo base pair (kbp) at 72°C for each cycle. The final extension was for 5 min at 72°C. Following the final extension the reaction tubes were cooled at 20°C for 5 min or until the PCR tubes were removed from the thermal cycler. Reaction mixtures not required straight away were stored at -20°C.

2.5. Restriction digestion

Restriction digest cuts DNA into smaller pieces with RE that recognise RE sites in the DNA. In this study, restriction digests were performed to either confirm the presence of a known insert within the plasmid DNA or to release DNA inserts for religation.

To confirm the presence of the insert in a recombinant plasmid, 1 µg of plasmid DNA was digested in a 10 µl reaction mixture containing 1 µl 10x reaction enzyme specific buffer and 0.5 µl of each RE (10 U/µl). The mixture was incubated at 37°C for 2-3 h in a Grant GD100 water bath. After digestion, if not required straight away, the reaction mixture was stored at -20°C.

To prepare an insert or vector for ligation (plasmid or purified PCR product) the same conditions were used as above with the exception that the total reaction volume was 100 µl. The reaction mixture contained 50 µl plasmid DNA, 10 µl

10x reaction enzyme specific buffer, 10 µl of each RE and 30 µl ddH_2O. After digestion, if not required straight away, the reaction mixture was stored at -20°C.

2.6. Agarose gel electrophoresis

Agarose gel electrophoresis was used to either separate or identify original PCR products and digested plasmids. Here, 2x 0.5 g of agarose tablets were added to 100 ml TAE buffer (0.4 M Tris acetate, 0.01 M EDTA, pH 8.3), left for 10-15 min at room temperature (RT) to disperse the tablets and heated in a microwave oven until the agarose had completely dissolved to produce a 1% gel. 10 µl of ethidium bromide (10 mg/ml) was added to the solution and mixed by swirling. The gel was then poured into the casting tray (Whatman, Maidstone, UK) with a comb to form the sample wells and allowed to solidify at RT. Once the gel had solidified, the comb was removed and TAE buffer was added to the tank to cover the gel. 5 µl or 100 µl of DNA sample were mixed with 6x DNA loading buffer (0.25% [v/v] bromophenol blue, 30% [v/v] glycerol) and then pipetted into the wells of the gel. A 1.0 kb HyperLadder™ was used to estimate the size of the DNA fragments. Using a PowerPac 200 (BioRad, Herts, UK) the gel was run at 100 volts (V) for 15-30 min, then removed from the tank, placed on the GelDoc machine (BioRad, Herts, UK) and viewed under Trans UV light.

2.7. DNA extraction and purification

The QIAquick gel extraction kit was used to extract and purify DNA from agarose gel or solution (e.g. after restriction digestion of excised DNA to be used for ligation [see section 2.8]), as directed by the manufacturer. This removes enzymes, dNTPs, nucleotides, primers, salts, agarose, ethidium bromide and other impurities from the DNA samples.

Using a clean scalpel under trans-UV light, the band of interest was excised from the agarose gel and weighed in a 2 ml microcentrifuge tube of known weight. The gel band was heated at 50°C in a volume of QG buffer (µl) equivalent to 3 times the gel weight (µg) using a Grant heating block (Cambridgeshire, UK) with periodic mixing to dissolve the gel piece. A volume of isopropanol (µl) equivalent to the gel weight (µg) was added, the sample was then mixed and added to a QIAquick spin column. This was centrifuged in a table top Eppendorf 5415D centrifuge for 1 min at 16000 xg and the flow through discarded. If necessary, the centrifugation was repeated to add more sample to the spin column. The column was washed with 750 µl of buffer PE, centrifuged (1 min, 16000 xg) and the flow through was discarded. The column was further centrifuged (1 min, 16000 xg) to completely remove any residual ethanol. The column was then transferred to a clean 1.5 ml microcentrifuge tube and 50 µl of buffer EB (10 mM Tris, pH 8.5) added to the column and left to sit for 1 min before centrifugation for 1 min at 16000 xg to elute DNA.

To purify DNA after RE digestion, the above protocol was followed. However, 450 µl of buffer QG was added directly to 100 µl digested product and the solution was not heated. 150 µl of isopropanol was added and the mixture applied to the QIAquick spin column as described above. Additionally, DNA was eluted with 30 µl of buffer EB.

2.8. DNA ligation

Ligation was used to join DNA fragments by covalent bonds. To generate the GFP epitope tagged hGLP-1R constructs and other fluorescently tagged constructs, inserts released from existing constructs by RE or isolated by PCR amplification and digested with RE and an empty vector digested with the same RE or ligation compatible RE were ligated. The insert and vector were prepared by RE digest as described (section 2.5). The total reaction volume of the ligation mixture was 10 µl and contained 5 µl 2x ligation buffer, 1 µl T4 DNA Ligase, 1 µl

vector, 3 µl insert or water (for the negative control). The ligation mixture was mixed and centrifuged briefly in a table top Eppendorf 5415D centrifuge to collect at the bottom of the microcentrifuge tube. The reaction was carried out at 4°C for a minimum of 24 h. 5 µl of the ligation mixture was used to transform into 100 µl of ultracompetent XL1-Blue cells followed by selection with the appropriate antibiotic conferred by the vector for purification of plasmid DNA (see section 2.3).

2.9. Site-directed mutagenesis

2.9.1. Point mutations

Point mutations within the hGLP-1R construct were generated using the QuikChange II XL Site-Directed Mutagenesis Kit as directed by the manufacturer. Point mutations were introduced using PCR primers (Table 2.2). The DNA template used was either the SP-VSVG-hGLP-1RΔN23-GFP, VSVG-hGLP-1R-GFP or VSVG-hGLP-1RΔN23-GFP construct. A reaction mixture was made with the addition of 1 µl 10x reaction buffer, 50 ng DNA template, 0.125 µl of 100 µM 5' primer and 0.125 µl of 100 µM 3' primer, 0.2 µl dNTP mix, 0.6 µl of QuikSolution and 7.5 µl of ddH_2O to a total reaction volume of 10 µl. To this 0.2 µl of *PfuUltra* HF DNA polymerase (2.5 U/µl) was added to the reaction mixture.

PCR for generating mutated PCR products was proceeded with initial denaturation, 18 cycles of denaturation, annealing and elongation, and final extension using the GeneAmp PCR System 2400. The initial denaturation was carried out at 95°C for 2 min. The denaturation in each was at 95°C for 1 min. Annealing was performed at 60°C for 50 s in each cycle. The elongation temperature was for 7 min (1 min per kbp DNA) at 68°C for each cycle. The final extension was for 7 min at 68°C. Following the final elongation, the reaction tubes were cooled at 20°C for 5 min or until the PCR tubes were removed from the GeneAmp PCR System 2400.

The PCR product was then digested with 0.4 µl of *Dpn*I RE (10 U/µl) at 37°C for 2 h. 2 µl of product was then transformed into 50 µl of XL1 Blue ultracompetent cells for purification of plasmid DNA (see section 2.3).

2.9.2. Deletion mutations

Deletions within the hGLP-1R was generated using the Q5® Site-Directed Mutagenesis Kit as directed by the manufacturer. Deletions were introduced using PCR primers (Table 2.3). The DNA template used was the SP-VSVG-hGLP-1RΔN23-GFP construct. A reaction mixture was made with the addition of 5 µl Q5 hot start fidelity 2x master mix, 10 ng template, 0.5 µl of 10 µM 5' primer and 0.5 µl of 10 µM 3' primer and 3 µl of ddH_2O to a total volume of 10 µl.

PCR for generating mutated PCR products was proceeded with initial denaturation, 25 cycles of denaturation, annealing and elongation, and final extension using the GeneAmp PCR System 2400. The initial denaturation was carried out at 98°C for 30 s. The denaturation in each was at 98°C for 10 s. Annealing was performed at 60°C for 30 s in each cycle. The elongation temperature was for 3.5 min (30 s per kbp DNA) at 72°C for each cycle. The final extension was for 2 min at 72°C. Following the final elongation, the reaction tubes were cooled at 4°C for 5 min or until the PCR tubes were removed from the GeneAmp PCR System 2400.

The PCR product was then subjected to KLD (oligonucleotide kinase, T4 DNA ligase and *Dpn*I) reaction. A reaction mixture was made up of 0.5 µl of PCR product, 2.5 µl 2x KLD reaction buffer, 0.5 µl 10x KLD enzyme mix and 1.5 µl ddH_2O and incubated at RT for 1 h. 5 µl of product was then transformed into 50 µl of NEB 5-alpha competent *E. coli* or XL1 Blue ultracompetent cells for purification of plasmid DNA (see section 2.3).

2.10. DNA sequencing

The mutations, deletions and right reading frames were confirmed by automated sequencing (DNA Sequencing Services ™, within the of Life Sciences, University of Dundee, Scotland, UK). For each sequencing, 600 ng of plasmid and 3.2 μM of primer was made up to 30 μl with ddH_2O was supplied.

2.11. Mammalian cell culture

2.11.1. Growth and maintenance

HEK293 cell were maintained at 37°C in a 5% CO_2 humidified environment in Dulbecco's modified Eagle medium (DMEM; serum free medium [SFM], LM-D1110, Biosera, East Sussex, UK) containing 4500 mg glucose/L, L-glutamine, sodium bicarbonate and pyridoxine HCl, supplemented with 10% (v/v) fetal calf serum (FCS), 2 mM (v/v) glutamine, 100 U/ml (v/v) penicillin and 0.1 mg/ml (v/v) streptomycin (full serum medium [FSM]; Invitrogen, Paisley, UK) in a Galaxy S Incubator (Wolf Laboratories, York, UK). Once cells had reached approximately 90-100% confluency, cells were subcultured.

To subculture, the FSM was aspirated (Integra Biosciences, NH, USA) and cells washed gently with 1.5 ml Dulbecco's PBS (without $CaCl_2$ or $MgCl_2$). This was aspirated and 1.0 ml trypsin-EDTA (0.05% [w/v] trypsin, 0.04% [w/v] EDTA in PBS) gently added to cells. After being left for 2 min at 37°C, cells were resuspended in 10 ml FSM. The cell suspension was vortexed to prevent cells from clumping together and the appropriate volume of cells were transferred into a new cell culture dish. Cells were passaged every 3-4 days depending on growth rate.

2.11.2. Cell counting and viability determination

Following trypsinisation of adherent cells (see section 2.11.1), cells in suspension were counted using the Countess® automated cell counter (Invitrogen, Paisley, UK) to determine cell number and viability. 10 µl of 0.2% (v/v) trypan blue stain was mixed with 10 µl of cells in suspension in microcentrifuge tube. This was immediately added to the counter chamber slide and placed inside the Countess®. The information given by the Countess® included the total number of cells, the number of live and dead cells, percentage viability and the average size of the cell population.

2.11.3. Resuscitation of frozen cells

Frozen cells were removed from liquid nitrogen and quickly thawed to minimise any damage to the cell membranes. The cells were added into 15 ml of prewarmed (37°C) FSM in a 50 ml universal and then vortexed to avoid clumping. The cells were then transferred into a 10 cm tissue culture plate and cultured under normal growth conditions after 24 h incubation (section 2.11.1).

2.11.4. Freezing cells for storage

HEK293 cells grown to 100% confluency were resuspended in 10 ml FSM following trypsinisation as described in section 2.11.1 Cells were then centrifuged at 500 xg for 5 min at RT using a Heraeus Biofuge Primo R centrifuge (DJB LAbcare Ltd, Buckinghamshire, UK). The cell pellet was resuspended in 1 ml of cryopreservation medium (65% [v/v] SFM, 25% [v/v] FCS, 10% [v/v] DMSO) and transferred to a sterile 2 ml cryovial. These cryovials were placed in a Nalgene™ Cyro 1°C freezing container (Thermo Scientific, Northumberland, UK), filled with isopropanol and placed at -80°C overnight, which reduced the temperature by 1°C per min. The cryovials were transferred and stored in liquid nitrogen (section 2.11.3).

2.12. Transient transfection of plasmid DNA

Transfection is the process of introducing DNA into mammalian cells using non-viral methods. HEK293 cells grown in the appropriate cell culture dish were transfected using Polyplus JetPRIME® transfection reagent, following manufacturer's instructions. The cells were plated 24 h before transfection and allowed to adhere overnight. Briefly, the appropriate volume of plasmid DNA was diluted in the appropriate volume of JetPRIME® buffer (see Table 2.4). The appropriate volume of JetPRIME ® transfection reagent (2 µl per 1 µg plasmid DNA) was added. These mixtures were incubated at RT for 15 min. The DNA-JetPrime® mixture was added dropwise to the cells followed by gently rocking to mix. 24 h after transfection, the medium was changed. Cells were used for experimentation 48 h post transfection.

Table 2.4. JetPRIME® transfection guidelines depending on culture plate.

Culture Plate	Concentration of DNA (µg)	Volume of JetPRIME® buffer (µl)	Volume of JetPRIME® reagent (µl)
24-well	0.25	50	0.5
12-well	0.5	75	1
6-well/3 cm	1	200	2
6 cm	2	200	4
10 cm	5	500	10

The table shows the concentration of DNA, volume of JetPRIME® buffer and reagent used depending on culture plate.

2.13. Enzyme linked immunosorbent assay (ELISA)

Cell surface receptor expression, in the absence and presence of agonists, was assessed by ELISA (Daunt et al, 1997; Kanamarlapudi et al, 2012). Transiently transfected HEK293 cells expressing the hGLP-1R plasmid construct from 10 cm or 6 cm plates were replated (as described in section 2.11.1) in duplicate using FSM into wells of a 48-well plate coated with poly-L-lysine (0.1 mg/ml in PBS, 10 mM phosphate buffer, 2.7 mM KCl and 137 mM sodium hydroxide [NaOH], pH 7.4) and incubated at 37°C/5% CO_2 for 24 h.

Following overnight incubation, cells were serum starved. The medium was aspirated, washed 3 times with SFM and then incubated with 100 µl of SFM per well for 1 h at 37°C/5%CO_2. Cells were then left untreated or treated with an appropriate concentration of agonist in 0.5% (w/v) fat free bovine serum albumin (BSA)/SFM and incubated at 37°C/5% CO_2 for the required length of time. Cells were fixed immediately with 4% (w/v) paraformaldehyde (PFA) in PBS for no longer than 5 min on a SSL4 see-saw rocker (Stuart, Staffordshire, UK). If the PFA was left for longer than 5 min it would perforate the cell membrane, which was not desirable. The PFA was removed and the wells washed 3 times with tris-buffered saline (TBS, 10 mM Tris HCl, 150 mM NaCl, pH 7.4) and non-specific binding blocked in 1% (w/v) BSA/TBS for 45 min with rocking. The cells were then incubated with 100 µl per well of anti-hGLP-1R antibody or anti-VSVG antibody diluted 1:15000 in 1% (w/v) BSA/TBS for 1 h at RT with rocking. After incubation with primary antibody, cells were washed 3 times with TBS and then incubated with 100 µl per well of HRP-linked anti-mouse IgG diluted 1:5000 in 1% (w/v) BSA/TBS for 1 h with rocking at RT. Again the washes were repeated and then developed by adding 100 µl per well of 1-stepTM Ultra TMB-ELISA substrate for 15 min at RT with rocking. 30 µl of the developing solution was transferred in triplicate to a 96-well plate and the reaction stopped by adding an equal volume of 2 M sulphuric acid (H_2SO_4). The optical density was read at 450 nm using a Biotek plate reader (Northstar Scientific Ltd, Leeds, UK). The data obtained was analysed to show either receptor cell surface expression or percentage cell surface receptor loss.

To examine the concentration dependency of receptor internalisation by ELISA, cells were stimulated with a range of concentrations for 60 min. To investigate the time dependent effect of agonists on receptor internalisation by ELISA, cells were stimulated with a single concentration of agonist (100 nM GLP-1, 10 µl compound 2 and compound B) for 0-240 min. Where indicated, cells were preincubated with antagonists or inhibitors for the indicated time at 37°C/5% CO_2 prior to agonist stimulation and during agonist stimulation. The rest of the protocol was followed as detailed above.

2.14. Immunofluorescence

Intracellular localisation of hGLP-1R expression in response to agonist stimulation was assessed by immunofluorescence as previously described (Kanamarlapudi et al, 2012). Cells transiently transfected with hGLP-1R plasmid DNA were seeded (see section 2.11.1) onto poly-L-lysine coated 13 mm coverslips in a 24-well plate using FSM and incubated at 37°C/5% CO_2 for a further 24 h. After 24 h, cells were serum starved for 1 h at 37°C/5% CO_2 in 200 µl SFM per well. The medium was removed and cells were incubated with either the anti-hGLP-1R or anti-VSVG antibody diluted 1:5000 in 1% (w/v) BSA/SFM for 1 h at 4°C on a see-saw rocker. The cells were washed twice with ice cold PBS and either left untreated or treated with an appropriate concentration of agonist in 0.5% (w/v) fat free BSA/SFM and incubated at 37°C/5% CO_2 for the required length of time. Cells were then fixed immediately with 4% (w/v) PFA in PBS for 30 min with rocking. The PFA was removed and the wells washed 3 times with PBS, permeabilised with 0.2% (v/v) Triton-X100 in PBS for 10 min and non-specific binding sites blocked with 1% (w/v) BSA/PBS-T (PBS-0.1% (v/v) Triton-X100) for 30 min with rocking. Cells were then incubated with 200 µl of Cy™3-conjugated anti-mouse IgG secondary antibody, diluted 1:200 in 1% (w/v) BSA/PBS-T, in the dark for 1 h with rocking. Cells were washed 3 times in PBS and incubated with DAPI (1 mg/ml), diluted 1:2000 in PBS, in the dark for 5

min with rocking to stain nuclei. Lastly, the coverslips were mounted onto glass slides using 10 µl of mounting solution (0.1 M Tris HCl pH 8.5, 10% [w/v] Mowiol, 50% [v/v] glycerol) containing 2.5% (v/v) 1,4 diazabicyclo (2.2.2) octane (DABCO, anti-fading reagent) and kept in the dark at 4°C until slides were ready to be imaged.

Slides were examined and imaged using a confocal microscope (Carl Zeiss, LSM710) with a 63x oil-immersion objective lens and a 488 nm Kr/Ar laser. Emission wavelengths used were 405 nm for DAPI, 488 nm for GFP and 543 nm for Cy™3-conjugated anti-mouse IgG secondary antibody. Scale bar in confocal images represents 10 µm. The confocal images shown in figures are representative of 3 independent cell preparations.

To examine the concentration dependency of hGLP-1R internalisation by immunofluorescence, cells were stimulated with a range of concentrations for 60 min. To investigate the time dependent effect of agonists on hGLP-1R internalisation by immunofluorescence, cells were stimulated with a single concentration of agonist (100 nM GLP-1, 10 µl compound 2 and compound B) for 0-240 min. Where indicated, cells were preincubated with antagonist or inhibitors for the indicated time at 37°C/5% CO_2 prior to agonist stimulation, during antibody incubations and agonist stimulation. The rest of the protocol was followed as detailed above.

2.15. Live cell imaging

For live cell imaging, transiently transfected HEK293 cells were plated into 8-chamber glass bottom slides (Thermo Scientific, Northumberland, UK) pre-coated with poly-L-lysine and incubated at 37°C/5% CO_2 in FSM. After 24 h, cells were washed 3 times and serum starved with 200 µl per well of SFM for 1 h at 37°C/5% CO_2. Cells were then imaged twice (0 and 3 min) with no agonist added and for every 3 min after stimulating with agonist (diluted in 0.5% (w/v)

fat-free BSA/SFM) at 37°C for 60 min. Cells were imaged using a confocal microscope (Carl Zeiss, LSM710) with a 63x oil-immersion objective lens and a 488 nm Kr/Ar laser. Emission wavelengths used were 405 nm for DAPI, 488 nm for GFP and 543 nm for Cy™3-conjugated anti-mouse IgG secondary antibody. Scale bar in confocal images represents 10 μm. The confocal images shown in figures are representative of 3 independent cell preparations.

Where indicated cells were preincubated with antagonist for the indicated time at 37°C/5% CO_2 prior to agonist stimulation, during antibody incubations and agonist stimulation. The rest of the protocol was followed as detailed above.

2.16. Methylthiazol tetrazolium (MTT) assay

The methylthiazol tetrazolium (3-(4,5-dimethlthiazol-2-yl)-2,5-diphenyltetrazolium bromide, MTT) assay was performed to assess the cytotoxicity of GLP-1, compound 2 and compound B on cells (Bromberg & Alakhov, 2003). HEK293 cells were seeded into poly-L-lysine coated 96-well plates at a density of $2.75x10^4$ cells per well. PBS was added to wells surrounding the cell to prevent dehydration. After 24 h of plating, cells were washed and serum starved for 1 h in SFM at 37°C/5% CO_2. Cells were either left untreated or incubated with varying concentrations of agonist in 0.5% (w/v) fat-free BSA/SFM for a further 1 h at 37°C/5% CO_2. MTT stock reagent (5 mg/ml in PBS) diluted 1:5 in 0.5% (w/v) fat-free BSA/SFM was then added to the cells and incubated for 5 h at 37°C/5% CO_2 in the dark. After 5 h, the MTT reagent was removed and the reaction product accumulated in cells was solubilised in DMSO for 30 min. The solubilised product was quantified at 550 nm using a FLUOstar OPTIMA (BMG Labtech, Buckinghamshire, UK) plate reader. Each concentration was performed in triplicate with 3 independent cell preparations.

2.17. Luciferase assay

HEK293 cells cotransfected with the hGLP-1R plasmid and luciferase reporter plasmid for cAMP (pGL4.29-Luc-CRE) or intracellular Ca^{2+} (pGL4.30-Luc-NFAT) or ERK phosphorylation (pGL4.33-Luc-SRE) were plated in a poly-L-lysine coated 96-well half area white opaque with clear bottom plates and incubated for 24 h at 37°C/5% CO_2. Cells were treated with 25 µl increasing concentrations of agonists for 4 h (cAMP and ERK) or 8 h (Ca^{2+}) in 0.5% (w/v) BSA/SFM at 37°C/5% CO_2. After incubation, plates were left to cool to RT for 15 min and an equal volume (25 µl) of 2x ONE-Glo™ lysis buffer containing luciferase substrate was added to each well. The plate was left for 3 min on a Heidolph Tetramax 100 shaker (Heidolph UK, Essex, UK) at 250 rpm. Luminescence (relative light units [RLU]) was immediately measured using a FLUOstar OPTIMA plate reader. Each concentration was performed in triplicate with 3 independent cell preparations.

2.18. cAMP assay

2.18.1. Preparation of hGLP-1R cAMP samples

HEK293 cells transiently transfected with hGLP-1R plasmid DNA were seeded into poly-L-lysine coated 12-well plates and incubated at 37°C/5% CO_2. After 24 h, the FSM was aspirated and serum starved for 1 h at 37°C/5% CO_2. After serum starvation, cells were incubated without or with agonist in the presence of 250 µM Ro201724. The media was aspirated and 150 µl 0.1 M HCl was added to each well. Cells were harvested using a rubber policeman and transferred to a 1.5 ml microcentrifuge tube. The cell lysate was dissociated by vortexing until the suspension was homogeneous and incubated at RT for 20 min. The lysate was centrifuged at 16000 xg for 10 min in a table top Eppendorf 5415D centrifuge. The supernatant was collected into a new microcentrifuge tube and if not required straight away was stored at -80°C.

2.18.2. Preparation of cAMP Standard Curve

cAMP standards were prepared by diluting 100 pM/µl cAMP stock in 0.1 M HCl to the concentrations of 100, 20, 4, 0.8, 0.16, 0.032, 0 and 0_B (0 with no antibody added) pM/µl. 50 µl of 0.2 M NaOH was added to 100 µl of cAMP standard or sample (see section 2.18.1) to neutralise and made up to 1 ml with 850 µl TBS-0.05% (v/v) Tween 20. Samples were ready for quantification.

2.18.3. Quantification of cAMP

24 h prior to quantification 1x8 flat well strips were coated with 50 µl/well of 1 mg/ml unconjugated goat-anti rabbit diluted in coating buffer (sodium bicarbonate buffer, pH 9.5) and incubated overnight with gentle agitation using a Heidolph Tetramax 100 shaker.

The coating buffer was removed and 100 µl/well 0.5% (w/v) BSA/TBS-0.05% (v/v) Tween 20 was added for 2 h at RT to block non-specific binding sites. The blocking buffer was removed and the plate was washed twice with TBS-0.05% (v/v) Tween 20. 25 µl/well of standard cAMP and sample was added to the 96-well plate in duplicate. 12.5 µl/well of cAMP polyclonal antibody diluted 1 in 10000 in 0.5% (w/v) BSA/TBS-0.05% (v/v) Tween 20 was added to all wells except 0_B where 25 µl of 0.5% (w/v) BSA/TBS-0.05% (v/v) Tween 20 was added. The plate was incubated at RT for 1 h with gentle agitation, after which, 12.5 µl/well of cAMP-HRP antibody diluted 1 in 10000 in 0.5% (w/v) BSA/TBS-0.05% (v/v) Tween 20 was added to all wells. All wells were washed 5 times with 0.5% (w/v) BSA/TBS-0.05% (v/v) Tween 20 and 50 µl/well of 1-step Ultra TMB ELISA substrate was added and left to incubate at RT for 5 min with gentle agitation. The reaction was stopped with the addition of 50 µl/well 2 M H_2SO_4. The optical density was read at 450 nm using a Biotek plate reader. The data obtained was analysed to show percentage cAMP production compared to control.

2.19. Flow cytometry

Flow cytometry allows specific cell populations to be analysed by hydrodynamically focusing cells. Cells intercept a laser beam resulting in a pulse of scattered light proportional to the size of the cell. The forward scatter is relative to the size of the cell and the side scatter is relative to the granularity of the cell. When fluorescent labelled cells intercept the laser light, electrons are excited to a higher energy state and then emit fluorescent light when the electron returns back down to its ground state (Radcliff & Jaroszeski, 1998). See Table 2.5 for the fluorochromes used with each antibody.

HEK293 cells plated in 10 cm plates were transiently transfected with hGLP-1R plasmid DNA and incubated at 37°C/5% CO_2. After 24 h, FSM was aspirated and cells were resuspended in 10 ml FSM. Cells were then counted and their viability determined (section 2.11.2), a minimum of $1x10^6$ cells/ml were used. Cells were centrifuged at 500 xg for 5 min at 4°C using an Eppendorf 5810R centrifuge and the FSM aspirated off. Cells were washed in 2 ml ice cold PBS, centrifuged at 500 xg for 5 min at 4°C and blocked in blocking buffer (0.2% [w/v] BSA/PBS) for 1 h at 4°C. The blocking buffer was removed by centrifugation, cells were resuspended in 3 ml ice cold PBS and 1 ml of this added into 3x 1.5 ml microcentrifuge tubes. Cells were again centrifuged at 500 xg for 5 min, the PBS was aspirated from the 3x 1.5 ml microcentrifuge tubes and replaced with either 200 µl of either no antibody (unstained), anti-VSVG antibody, or anti-hGLP-1R antibody diluted 1:100 in 0.2% (w/v) BSA/PBS for 1 h at 4°C. After the primary antibody incubation, cells were centrifuged (500 xg, 5 min, 4°C) and the primary antibody removed. Cells were then washed 3 times in 1 ml ice cold PBS by centrifugation (500 xg, 5 min, 4°C) and finally resuspended in 200 µl of Cy™3-conjugated anti-mouse IgG secondary antibody, diluted 1:100 in 0.2% (w/v) BSA/PBS for 1 h at 4°C in the dark. The secondary antibody was removed and cells were washed 3 times in 1 ml ice cold PBS by centrifugation (500 xg, 5 min, 4°C), but on the final wash cells were split into 2 further 1.5 ml microcentrifuge tubes without and with 7-aminoactinomycin D (7-AAD) staining prior to the final centrifugation. Cells were resuspended in 100

µl 7-AAD (Invitrogen) diluted 1:100 in 0.2% (w/v) BSA/PBS for 5 min at 4°C in the dark. Cells were centrifuged (500 xg, 5 min, 4°C) to remove the 7-AAD stain, resuspended in 1 ml fluorescence activated cell sorting (FACS) buffer (0.2% [w/v] BSA, 0.05% [v/v] sodium azide in PBS) and transferred to FACS tubes (BD Biosciences, Oxford, UK). FACS tubes were centrifuged (500 xg, 5 min, 4°C), the buffer aspirated and cells were resuspended in a final volume of 200 µl FACS buffer.

Cells were quantified by BD FACS Aria flow cytometer (BD Bioscience) and analysed using BD FACS DIVA software. BD Cytometer Setup and Tracking (CST) settings were used with 70 micron default, 3 laser, 9 colour (4-2-3) setup. Cells in suspension were topped up with FACS Flow (IsoFlow™ Sheath Fluid, Beckman Coulter Ltd, High Wycombe, UK) until a flow rate of between 2000 and 3000 cells/s was achieved. Firstly, cells were sorted by gating the forward and side scatter profiles (P1, Figure 2.2A). Cells were then sorted into dead cells (P2, high 7-AAD PE-Texas red) and live cells (P3, low 7-AAD PE-Texas red) (Figure 2.2B). The P3 population of cells (the cells of interest) were further analysed and sorted into 2 populations. Cells with high FITC emission (pEGFP transfected cells) was selected for (P4, Figure 2.2C) and used for further analysis. A dot plot was used to select for low 7-AAD PE-Texas Red but with high FITC emission (Q1-1, Figure 2.2D). The Q1-1 population of cells were then further analysed to look for PE antibody staining (VSVG or hGLP-1R antibodies) by histograms (Figure 2.2E) and dot plots to assess expression and cells of interest were gated (Q2, Figure 2.2F). There is a high chance of spectral overlap because 3 fluorochromes were used. Therefore, using the unstained controls (without GFP epitope tag, without primary antibody and without 7-AAD staining) compensation was used to correct for spectral overlap that could have occurred when 2 or more fluorochromes were used. This ensured that the fluorescence output of each fluorochrome was representative of its designated channel (Alvarez et al, 2010). The data obtained was analysed to show cell surface expression of GFP positive cells. Plots shown in figures are representative of 3 independent cell preparations.

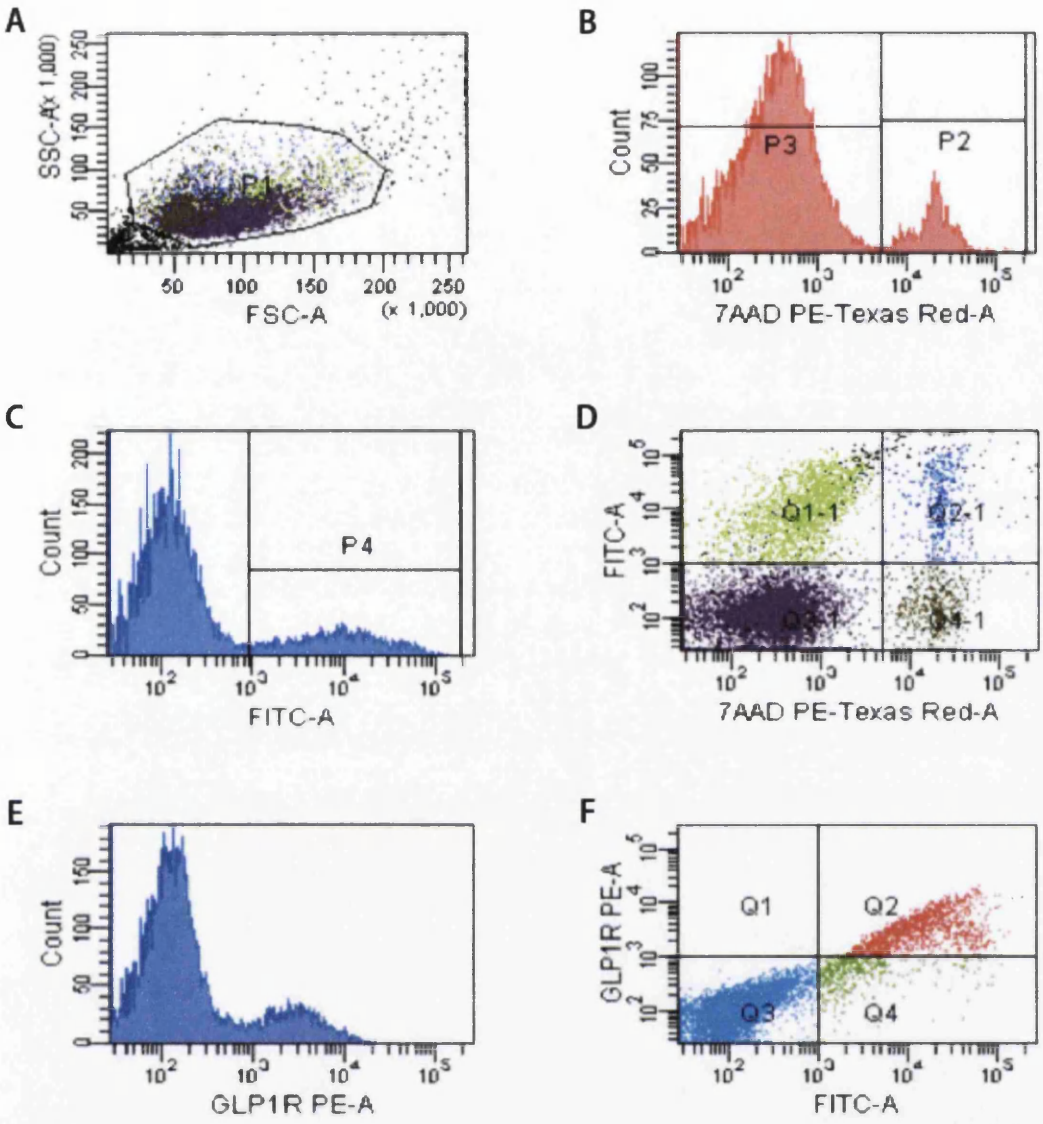

Figure 2.2. Example of gating used for flow cytometry analysis. Example of SP-VSVG-hGLP-1RΔN23-GFP transfected HEK293 cells analysed by flow cytometry. (A) A dot plot showing the P1 population of cells sorted by forward scatter and side scatter. (B) A histogram representing the P2 population with high 7-AAD staining (represents dead cells). P3 population representing live cells that have very low 7-AAD staining. This population (the cells of interest) was used for further analysis. (C) The P4 population representing cells expressing the GLP-tagged hGLP-1R and showing high FITC emission in a histogram. (D) A dot plot representing low 7-AAD and high FITC emission. The Q1-1 gated cells (the cells of interest) were used for further analysis. Cells from the Q1-1 population showing either VSVG or hGLP-1R antibody staining in a histogram (E) or dot plot (F).

Table 2.5. Fluorochromes used in flow cytometry for hGLP-1R analysis.

Epitope Tag/ Antibody	Fluorochrome	Emission (nm)
GFP	Flourescein (FITC)	519
Anti-VSVG	Phycoerythrin (PE)	578
Anti-hGLP-1R	Phycoerythrin (PE)	578
7-AAD	PE-Texas red	616

The table shows the fluorochromes and emission wavelengths for the detection of the GFP epitope tag and the anti-VSVG, anti-hGLP-1R and 7-AAD antibodies used for flow cytometry analysis.

2.20. Cell surface biotinylation

HEK293 cells transiently transfected with hGLP-1R constructs were grown to 90-100% confluency in 6-well plates and subjected to cell surface biotinylation (Alken et al, 2005; Schlondorff et al, 2009). Cells were washed and incubated at 4°C for 10 min in ice cold PBS containing 1 mM $CaCl_2$ and 1 mM $MgCl_2$. Cells were then incubated at 4°C for 1 h in 1 ml of ice cold PBS containing 1 mM $CaCl_2$ and 1mM $MgCl_2$ supplemented with 0.5 mg/ml No-weigh™ Sulpho-NHS-LC-Biotin (Thermo Scientific, Northumberland, UK). The biotin solution was removed and cells were incubated for 10 min at 4°C with 100 mM glycine in TBS to quench any remaining reactive biotin cross linker. Cells were then lysed in 250 µl of ice cold modified radio-immunoprecipitation assay (RIPA) lysis buffer (10 mM Tris HCl pH 7.5, 10 mM EDTA pH 8.5, 1% [v/v] nonyl phenoxypolyethoxylethanol [NP40], 0.1% [v/v] sodium dodecyl sulphate [SDS], 0.5% [w/v] sodium deoxycholate, 150 mM NaCl, 1% [v/v] mammalian protease

inhibitors), harvested using a rubber policeman and transferred to a 1.5 ml microcentrifuge tube. The cell lysate was sheared using a 21-gauge needle and syringe and then incubated on ice for 15 min. The lysate was centrifuged at 22000 xg for 10 min at 4°C and the supernatant was collected into a new microcentrifuge tube. A 50 µl aliquot of supernatant was collected and ½ volume of 3x sample loading buffer (3% [w/v] SDS, 75 mM Tris HCl pH 6.8, 30% [v/v] glycerol, 0.003% [w/v] bromophenol blue, 300 mM dithiothreitol [DTT]) was added, incubated at RT for 1 h and was used to assess total hGLP-1R expression. The remaining lysate was incubated with 50 µl of Dynabeads® MyOne™ Streptavidin T1 Magnetic Beads (Life technology, Paisley, UK) at 4°C for 2 h. The beads were separated on a magnet and washed 3 times with 1 ml lysis buffer. The bound receptor was eluted in 50 µl 1x sample loading buffer (1% [w/v] SDS, 25 mM Tris HCl pH 6.8, 10% [v/v] glycerol, 0.001% [w/v] bromophenol blue, 100 mM DTT) and left at RT for 1 h. Samples that were not required straight away were stored at -20°C. Total and biotinylated cell surface receptors were detected by immunoblotting as described in section 2.23.

2.21. Coimmunoprecipitation

2.21.1. Preparation of Dynabeads® and antibody binding

In a microcentrifuge tube, 25 µl (0.75 mg) of protein G Dynabeads® (Life technology, Paisley, UK) was added. Dynabeads® were collected by placing the microcentrifuge tube on a magnet and resuspended in 100 µl binding and wash buffer (PBS-0.02% [v/v] Tween 20, pH 7.4) containing 0.5 µg of antibody (2.5 µl anti-GFP, 2.5 µl anti-RFP and 5 µl anti-CAV-1). The microcentrifuge tube was rotated for 10 min at RT. The beads were washed 3 times by gentle mixing with 750 µl binding and washing buffer and placing the microcentrifuge tube on a magnet.

2.21.2. Coimmunoprecipitation

Transiently transfected HEK293 cells grown to 90-100% confluency in poly-L-lysine coated 10 cm plates were subjected to coimmunoprecipitation. After 48 h of transfection, the FSM was aspirated from plates and the cells washed 3 times in ice cold PBS. Ice cold lysis buffer was added (1 mM $CaCl_2$, 1% [v/v] TritonX-100, 0.5% [w/v] SDS in PBS) and harvested as described in section 2.20. A 50 µl aliquot of supernatant was collected and ½ volume of 3x sample loading buffer (see section 2.20) was added, incubated at RT for 1 h and was used to assess total hGLP-1R expression. The remaining lysate was incubated with 25 µl of antibody coupled Protein G Dynabeads® at 4°C for 2 h. The beads were separated on a magnet and washed once with 1 ml lysis buffer and twice with binding and wash buffer (see section 2.21.1). The bound receptor was eluted in 50 µl 1x sample loading buffer (see section 2.20) and left at RT for 1 h. Samples that were not required straight away were stored at -20°C. Total and immunoprecipitated hGLP-1R were detected by immunoblotting as described in section 2.23.

2.22. Protein estimation (bicinchoninic acid (BCA) assay)

Protein standards were made by diluting 2 mg/ml BSA stock in ddH_2O to the concentrations of 0, 0.2, 0.4, 0.6, 0.8, 1.0 mg/ml. 10 µl of protein standard was pipetted into wells of a 96-well flat bottom plate, in duplicate. All protein samples were diluted (1:5 and 1:10) in ddH_2O and added to the plate, in duplicate. A reaction mixture of copper sulphate and BCA solution (1:50, v/v) was made up and 80 µl added to each well containing either the standard or samples. The plate was then incubated at 37°C for 30 min in an Incucell incubator and the absorbance measured at 490 nm using the Biotek plate reader. Standard Curves were fitted using Microsoft Office Excel 2011 (Microsoft Corporation, WA, USA) and the unknown protein concentrations were calculated by interpolation of the standard curve.

2.23. Immunoblotting

2.23.1. Preparation of hGLP-1R transfected whole cell lysates

HEK293 cells transiently transfected with the hGLP-1R constructs were grown to 90-100% confluency in 6-well plates. The medium was aspirated and cells were washed 3 times with ice cold PBS. Cells were lysed by the addition of 250 µl ice cold modified RIPA lysis buffer and harvested as previously described in section 2.20. A 10 µl aliquot of each sample was retained for protein estimation (see section 2.22). The supernatant was collected and ½ volume of 3x sample loading buffer (see section 2.20) was added to the remaining lysate and incubated at RT for 1 h. Samples that were not required straight away were stored at -20°C.

2.23.2. Preparation of ERK1/2 phosphorylation cell lysates

Transiently transfected HEK293 cells were grown to 90-100% confluency in poly-L-lysine coated 6-well plates. After 24 h the FSM was aspirated and cells serum starved for 1 h at 37°C/5% CO_2. Where indicated cells were preincubated with inhibitors for 30 min at 37°C/5% CO_2 prior to agonist stimulation and then incubated without or with agonist for 5 min at the required concentration. The media was aspirated and cells were lysed by the addition of 250 µl of ice cold modified RIPA lysis buffer for ERK phosphorylation (50 mM Tris HCl pH 7.5, 0.2 M NaCl, 10 mM $MgCl_2$, 0.1% [v/v] SDS, 0.5% [w/v] sodium deoxycholate, 1% [v/v] TritonX-100, 5% [v/v] glycerol, 1% [v/v] mammalian protease inhibitors). Cells were harvested as described in section 2.20. A 10 µl aliquot of each sample was retained for protein estimation (see section 2.22). The supernatant was collected and ¼ volume of 5x sample loading buffer (5% [w/v] SDS, 125 mM Tris HCl pH 6.8; 50% [v/v] glycerol; 0.025% [w/v] bromophenol blue; 20% [v/v] β-Mercaptoethanol) was added to the remaining lysate, and the lysate boiled at 100°C for 5 min using a Grant heating block. Samples that were not required straight away were stored at -20°C.

2.23.3. SDS-Polyacrylamide Gel Electrophoresis (SDS-PAGE)

The required percentage of running gel was made by adding 4x Tris SDS pH 8.8, 30% (v/v) acrylamide, N, N, N', N'-tetramethylethylenediamine (TEMED) and ammonium persulphate (APS) (see Table 2.6 for recipes). The solution was mixed and poured between a spacer plate and short plate (BioRad, Herts, UK). Water-saturated butanol was added to ensure a level edge. After polymerisation (~30 min), the water-saturated butanol was washed off with ddH_2O. The stacking gel (125 mM Tris HCl pH 6.8, 0.1% [w/v] SDS, 5% [v/v] acrylamide, 0.01% [v/v] TEMED, 0.01% [w/v] APS) was poured onto the running gel and a comb added to form loading wells. The gel was left to polymerise (~20 min), after which the comb was removed and the wells rinsed with ddH_2O.

The gels were assembled into a clamping frame and placed in a mini tank (BioRad, Herts, UK). The central reservoir was completely filled and the tank half filled with running buffer (25 mM Tris HCl, 192 mM glycine, 0.1% [w/v] SDS, pH 8.3). Up to 25 µl of sample and 5 µl protein standard was loaded into each well. Electrophoresis was carried out at 200 V until the loading dye front reached the bottom of the gel (~40 min) using the PowerPac Basic (BioRad, Herts, UK).

Table 2.6. Running gel recipes.

Reagent	7.5% ~37-250kDa	10% ~25-150kDa	12% ~15-100kDa	15% ~10-75kDa
Water	5 ml	4.2 ml	3.5 ml	2.5 ml
4x Tris SDS (pH 8.8)	2.5 ml	2.5 ml	2.5 ml	2.5 ml
30% Acrylamide	2.5 ml	3.3 ml	4 ml	5 ml
TEMED	10 µl	10 µl	10 µl	10 µl
APS	1 small spatula	1 small spatula	1 small spatula	1 small spatula

The table shows volumes required of water, 4x Tris SDS, 30% acrylamide, APS and TEMED to produce a 7.5%, 10%, 12% or 15% gel depending on the molecular weight of the protein of interest.

2.23.4. Semi-Dry Membrane Transfer

A 'semi dry' method was used to transfer proteins from gels to polyvinylidene fluoride (PVDF) membranes (pore size 0.45 µM). The filter paper and PDVF were precut to the size of the gel. Here, PVDF membrane was soaked in methanol for 30 s, and then in transfer buffer (25 mM Tris HCl, 192 mM glycine, 20% [v/v] methanol, pH 8.3, chilled to 4°C) for 5 min. After electrophoresis, the gel was carefully removed from the casting plates, the stacking gel removed and the running gel soaked in transfer buffer for 5 min. Using a Trans-Blot® SD Semi-Dry Transfer Cell machine (BioRad, Herts, UK) a piece of presoaked PDVF membrane was placed on top of 3 layers of presoaked filter paper, the gel was placed on top of this and finally 3 more sheets of presoaked filter paper added.

The transfer was performed at 15 V for 75 min using a PowerPac 200 (BioRad, Herts, UK).

2.23.5. Immunoblotting

Once transfer was completed, proteins were visualised with ponceau red stain (0.1% [w/v] ponceau S and 5% [w/v] acetic acid) to ensure good transfer had occurred. Once proteins had stained, the PDVF membrane was washed with TBS-Tween 20 (10 mM Tris HCl pH 7.4, 150 mM NaCl, 0.05% [v/v] Tween 20) on a SSL4 see-saw rocker, to remove the stain. The membrane was then blocked in 5% (w/v) non-fat milk powder (Marvel, Lincolnshire, UK) prepared in TBS-Tween 20 (5% [w/v] milk-TBS-Tween 20) on a rocker for 1 h at RT or overnight at 4°C. After blocking, the membrane was sealed in a bag with 2 ml of 5% (w/v) milk-TBS-Tween 20 containing primary antibody at an appropriate dilution (Table 2.7). The sealed bags were placed in TBS-Tween 20 for 1 h at RT or overnight at 4°C with rocking. After incubating with the primary antibody, the membrane was washed 5 times for 5 min in TBS-Tween 20. Again the membrane was sealed in a bag with 2 ml of secondary antibody diluted 1:5000 (Table 2.7) in 5% (w/v) milk-TBS-Tween 20 and incubated for 1 h at RT with rocking. The membrane was once again washed 5 times for 5 min in TBS-Tween 20.

Visualisation of bands on the membrane was achieved using Amersham ECL Select immunoblotting Detection Reagent. The detection reagent was made up by adding equal volumes of detection reagents 1 and 2. The membrane was placed face down in the detection reagent for 1 min and then placed face up in the ChemiDoc™ XRS imaging machine (BioRad, Herts, UK). The membrane was exposed for 1, 10, 30, 90 and 270 s using Quantity One software (BioRad, Herts, UK). Membranes were stored at 4°C. Image-J software (Gallwitz, 2010) was used for densitometry analysis. The blots shown in figures are representative of 3 independent cell preparations.

Table 2.7. Series of antibodies used in immunoblotting.

Primary Antibody	Secondary Antibody
Polyclonal anti-phospho p44/42 MAPK (1:1000 dilution)	Donkey anti-rabbit IgG, HRP-linked (1:5000 dilution)
Polyclonal anti-p44/42 MAPK (1:1000 dilution)	Donkey anti-rabbit IgG, HRP-linked (1:5000 dilution)
Polyclonal anti-VSVG tag (Biotin) (1:1000 dilution)	Donkey anti-rabbit IgG, HRP-linked (1:5000 dilution)
Monoclonal anti-GFP (1:500 dilution)	Sheep anti-mouse IgG, HRP-linked (1:5000 dilution)
Monoclonal anti-hGLP-1R (1:500 dilution)	Sheep anti-mouse IgG, HRP-linked (1:5000 dilution)

The table shows the primary and secondary antibody used for immunoblotting and their dilutions.

2.23.6. Stripping and reprobing

Previously probed membranes were sealed in a bag with 2 ml immunoblot stripping buffer (Thermo Scientific, Northumberland, UK) and left at RT for ~15 min with gentle rocking. Once membranes were stripped, blots were washed twice with ddH_2O for 1 min and then once in TBS-Tween 20 for 5 min. The membrane was then blocked, reprobed with the required primary and secondary antibody and finally visualised as described in section 2.23.5.

2.24. Tunicamycin treatment

This assay was carried out as described previously (Whitaker et al, 2012). HEK293 cells were either left untreated (DMSO) or treated with 5 μg/ml tunicamycin in FSM at time of transfection. Cells were lysed and harvested for immunoblotting 48 h post transfection as described in section 2.23.1.

2.25. Glycosidase treatment

2.25.1. Preparation of post nuclear supernatant fractions

This assay was carried out as described previously (Huang et al, 2010). HEK293 cells transiently transfected with the hGLP-1R DNA plasmid was grown to confluency in a 10 cm plate. 48 h after transfection the medium was aspirated and cells were washed twice with ice cold PBS. Cells were harvested with a rubber policeman in 2 ml ice cold PBS. Cells were centrifuged at 200 xg for 2 min at 4°C in an Eppendorf 5810R centrifuge. The supernatant was removed and the pellet resuspended in 1 ml homogenisation buffer (1 mM EDTA, 10 mM Tris HCl pH 7.5, 1 mM phenylmethanesulfonylfluoride [PMSF], 1% [v/v] mammalian protease inhibitors) and incubated on ice for 15 min. Cells were then sonicated at 80% amplitude for 3 x 10 s with 1 min intervals using a Sonics Vibra Cell VCX130 (Jencons-Pls, Bedfordshire, UK). The lysate was centrifuged at 300 xg for 10 min at 4°C in an Eppendorf 5810R centrifuge to pellet nuclei and unbroken cells. The supernatant was collected into a new microcentrifuge tube and a 10 μl aliquot of each sample retained for protein estimation (see section 2.22). The post-nuclear supernatant fraction was diluted with ice cold glycerol to 5 mg/ml and stored in aliquots at -80°C.

2.25.2. Glycosidase treatment

A 36 µl aliquot of 5 mg/ml post-nuclear supernatant fraction was used for each treatment following manufacturer's instructions. Briefly, 4 µl of 10x glycoprotein denaturing buffer was added to the 36 µl aliquot of 5 mg/ml post-nuclear supernatant fraction and incubated at RT for 1 h. The sample was separated into 3 microcentrifuge tubes and the proteins were either left untreated or treated with either 500 units of PNGase F or Endo H in a total reaction volume of 20 µl containing 1% (v/v) NP40 and either 1x G7 or G5 reaction buffer, respectively for 1 h at 37°C. Reactions were stopped with the addition of ½ volume of 3x sample loading buffer (section 2.20) for 1 h at RT. Proteins were then subjected to immunoblotting as described in section 2.23.

2.26. Data analysis

Data were analysed using the GraphPad Prism program. All data are presented as means ± standard error of the mean (SEM) of three independent experiments. Statistical comparisons between the control and test value was made by a two-tailed unpaired student t-test. Statistical analysis between multiple groups were determined by the Bonferroni's post test after one-way or two-way analysis of variance (ANOVA), where $p>0.05$ was considered as statistically not significant (n.s.), and $p<0.05$, $p<0.01$ and $p<0.001$ shown as *, ** and *** respectively, was considered statistically significant. Concentration response curves were also fitted using Prism, according to a standard logistic equation. Scale bar in confocal images represents 10 µm. Confocal images shown in the figures are representative of 190-200 transfected cells from three different experiments. Similarly, immunoblotting data shown in the figures are representative of three independent experiments. Cluster Omega (1.2.1) was used for multiple sequence alignment (Goujon et al, 2010; McWilliam et al, 2013; Sievers et al, 2011).

3. The Region After the Signal Peptide is Critical for Human Glucagon Like Peptide-1 Receptor Cell Surface Expression

3.1. Introduction

Glucagon like peptide-1 (GLP-1) is a polypeptide hormone secreted by the intestinal L-cells into the blood in response to food intake (Drucker et al, 1987; Holst, 2007; Thompson & Kanamarlapudi, 2013). It is an effective insulinotropic agent, which lowers blood glucose levels and increases insulin secretion (Doyle & Egan, 2007; Holz et al, 1999; Thompson & Kanamarlapudi, 2013). It acts as an agonist to the GLP-1 receptor (GLP-1R), a family B G-protein coupled receptor (GPCR). The binding of GLP-1 to the GLP-1R results in insulin secretion from pancreatic β-cells, making human GLP-1R (hGLP-1R) an important target in the treatment of type 2 diabetes (Gallwitz, 2010; Thompson & Kanamarlapudi, 2013).

Family B GPCRs contain a N-terminal domain signal peptide (SP) sequence that is often critical for the synthesis and processing of the receptor (Kochl et al, 2002). The SP is about 20 amino acids (aa) long and contains a run of hydrophobic residues. The first stage of protein targeting, during its synthesis, is insertion into the endoplasmic reticulum (ER) by binding to the signal recognition particle (SRP), which is usually mediated by the SP (Hegde & Lingappa, 1997). For example, deleting the SP sequence of the thyrotropin receptor (TR) abolished its functionality (Akamizu et al, 1990; Ban et al, 1992). However, the SP of the corticotropin-releasing factor (CRF) type 2a receptor although present, is incapable of mediating ER targeting (Rutz et al, 2006; Schulz et al, 2010). Further, the SP of the CRF_1 receptor is required for its expression but not for its function (Alken et al, 2005). The GLP-1R contains a cleavable N-terminal SP (23aa long), its cleavage was not required for synthesis

of the receptor but was essential for cell surface expression of the receptor (Huang et al, 2010). Mutation of the SP ($Ala^{21}Arg$) to prevent its cleavage has been shown to result in retention of the GLP-1R within the ER. Further, a mutation of Glu^{34} was shown to facilitate GLP-1R cell surface expression when the SP was deleted (Huang et al, 2010). The aa sequence following the SP in the GLP-1R, Gly^{27}-Trp^{39}, is relatively hydrophobic and it has previously been suggested that this region may be recognised by the SRP for synthesis of the receptor (Hatsuzawa et al, 1997; Huang et al, 2010).

GPCRs synthesised in the ER translocate to the Golgi before being targeted to the cell surface. In this process, GPCRs undergo post- or co-translational modifications including glycosylation, methylation, phosphorylation, sulfation and lipid addition (Achour et al, 2008; Duvernay et al, 2005). The *N*-linked glycosylated GPCRs are processed further in the ER and Golgi before translocation and insertion into the plasma membrane (Wallin & Vonheijne, 1995). The GLP-1R has been shown to undergo *N*-linked glycosylation at positions Asn^{63}, Asn^{82} and Asn^{115} within the ER (Chen et al, 2010; Whitaker et al, 2012).

The hGLP-1R has three residues, Trp^{39}, Tyr^{69} and Tyr^{88}, within its N-terminal domain that are important for agonist binding (Runge et al, 2008; Underwood et al, 2010; Van Eyll et al, 1996). Trp^{39} has importance in maintaining the structure of the N-terminal domain of the GLP-1R by interacting with Tyr^{42}, Phe^{66} and the adjacent disulphide bond (Cys^{46}-Cys^{71}) (Parthier et al, 2007). It has been demonstrated that GLP-1 could not bind and activate the GLP-1R when Trp^{39} was substituted with Ala or Phe (Van Eyll et al, 1996). Further, Phe^{22}, Ile^{23} and Leu^{26} of GLP-1 interacts with Trp^{39} in addition to Val^{36}, Asp^{67}, Tyr^{69}, Arg^{121} and Leu^{123} of the GLP-1R (Underwood et al, 2010). Tyr^{69}, which is centrally located within the N-terminal domain, interacts with Asp^{67} and has been shown to be involved in GLP-1 binding to its receptor (Runge et al, 2008). Tyr^{88} is involved in making the hydrophobic agonist binding site, which interacts with Leu^{32} of GLP-1 and Leu^{26} of Exendin-4 (Runge et al, 2008; Underwood et al, 2010). Although, Trp^{39}, Tyr^{69} and Tyr^{88} residues within the GLP-1R have been shown to

be required for agonist binding, their role in hGLP-1R trafficking, function and *N*-linked glycosylation are currently unknown.

The GLP-1R is a major therapeutic target in the treatment of type 2 diabetes, therefore a better understanding of its membrane trafficking is of high importance. This study determined that the SP is cleaved in the mature hGLP-1R. Cell surface expression was almost abolished with a mutation of the SP (A21R) to prevent its cleavage, demonstrating that the cleavage of the SP was essential for cell surface expression of the hGLP-1R. Although the role of the SP in family B GPCR trafficking is well established, the significance of the hydrophobic region after the SP (HRASP) is unclear. Here, the HRASP was shown to be necessary for efficient hGLP-1R trafficking to the cell surface. Further, this study indicated that the hGLP-1R undergoes *N*-linked glycosylation and only the mature fully glycosylated form is found at the cell surface. It was also demonstrated that preventing cleavage of the SP inhibited hGLP-1R cell surface expression by affecting *N*-linked glycosylation. Additionally, mutating Trp^{39}, Tyr^{69} and Tyr^{88} within the hGLP-1R abolished cell surface expression of the receptor without affecting *N*-linked glycosylation and cleavage of the SP.

3.2. Materials and methods

3.2.1. Materials

The primary antibodies used were rabbit anti-vesicular stomatitis virus glycoprotein (VSVG) (Immunoblotting, Abcam Biochemicals), mouse anti-VSVG (ELISA and immunofluorescence, Sigma), mouse anti-green fluorescent protein (GFP) (Roche), mouse anti-hGLP-1R (ELISA and immunofluorescence, R&D Systems), mouse anti-hGLP-1R (Immunoblotting, Santa Cruz). The Cy3-conjugated anti-mouse immunoglobulin G (IgG) secondary antibody (Jackson Laboratories) was used for immunofluorescence. The horseradish peroxidase (HRP)-conjugated anti-mouse and anti-rabbit IgG (GE Healthcare) secondary antibodies were used for immunoblotting. Enhanced chemiluminescence (ECL)

select reagent was obtained from GE Healthcare. The cyclic monophosphate (cAMP) polyclonal antibody and cAMP-HRP were obtained from Genscript. GLP-1 (Liraglutide) was from Novo Nordisk. All other chemicals were from Sigma unless otherwise stated.

3.2.2. Plasmids

The full-length hGLP-1RΔN23 cDNA was amplified from mammalian gene collection (MGC) clone 142053 (Source Bioscience) by polymerase chain reaction (PCR) using High Fidelity Taq DNA polymerase (Roche Applied Science) and sequence specific primers containing *Eco*RI restriction site and VSVG-tag coding sequence (5' primer), and *Sal*I restriction site and no stop codon (3' primer). SP-VSVG-hGLP-1RΔN23 cDNA was amplified by overlap PCR using VSVG-hGLP-1RΔN23 cDNA as the template, the sense primer, containing *Eco*RI restriction site, the SP (1-23aa) coding sequence followed by VSVG coding sequence and 3' primer. The cDNA was digested with *Eco*RI and *Sal*I, and cloned in frame into the same sites of pEGFP-N1 vector (Clontech) for expression as the N-terminus VSVG-tagged (after the SP) and the C-terminus GFP-tagged fusion protein in mammalian cells (SP-VSVG-hGLP-1RΔN23-GFP). The point mutations within the hGLP-1R were generated using Quickchange II XL site-directed mutagenesis kit (Stratagene) and SP-VSVG-hGLP-1RΔN23-GFP plasmid as the template. The mutants with internal deletions (Δ) within the N-terminus of hGLP-1R were generated using Q5 site-directed mutagenesis kit (New England Biolabs) and SP-VSVG-hGLP-1RΔN23-GFP plasmid as the template. See Table 3.1 for constructs used in this study.

Table 3.1. Series of hGLP-1R constructs used in this study.

	Construct Name	Abbreviation	Epitope Tags
1	SP-VSVG-hGLP-1RΔN23-GFP	SP-VSVG	VSVG GFP
2	VSVG-hGLP-1R-GFP	VSVG-SP	VSVG GFP
3	VSVG-hGLP-1R	VSVG-hGLP-1R	VSVG
4	hGLP-1R-GFP	hGLP-1R-GFP	GFP
5	hGLP-1R	hGLP-1R	-
6	hGLP-1RΔN23	hGLP-1RΔN23	-
7	VSVG-hGLP-1RΔN23-GFP	ΔSP	VSVG GFP
8	VSVG-VSP-hGLP-1RΔN23-GFP	VSP-ΔSP	VSVG GFP
9	VSVG-hGLP-1R A21R-GFP	A21R	VSVG GFP
10	VSVG-hGLP-1RΔN24-GFP	ΔN24	VSVG GFP
11	VSVG-hGLP-1RΔN30-GFP	ΔN30	VSVG GFP
12	VSVG-hGLP-1RΔN35-GFP	ΔN35	VSVG GFP
13	VSVG-hGLP-1RΔN40-GFP	ΔN40	VSVG GFP
14	SP-VSVG-hGLP-1RΔN23 Δ31-40-GFP	Δ31-40	VSVG GFP

15	VSVG-hGLP-1RΔN145-GFP	ΔN145	VSVG GFP
16	SP-VSVG-hGLP-1RΔN23 N63,82,115L-GFP	N63,82,115L	VSVG GFP
17	SP-VSVG-hGLP-1RΔN23 E34K-GFP	E34K	VSVG GFP
18	SP-VSVG-hGLP-1RΔN23 W39A-GFP	W39A	VSVG GFP
19	SP-VSVG-hGLP-1RΔN23 Y69A-GFP	Y69A	VSVG GFP
20	SP-VSVG-hGLP-1RΔN23 Y88A-GFP	Y88A	VSVG GFP

The table shows the hGLP-1R constructs full name, abbreviated name and epitope tags.

3.2.3. Cell culture and transfection

Human embryonic kidney 293 (HEK293) cells were maintained at 37°C in a 5% CO_2 humidified environment in Dulbecco's modified Eagle medium (DMEM; serum free medium [SFM]) supplemented with 10% fetal calf serum, 2 mM glutamine, 100 U/ml penicillin and 0.1 mg/ml streptomycin (full serum medium [FSM]). Cells were transiently transfected for 48 h using JetPrime transfection reagent (Polyplus; 2 µl/µg DNA) according to the manufacturer's instructions.

3.2.4. Enzyme linked immunosorbent assay (ELISA)

This is carried out as described previously with unpermeabilised cells to quantify cell surface expression (Kanamarlapudi et al, 2012). Briefly, HEK293 cells expressing the hGLP-1R were serum starved for 1 h and then stimulated without or with agonist at 37°C/5% CO_2. Where indicated, cells were incubated

without or with inhibitors for 30 min prior to stimulation with agonist at 37°C/5% CO_2. Cells were then fixed with 4% paraformaldehyde (PFA) for 5 min and non-specific binding sites blocked with 1% bovine serum albumin (BSA) made in Tris buffered saline (TBS) (1% BSA/TBS) for 45 min. Cells were incubated with either the anti-hGLP-1R or anti-VSVG mouse antibody (diluted 1:15000) in 1% BSA/TBS for 1 h, washed with TBS and then incubated with the HRP-conjugated anti-mouse IgG (diluted 1:5000) in 1% BSA/TBS for 1 h. Cells were washed and developed using 1-step Ultra TMB-ELISA substrate (Bio-Rad) for 15 min and the reaction stopped by adding an equal volume of 2 M sulphuric acid. The optical density was read at 450 nm using a plate reader.

3.2.5. Immunofluorescence

Intracellular localisation of hGLP-1R expression was assessed by immunofluorescence as described previously (Kanamarlapudi et al, 2012). Briefly, cells were serum starved for 1 h and where indicated cells were preincubated without or with inhibitors at the indicated concentration for 30 min. Cells were then incubated with either the anti-hGLP-1R or anti-VSVG mouse antibody (diluted 1:5000) in 1% BSA/SFM for 1 h at 4°C and then stimulated without or with agonist in the presence of inhibitor at 37°C/5% CO_2. Cells were then fixed with 4% PFA for 30 min. Cells were permeabilised with 0.2% Triton X-100 made in phosphate buffered saline (PBS) for 10 min, blocked in blocking buffer (1% BSA made in wash buffer [0.1% Triton X-100 in PBS]) for 30 min and then incubated with the Cy3-conjugated anti-mouse antibody (diluted 1:200 in blocking buffer) for 1 h. Cells were then washed 3 times with wash buffer and incubated with DAPI (4′,6-diamidino-2-phenylindole dihydrochloride, 1 mg/ml) diluted 1:2000 in PBS to stain nucleus. Coverslips were mounted on glass microscopic slides using mounting solution (0.1 M Tris-hydrochloric acid [HCl], pH 8.5, 10% Mowiol 50% glycerol) containing 2.5% DABCO (1,4 diazabicyclo (2.2.2) octane). Immunofluorescence staining was visualised using a Zeiss LSM710 confocal microscope fitted with a 63x oil immersion lens.

3.2.6. cAMP assay

Cells were serum starved for 1 h and then stimulated without or with 100 nM GLP-1 for 1 h at 37°C/5% CO_2 in the presence of 0.25 mM phosphodiesterase inhibitor Ro201724. Cells were lysed and cAMP levels in the cell lysates were estimated using the cAMP direct immunoassay kit (Abcam).

3.2.7. Flow cytometry

Cells in suspension were incubated in blocking buffer (0.2% BSA/PBS) for 1 h at 4°C and then with either the anti-hGLP-1R or anti-VSVG mouse antibodies (diluted 1:100 in blocking buffer) for 1 h at 4°C. Cells were washed 3 times with PBS and incubated with the Cy3-conjugated anti-mouse antibody, diluted 1:100 in blocking buffer for 1 h at 4°C in the dark. Cells were washed 3 times and incubated with 7-AAD diluted 1:100 in blocking buffer for 5 min at 4°C in the dark. Cells were resuspended in 1 ml fluorescence-activated cell sorting (FACS) buffer (0.2% BSA, 0.05% sodium azide in PBS) and analysed using BD FACS Aria flow cytometer (BD Bioscience) and BD FACS DIVA software.

3.2.8. Cell lysates

To make cell lysates, HEK293 cells expressing the hGLP-1R were washed 3 times with ice cold PBS and lysed in ice cold modified RIPA lysis buffer (10 mM Tris HCl, pH 7.5 containing 10 mM ethylenediaminetetraacetic acid [EDTA], 1% Nonidet P40 [NP40], 0.1% sodium dodecyl sulphate [SDS], 0.5% sodium deoxycholate and 150 mM sodium chloride [NaCl]) with 1% mammalian protease inhibitors. Cell lysates were incubated at 4°C for 15 min and then centrifuged at 22000 xg for 10 min at 4°C. The supernatant was collected and ½ volume of 3x SDS-polyacrylamide gel electrophoresis (PAGE) sample loading buffer (75 mM Tris HCl, pH 6.8 containing 3% SDS, 30% glycerol, 0.003% bromophenol blue and 0.3 M dithiothreitol [DTT]) was added and left at room temperature for 1 h. These cell lysates were used to detect hGLP-1R expression by immunoblotting using the anti-GFP and anti-VSVG antibodies.

3.2.9. Surface biotinylation

This was performed as described previously (Alken et al, 2005). Cells were washed with ice cold containing 1 mM calcium chloride ($CaCl_2$) and 1 mM magnesium chloride ($MgCl_2$) and incubated at 4°C for 1 h with 0.5 mg/ml Sulpho-NHS-LC-Biotin (Thermo Scientific). Cells were then incubated for 10 min at 4°C with 100 mM glycine in TBS to quench any remaining reactive biotin cross linker and lysed in ice cold modified RIPA lysis buffer with 1% mammalian protease inhibitors. Cell lysates were incubated with Streptavidin Magnetic Beads (Invitrogen) at 4°C for 2 h. Beads were washed 3 times with lysis buffer and the bound protein eluted in 1x SDS-PAGE sample loading buffer (25 mM Tris HCl, pH 6.8, containing 1% SDS, 10% glycerol, 0.001% bromophenol blue and 0.1 M dithiothreitol [DTT]). The lysate not incubated with beads was mixed with ½ volume of 3x SDS PAGE sample loading buffer and used to assess total hGLP-1R. Total and biotinylated cell surface receptors were detected by immunoblotting.

3.2.10. Immunoblotting

Proteins were separated in a SDS-PAGE gel by electrophoresis and transferred onto polyvinylidene fluoride (PDVF) membrane. Membranes were blocked with TBST (TBS with 0.1% tween 20) containing 5% milk powder (blocking buffer) for 1 h at room temperature or overnight at 4°C. Membranes were immunoblotted with the anti-GFP mouse antibody (diluted 1:500 in blocking buffer) for 1 h at room temperature or overnight at 4°C. Membranes were washed and then incubated with the HRP-conjugated anti-mouse secondary antibody (diluted 1:2500 in blocking buffer) for 1 h at room temperature. Membranes were then incubated in ECL select substrate and bands visualised using the ChemiDoc™ XRS system (Bio-Rad). Blots probed with the anti-GFP mouse antibody were stripped with western blot stripping buffer (Thermo Scientific) and reprobed with the anti-VSVG rabbit antibody (diluted 1:1000 in blocking buffer) and the HRP-conjugated anti-rabbit secondary antibody (diluted 1:2500 in blocking buffer) as described above.

3.2.11. Tunicamycin treatment

This was carried out as described previously (Whitaker et al, 2012). Briefly, cells were treated with 5 μg/ml tunicamycin at the time of transfection. After 48 h of transfection, cells were lysed and subjected to immunoblotting.

3.2.12. Glycosidase treatment

This assay was carried out as described previously (Huang et al, 2010). Cells harvested from a 10 cm plate by trypsinisation were resuspended in 1 ml homogenisation buffer (10 mM Tris HCl, pH 7.5, 1 mM EDTA, 1 mM phenylmethanesulfonylfluoride [PMSF]) containing 1% mammalian protease inhibitors and incubated on ice for 15 min. Cells were then sonicated at 80% amplitude for 3x 10 s with 1 min intervals. The lysate was centrifuged at 300 xg for 10 min at 4°C to pellet nuclei and unbroken cells. An aliquot of post-nuclear supernatant fraction (50 μg of protein) was incubated with glycoprotein denaturing buffer at room temperature for 1 h and then treated without or with 500 units of either PNGase F or Endo H for 1 h at 37°C. Reactions were stopped with the addition of ½ volume of 3x SDS-PAGE sample loading buffer and subjected to immunoblotting.

3.2.13. Data analysis

Data were analysed using the GraphPad Prism program. All data are presented as means ± standard error of the mean (SEM) of three independent experiments. Statistical comparisons between the control and test value was made by a two-tailed unpaired student t-test. Statistical analysis between multiple groups were determined by the Bonferroni's post test after one-way or two-way analysis of variance (ANOVA), where $p>0.05$ was considered as statistically not significant (n.s.), and $p<0.05$, $p<0.01$ and $p<0.001$ shown as *, ** and *** respectively, was considered statistically significant. Concentration response curves were also fitted using Prism, according to a standard logistic equation. Scale bar in confocal images represents 10 μm. Confocal images shown in the figures are representative of 190-200 transfected cells from three

different experiments. Similarly, immunoblotting data shown in the figures are representative of three independent experiments.

3.3. Results

3.3.1. HGLP-1R expressing at the cell surface shows no SP

It has been shown previously that the mature hGLP-1R expressing at the cell surface is without the SP (1-23aa) (Huang et al, 2010). To confirm whether the SP is cleaved off from the mature hGLP-1R that is targeted to the plasma membrane, constructs containing a GFP-epitope at the C-terminus and VSVG-epitope at the N-terminus before (SP-VSVG) or after the SP (VSVG-SP) were generated (Figure 3.1A). HEK293 cells transfected with these constructs were analysed for hGLP-1R cell surface expression by ELISA (Figure 3.1D), immunofluorescence (Figure 3.1F) and flow cytometry (Figure 3.1G) using the anti-hGLP-1R and anti-VSVG antibodies. HEK293 cells expressing the SP-VSVG construct showed cell surface expression of the receptor with both antibodies. However, HEK293 cells expressing the VSVG-SP construct showed signal at the cell surface with the anti-hGLP-1R antibody but not with the VSVG antibody (100.0 ± 0.6% versus 0.0 ± 0.6% by ELISA and 93.8 ± 2.6% versus 1.8 ± 1.1% by flow cytometry with the anti-hGLP-1R antibody [$p<0.001$] versus the anti-VSVG antibody [$p>0.05$], respectively). This result suggested that the SP is cleaved in the membrane targeted hGLP-1R.

Both the SP-VSVG and VSVG-SP constructs showed a doublet (~65 kDa and ~85 kDa in size) when the lysates of HEK293 cells transfected with these constructs were immunoblotted with the anti-GFP antibody (Figure 3.1C). In addition, the SP-VSVG but not the VSVG-SP construct showed a doublet in the immunoblot probed with the anti-VSVG antibody, indicating that the SP is cleaved off from the hGLP-1R before it is targeted to the cell surface. Further, when HEK293 cells expressing these constructs were subjected to cell surface biotinylation, only a single band at ~85 kDa was observed in the total lysate (Figure 3.1B). This

demonstrated the ~85 kDa band represents the mature form of the hGLP-1R that targeted to the cell surface.

The GLP-1R is a $G\alpha_s$ coupled GPCR and therefore the activity of the receptor was assessed by measuring cAMP produced in hGLP-1R expressing cells stimulated with agonist (Figure 3.1E). The VSVG-SP construct had 99.6 ± 0.4% ($p>0.05$) cAMP accumulation compared to the SP-VSVG construct, confirming the VSVG-SP is functionally no different from the SP-VSVG construct. Furthermore, the cAMP activity of SP-VSVG (which contains both VSVG and GFP tags) is similar to that of the hGLP-1R with no tag or either of the VSVG-tag or GFP-tag, indicating that the attachment of the VSVG and GFP tags to the hGLP-1R had no effect on the activity of the receptor (see Chapter 4, Figure 4.2A,C-D). For further experimentation the SP-VSVG construct was used as the wild type (WT) control.

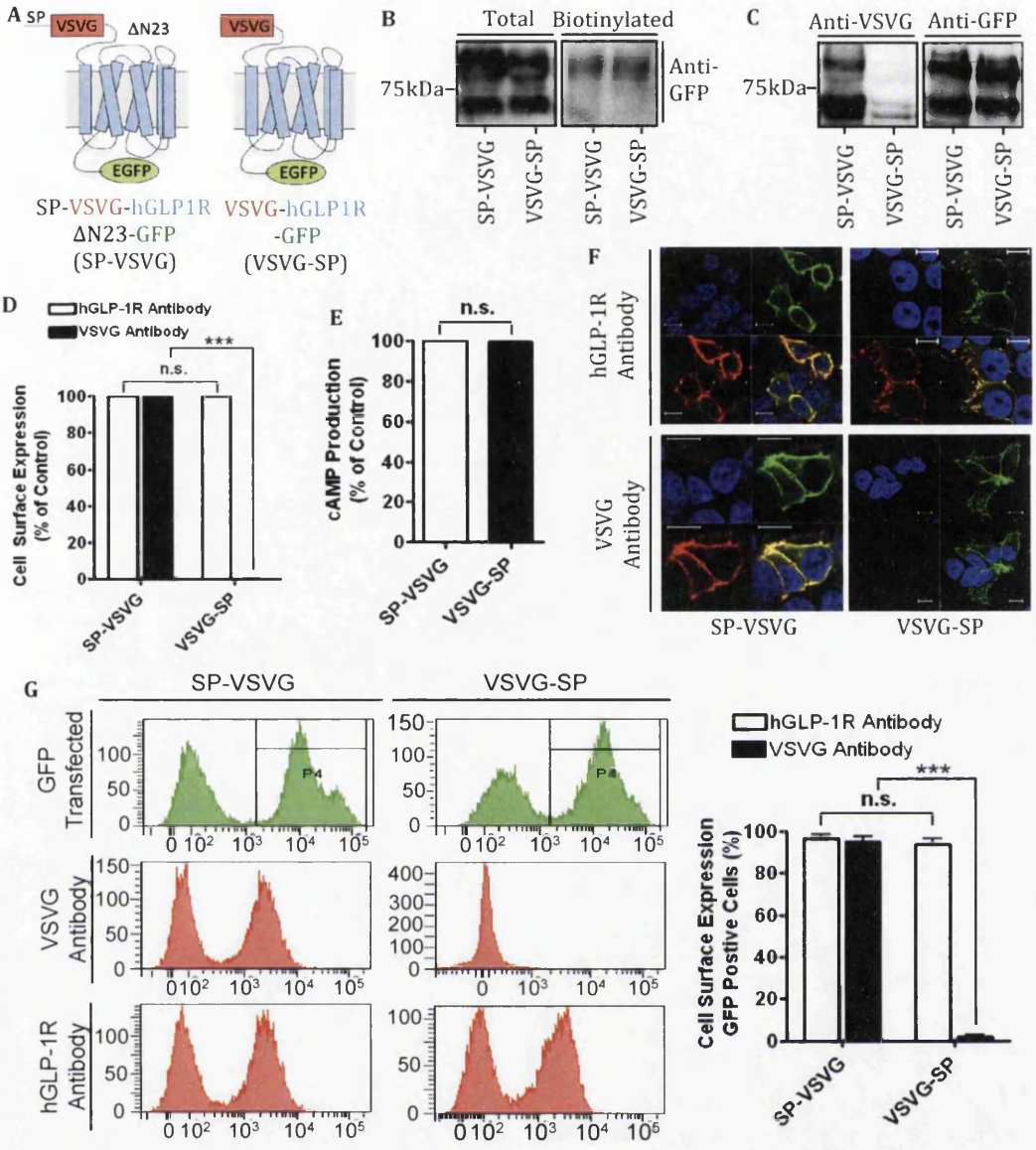

Figure 3.1. HGLP-1R expressing at the cell surface shows no SP. (A) HEK293 cells transfected with SP-VSVG and VSVG-SP constructs. (B) Total and cell surface biotinylated hGLP-1R expression was assessed by immunoblotting using the anti-GFP antibody. (C) Total hGLP-1R expression was assessed by immunoblotting using the anti-VSVG and anti-GFP antibodies. (D) Cell surface expression was assessed by ELISA using the anti-VSVG and anti-hGLP-1R antibodies. (E) cAMP production was measured in cells stimulated with 100 nM GLP-1 for 60 min to assess hGLP-1R activity. (F) Immunofluorescence showing cell surface expression of hGLP-1R, EGFP (green) and the anti-hGLP-1R antibody (red) overlay shown in yellow and nuclear staining with DAPI in blue. (G) Cell surface expression of hGLP-1R constructs assessed by flow cytometry. Data are mean ± SEM, n=3. Data were analysed by two-tailed unpaired t-test; values differ from control, n.s. $p>0.05$, *** $p<0.001$.

3.3.2. Cleavage of the SP is necessary for targeting the hGLP-1R to the cell surface

Next, the importance of the SP cleavage in hGLP-1R cell surface expression was determined. Cell surface expression of the hGLP-1R without the SP (ΔSP), the hGLP-1R containing the SP replaced with viral SP (VSP-ΔSP) and the hGLP-1R defective in cleaving the SP (A21R) was compared to the SP-VSVG WT control (Figure 3.2A). HEK293 cells transfected with these constructs were analysed for their effect on hGLP-1R cell surface expression (assessed by ELISA [Figure 3.2C], immunofluorescence [Figure 3.2E] and flow cytometry [Figure 3.2F] using the anti-hGLP-1R antibody) and activity (assessed by cAMP [Figure 3.2D]). The ΔSP construct showed cell surface expression (assessed by ELISA [97.4 ± 2.6%, $p>0.05$], immunofluorescence and flow cytometry [100.0 ± 0.6%, $p>0.05$]) similar to that of the SP-VSVG WT control. Additionally, the ΔSP construct showed 95.2 ± 2.6% ($p>0.05$) agonist induced cAMP production, confirming the hGLP-1R without the SP is functionally similar to the control hGLP-1R. In contrast, VSP-ΔSP and A21R constructs showed very little cell surface expression (2.3 ± 0.6% and 7.8 ± 2.7% by ELISA, and 1.9 ± 1.7% and 4.4 ± 2.2% by flow cytometry, $p<0.001$, respectively), which was confirmed by immunofluorescence. The cAMP activity of the VSP-ΔSP and A21R constructs in agonist stimulated cells was also low (16.2 ± 1.3% and 24.1 ± 1.5%, $p<0.001$, respectively). Immunoblotting of the cell lysates expressing the above mentioned constructs suggested that the SP of VSP-ΔSP and A21R was not cleaved and as a result produced a single band at the lower molecular weight of ~65 kDa with both the anti-GFP and anti-VSVG antibodies (Figure 3.2B), confirming the expression of an immature receptor. This result demonstrated that the SP is specific to the hGLP-1R and mutating this sequence prevents cleavage of the SP and thereby targeting of the hGLP-1R to the cell surface.

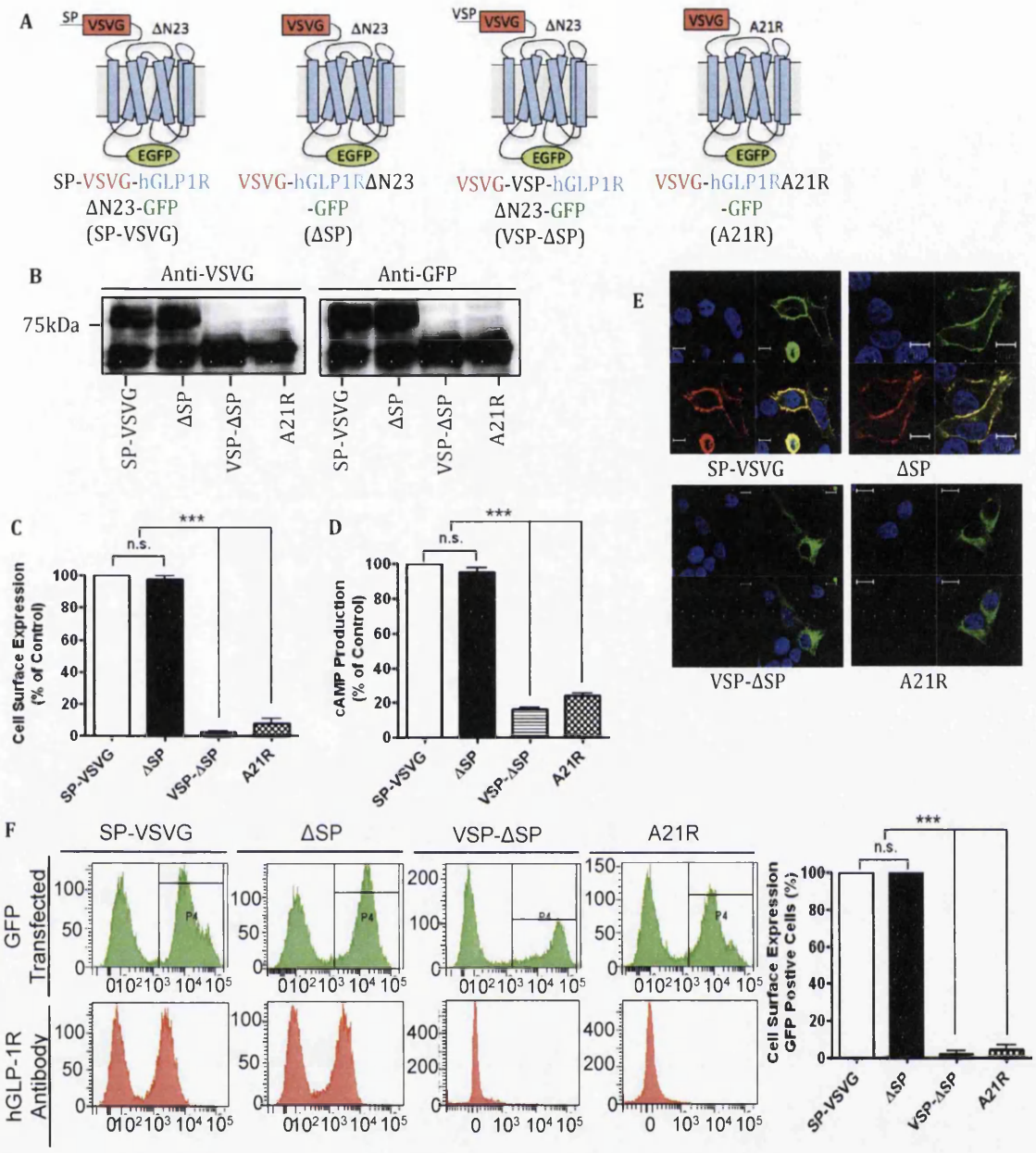

Figure 3.2. Cleavage of the SP is required for hGLP-1R cell surface expression. (A) HEK293 cells transfected with VSVG-tagged hGLP-1R constructs. (B) Total hGLP-1R expression was assessed by immunoblotting using the anti-VSVG and anti-GFP antibodies. (C) Cell surface expression was assessed by ELISA using the anti-hGLP-1R antibody. (D) cAMP production was measured in cells stimulated with 100 nM GLP-1 for 60 min to assess hGLP-1R activity. (E) Immunofluorescence showing cell surface expression of hGLP-1R, EGFP (green) and the anti-hGLP-1R antibody (red) overlay shown in yellow and nuclear staining with DAPI in blue. (F) Cell surface expression of hGLP-1R constructs by flow cytometry. Data are mean ± SEM, n=3. Data were analysed by Bonferroni's post test after one-way ANOVA; values differ from control, n.s. $p>0.05$, *** $p<0.001$.

3.3.3. The sequence after the SP is required for hGLP-1R cell surface expression

A number of deletions were made within the HRASP of the hGLP-1R and analysed for their effect on cell surface expression and activity of the receptor (Figure 3.3A). For this purpose, cell surface expression of the N-terminal deleted hGLP-1R mutants in HEK293 cells was analysed by ELISA (Figure 3.3C). Removal of either 24aa (ΔN24) or 30aa (ΔN30) from the N-terminal domain had no effect on hGLP-1R cell surface expression (98.2 ± 2.1% and 94.4 ± 2.7%, $p>0.05$, respectively). However, deleting 35aa (ΔN35) from the N-terminus significantly reduced hGLP-1R cell surface expression and deleting 40aa (ΔN40) abolished cell surface expression altogether (17.8 ± 0.6% and 0.2 ± 0.2, $p<0.001$, respectively). These results were also confirmed by immunofluorescence (Figure 3.3E). Additionally, the cAMP production of the receptor in agonist stimulated cells reflected cell surface expression of the receptor (Figure 3.3D). Agonist induced cAMP production of the ΔN24 and ΔN30 mutants (96.7 ± 3.3% and 98.2 ± 0.9%, $p>0.05$, respectively) were similar to that produced by the WT. In contrast, hGLP-1R activity was significantly reduced when either 35aa (ΔN35) or 40aa (ΔN40) were deleted from the N-terminal domain (28.8 ± 6.3% and 17.5 ± 3.0%, $p<0.001$, respectively). Consequently, the region between 31-40aa was deleted (Δ31-40) from the hGLP-1R and analysed for the deletion's effect on hGLP-1R cell surface expression and cAMP production. Cell surface expression (1.2 ± 1.3%, $p<0.001$) and cAMP production (16.4 ± 0.2%, $p<0.001$) of the hGLP-1R were almost abolished in the Δ31-40 mutant when compared to that of the WT, indicating the importance of this region in trafficking the receptor to the cell surface. Immunofluorescence confirmed these results and showed hGLP-1R expression to be intracellular. Immunoblotting confirmed that the reduced cell surface expression of these deletion mutants was not due to alterations in their expression levels (Figure 3.3B).

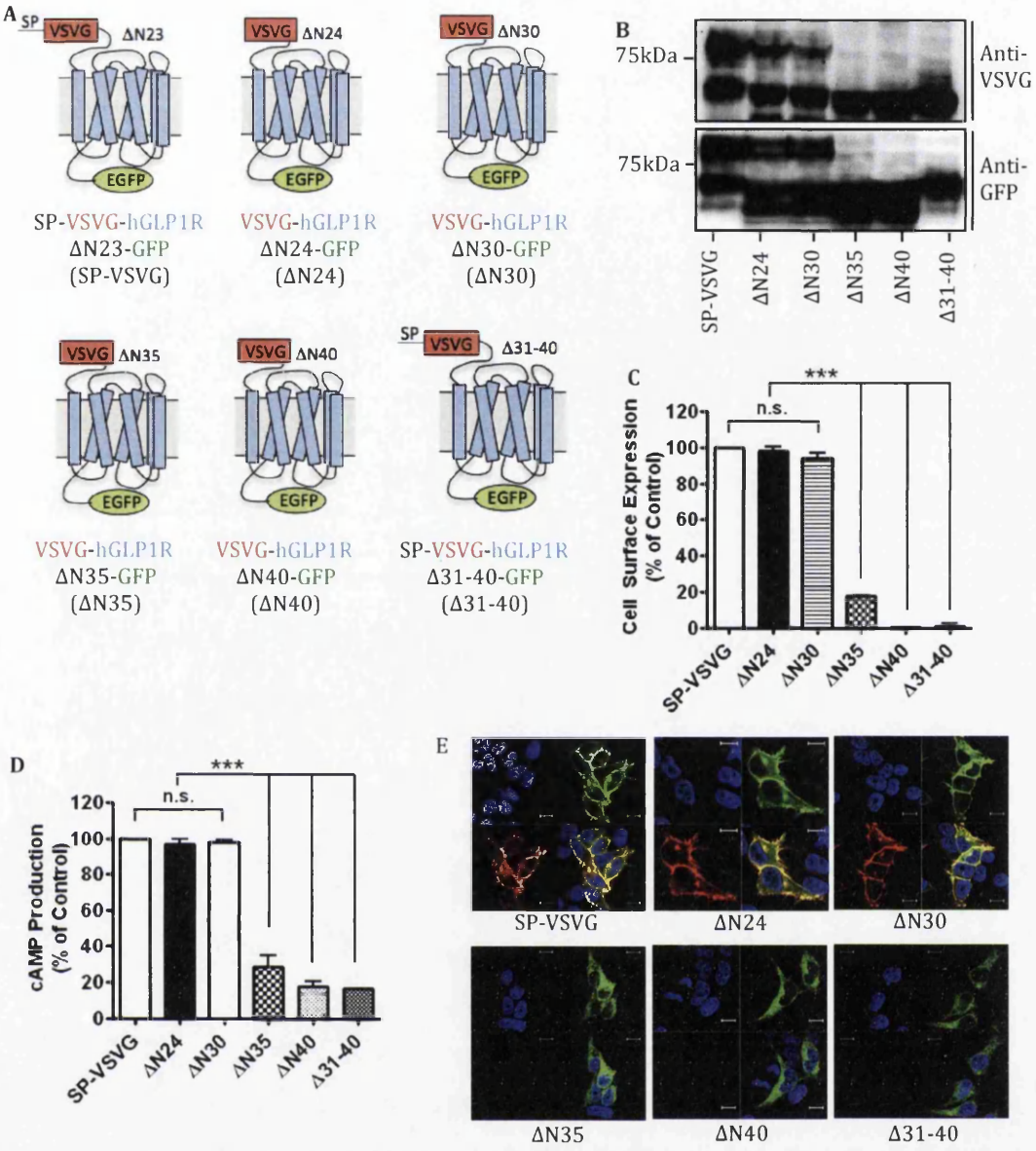

Figure 3.3. The sequence after the SP is essential for hGLP-1R cell surface expression. (A) HEK293 cells were transfected with the indicated N-terminal deleted constructs. (B) Total hGLP-1R expression was assessed by immunoblotting using the anti-VSVG and anti-GFP antibodies. (C) Cell surface expression using was assessed by ELISA using the anti-hGLP-1R antibody. (D) cAMP production was measured in cells stimulated with 100 nM GLP-1 for 60 min to assess hGLP-1R activity. (E) Immunofluorescence showing cell surface expression of hGLP-1R, EGFP (green) and the anti-hGLP-1R antibody (red) overlay shown in yellow and nuclear staining with DAPI in blue. Data are mean ± SEM, n=3. Data were analysed by Bonferroni's post test after one-way ANOVA; values differ from control, n.s $p>0.05$, *** $p<0.001$.

3.3.4. *N*-linked glycosylation is essential for hGLP-1R cell surface expression

The hGLP-1R has been shown to be *N*-linked glycosylated at positions Asn^{63}, Asn^{82} and Asn^{115} within the ER (Chen et al, 2010; Whitaker et al, 2012). Therefore, HEK293 cells transfected with either the WT SP-VSVG, ΔN145 or N63,82,115L constructs (Figure 3.4A) were used to assess the importance of *N*-linked glycosylation in hGLP-1R cell surface expression. Immunoblotting of the SP-VSVG WT control showed the doublet at ~65 kDa and ~85 kDa (Figure 3.4B). Treatment of SP-VSVG with a *N*-linked glycosylation inhibitor, tunicamycin, shifted this doublet to ~60 kDa and 65 kDa. This shift is used as a readout assay to assess hGLP-1R *N*-linked glycosylation and showed that the hGLP-1R is *N*-linked glycosylated. The hGLP-1R with the N-terminal domain removed (ΔN145) showed only a single band at ~50 kDa in immunoblotting. As the glycosylation sites were removed in the ΔN145 mutant, no change in mobility was seen when treated with tunicamycin. Additionally, the N63,82,115L mutant, with all three *N*-linked glycosylation sites mutated, of the hGLP-1R showed a single band at ~60 kDa, which was also unaltered by treatment with tunicamycin.

HGLP-1R glycosylation can be removed by treatment with both PNGase F and Endo H enzymes, indicating the receptor is *N*-linked glycosylated (Maley et al, 1989). PNGase F cleaves oligomannoses and both hybrid and complex *N*-glycans whereas Endo H cleaves oligomannoses and some hybrid glycans. Therefore, the WT SP-VSVG, ΔN145 or N63,82,115L constructs were digested with Endo H or PNGase F enzymes and analysed for their band pattern by immunoblotting (Figure 3.4C). Treatment of the SP-VSVG WT control lysate with Endo H caused a shift in the lower band mobility only from ~65 kDa to ~60 kDa. However, treatment with PNGase F shifted both bands to ~60 kDa and 65 kDa, which mimicked the effect of tunicamycin and thereby confirmed that the hGLP-1R is *N*-linked glycosylated by oligomannoses and both hybrid and complex *N*-glycans in the mature form. In contrast, the lysates of HEK293 cells expressing either the ΔN145 or N63,82,115L mutants showed no shift in band pattern

when treated with either Endo H or PNGase F, confirming that they are not glycosylated.

The deleted (ΔN145) and mutated (N63,82,115L) hGLP-1R constructs were used to assess the importance of *N*-linked glycosylation for cell surface expression of the receptor by ELISA (Figure 3.4E) and immunofluorescence (Figure 3.4G). HGLP-1R cell surface expression was abolished in both mutations when compared to the WT (0.5 ± 0.5% and 0.1 ± 0.1%, $p<0.001$, respectively). Further, when cells expressing the SP-VSVG control construct were treated with tunicamycin, cell surface expression was abolished (1.9 ± 0.6%, $p<0.001$). This was confirmed further by immunofluorescence where cell surface expression was seen for the SP-VSVG construct with good colocalisation between GFP-tag and cell surface staining with the anti-hGLP-1R antibody. However, the ΔN145 and N63,82,115L mutants and the SP-VSVG construct treated with tunicamycin, only showed intracellular expression of GFP and no cell surface expression with the anti-hGLP-1R antibody. Immunoblotting demonstrated that the reduction in cell surface expression of the mutants was not a result of reduced protein expression (Figure 3.4D). Consistent with the reduced cell surface expression, the ΔN145 and N63,82,115L mutants and the SP-VSVG construct treated with tunicamycin caused reduced cAMP production in agonist stimulated cells (14.3 ± 0.3%, 13.6 ± 0.9% and 11.1 ± 1.6%, $p<0.001$, respectively, Figure 3.4F). Therefore, preventing hGLP-1R glycosylation by either deleting the N-terminal domain or mutating the glycosylation sites within the N-terminal domain drastically reduced cell surface expression of the receptor.

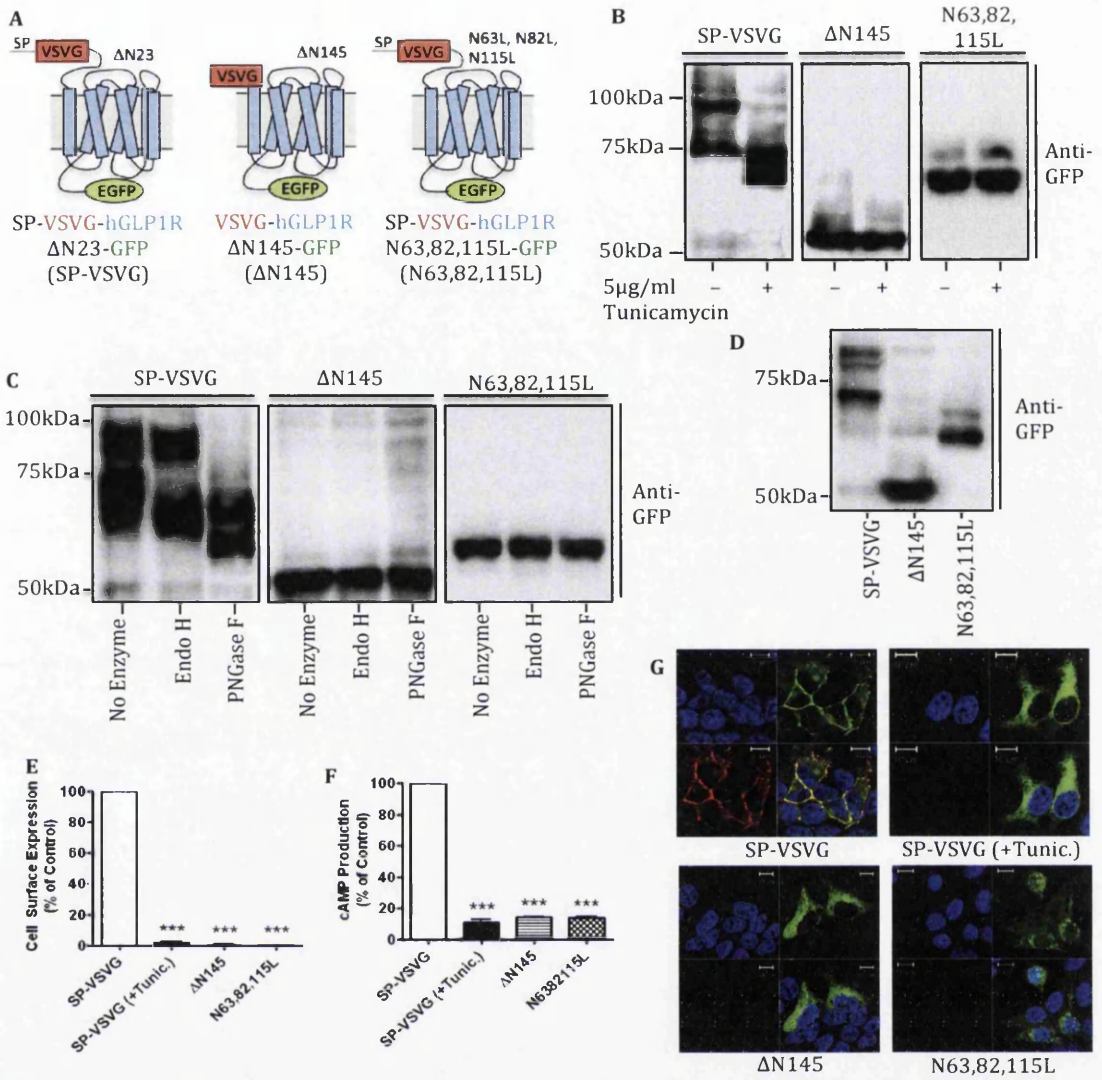

Figure 3.4. *N*-linked glycosylation is essential for hGLP-1R cell surface expression. (A) HEK293 cells were transfected with either SP-VSVG, ΔN145 or N63,82,115L plasmid DNA. (B) Cells were treated without or with 5 μg/ml tunicamycin for 48 h. The cells were lysed and the cell lysates were immunoblotted with the anti-GFP antibody. (C) Post nuclear supernatant fractions of HEK293 cells were treated with either no enzyme, Endo H or PNGase F for 60 min at 37°C and immunoblotted with the anti-GFP antibody. (D) Total hGLP-1R expression was assessed by immunoblotting using the anti-GFP antibody. (E) Cell surface expression was assessed by ELISA using the anti-hGLP-1R antibody. (F) cAMP production was measured in cells stimulated with 100 nM GLP-1 for 60 min to assess hGLP-1R activity. (G) Immunofluorescence showing cell surface expression of hGLP-1R, EGFP (green) and the anti-hGLP-1R antibody (red) overlay shown in yellow and nuclear staining with DAPI in blue. Data are mean ± SEM, n=3. Data were analysed by Bonferroni's post test after one-way ANOVA; values differ from control, *** $p<0.001$.

3.3.5. Effect of point mutations within the N-terminal domain on cell surface expression of the hGLP-1R

A number of N-terminal residues conserved across the family B GPCRs were mutated within the hGLP-1R to assess their effect on cell surface expression of the receptor (estimated by ELISA [Figure 3.5B] and immunofluorescence [Figure 3.5D]) and activity (assessed by cAMP accumulation [Figure 3.5C]). The total protein expression of the mutants was determined by immunoblotting using both the anti-GFP and anti-VSVG antibodies (Figure 3.5A). Substitution of the negatively charged Glu^{34} with a positively charged Lys residue (E34K) had no significant effect on cell surface expression (101.6 ± 1.6%, $p>0.05$) or activity (98.5 ± 0.3%, $p>0.05$) of the receptor. Total protein expression levels of the E34K mutant were similar to that of the SP-VSVG control construct. The W39A mutation significantly reduced hGLP-1R cell surface expression (25.1 ± 2.4%, $p<0.001$) and agonist stimulated cAMP production (21.7 ± 2.4%, $p<0.001$). Additionally, the Y69A mutant of the hGLP-1R showed very low cell surface expression (3.7 ± 0.8%, $p<0.001$) and reduced agonist induced cAMP production (18.9 ± 2.3%, $p<0.001$). Further, the Y88A mutation within the N-terminal domain of the hGLP-1R almost abolished cell surface expression of the receptor (2.3 ± 1.1%, $p<0.001$) and showed an even further reduction in cAMP production (16.4 ± 3.7%, $p<0.001$). Immunoblot analysis confirmed that the reduction in cell surface expression of these mutants was not due to alterations in the mutants protein expression. Consistent with the reduction in cell surface expression and cAMP producing activity of the receptor, only a single band was seen at ~65 kDa for these three mutations, indicating the immature receptor. Immunofluorescence also supported the ELISA results as intracellular expression was seen with GFP but no cell surface staining was observed with the anti-hGLP-1R antibody.

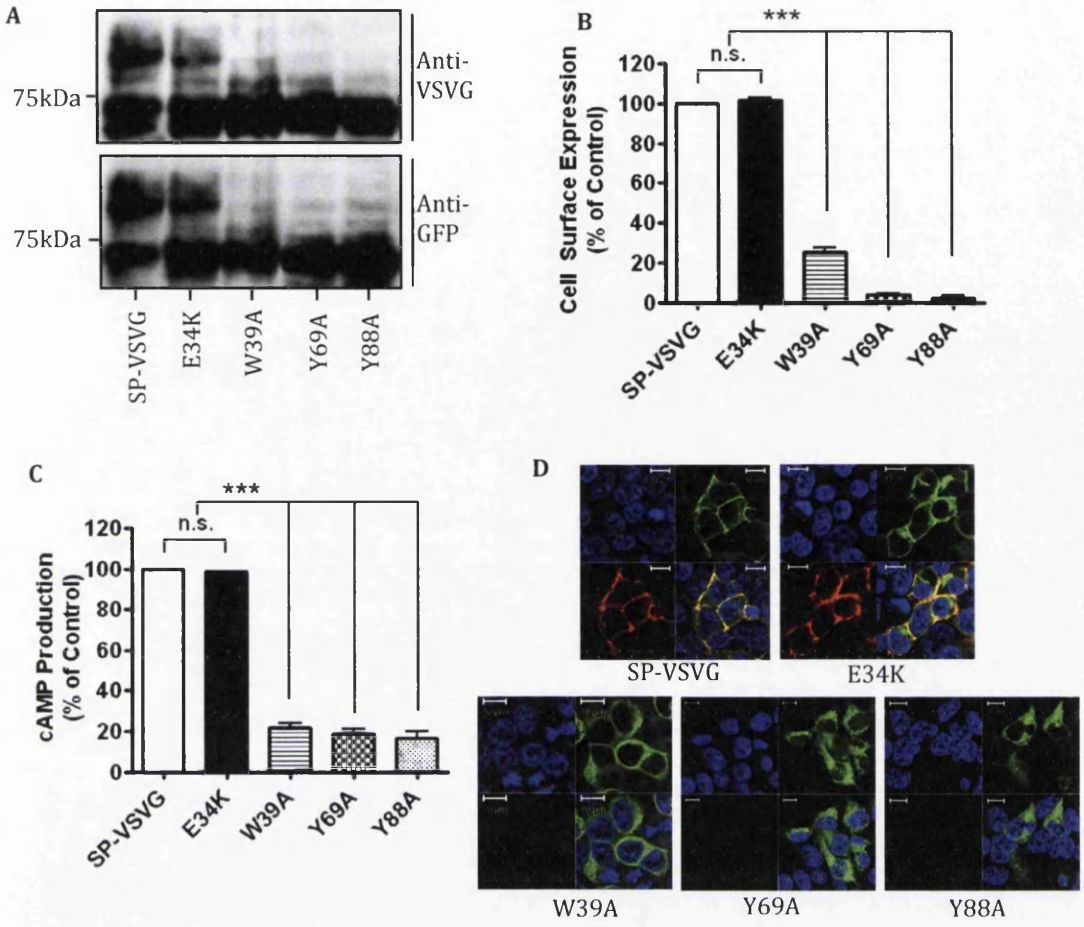

Figure 3.5. The effect of various point mutations within the N-terminal domain of the hGLP-1R on cell surface expression of the receptor. (A) HEK293 cells were transfected with the indicated N-terminal mutated constructs. Total hGLP-1R expression was assessed by immunoblotting using the anti-VSVG and anti-GFP antibodies. (B) Cell surface expression was assessed by ELISA using the anti-hGLP-1R antibody. (C) cAMP production was measured in cells stimulated with 100 nM GLP-1 for 60 min to assess hGLP-1R activity. (D) Immunofluorescence showing cell surface expression of hGLP-1R, EGFP (green) and the anti-hGLP-1R antibody (red) overlay shown in yellow and nuclear staining with DAPI in blue. Data are mean ± SEM, n=3. Data were analysed by Bonferroni's post test after one-way ANOVA; values differ from control, n.s $p>0.05$, *** $p<0.001$.

3.3.6. Effect of SP, HRASP and conserved residue mutants on hGLP-1R *N*-linked glycosylation

The importance of the SP, the HRASP and conserved residues (Glu^{34}, Trp^{39}, Tyr^{69} and Tyr^{88}) within the hGLP-1R N-terminus on its *N*-linked glycosylation was determined. For this purpose, cells expressing the constructs were treated without or with tunicamycin and the cell lysates analysed by immunoblotting using the anti-GFP antibody. Like the SP-VSVG WT control construct, the SP deleted construct (ΔSP) showed a doublet in immunoblotting and the doublet mobility was altered with tunicamycin treatment. This suggested the ΔSP mutant was *N*-linked glycosylated in the same way as the WT. The hGLP-1R mutants that prevented cleavage of the SP (VSP-ΔSP and A21R) only showed a single band at ~65 kDa and the band mobility was unaltered when treated with tunicamycin, indicating that these mutants were not *N*-linked glycosylated (Figure 3.6A). This is most likely because the SP prevents access to the *N*-linked glycosylation sites, as it is not cleaved in these mutants. Additionally, the mutants with deletions within the HRASP of the N-terminus (ΔN35, ΔN40 and Δ31-40) showed a single band at ~65 kDa and a shift in the doublet mobility was seen when treated with tunicamycin, which suggests that these mutants are still glycosylated (Figure 3.6B).

When the W39A, Y69A and Y88A mutants were left untreated with tunicamycin, a single band at ~65 kDa was observed indicating the immature form of the receptor. However, when treated with tunicamycin there was a shift in the doublet mobility to ~60 kDa and 65 kDa demonstrating these mutations still allowed the receptor to be *N*-linked glycosylated (Figure 3.6C). Additionally, the E34K mutant showed a doublet similar to that of the WT control in immunoblotting and the doublet mobility also altered with tunicamycin treatment. These results suggest that *N*-linked glycosylation of the receptor is unaltered with the E34K mutation.

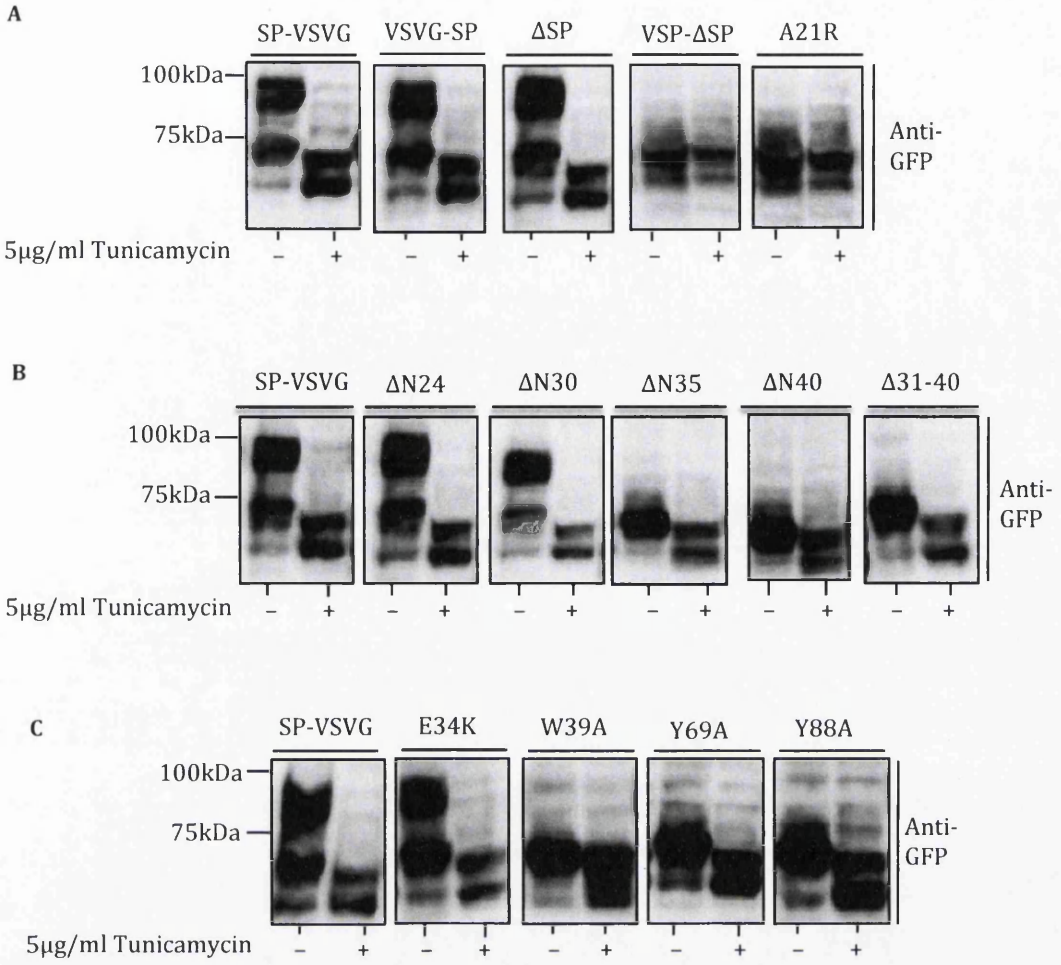

Figure 3.6. The effect of the SP, HRASP and conserved residue mutations on hGLP-1R glycosylation. HEK293 cells transfected with SP (A), HRASP (B) or the conserved residue (C) mutant constructs treated without or with 5 μg/ml tunicamycin for 48 h. The cells were lysed and the cell lysates were immunoblotted with the anti-GFP antibody.

3.3.7. The W39A, Y69A and Y88A mutations do not affect cleavage of the SP

The W39A, Y69A and Y88A mutants in the SP-VSVG, VSVG-SP and ΔSP constructs were used to determine whether these mutations affect cleavage of the SP. The lysates of HEK293 cells expressing these mutants were subjected to immunoblotting with both the anti-GFP and anti-VSVG antibodies to assess total hGLP-1R expression and their effect on its SP cleavage (Figure 3.7A). The W39A, Y69A and Y88A mutations did not prevent cleavage of the SP when expressed in the SP-VSVG construct. This and expression of these mutants in the ΔSP construct showed expression with both the anti-GFP and anti-VSVG antibodies. However, expression of the VSVG-SP construct with these mutations only showed signal with the anti-GFP antibody but not with the VSVG antibody, suggesting the SP is still cleaved. If the mutations had affected cleavage of the SP, then the mutation would have abolished expression of the VSVG-SP construct and allowed expression of the ΔSP construct at the cell surface. This is because there would be no SP to be cleaved in the ΔSP construct. In immunofluorescence, hGLP-1R cell surface expression was seen with good colocalisation of GFP and the anti-hGLP-1R antibody in all constructs (SP-VSVG, VSVG-SP and ΔSP) without the mutations. Whereas, only intracellular expression was seen with GFP and no cell surface staining with the anti-hGLP-1R antibody for all constructs with the N-terminal mutations (Figure 3.7B). Taken together, these results suggest that the W39A, Y69A and Y88A mutations did not affect hGLP-1R cell surface expression by preventing cleavage of the SP.

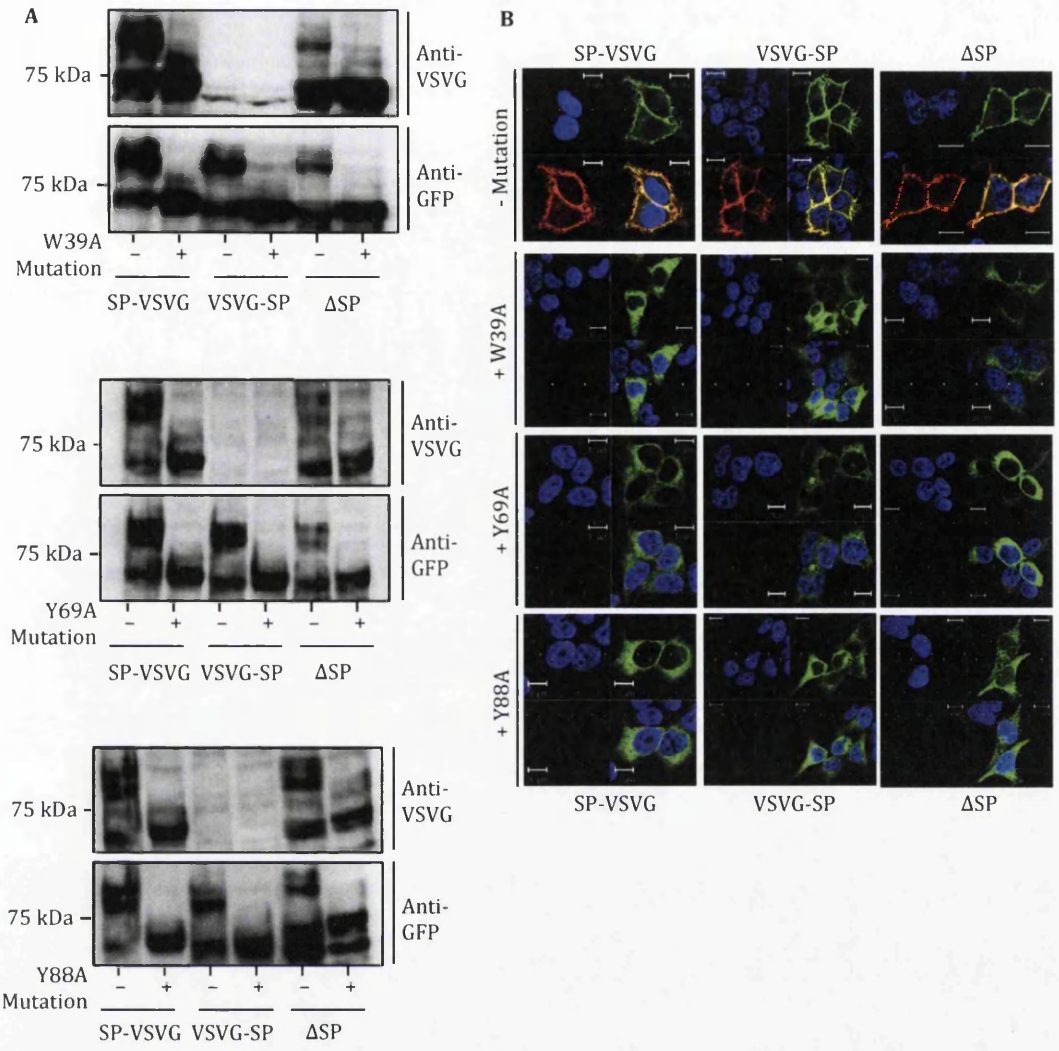

Figure 3.7. W39A, Y69A and Y88A mutations do not affect cleavage of the SP within the hGLP-1R. (A) Total hGLP-1R expression of W39A, Y69A and Y88A mutants in SP-VSVG, VSVG-SP or ΔSP constructs was assessed by immunoblotting using the anti-VSVG and anti-GFP antibodies. (B) Immunofluorescence showing cell surface expression of hGLP-1R, EGFP (green) and the anti-hGLP-1R antibody (red) overlay shown in yellow and nuclear staining with DAPI in blue.

3.4. Discussion

The hGLP-1R construct containing the VSVG-epitope tag at the N-terminal domain before the SP sequence (VSVG-SP) showed signal with the anti-hGLP-1R antibody but not with the anti-VSVG antibody, which indicated that the mature receptor expressed at the cell surface is without its SP. Further, stimulation of cells expressing the VSVG-SP with GLP-1 still stimulated cAMP production, confirming that the receptor without the SP is functionally active. These results are in agreement with a previous study, which showed the mature hGLP-1R expressed at the cell surface is without the SP (Huang et al, 2010). These findings are also consistent with that of other family B GPCRs including the vasoactive intestinal peptide (VPAC1) receptor (Couvineau et al, 2004) and CRF_1 receptor (Alken et al, 2005) where the SP is cleaved during synthesis. However, the SP of VPAC1 was found to play a critical role in targeting the receptor, as deletion of the SP resulted in the synthesis but prevented trafficking of the receptor to the cell surface. It was suggested that the SP of the VPAC1 receptor is cleaved during trafficking to the plasma membrane, most likely in the ER (Couvineau et al, 2004). Additionally, the SP is of the CRF_1 receptor reduced cell surface expression but still retained its functionality (Alken et al, 2005). The hGLP-1R with the SP deletion (ΔSP), was shown in this study to function exactly like the receptor with the SP present. This contradicts a previous study, which showed the SP deleted hGLP-1R is synthesised but does not express at the cell surface (Huang et al, 2010). The reason for the variation in results is unclear. In this study, the hGLP-1RΔSP was expressed with the VSVG-epitope tag at the N-terminus whereas Huang et al (2010) expressed the same deletion construct with a HA-epitope tag. However, it was observed that the hGLP-1RΔSP without any epitope tag at the N-terminus also targets to the cell surface, indicating that the difference in the N-terminal tag between studies may not be the reason for variation in the results (see Chapter 4). Within this study, the hGLP-1R showed specificity to its SP sequence because replacing it with the viral SP (VSP-ΔSP) allowed protein synthesis but cell surface expression of the receptor was reduced. The A21R mutation (-3 position of the SP cleavage site) allowed synthesis of the hGLP-1R but prevented cleavage of

the SP and therefore cell surface expression was reduced, which is consistent with a previous study (Huang et al, 2010). Taken together, this study demonstrates that cleavage of the SP is required for hGLP-1R cell surface expression and the SP sequence is specific to the hGLP-1R. This is similar to the specificity demonstrated for the CRF_1, as replacement of the CRF_1 SP with the CRF_{2a} SP abolished expression of the receptor (Schulz et al, 2010).

The aa sequence following the SP, Gly^{27}-Trp^{39}, is relatively hydrophobic (HRASP) and it has previously been suggested that this region may be recognised by the SRP and allow for subsequent synthesis of the receptor (Hatsuzawa et al, 1997; Huang et al, 2010). A similar region within the endothelin B receptor (ET_BR), Gln^{28}-Trp^{34}, was shown to be important in receptor trafficking to cell surface by facilitating translocation across the ER membrane (Alken et al, 2009). To examine the role of the HRASP in hGLP-1R trafficking, deletions were made within the HRASP region and assessed for their effect on hGLP-1R cell surface expression. Deleting up to 30aa of the N-terminal domain of the hGLP-1R had no effect on cell surface expression of the receptor, whereas deletion of up to 40aa or 31-40aa abolished hGLP-1R cell surface expression. Therefore, these results suggest that residues 31-40 within the HRASP are important for hGLP-1R cell surface expression and cAMP production. However, the 31-40aa deletion within the hGLP-1R had no effect on the cleavage of the SP or *N*-linked glycosylation, indicating that the HRASP is not required for either cleavage of the SP or *N*-linked glycosylation of the receptor. It is possible that, like in the ET_BR, this region may be important in hGLP-1R translocation across the ER membrane, but requires further studies to confirm this possibility.

The GLP-1R expressed in CCL39 fibroblasts (Widmann et al, 1995) and transfected HEK293 (Huang et al, 2010) and CHO cells (Whitaker et al, 2012) has previously been shown to produce a two band pattern in immunoblotting, representing different *N*-linked glycosylation states. Consistent with this, the hGLP-1R expressed in HEK293 cells in this study showed a doublet in immunoblotting. Further, treatment with tunicamycin, an *N*-linked

glycosylation inhibitor (Varki et al, 2009), or deletion of the N-terminus (ΔN145) or mutating the glycosylation sites (N63,82,115L) prevented glycosylation of the hGLP-1R, confirming the hGLP-1R is glycosylated in the N-terminus. Moreover, hGLP-1R glycosylation can be removed by treatment with both PNGase F and Endo H, indicating the receptor is *N*-linked glycosylated. The lysates of cell surface biotinylated hGLP-1R expressing cells showed only the top band of the characteristic two band pattern in immunoblotting, demonstrating it as the fully glycosylated and mature receptor present at the cell surface. This is consistent with a previous study, which showed that only the high molecular weight band of the rat GLP-1R binds the GLP-1 agonist (Widmann et al, 1995). Taken together, the data in this study confirmed that only the fully glycosylated and mature receptor is found at the cell surface and that mutations and deletions of the glycosylation sites prevented cell surface expression and activity of the receptor. Additionally, tunicamycin inhibited glycosylation of the SP deleted (ΔSP) mutant confirming it also underwent *N*-linked glycosylation. This study demonstrated that preventing cleavage of the SP (A21R or VSP) also inhibits *N*-linked glycosylation, suggesting the SP may prevent access to the glycosylation sites required for hGLP-1R cell surface expression.

In addition to conserved glycosylation sites, the hGLP-1R contains a number of aa within the N-terminal domain that are highly conserved among family B GPCRs. A substitution of Glu^{34} to a positively charged residue has previously been shown to partially compensate for the lack of the SP, where no GLP-1R expression was demonstrated (Huang et al, 2010). However, in this study the E34K mutation within the hGLP-1R showed no significant effect on the cell surface expression of the receptor. This is expected since the SP deleted (ΔSP) mutant showed no effect on hGLP-1R cell surface expression. It has previously been shown that a mutation of Trp^{39} abolished GLP-1 binding to the GLP-1R, as the imidazole ring structure in this position is important for agonist binding (Runge et al, 2008; Van Eyll et al, 1996). In this study, the W39A mutation abolished hGLP-1R cell surface expression, demonstrating that the imidazole ring structure at this position is also required for cell surface expression of the

receptor. Tyr^{69} and Tyr^{88} within the hGLP-1R have also been shown to be important in binding to the agonist, Exenatide, but the reason for this was undetermined (Runge et al, 2008; Underwood et al, 2010). In this study, the Tyr^{69} and Tyr^{88} mutations caused a significant loss in hGLP-1R cell surface expression. The Trp^{39}, Tyr^{69} and Tyr^{88} mutants interfered with neither cleavage of the SP nor *N*-linked glycosylation of the receptor and therefore it is unlikely that these mutations had any effect on the stability of the receptor. The exact reason for these mutations affecting hGLP-1R maturation and thereby its cell surface expression is still unclear. However, it is possible that these mutations may affect trafficking of the *N*-linked glycosylated hGLP-1R to the Golgi or interfere with further processing within the ER and Golgi. This is an area requiring further investigation.

In summary, this study revealed that the SP sequence of the hGLP-1R is cleaved during processing of the receptor. Cleavage of the SP is not essential for hGLP-1R synthesis but is required for glycosylation and trafficking of the receptor to the cell surface. Moreover, the SP is specific to the hGLP-1R. The hGLP-1R is *N*-linked glycosylated and only a fully glycosylated receptor is present at the cell surface. Furthermore, the sequence within the HRASP, 31-40, was found to be critical for hGLP-1R cell surface expression but not for cleavage of the SP or glycosylation of the receptor. The conserved residues, Trp^{39}, Tyr^{69} and Tyr^{88}, within the N-terminal domain were required for cell surface expression of the hGLP-1R as mutating these residues abolished cell surface expression while not interfering with cleavage of the SP or glycosylation of the receptor. Overall, the results presented in this study suggest that the SP may prevent access to Asn^{63}, Asn^{82} and Asn^{115} glycosylation sites within hGLP-1R. With cleavage of the SP, the glycosylation sites are exposed and the receptor undergoes *N*-linked glycosylation. The glycosylated receptor traffics to the Golgi and then onto the plasma membrane. The HRASP (31-40aa) and Trp^{39}, Tyr^{69} and Tyr^{88} residues are critical for hGLP-1R cell surface expression and most likely play a role in trafficking the receptor from the ER or interfere with further processing within the ER and Golgi (Figure 3.8).

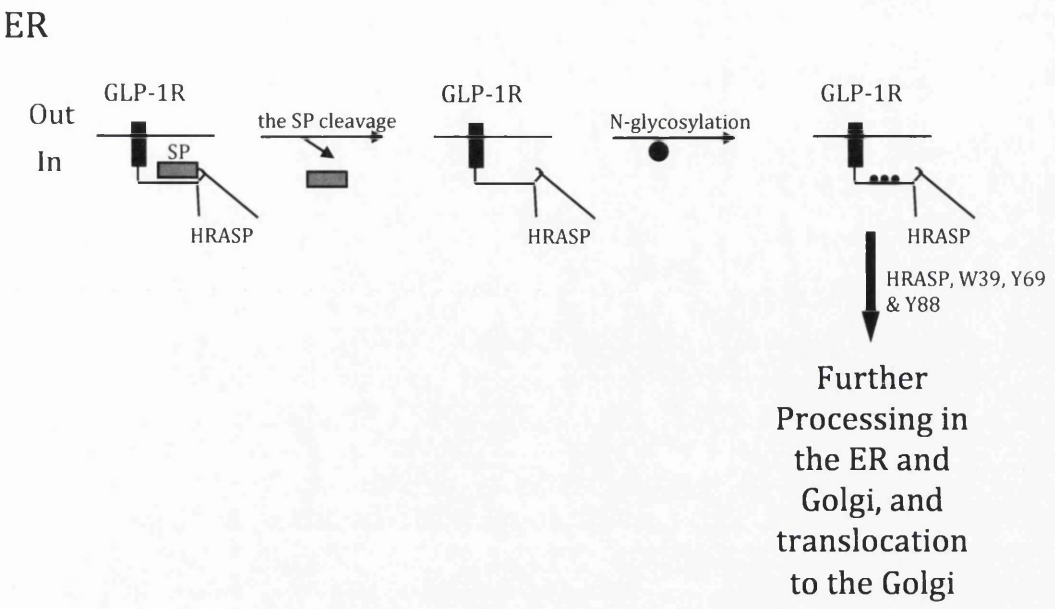

Figure 3.8. Proposed schematic model of hGLP-1R trafficking pathway as deduced from the present study. A simplified scheme of hGLP-1R cell surface expression. Within the ER the SP is cleaved to reveal *N*-linked glycosylation sites. The receptor is then glycosylated within the ER and Golgi prior to trafficking to the plasma membrane.

4. Characterisation of Two Small Molecule Agonists of the Human Glucagon Like Peptide-1 Receptor

4.1. Introduction

The actions of glucagon like peptide-1 (GLP-1) have been well studied over the last twenty years due to its effectiveness in lowering blood glucose levels by increasing insulin secretion in type 2 diabetic patients (Doyle & Egan, 2007; Holz et al, 1999; Thompson & Kanamarlapudi, 2013). GLP-1 exerts its actions through the GLP-1 receptor (GLP-1R). The agonist occupied GLP-1R activates the $G\alpha_s$ subunit, which in turn activates adenylyl cyclase (AC). AC produces cyclic adenosine monophosphate (cAMP), which potentiates insulin secretion in β-cells (Drucker et al, 1987; Thompson & Kanamarlapudi, 2013; Willard & Sloop, 2012).

GLP-1 is produced from the breakdown of proglucagon within the intestinal L-cells by prohormone convertase 1 (PC1) (Dhanvantari et al, 2001). In secretory vesicles, the first six amino acids of GLP-1 are cleaved from the N-terminus to form the bioactive peptides, GLP-1 (7-36)-NH_2 and GLP-1 (7-37). Approximately 80% of secreted GLP-1 is in the GLP-1 (7-36)-NH_2 form, whereas the remaining 20% is released as GLP-1 (7-37) (Vahl et al, 2003). Both GLP-1 (7-37) and GLP-1 (7-36)-NH_2 bind to the GLP-1R with similar affinity and show similar potency (Orskov et al, 1993). *In vivo*, both bioactive types of GLP-1 have a very short half-life (~1.5 minutes) due to their rapid proteolytic degradation by dipeptidyl peptidase-IV (DPP-IV) (Hansen et al, 1999; Larsen et al, 2001; Mentlein, 2009; Vilsboll et al, 2003). This enzyme cleaves the active GLP-1 (7-36)-NH_2/(7-37) to its inactive GLP-1 (9-36)-NH_2/(9-37) form by removing two amino acids at the N-terminus of the peptide (Kieffer et al, 1995; López de Maturana & Donnelly, 2002; Mentlein, 2009; Montrose-Rafizadeh et al, 1997).

Exendin-4 also acts as an agonist to the GLP-1R, which is found in the saliva of the Gila monster lizard (*Heloderma suspectum*) (Goke et al, 1993; Thorens et al, 1993). It shares approximately 53% homology to GLP-1 (7-36)-NH_2 and contains an additional nine amino acids at the C-terminus (Goke et al, 1993; Kim & Egan, 2008; Young et al, 1999). In contrast to the active forms of GLP-1, exendin-4 does not contain an alanine as the second amino acid, which makes it resistant to proteolytic degradation by DPP-IV (Green et al, 2006). Truncated versions of GLP-1 (GLP-1 [9-36]-NH_2/[9-37]) and exendin-4 (exendin-3, Ex[9-39]) also bind to the GLP-1R but function as antagonists (Goke et al, 1993; López de Maturana & Donnelly, 2002; Serre et al, 1998; Thorens et al, 1993). Exendin-4 can be truncated by two amino acids at the N-terminus (Ex[9-39]) without loss of affinity to the receptor, whereas GLP-1 (9-36)-NH_2 is highly sensitive to N-terminal cleavage rendering it inactive in binding to the receptor (Kieffer et al, 1995; Montrose-Rafizadeh et al, 1997; Serre et al, 1998).

The main limitation of using GLP-1 as an agonist is the very short half-life (~1.5 minutes) of the native bioactive peptide as a result of the rapid proteolytic degradation by DPP-IV (Hansen et al, 1999; Larsen et al, 2001; Vilsboll et al, 2003). Therefore, therapeutic strategies that improve GLP-1 stability have been extensively studied, which has led to the development of a DPP-IV resistant GLP-1R agonist, Liraglutide, with prolonged duration of action (Gonzalez et al, 2006). Exenatide, a synthetic version of exendin-4, has also been developed (Eng et al, 1992). Both GLP-1R agonists, Liraglutide and Exenatide, are currently in use as drugs for the treatment of type 2 diabetes. They are effective insulinotropic agents that regulate blood glucose levels by increasing insulin secretion and supressing glucagon secretion in a glucose dependent manner (Bond, 2006; Edavalath & Stephens, 2010; Kim Chung le et al, 2009). The long-term requirement to administer these injectable drugs has necessitated the search for orally active agonists of the GLP-1R, a member of the family B G-protein coupled receptors (GPCR) (Coopman et al, 2010). Small molecule agonists are being sought after because they have the potential of oral administration (Cheong et al, 2012; Irwin et al, 2010). However, the discovery of small molecule orally active agonists that bind to the orthosteric site and

mimic the effects of the natural agonist has been difficult because they do not have the physiochemical properties to be orally active (Sloop et al, 2010; Wootten et al, 2013). Therefore, the discovery of non-peptide small molecule agonists that bind to a site distinct from the orthosteric site and act as positive allosteric agonists is advantageous for the development of orally active small molecule agonists in the treatment of type 2 diabetes.

Many GPCRs have been shown to have allosteric binding sites that are spatially and often functionally distinct from the primary agonist (orthosteric) binding site (Schwartz & Holst, 2007; Wang et al, 2009). Small molecule allosteric agonists can either increase or decrease the binding efficiency of an orthosteric agonist (De Amici et al, 2010). Allosteric agonists may provide novel therapeutic drugs as well as have a number of advantages compared to the classical orthosteric agonist. They are beneficial where selective orthosteric agonist based therapy has been difficult (for example, where the orthosteric site is highly conserved). Targeting the allosteric site allows for greater selectivity to be obtained and may be selectively regulated by endogenous agonists (Kenakin, 2009; Urban et al, 2007). Finally, low molecular weight agonists that have the potential for oral administration can be used to target allosteric binding sites (Schwartz & Holst, 2007). Some small molecule agonists, named ago-allosteric agonists, can bind to GPCRs and act as both agonists and allosteric modulators in the absence of orthosteric agonists. It is unknown how these agonists affect the binding or efficiency of compounds acting at the orthosteric site. Compounds with allosteric or ago-allosteric properties increase the potential for GPCR subtype selectivity. This allows for improved, targeted and novel therapeutics (Bridges & Lindsley, 2008).

A small molecule agonist of the GLP-1R, compound 1 (2- [2' methyl] thiadiazolylsulfanyl-3-trifluoromethyl-6,7-dichloroquinoxaline), has been identified as demonstrating low affinity, low potency allosteric agonism to the GLP-1R. In an effort to produce a more potent agonist, compound 2 (6,7-dichloro-2-methylsulfonyl-3-*N*-*tert*-butylaminoquinoxaline) has been developed. Compound 2 is an ago-allosteric modulator of GLP-1R, which also

acts as an agonist. Additionally, Ex(9-39) antagonist did not inhibit compound 2 binding, suggesting a second binding site on the GLP-1R distinct from the orthosteric binding site (Knudsen et al, 2007). The effectiveness of compound 2 to stimulate insulin secretion has also been assessed *in vivo*. Although compound 2 stimulates insulin secretion, it is not as effective in doing so as GLP-1 (7-36)-NH_2, Liraglutide or Exenatide. Further, combining compound 2 with either GLP-1, Liraglutide or Exenatide does not improve insulin secretion response in mice (Irwin et al, 2010). However, compound 2 has been shown to near-normalise insulin secretion in human islets isolated from a donor with type 2 diabetes (Sloop et al, 2010). Two additional small molecule agonists of the GLP-1R, compound A (4-(3,4-dichlorophenyl)-2-(ethanesulfonyl)-6-(trifluoromethyl) pyrimidine) and compound B (4-(3-(benzyloxy)phenyl)-2-(ethylsulfinyl)-6-(trifluoromethyl)), have also demonstrated ago-allosteric properties. Like compound 2, these compounds increase GLP-1R activity and insulin secretion from rodent islets and in animal studies.

The agonist occupied GLP-1R signals through both the $G\alpha_s$ and $G\alpha_q$ coupled pathways to stimulate insulin secretion (Drucker et al, 1987; Thompson & Kanamarlapudi, 2013; Willard & Sloop, 2012). Coupling to the $G\alpha_s$ pathway results in cyclic adenosine monophosphate (cAMP) production whereas coupling to the $G\alpha_q$ pathway leads to intracellular calcium (Ca^{2+}) accumulation. Upon agonist binding, GLP-1R signals through the phosphorylation of extracellular signal-regulated kinase (ERK). In this study, the effect of small molecule agonists, compound 2 and compound B were assessed for their effects on cAMP production, intracellular Ca^{2+} accumulation, ERK phosphorylation and hGLP-1R internalisation. Compounds 2 and B caused cAMP production similar to that of GLP-1 but did not induce intracellular Ca^{2+} accumulation, ERK phosphorylation or agonist induced hGLP-1R internalisation. Using antagonists Ex(9-39) (Goke et al, 1993; Thorens et al, 1993) and JANT-4 (Patterson et al, 2011), compounds 2 and B were shown to be allosteric modulators of GLP-1R, which bind to a site different from that of GLP-1 on the receptor. Consistent with this, a mutation to the orthosteric binding site (V36A) abolished GLP-1 induced cAMP production but had no effect on cAMP production stimulated by

compound 2 and compound B. However, the mutation of K334, which is required for efficient coupling of the receptor to the $G\alpha_s$ subunit, to alanine (K334A) in the hGLP-1R, inhibited cAMP production induced by GLP-1, compound 2 and compound B. These results demonstrated that both small molecule agonists and GLP-1 induce similar conformational changes in the GLP-1R for $G\alpha_s$ coupling, although they bind at different sites on the GLP-1R. Further, preincubation of the receptor with small molecule agonists inhibited GLP-1 induced hGLP-1R internalisation, intracellular Ca^{2+} accumulation and ERK phosphorylation.

4.2. Materials and methods

4.2.1. Materials

The primary antibodies used were rabbit anti-vesicular stomatitis virus glycoprotein (VSVG) (Immunoblotting, Abcam Biochemicals), mouse anti-VSVG (ELISA, Sigma), mouse anti-green fluorescent protein (GFP) (Roche) mouse anti-hGLP-1R (R&D Systems), rabbit anti-phospho ERK1/2 (pERK1/2) and rabbit anti-ERK1/2 (New England Biolabs). The Cy3-conjugated anti-mouse immunoglobulin G (IgG) secondary antibody (Jackson Laboratories) was used for immunofluorescence. The horseradish peroxidase (HRP)-conjugated anti-mouse and anti-rabbit IgG (GE Healthcare) secondary antibodies were used for immunoblotting. Enhanced chemiluminescence (ECL) select reagent was obtained from GE Healthcare. The cAMP polyclonal antibody and cAMP-HRP were obtained from Genscript. GLP-1 (7-37) (Liraglutide) was from Novo Nordisk and GLP-1 (7-36)-NH_2 was from Tocris. Exendin-4 (Exenatide) was from Eli Lilly and Company Limited. Compound 2, compound B and Ex(9-39) were purchased from Calbiochem. Antagonist JANT-4 was from Prof. Richard DiMarchi, Indiana University (IN, USA) (Patterson et al, 2011). All other chemicals were from Sigma unless otherwise stated.

4.2.2. Plasmids

The full-length hGLP-1RΔN23 cDNA was amplified from mammalian gene collection (MGC) clone 142053 (Source Bioscience) by polymerase chain reaction (PCR) using High Fidelity Taq DNA polymerase (Roche Applied Science) and sequence specific primers containing *Eco*RI restriction site and VSVG-tag coding sequence (5' primer), and *Sal*I restriction site and no stop codon (3' primer). SP-VSVG-hGLP-1RΔN23 cDNA was amplified by overlap PCR using VSVG-hGLP-1RΔN23 cDNA as the template, the sense primer, containing *Eco*RI restriction site, the signal peptide (SP, 1-23 amino acids) coding sequence followed by VSVG coding sequence and 3' primer. The cDNA was digested with *Eco*RI and *Sal*I, and cloned in frame into the same sites of pEGFP-N1 vector (Clontech) for expression as the N-terminus VSVG-tagged (after the SP) and the C-terminus GFP-tagged fusion protein in mammalian cells (SP-VSVG-hGLP-1RΔN23-GFP). The V36A (SP-VSVG-hGLP-1RΔN23 V36A-GFP) and K334A (SP-VSVG-hGLP-1RΔN23 K334A-GFP) point mutations within the hGLP-1R was generated using Quickchange II XL site-directed mutagenesis kit (Stratagene) and SP-VSVG-hGLP-1RΔN23-GFP plasmid as the template. Luciferase pGL4.29-Luc-CRE, pGL4.30-Luc-NFAT and pGL4.33-Luc-SRE reporter plasmids were from Promega.

4.2.3. Cell culture and transfection

Human embryonic kidney 293 (HEK293) cells were maintained at 37°C in a 5% CO_2 humidified environment in Dulbecco's modified Eagle medium (DMEM; serum free medium [SFM]) supplemented with 10% fetal calf serum, 2 mM glutamine, 100 U/ml penicillin and 0.1 mg/ml streptomycin (full serum medium [FSM]). Cells were transiently transfected for 48 h using JetPrime transfection reagent (Polyplus; 2 µl/µg DNA) according to the manufacturer's instructions.

4.2.4. Methylthiazol tetrazolium (MTT) assay

Performed to assess the cytotoxicity of GLP-1, compound 2 and compound B on cells (Bromberg & Alakhov, 2003). HEK293 cells were seeded at a density of $2.75x10^4$ cells per well. After 24 h of plating, cells were washed and serum

starved for 1 h in SFM at 37°C/5% CO_2. Cells were either left untreated or incubated with varying concentrations of agonist for 1 h at 37°C/5% CO_2. Then MTT reagent (5 mg/ml made in PBS) diluted 1:5 in SFM was added to the cells and the plate incubated for 5 h at 37°C/5% CO_2 in the dark. After 5 h, the MTT reagent was removed and the reaction product accumulated in cells was solubilised in DMSO for 30 min. The solubilised product was quantified at 550 nm using a plate reader. Each concentration was performed in triplicate with 3 independent cell preparations.

4.2.5. Enzyme linked immunosorbent assay (ELISA)

This is carried out as described previously with unpermeabilised cells to quantify cell surface expression (Kanamarlapudi et al, 2012). Briefly, HEK293 cells expressing the hGLP-1R were serum starved for 1 h and then stimulated without or with agonist at 37°C/5% CO_2. Where indicated, cells were incubated without or with antagonist for 30 min or small molecule agonists for 60 min prior and during stimulation with agonist at 37°C/5% CO_2. Cells were then fixed with 4% paraformaldehyde (PFA) for 5 min and non-specific binding sites blocked with 1% bovine serum albumin (BSA) made in Tris buffered saline (TBS) (1% BSA/TBS) for 45 min. Cells were incubated with the anti-hGLP-1R or anti-VSVG mouse antibody (diluted 1:15000) in 1% BSA/TBS for 1 h, washed with TBS and then incubated with the HRP-conjugated anti-mouse IgG (diluted 1:5000) in 1% BSA/TBS for 1 h. Cells were washed and developed using 1-step Ultra TMB-ELISA substrate (Bio-Rad) for 15 min and the reaction stopped by adding an equal volume of 2 M sulphuric acid. The optical density was read at 450 nm using a plate reader.

4.2.6. Immunofluorescence

Intracellular localisation of hGLP-1R expression was assessed by immunofluorescence as described previously (Kanamarlapudi et al, 2012). Briefly, cells were serum starved for 1 h and where indicated cells were preincubated without or with antagonist for 30 min or small molecule agonists for 60 min. Cells were then incubated with the anti-hGLP-1R mouse antibody

(diluted 1:5000) in 1% BSA/SFM for 1 h at 4°C and then stimulated without or with agonist in the absence or presence of antagonist or small molecule agonists at 37°C/5% CO_2. Cells were then fixed with 4% PFA for 30 min. Cells were permeabilised with 0.2% Triton X-100 made in phosphate buffered saline (PBS) for 10 min, blocked in blocking buffer (1% BSA made in wash buffer [0.1% Triton X-100 in PBS]) for 30 min and then incubated with the Cy3-conjugated anti-mouse antibody (diluted 1:200 in blocking buffer) for 1 h. Cells were then washed 3 times with wash buffer and incubated with DAPI (4′,6-diamidino-2-phenylindole dihydrochloride, 1 mg/ml) diluted 1:2000 in PBS to stain nucleus. Coverslips were mounted on glass microscopic slides using mounting solution (0.1 M Tris-hydrochloric acid [HCl], pH 8.5, 10% Mowiol 50% glycerol) containing 2.5% DABCO (1,4 diazabicyclo (2.2.2) octane). Immunofluorescence staining was visualised using a Zeiss LSM710 confocal microscope fitted with a 63x oil immersion lens.

4.2.7. Live cell imaging

For live cell imaging, transiently transfected HEK293 cells were plated into 8-chamber glass bottom slides (Thermo Scientific, Northumberland, UK) pre-coated with poly-L-lysine and incubated at 37°C/5% CO_2 in FSM. After 24 h, cells were washed 3 times with and incubated in 250 µl per well of SFM for 1 h at 37°C/5% CO_2 for serum starvation. Cells were then imaged by live cell imaging, using a Zeiss LSM710 confocal microscope fitted with a 63x oil immersion lens. Cells were imaged twice (0 and 3 min) with no agonist added and for every 3 min after stimulating with agonist (diluted in 0.5% fat-free BSA/SFM) at 37°C for 60 min.

4.2.8. cAMP, Ca^{2+} and ERK luciferase assay

HEK293 cells cotransfected with the hGLP-1R plasmid and luciferase reporter plasmid for cAMP (pGL4.29-Luc-CRE) or intracellular Ca^{2+} (pGL4.30-Luc-NFAT) or ERK phosphorylation (pGL4.33-Luc-SRE) were treated with increasing concentrations of agonist for 4 h (cAMP and ERK) or 8 h (Ca^{2+}) at 37°C/5% CO_2. After incubation, an equal volume of ONE-Glo™ lysis buffer containing

luciferase substrate (Promega) was then added to each well and luminescence (relative light units [RLU]) measured using a plate reader in accordance with the manufacturer's instructions.

4.2.9. Cell lysates

To make cell lysates, HEK293 cells expressing the hGLP-1R were washed 3 times with ice cold PBS and lysed in ice cold modified RIPA lysis buffer (10 mM Tris HCl, pH 7.5 containing 10 mM ethylenediaminetetraacetic acid [EDTA], 1% nonyl phenoxypolyethoxylethanol [NP40], 0.1% sodium dodecyl sulphate [SDS], 0.5% sodium deoxycholate and 150 mM sodium chloride [NaCl]) with 1% mammalian protease inhibitors. Cell lysates were incubated at 4°C for 15 min and then centrifuged at 22000 xg for 10 min at 4°C. The supernatant was collected and ½ volume of 3x SDS-polyacrylamide gel electrophoresis (PAGE) sample loading buffer (75 mM Tris HCl, pH 6.8 containing 3% SDS, 30% glycerol, 0.003% bromophenol blue and 0.3 M dithiothreitol [DTT]) was added and left at room temperature for 1 h. The cell lysates were used to detect hGLP-1R expression by immunoblotting using the anti-GFP and anti-VSVG antibodies.

For assessing ERK1/2 phosphorylation, HEK293 cells expressing the hGLP-1R were lysed in ice cold modified RIPA lysis buffer (50 mM Tris HCl, pH 7.5, containing 0.2 M NaCl; 10 mM $MgCl_2$; 0.1% SDS; 0.5% sodium deoxycholate; 1% TritonX-100; 5% Glycerol) with 1% mammalian protease inhibitors. Cell lysates were incubated at 4°C for 15 min and centrifuged at 22000 xg for 10 min at 4°C. The supernatant was collected and ¼ volume of 5x SDS-PAGE sample loading buffer (125 mM Tris HCl, pH 6.8 containing 5% SDS, 50% glycerol, 0.005% bromophenol blue and 5% β-mercaptoethanol) was added and heated at 100°C for 5 min. These cell lysates were used to detect phosphorylated ERK and total ERK by immunoblotting using the anti-pERK1/2 and anti-ERK1/2 antibodies.

4.2.10. Immunoblotting

Proteins were separated in a SDS-PAGE gel by electrophoresis and transferred onto polyvinylidene fluoride (PDVF) membrane. Membranes were blocked with

TBST (TBS with 0.1% tween 20) containing 5% milk powder (blocking buffer) for 1 h at room temperature or overnight at 4°C. Membranes were immunoblotted with the anti-GFP mouse antibody (diluted 1:500 in blocking buffer) to assess protein expression levels or the anti-pERK1/2 rabbit antibody (diluted 1:1000 in blocking buffer) to assess ERK1/2 phosphorylation for 1 h at room temperature or overnight at 4°C. Membranes were washed and then incubated with the HRP-conjugated anti-mouse or anti-rabbit secondary antibody (diluted 1:2500 in blocking buffer) for 1 h at room temperature. Membranes were then incubated in ECL select substrate and bands visualised using the ChemiDoc™ XRS system (Bio-Rad). Blots probed with the anti-GFP mouse antibody were stripped with western blot stripping buffer (Thermo Scientific) and reprobed with the anti-VSVG rabbit antibody (diluted 1:1000 in blocking buffer) to assess protein expression levels. Blots probed with the anti-pERK1/2 rabbit antibody were stripped and reprobed with the anti-ERK1/2 rabbit antibody (diluted 1:1000 in blocking buffer) to assess ERK1/2 phosphorylation. The HRP-conjugated anti-rabbit secondary antibody (diluted 1:2500 in blocking buffer) was used as described above.

4.2.11. Data analysis

Data were analysed using the GraphPad Prism program. All data are presented as means ± standard error of the mean (SEM) of three independent experiments. Statistical comparisons between the control and test value was made by a two-tailed unpaired student t-test. Statistical analysis between multiple groups were determined by the Bonferroni's post test after one-way or two-way analysis of variance (ANOVA), where $p>0.05$ was considered as statistically not significant (n.s.), and $p<0.05$, $p<0.01$ and $p<0.001$ shown as *, ** and *** respectively, was considered statistically significant. Concentration response curves were also fitted using Prism, according to a standard logistic equation. Scale bar in confocal images represents 10 μm. Confocal images shown in the figures are representative of 190-200 transfected cells from three different experiments. Similarly, immunoblotting data shown in the figures are representative of three independent experiments.

4.3. Results

4.3.1. Initial characterisation of the hGLP-1R

Agonist induced internalisation of the hGLP-1R into intracellular compartments of the cell is important for regulation of the receptor's activity (Bhaskaran & Ascoli, 2005; Kanamarlapudi et al, 2012). Therefore, the effect of agonists GLP-1 (7-36)-NH_2 (Tocris), GLP-1 (7-37) (Novo Nordisk) and exendin-4 (Eli Lilly) on hGLP-1R internalisation was assessed by ELISA (Figure 4.1A) and immunofluorescence (Figure 4.1B). The addition of 100 nM GLP-1 (7-36)-NH_2 to cells had a maximal internalisation effect of 66.3 ± 2.7% ($p<0.001$). 100 nM GLP-1 (7-37) and Exendin-4 internalised 65.6 ± 2.9% ($p<0.001$) and 66.5 ± 5.4% ($p<0.001$) of cell surface receptors, respectively. Immunofluorescence imaging of cells confirmed agonist induced internalisation of the hGLP-1R and showed good correlation between loss of the cell surface receptors detected by ELISA and internalisation of the receptor's identified by immunofluorescence (Figure 4.1B). All agonists showed very little variation in the internalisation effect and therefore GLP-1 (7-37) (mentioned as GLP-1) was used for further experimentation, as it was more readily available.

Further, the kinetics of agonist induced internalisation of the hGLP-1R with the N-terminal VSVG-tag (before and after the signal peptide [SP]) and C-terminal GFP-tag either present or absent (Figure 4.2A) was assessed for agonist induced internalisation (by ELISA [Figure 4.2B] and immunofluorescence [Figure 4.2D]) and cAMP activity (Figure 4.2C). All constructs showed similar kinetics (see Table 4.1) to that of the untagged hGLP-1R demonstrating that the N-terminal VSVG-tag and C-terminal GFP-tag had no effect on cell surface expression, agonist induced internalisation or cAMP production of the receptor. The hGLP-1R with the N-terminal VSVG-tag after the SP and C-terminal GFP-tag (SP-VSVG-hGLP-1RΔN23-GFP) was used in further experiments.

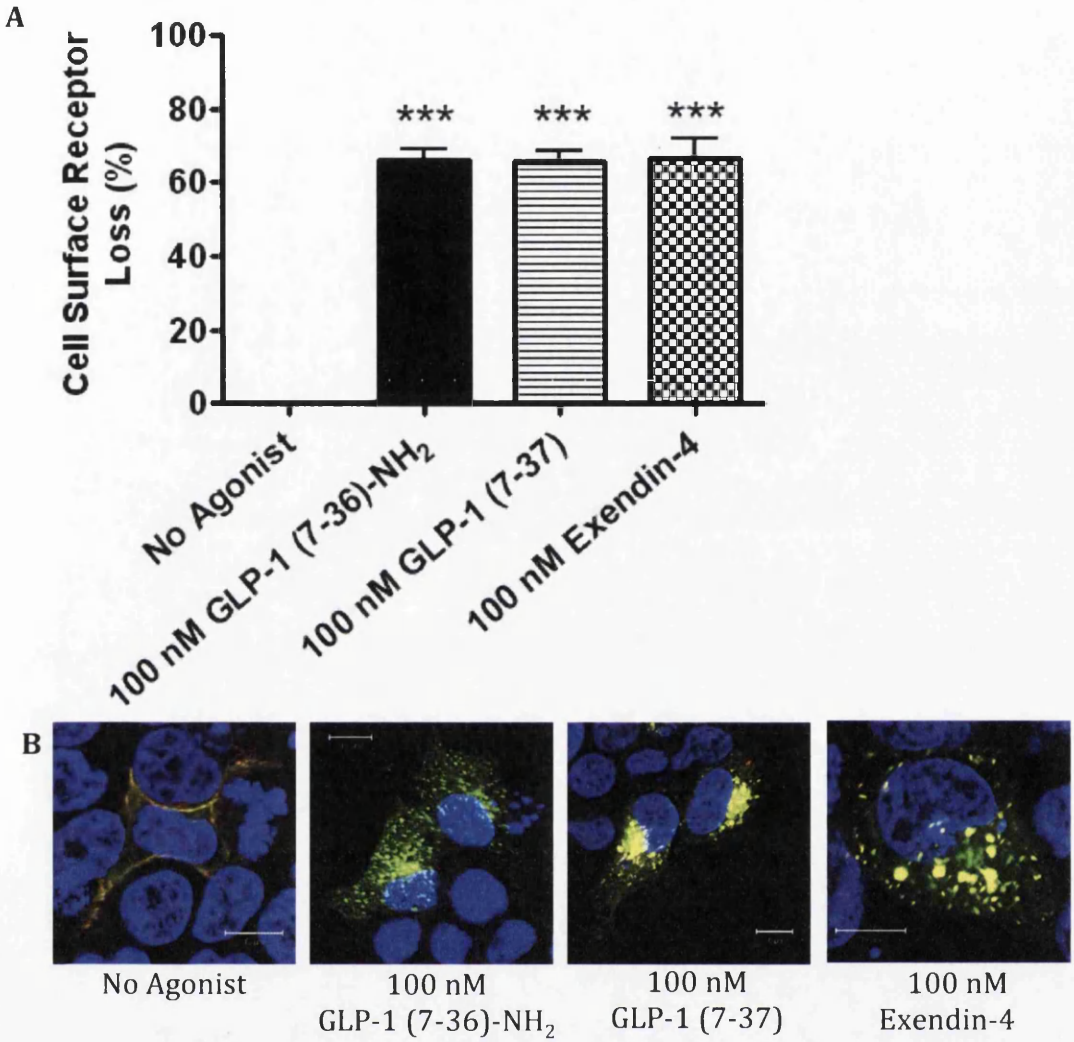

Figure 4.1. Agonist mediated internalisation of the hGLP-1R. HEK293 cells expressing the hGLP-1R were treated without or with 100 nM GLP-1 (7-36)-NH_2, GLP-1 (7-37) or Exendin-4 for 60 min to assess hGLP-1R internalisation by ELISA (A) and immunofluorescence (B) using the anti-hGLP-1R antibody. In immunofluorescence, EGFP (green) and the anti-GLP-1R antibody (red) overlay shown in yellow and nuclear staining with DAPI in blue. Data are percentage of total cell surface receptors and are mean ± SEM, n=3. Data were analysed by Bonferroni's post test after one-way ANOVA; values differ from control, *** $p<0.001$.

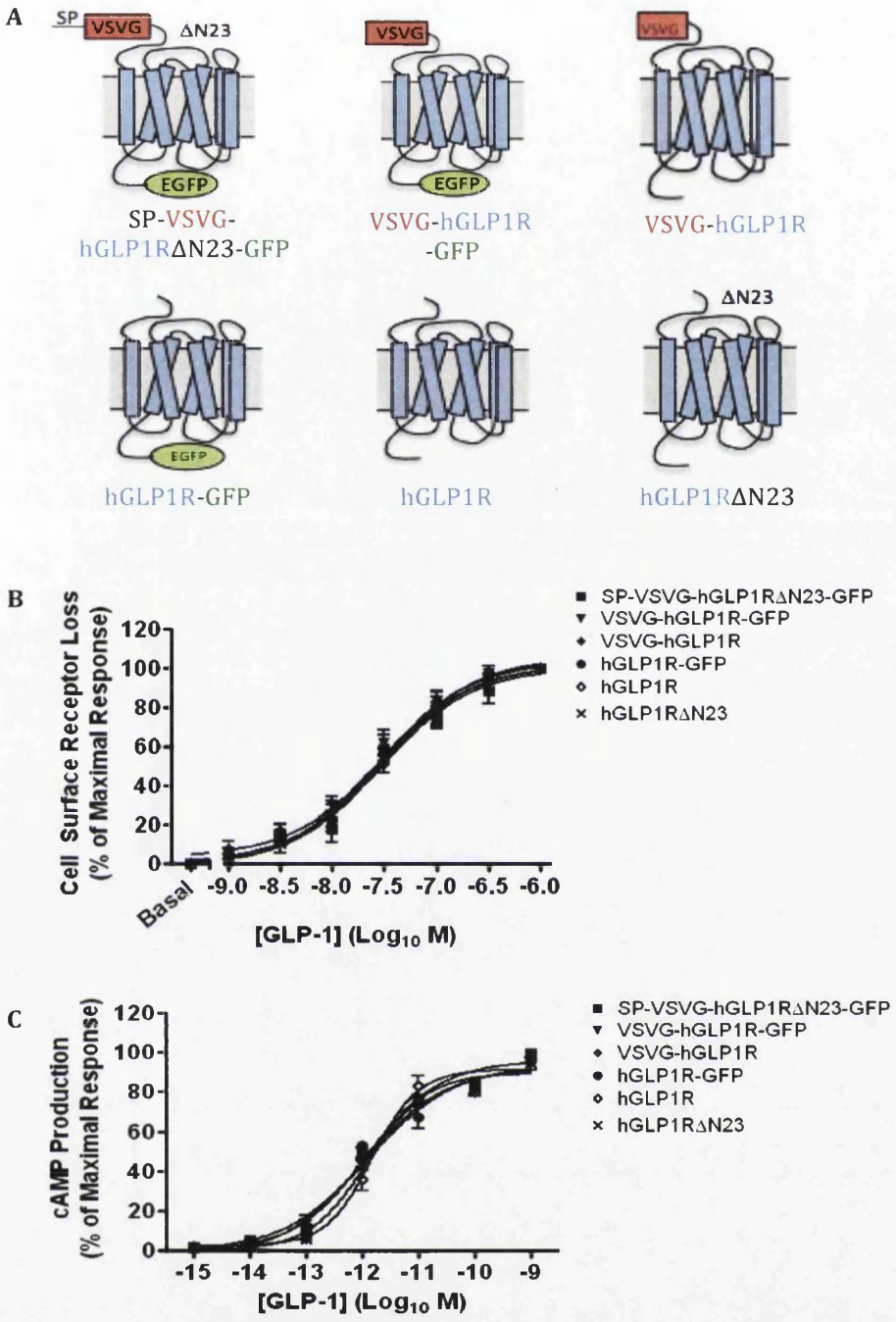

Figure 4.2. The effect of various epitope tags on hGLP-1R activity. HEK293 cells expressing various hGLP-1R epitope tagged constructs (A) were stimulated for 60 min with 100 nM GLP-1 and assessed for hGLP-1R internalisation by ELISA (B) using the anti-hGLP-1R antibody. (C) Agonist stimulated cAMP production was measured for 4 h to assess hGLP-1R activity by cotransfecting with a pGL4.29-Luc-CRE reporter plasmid. Data are mean ± SEM, n=3.

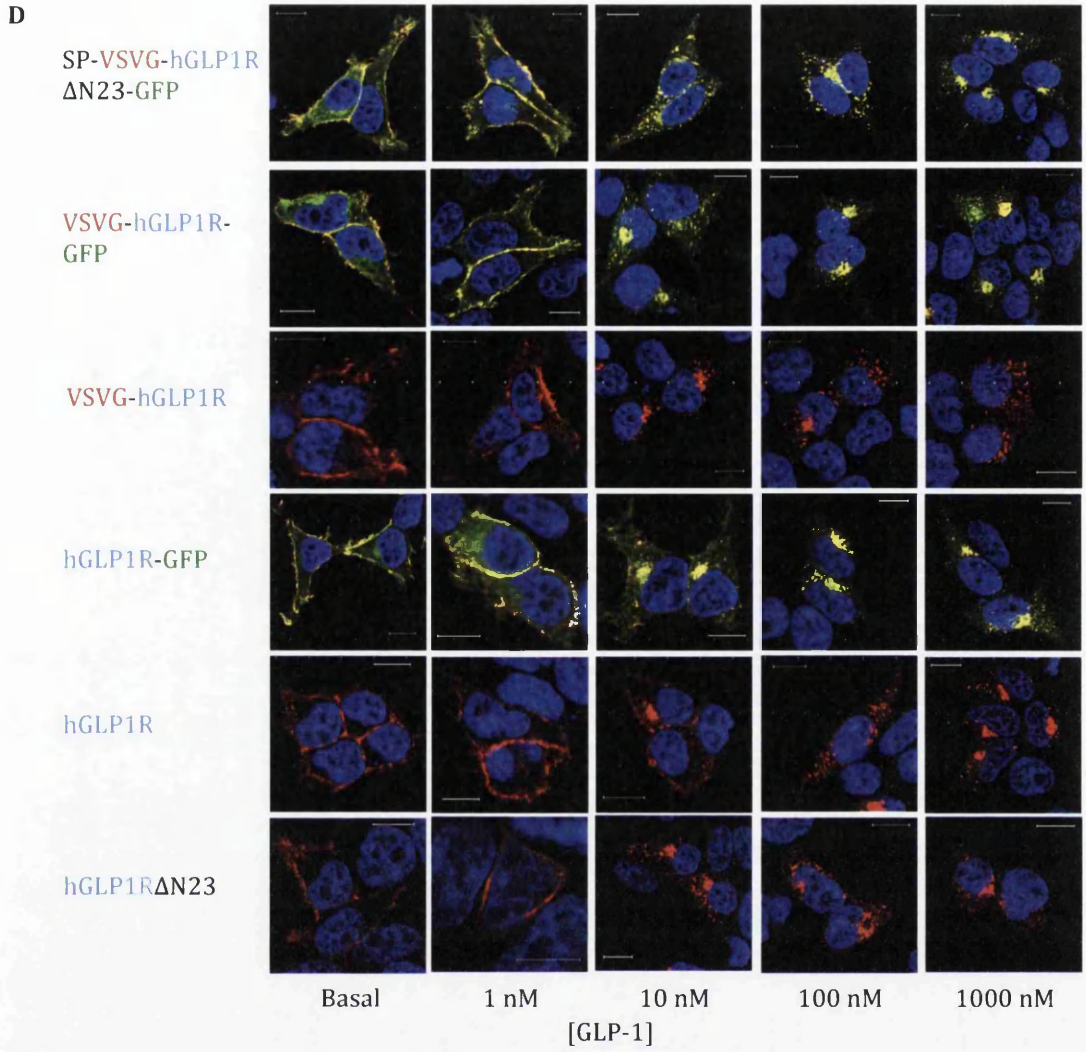

Figure 4.2 cont. The effect of various epitope tags on hGLP-1R activity. (D) Immunofluorescence showing expression of hGLP-1R, EGFP (green) and the anti-hGLP-1R antibody (red) overlay shown in yellow and nuclear staining with DAPI in blue. Data are mean ± SEM, n=3.

Table 4.1. EC_{50} values for the various epitope tagged hGLP-1R constructs stimulated with GLP-1

	ELISA (nM)	cAMP (pM)
SP-VSVG-hGLP-1RΔN23-GFP	29.34 ± 0.09	1.2 ± 0.09
VSVG-hGLP-1R-GFP	28.31 ± 0.07	1.23 ± 0.08
VSVG-hGLP-1R	28.64 ± 0.06	1.29 ± 0.09
hGLP-1R-GFP	29 ± 0.08	1.02 ± 0.15
hGLP-1R	30.34 ± 0.06	1.51 ± 0.09
hGLP-1RΔN23	27.29 ± 0.06	1.23 ± 0.08

The data shows no significant difference in the potency of GLP-1 to internalise the hGLP-1R or stimulate cAMP production in the various epitope tagged hGLP-1R constructs.

4.3.2. Characterisation of two small molecule agonists of the hGLP-1R

Two small molecule agonists of the hGLP-1R, compound 2 and compound B, were examined for their effects on hGLP-1R activity (using cAMP production, intracellular Ca^{2+} accumulation and ERK phosphorylation as readouts) and internalisation, and compared to that of GLP-1. Initially, compounds 2 and B were assessed for whether they affect the viability of HEK293 cells using the MTT assay. These compounds had no effect on HEK293 cell viability up to 33 μM. At 100 μM concentration, compound 2 and compound B reduced HEK293 cell viability to 71.7 ± 2.1% and 72.5 ± 1.6% respectively, demonstrating a small amount of cytotoxicity by these compounds at this concentration (Figure 4.3).

Compounds 2 and B were then assessed for their effects on agonist induced cAMP production (Figure 4.4A), intracellular Ca^{2+} accumulation (Figure 4.4B) and ERK phosphorylation (Figure 4.4C-D), and compared to that of GLP-1. GLP-1 stimulated a concentration dependent increase in cAMP production in HEK293 cells expressing the hGLP-1R with an EC_{50} of 3.6 ± 0.1 pM. Compound 2

and compound B also induced the same levels of cAMP production with an EC_{50} of 2.5 ± 0.2 μM and 4.4 ± 0.1 μM respectively, demonstrating compounds 2 and B both stimulate cAMP production with similar maximal cAMP responses to that of GLP-1. GLP-1 increased intracellular Ca^{2+} accumulation (EC_{50} of 53.7 ± 0.1 nM) and ERK phosphorylation (EC_{50} of 55.7 ± 0.1 nM) in a concentration dependent manner in hGLP-1R expressing cells. However, compounds 2 and B had no effect on intracellular Ca^{2+} accumulation (Figure 4.4B) and ERK phosphorylation (Figure 4.4C-D). Taken together, these results demonstrate compounds 2 and B induce cAMP production with similar maximal cAMP response to GLP-1 but do not activate intracellular Ca^{2+} accumulation or ERK phosphorylation.

Since intracellular Ca^{2+} accumulation and ERK phosphorylation are required for GLP-1 stimulated hGLP-1R internalisation (see Chapter 5), the effect of compounds 2 and B on hGLP-1R internalisation was assessed next. HEK293 cells expressing the hGLP-1R were challenged with increasing concentrations of GLP-1, compound 2 and compound B for 60 min and internalisation of the receptor was analysed by ELISA using the anti-hGLP-1R antibody (Figure 4.5A) and anti-VSVG antibody (Figure 4.5B). The orthosteric agonist, GLP-1, induced a concentration dependent increase in hGLP-1R internalisation and had a maximal effect of 76.0 ± 4.4% at 100 nM (EC_{50} of 33.7 ± 0.1 nM). Interestingly, compound 2 showed no induction of hGLP-1R internalisation up to 3.3 μM and at its highest concentration (100 μM) only 16.6 ± 7.0% of cell surface receptors were internalised (EC_{50} of 2233.6 ± 6.6 μM was calculated). Additionally, compound B showed no effect on internalisation of the receptor up to a concentration of 100 μM. When hGLP-1R internalisation was assessed by ELISA using the anti-VSVG antibody, the results obtained were similar to that obtained with the anti-hGLP-1R antibody (EC_{50} of 31.1 ± 0.1 nM for GLP-1, 2187.8 ± 8.4 μM for compound 2 was calculated, and no EC_{50} was determined for compound B, Figure 4.5B). This indicated the anti-hGLP-1R antibody does not interfere with compound 2 and compound B binding to the receptor and therefore only the anti-hGLP-1R antibody was used in further experiments. These results were confirmed by immunofluorescence analysis (Figure 4.5C) where intracellular

punctate structures, indicative of hGLP-1R internalisation, were observed for cells treated with GLP-1, but were absent in cells treated with compound 2 and B.

Additionally, the time dependent effect of GLP-1, compound 2 and compound B on hGLP-1R internalisation was determined using ELISA (Figure 4.6A) and live cell imaging (Figure 4.6B). GLP-1 induced hGLP-1R internalisation in a time dependent manner, reaching maximum internalisation of the receptor after approximately 60 min of stimulation (73.6 ± 5.8%). In contrast, no internalisation of the receptor was observed for compound 2 and compound B. Live cell imaging showed the appearance of intracellular punctate structures when challenged with GLP-1 but not with compound 2 or compound B, supporting the ELISA results. Together, these results demonstrate that unlike GLP-1, the small molecule agonists do not internalise the hGLP-1R most likely because they are unable to induce intracellular Ca^{2+} accumulation or ERK phosphorylation.

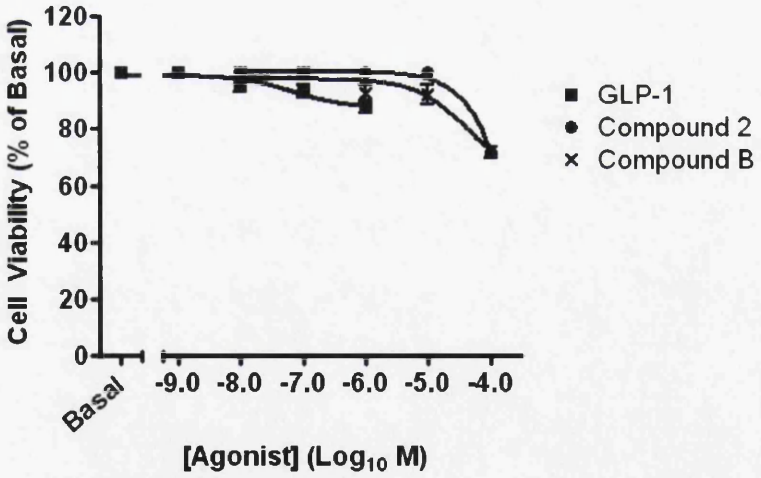

Figure 4.3. Viability of HEK293 cells treated with increasing concentrations of GLP-1, compound 2 and compound B. HEK293 cells were treated with the indicated concentrations of GLP-1, compound 2 and compound B for 60 min and assessed for their toxicity using a MTT assay. Data are mean ± SEM, n=3.

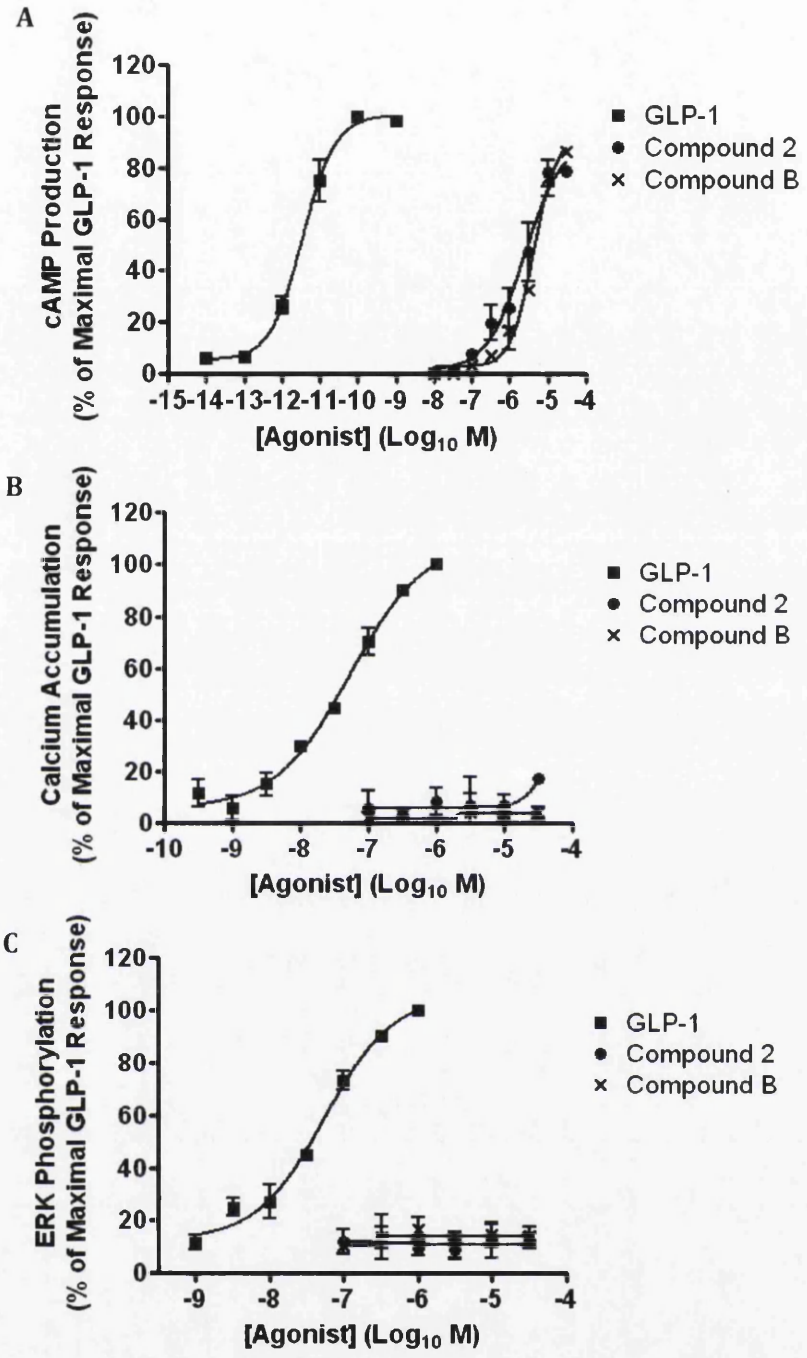

Figure 4.4. Small molecule agonists induced cAMP production but not intracellular Ca^{2+} accumulation or ERK phosphorylation. HEK293 cells cotransfected with the hGLP-1R plasmid and the luciferase reporter plasmid for cAMP (pGL4.29-Luc-CRE), intracellular Ca^{2+} (pGL4.30-Luc-NFAT) or ERK phosphorylation (pGL4.33-Luc-SRE) were stimulated with GLP-1, compound 2 and compound B as indicated for 4 h (cAMP and ERK phosphorylation) or 8 h (intracellular Ca^{2+} accumulation) to assess cAMP production (A), intracellular Ca^{2+} accumulation (B) and ERK phosphorylation (C). Data are mean ± SEM, n=3.

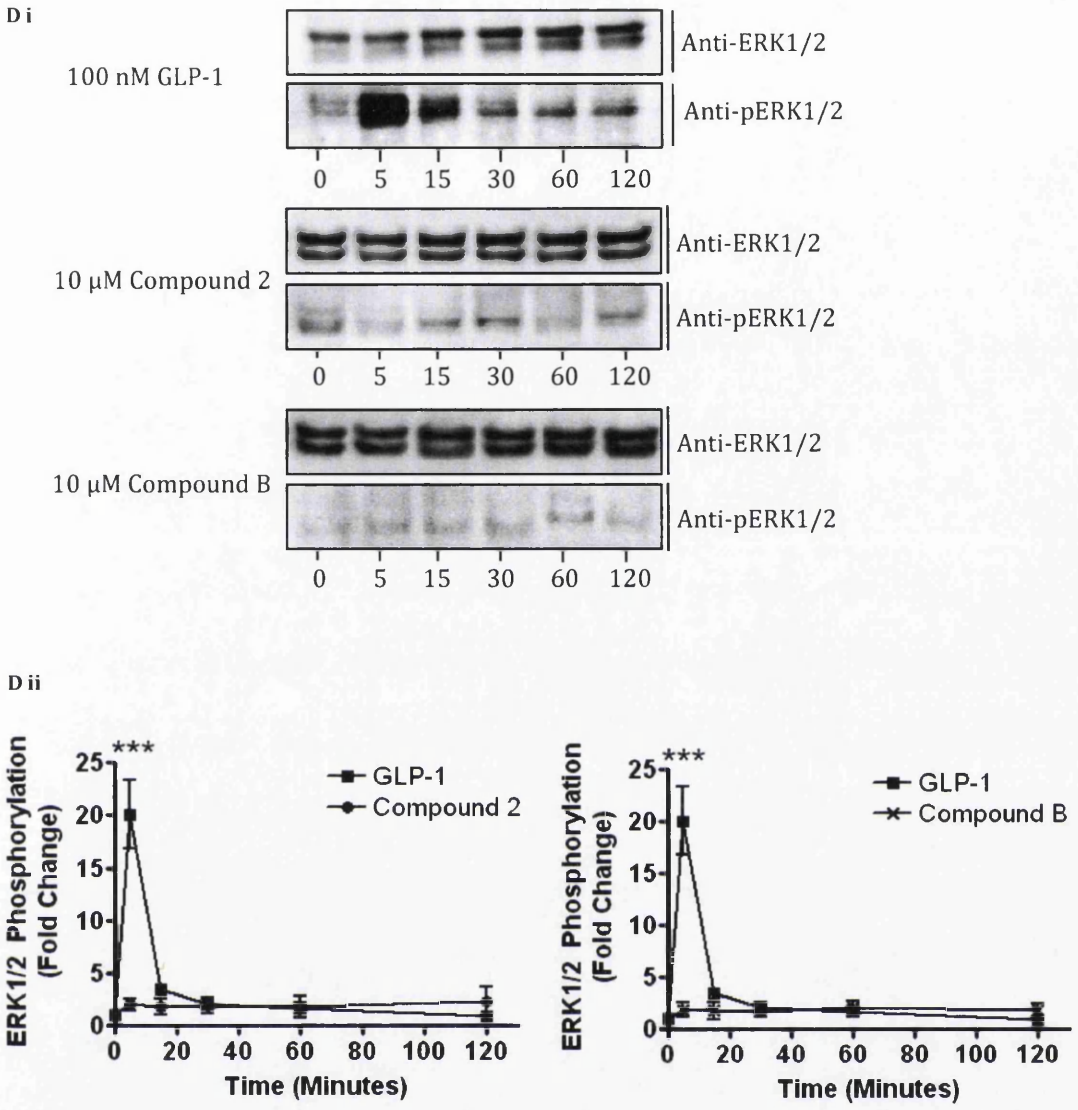

Figure 4.4 cont. Small molecule agonists induced cAMP production but not intracellular Ca^{2+} accumulation or ERK phosphorylation. (D) HEK293 cells expressing the hGLP-1R were stimulated with agonist for the indicated time and ERK1/2 phosphorylation was measured by immunoblotting (i) and quantified by densitometry and normalised to total ERK1/2 levels (ii). Data normalised to percentage stimulation of GLP-1 and are shown as mean ± SEM, n=3. Data were analysed by Bonferroni's post test after two-way ANOVA; values differ from control, ***p<0.001.

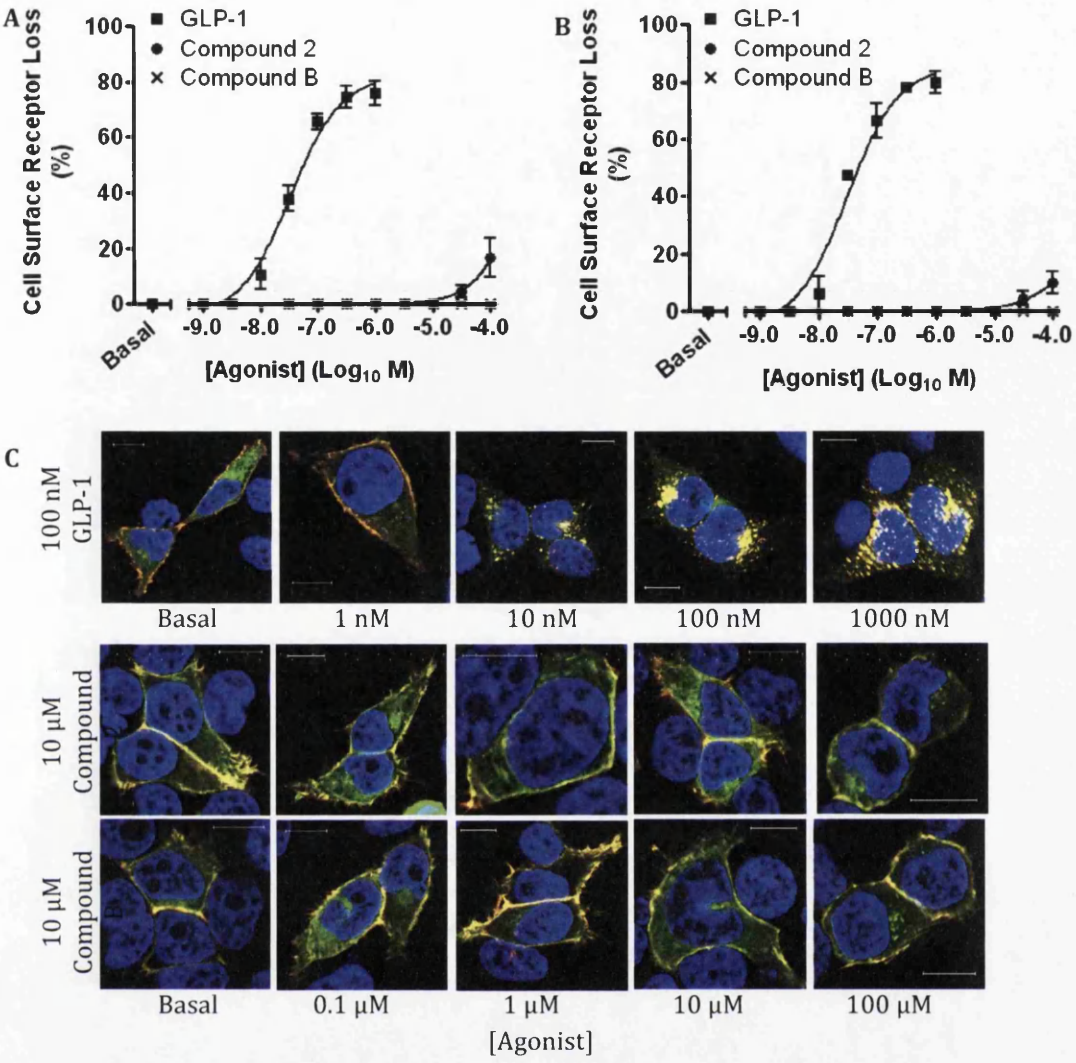

Figure 4.5. Concentration dependent stimulation of hGLP-1R internalisation by GLP-1, compound 2 and compound B. HEK293 cells expressing the hGLP-1R were stimulated with GLP-1, compound 2 and compound B at the indicated concentrations for 60 min and hGLP-1R internalisation was assessed by ELISA using the anti-hGLP-1R antibody (A) and the VSVG-antibody (B). (C) In immunofluorescence, EGFP (green) and the anti-hGLP-1R antibody (red) overlay shown in yellow and nuclear staining with DAPI in blue. Data are percentage of total cell surface receptors and are mean ± SEM, n=3.

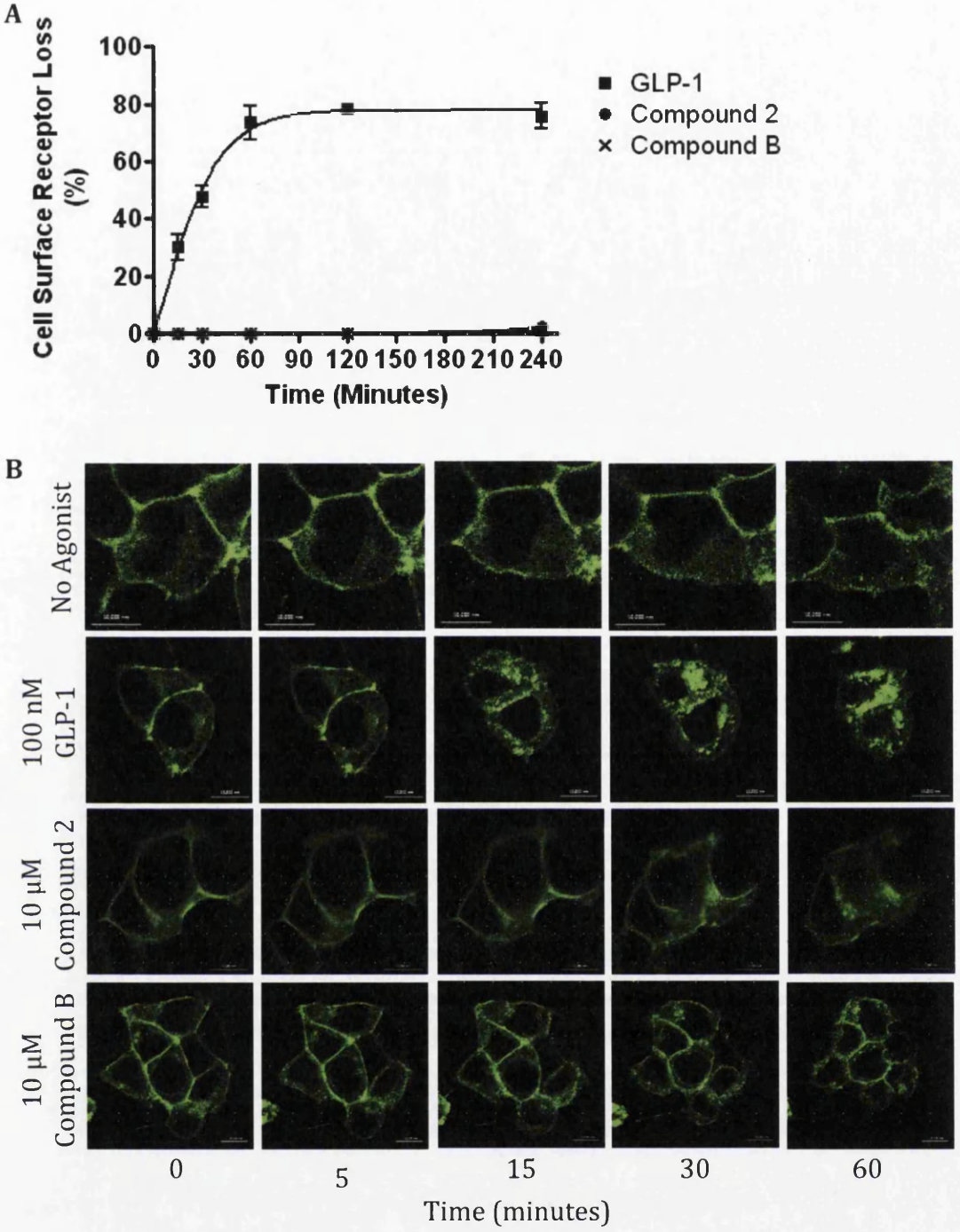

Figure 4.6. Time dependent stimulation of hGLP-1R internalisation by GLP-1, compound 2 and compound B. HGLP-1R internalisation stimulated with 100 nM GLP-1, 10 µM compound 2 and 10 µM compound B for the indicated times was assessed by ELISA (A) using the anti-hGLP-1R antibody. (B) Live cell imaging showing agonist induced internalisation of the hGLP-1R, with EGFP in green. Data are percentage of total cell surface receptors and are mean ± SEM, n=3.

4.3.3. Antagonists Ex(9-39) and JANT-4 inhibit the effects of GLP-1 but not compound 2 or compound B

Ex(9-39) and JANT-4 are known antagonists of the GLP-1R that work by binding to the orthosteric binding site, competitively inhibiting GLP-1 binding to the receptor (Goke et al, 1993; Montrose-Rafizadeh et al, 1997; Patterson et al, 2011; Thorens et al, 1993). Compound 2 and compound B have been described as ago-allosteric agonists (Coopman et al, 2010; Irwin et al, 2010; Knudsen et al, 2007; Sloop et al, 2010). To confirm this, the effect of antagonists Ex(9-39) and JANT-4 on these small molecule agonists was determined. The effects of Ex(9-39) and JANT-4 on GLP-1 (Figure 4.7A), compound 2 (Figure 4.7B) and compound B (Figure 4.7C) induced cAMP production was determined. GLP-1 stimulated a concentration dependent increase in cAMP production in HEK293 cells expressing the hGLP-1R with an EC_{50} of 2.3 ± 0.2 pM. In the presence of Ex(9-39) and JANT-4, cAMP production was reduced (14.5 ± 0.3 pM and 7.4 ± 0.5 pM, respectively). In contrast, Ex(9-39) and JANT-4 had no effect on compound 2 stimulated cAMP production (EC_{50} of 1.7 ± 0.1 μM with Ex[9-39] and 1.8 ± 0.1 μM with JANT-4 versus 2.1 ± 0.1 μM with no antagonist). Similarly, antagonists Ex(9-39) and JANT-4 had no effect on the cAMP production stimulated by compound B (EC_{50} of 4.2 ± 0.1 μM with Ex[9-39] and 4.0 ± 0.1 μM with JANT-4 versus 3.7 ± 0.1 μM with no antagonist). These results confirmed compound 2 and compound B do not bind to the orthosteric agonist binding site.

Additionally, the antagonists, Ex(9-39) and JANT-4, inhibited hGLP-1R internalisation, assessed by ELISA (A) and immunofluorescence (B), induced by GLP-1 in a concentration (Figure 4.8) and time dependent manner (Figure 4.9). GLP-1 increased hGLP-1R internalisation in a concentration dependent manner (EC_{50} of 30.7 ± 0.1 nM, Figure 4.8A). However, the addition of either Ex(9-39) or JANT-4 significantly reduced GLP-1 induced hGLP-1R internalisation and increased the EC_{50} value to 86.1 ± 0.3 nM and 227.5 ± 0.3 nM respectively. Immunofluorescence analysis supported these observations by demonstrating the inhibition of GLP-1 induced hGLP-1R internalisation by Ex(9-39) and JANT-4 antagonists in a concentration dependent manner (Figure 4.8B). Additionally,

Ex(9-39) and JANT-4 inhibited hGLP-1R internalisation induced by GLP-1 over time (Figure 4.9A). Agonist induced hGLP-1R internalisation was reduced to 60.3 ± 8.4% ($p<0.001$) by Ex(9-39) and 65.5 ± 6.5% ($p<0.001$) by JANT-4 at 60 min. These observations were confirmed by live cell imaging where inhibition of agonist induced internalisation (lack of punctate structures) was evident (Figure 4.9B). Taken together, these results demonstrate antagonists Ex(9-39) and JANT-4 non-competitively inhibit hGLP-1R activation by GLP-1 but not compounds 2 or B, confirming they act through a binding site or sites distinct from the orthosteric site on the GLP-1R.

The idea that compound 2 and compound B act through a binding site that is distinct from the orthosteric site was further assessed using two hGLP-1R mutants (V36A and K334A). The V36A mutant of hGLP-1R prevents agonist binding to the orthosteric site (Underwood et al, 2010), whereas the K334A mutant reduces cAMP production (Mathi, 1997; Takhar et al, 1996). The V36A and K334A mutants were assessed for their expression at protein level (determined by immunoblotting [Figure 4.10A]), cell surface expression and GLP-1 induced internalisation (determined by ELISA [Figure 4.10B-C] and immunofluorescence [Figure 4.10D]). The V36A and K334A total protein expression and cell surface expression was similar to that of the wild type (WT) control hGLP-1R (103.2 ± 9.6% and 108.9 ± 2.2%, $p>0.05$, respectively). As expected, GLP-1 induced hGLP-1R internalisation was almost abolished in the V36A mutant (12.4 ± 7.3%, $p<0.001$). In contrast, GLP-1 induced hGLP-1R internalisation in the K334A mutation was similar to that of the WT control (97.5 ± 3.7%, $p>0.05$). These results demonstrate that the V36A mutation abolishes GLP-1 induced hGLP-1R internalisation as suggested previously (Underwood et al, 2010). However, the K334A mutation had no effect on hGLP-1R expression or GLP-1 induced internalisation, which also confirms previous findings (Mathi, 1997; Takhar et al, 1996).

HEK293 cells expressing either the WT hGLP-1R, V36A mutant or K334A mutant were treated with increasing concentrations of GLP-1 (Figure 4.11A), compound 2 (Figure 4.11B) and compound B (Figure 4.11C) and assessed for

cAMP production. GLP-1 increased cAMP production in a concentration dependent manner with an EC_{50} of 2.2 ± 0.1 pM in WT expressing cells but not in the V36A mutant ($p<0.001$) expressing cells. Compound 2 stimulated cAMP production in a concentration dependent manner in both the WT and V36A mutant expressing cells (EC_{50} of 2.5 ± 0.1 μM and 2.9 ± 0.1 μM, respectively). Compound B also showed similar cAMP production in the WT and V36A mutant expressing cells (EC_{50} of 3.0 ± 0.1 μM and 3.2 ± 0.1 μM respectively). These results confirmed that the V36A mutation affects the orthosteric binding site of the hGLP-1R. Stimulation of cAMP production in the K334A mutant expressing cells was significantly reduced with GLP-1, compound 2 and compound B (EC_{50} of 7.9 ± 0.6 pM, 6.1 ± 0.1 μM, 4.7 ± 0.2 μM, $p<0.001$, respectively). This result confirmed that the K334A mutant inhibits cAMP production and suggests that although the small molecule agonists bind at a different site on the hGLP-1R, GLP-1, compound 2 and compound B alter the conformation of the receptor in a similar way so that the receptor couples to the $G\alpha_s$ pathway and induces cAMP production.

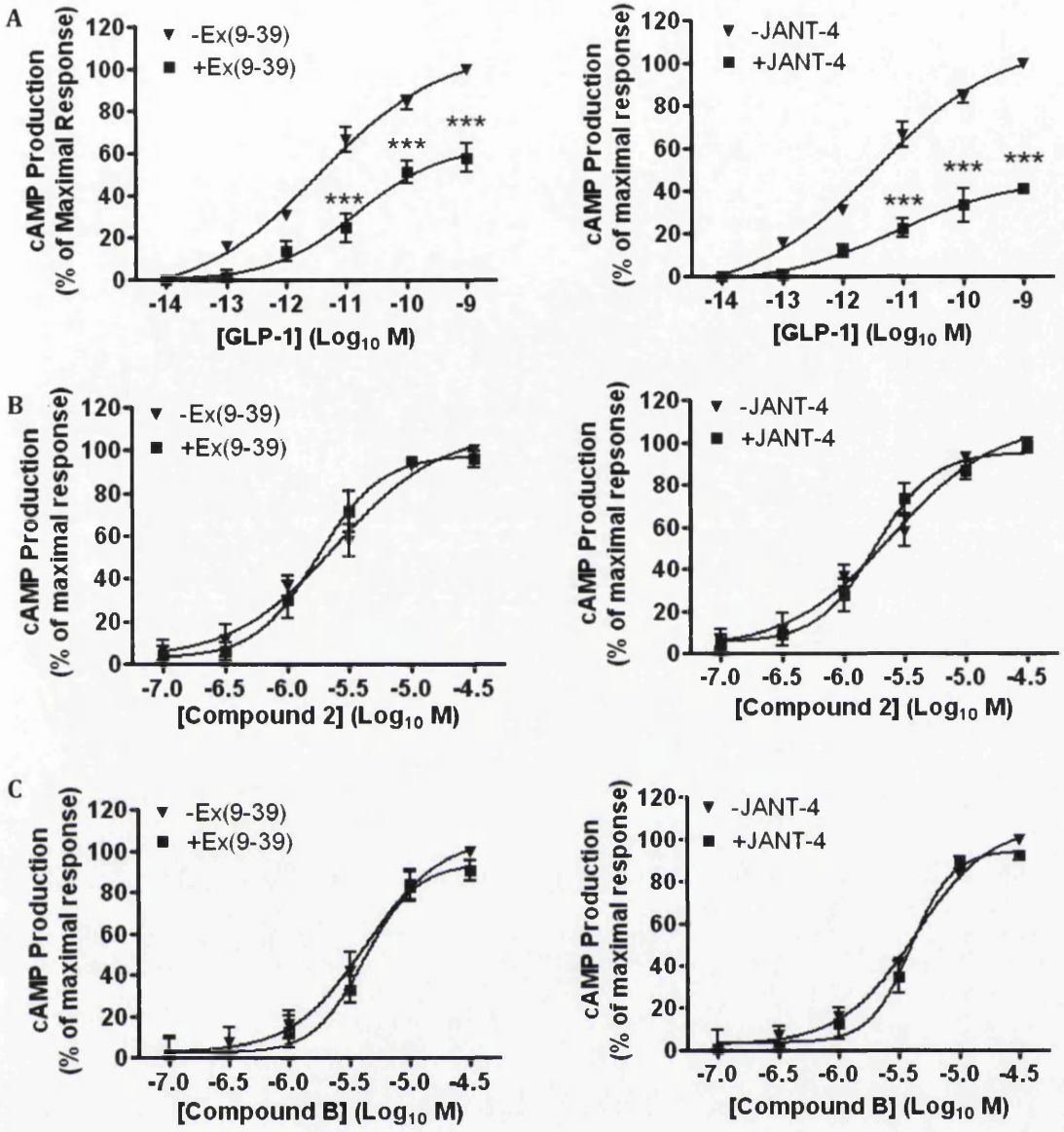

Figure 4.7. Antagonists Ex(9-39) and JANT-4 inhibit cAMP production induced by GLP-1 but not compound 2 or compound B. HEK293 cells cotransfected with the hGLP-1R plasmid and the luciferase reporter plasmid for cAMP (pGL4.29-Luc-CRE) were stimulated with GLP-1 (A), compound 2 (B) and compound B (C) in the presence of 100 nM Ex(9-39) (left panel) and JANT-4 (right panel) as indicated for 4 h to assess cAMP production. Data are mean ± SEM, n=3. Data were analysed by Bonferroni's post test after two-way ANOVA; values differ from control, ***p<0.001.

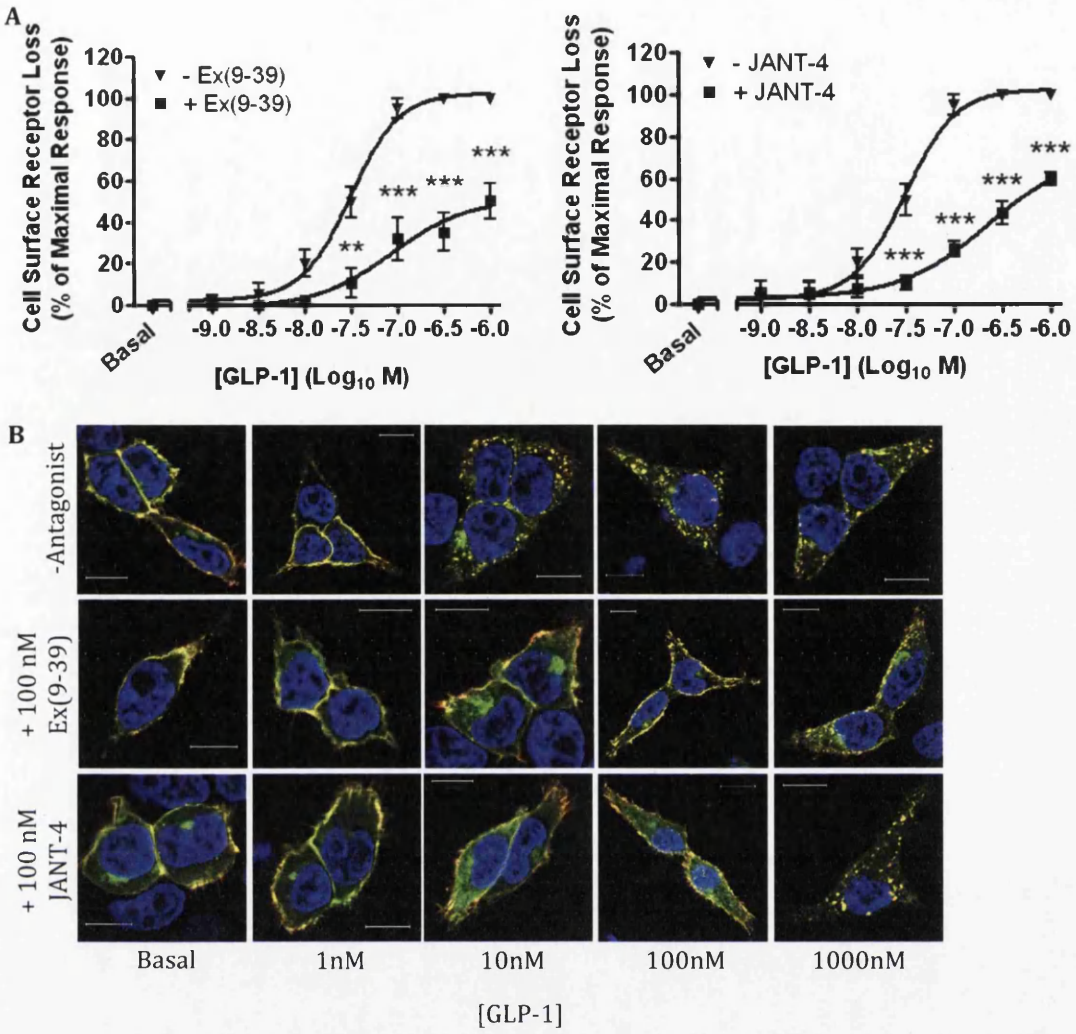

Figure 4.8. Concentration dependent stimulation of hGLP-1R internalisation by GLP-1 in the presence of antagonists Ex(9-39) and JANT-4. HEK293 cells expressing the hGLP-1R were stimulated with GLP-1 at the indicated concentrations for 60 min in the presence of 100 nM Ex(9-39) (left panel) and JANT-4 (right panel) and hGLP-1R internalisation was assessed by ELISA (A) and immunofluorescence (B) using the anti-hGLP-1R antibody. In immunofluorescence, EGFP (green) and the anti-hGLP-1R antibody (red) overlay shown in yellow and nuclear staining with DAPI in blue. Data are mean ± SEM, n=3. Data were analysed by Bonferroni's post test after two-way ANOVA; values differ from control, ** $p<0.01$, ***$p<0.001$.

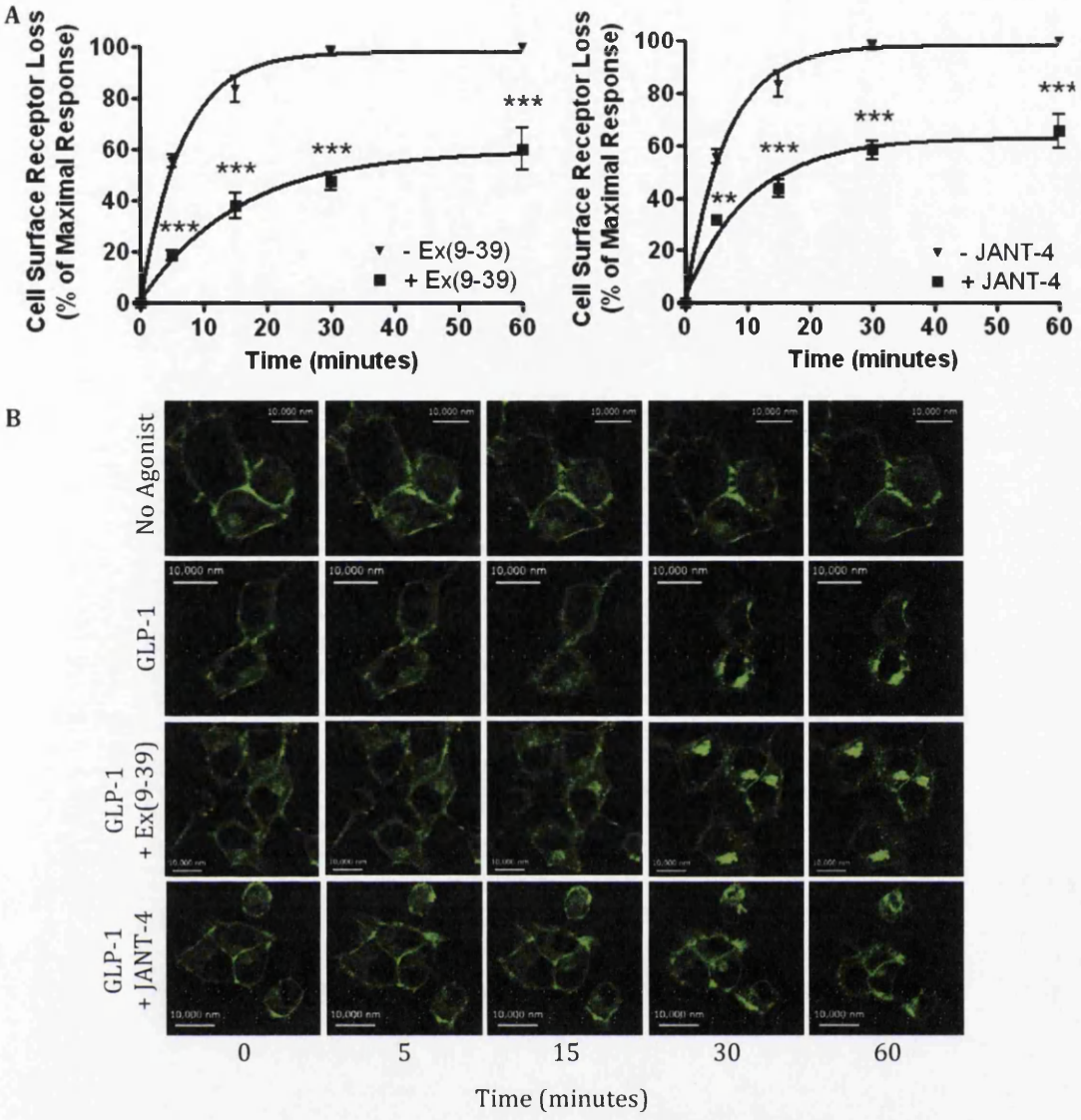

Figure 4.9. Time dependent stimulation of hGLP-1R internalisation by GLP-1 in the presence of antagonists Ex(9-39) and JANT-4. HEK293 cells expressing the hGLP-1R were stimulated with 100 nM GLP-1 at the indicated times in the presence of 100 nM Ex(9-39) (left panel) and JANT-4 (right panel) and hGLP-1R internalisation was assessed by ELISA (A) using the anti-hGLP-1R antibody. (B) Live cell imaging showing GLP-1 induced internalisation of the hGLP-1R in the presence of 100 nM Ex(9-39) and JANT-4, with EGFP in green. Data are mean ± SEM, n=3. Data were analysed by Bonferroni's post test after two-way ANOVA; values differ from control, ** $p<0.01$, *** $p<0.001$.

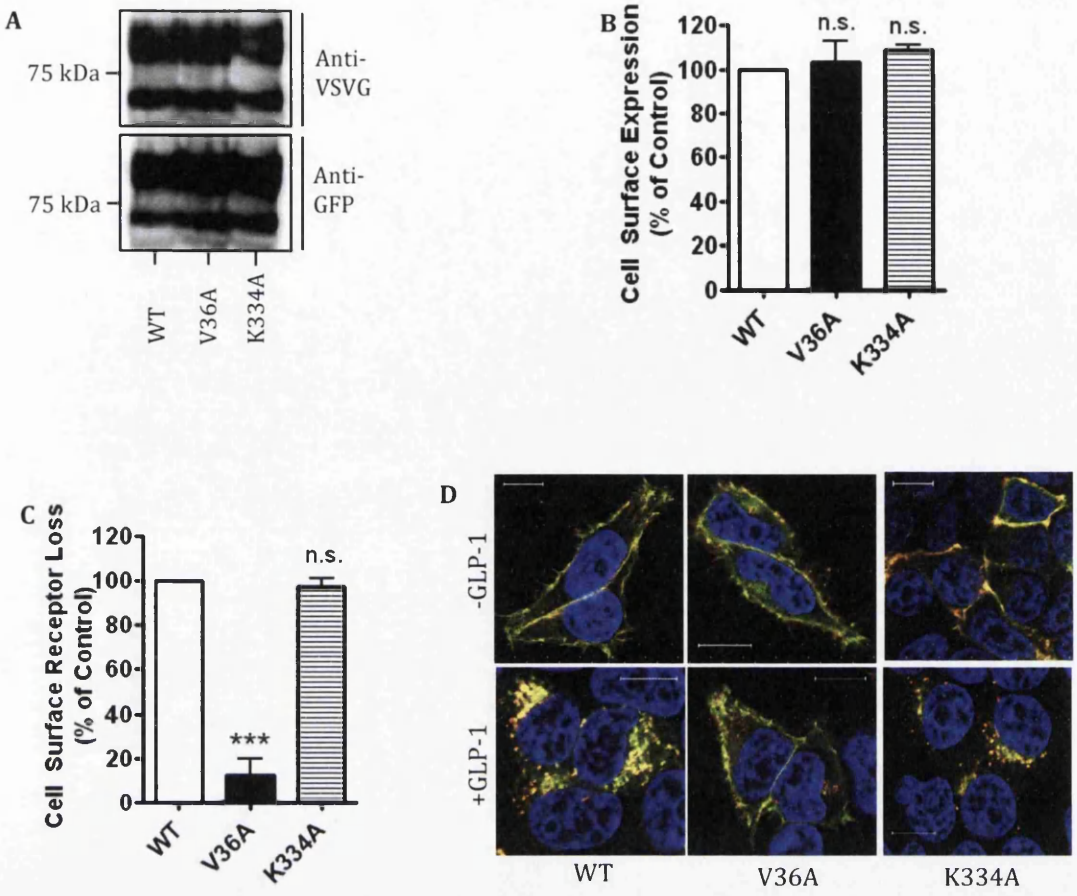

Figure 4.10. Effect of the V36A and K334A mutations on hGLP-1R cell surface expression and GLP-1 induced internalisation. HEK293 cells were transfected with the WT hGLP-1R or the V36A or K334A mutants for 48 h. (A) Total protein expression was assessed by immunoblotting using the anti-GFP and anti-VSVG antibodies. Cell surface expression (B) and 100 nM GLP-1 induced internalisation for 60 min (C) was assessed by ELISA using the anti-hGLP-1R antibody. (D) Immunofluorescence showing GLP-1 induced internalisation of the WT and mutant hGLP-1R, EGFP (green) and the anti-hGLP-1R antibody (red) overlay shown in yellow and nuclear staining with DAPI in blue. Data are mean ± SEM, n=3. Data were analysed by Bonferroni's post test after one-way ANOVA; values differ from control, n.s. $p<0.05$, *** $p<0.001$.

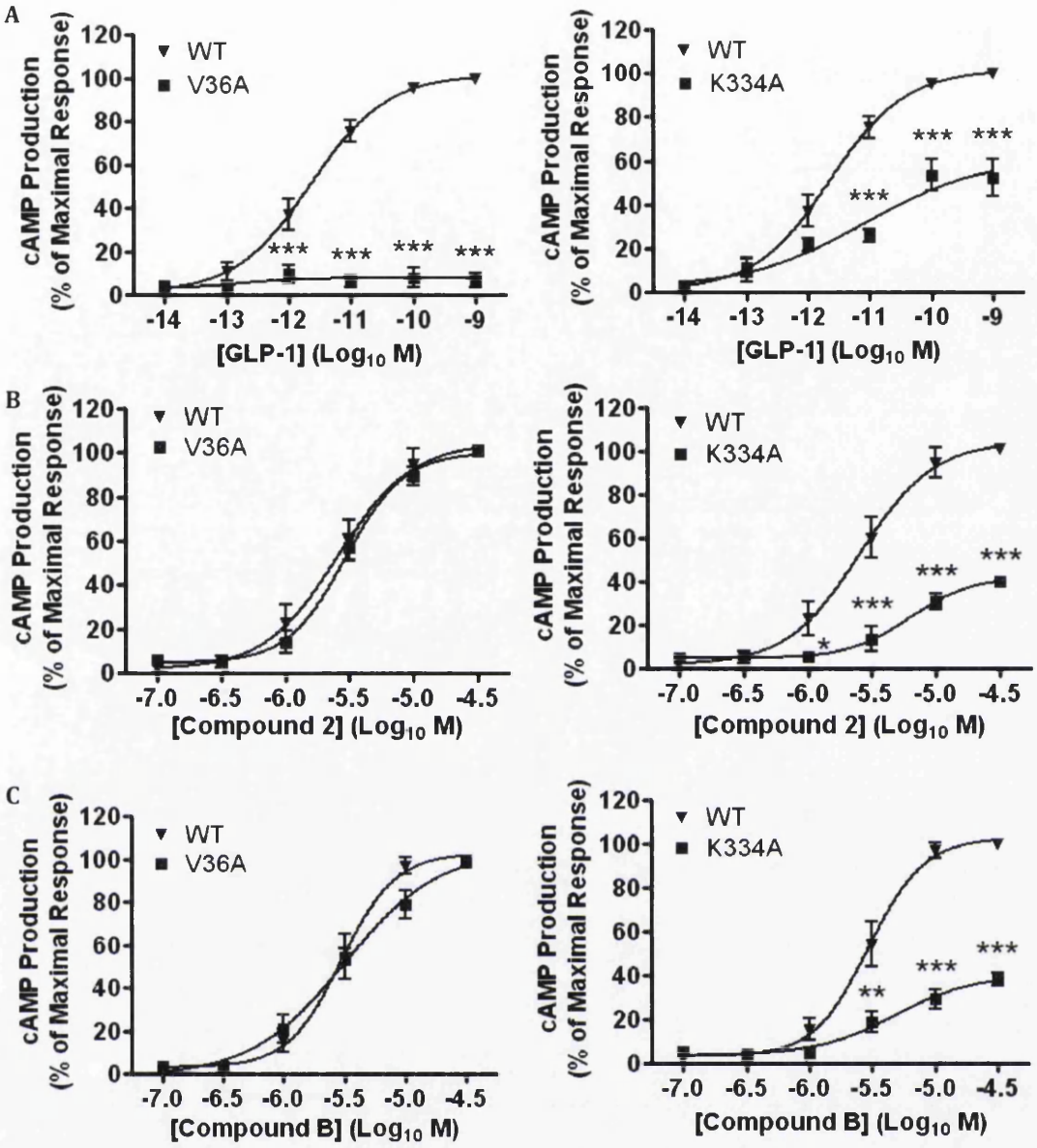

Figure 4.11. Effect of the V36A and K334A mutations on cAMP production. HEK293 cells transfected with the V36A (left panel) and K334A (right panel) mutation plasmid and the luciferase reporter plasmid pGL4.29-Luc-CRE were stimulated with GLP-1 (A), compound 2 (B) and compound B (C) as indicated for 4 h to assess cAMP production. Data are mean ± SEM, n=3. Data were analysed by Bonferroni's post test after two-way ANOVA; values differ from control, * $p<0.05$, ** $p<0.01$, *** $p<0.001$.

4.3.4. Antagonist effects of compound 2 and compound B

HEK293 cells expressing the hGLP-1R were preincubated with 10 μM compound 2 or compound B and then stimulated with increasing concentrations of GLP-1 and internalisation of the receptor was investigated by ELISA (Figure 4.12A) and immunofluorescence (Figure 4.12B). Interestingly, compound 2 and compound B reduced hGLP-1R internalisation with 10 nM GLP-1 from 31.3 ± 3.4% to just 6.3 ± 1.3% ($p<0.001$) and 8.4 ± 2.2% ($p<0.001$), respectively. The addition of 33 nM GLP-1 to cells challenged with 10 μM compound 2 or compound B also resulted in significant inhibition of internalisation of the receptor (from 56.9 ± 1.5% with GLP-1 alone to 38.3 ± 1.8% when preincubated with compound 2 and 37.9 ± 2.4% when preincubated with compound B, $p<0001$). Even with the addition of 100 nM GLP-1, a significant decrease in hGLP-1R internalisation was observed with compound 2 and compound B preincubation (from 71.8 ± 2.4% with GLP-1 alone to 55.0 ± 4.8% when preincubated with compound 2 and 47.0 ± 3.8% when preincubated with compound B, $p<0001$). This was further confirmed by immunofluorescence (Figure 4.12B).

As preincubation with compounds 2 and B showed reduced GLP-1 induced hGLP-1R internalisation, the effect of 10 μM compound 2 or compound B preincubation on GLP-1 induced cAMP production (Figure 4.13A), intracellular Ca^{2+} accumulation (Figure 4.13B) and ERK phosphorylation (Figure 4.13C) was assessed. Both small molecule agonists showed no significant effect on GLP-1 induced cAMP production. Interestingly, compound 2 and compound B significantly reduced intracellular Ca^{2+} accumulation with 10 nM GLP-1 from 921.3 ± 12.7 RLU to 335.3 ± 72.2 RLU ($p<0.001$) and 419.0 ± 114.6 RLU ($p<0.01$), respectively. The addition of 33 nM GLP-1 to cells challenged with 10 μM compound 2 or compound B also resulted in significant inhibition of intracellular Ca^{2+} accumulation (from 1015.3 ± 103.7 RLU with GLP-1 alone to 443.3 ± 147.0 RLU when preincubated with compound 2 and 420.0 ± 162.9 RLU when preincubated with compound B, $p<0001$). Even with the addition of 100 nM GLP-1, a significant decrease in intracellular Ca^{2+} accumulation was observed with compound 2 and compound B preincubation (from 1121.0 ± 62.6

RLU with GLP-1 alone to 555.3 ± 158.8 RLU and 545.3 ± 205.3 RLU, p<0001, when preincubated with compound 2 and compound B, respectively). Preincubation with either compound 2 or compound B also significantly reduced GLP-1 induced ERK phosphorylation. Addition of 10 nM GLP-1 to cells induced 1907.7 ± 139.7 RLU ERK phosphorylation, but preincubation with either compound 2 or compound B induced only 1286.7 ± 95.3 RLU or 1135.3 ± 138.3 RLU (p<0001) respectively. The addition of 33 nM GLP-1 to cells preincubated with compounds 2 and B reduced ERK phosphorylation from 2187.0 ± 170.6 RLU with GLP-1 alone to 1248.7 ± 72.1 RLU when preincubated with compound 2 and 1221.3 ± 68.5 RLU when preincubated with compound B (p<0001). ERK phosphorylation was still significantly reduced when induced by 100 nM GLP-1 after preincubation with compound 2 or compound B (from 2512.3 ± 29.0 RLU with GLP-1 alone to 1429.0 ± 135.3 RLU when preincubated with compound 2 and 1340.3 ± 102.7 RLU when preincubated with compound B, p<0001). These results demonstrate GLP-1 induced cAMP production was unaffected when preincubated with 10 μM compounds 2 and B, most likely because both small molecule agonists generate almost maximal cAMP production themselves. However, compounds 2 and B inhibited GLP-1 induced hGLP-1R internalisation, intracellular Ca^{2+} accumulation and ERK phosphorylation.

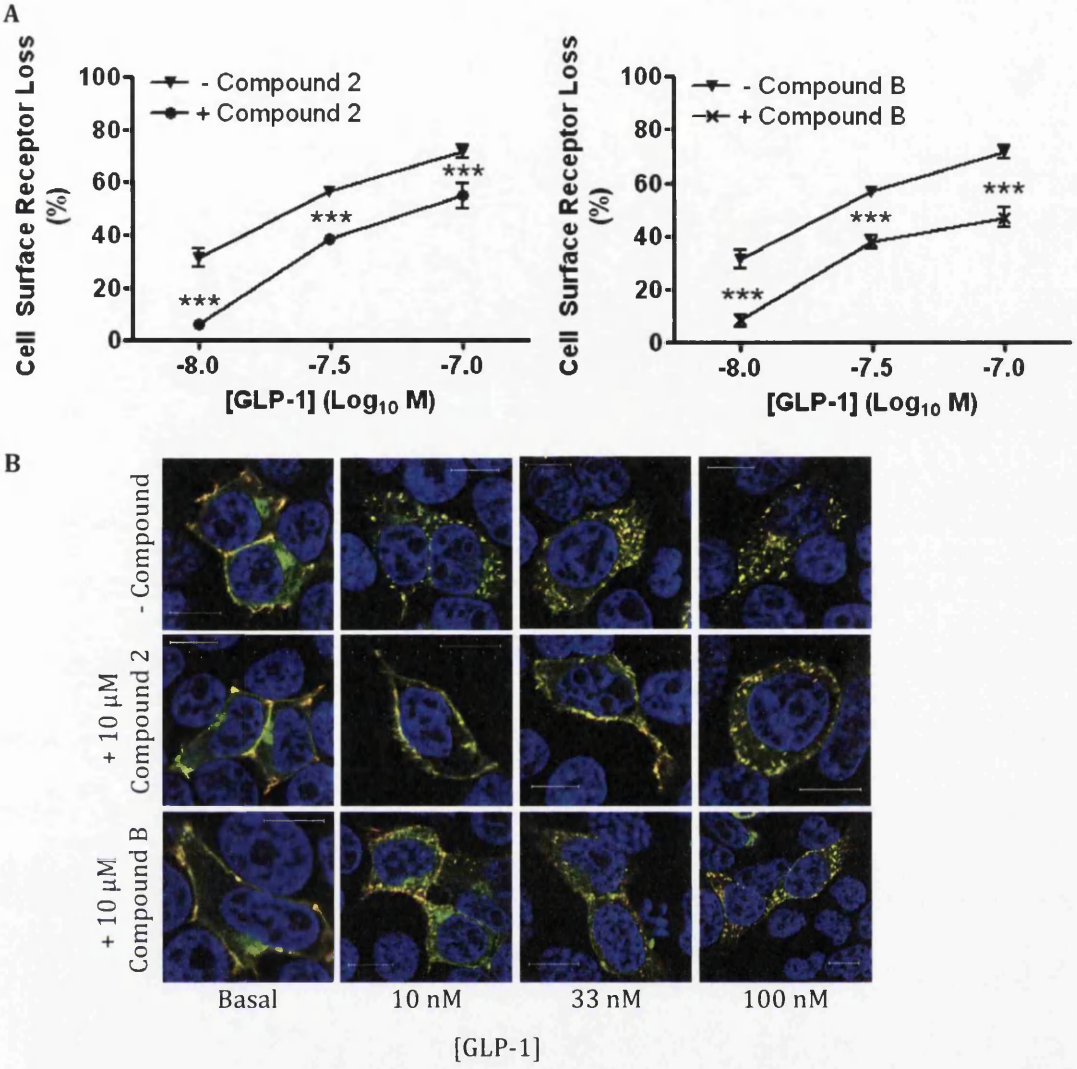

Figure 4.12. Preincubation of the hGLP-1R with compound 2 or compound B reduced GLP-1 induced internalisation. HEK293 cells were preincubated with either 10 µM compound 2 or compound B for 60 min. Cells were then stimulated with GLP-1 at the indicated concentrations for a further 60 min in the presence of 10 µM compound 2 (left panel) or compound B (right panel) and hGLP-1R internalisation was assessed by ELISA (A) and immunofluorescence (B) using the anti-hGLP-1R antibody. In immunofluorescence, EGFP (green) and the anti-hGLP-1R antibody (red) overlay shown in yellow and nuclear staining with DAPI in blue. Data are percentage of total cell surface receptors and are mean ± SEM, n=3. Data were analysed by Bonferroni's post test after two-way ANOVA; values differ from control, *** $p<0.001$.

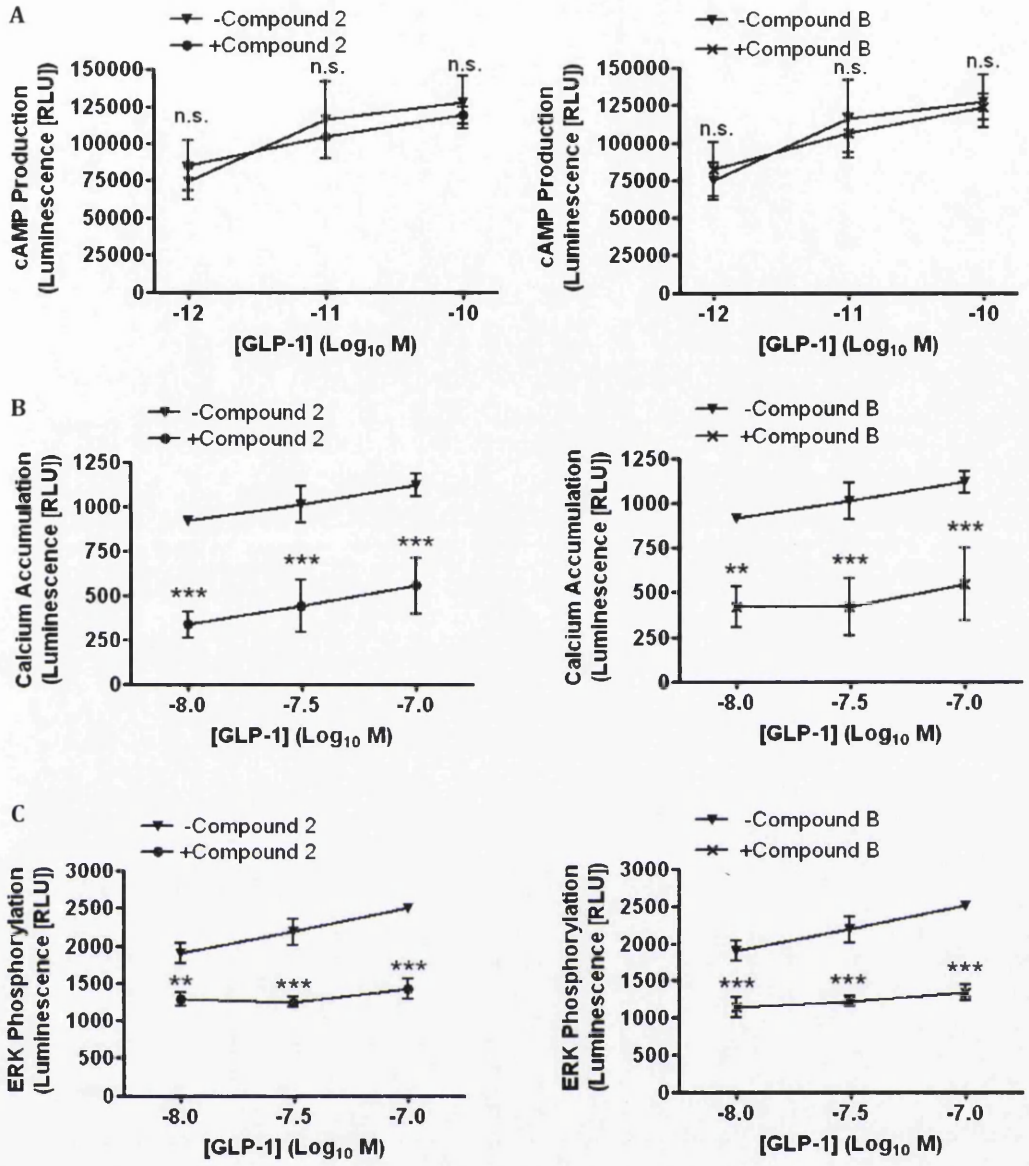

Figure 4.13. Preincubation of the hGLP-1R with compound 2 or compound B reduced GLP-1 stimulated intracellular Ca^{2+} accumulation and ERK phosphorylation. HEK293 cells cotransfected with the hGLP-1R plasmid and the luciferase reporter plasmid for cAMP (pGL4.29-Luc-CRE), intracellular Ca^{2+} (pGL4.30-Luc-NFAT) or ERK phosphorylation (pGL4.33-Luc-SRE) were preincubated with either 10 µM compound 2 or compound B for 60 min. Cells were then stimulated with GLP-1 at the indicated concentrations in the presence of 10 µM compound 2 (left panel) or compound B (right panel) for 4 h (cAMP and ERK phosphorylation) or 8 h (intracellular Ca^{2+} accumulation) to assess cAMP production (A), intracellular Ca^{2+} accumulation (B) and ERK phosphorylation (C). Data are mean ± SEM, n=3. Data were analysed by Bonferroni's post test after two-way ANOVA; values differ from control, n.s. $p>0.05$, ** $p<0.01$, *** $p<0.001$.

4.4. Discussion

Although the commercially available drugs, Liraglutide and Exenatide, have therapeutic potential, they are very expensive and have difficulties associated with the long-term administration of these injectable drugs. This has driven the need to find relatively less expensive and orally active small molecule agonists of the GLP-1R. Allosteric small molecule drugs not only have the potential of oral bioactivity but also the potential benefit of binding to a site on the receptor that is distinct from that used by the orthosteric agonist. Therefore, allosteric agonists can act upon the receptor at the same time as the endogenous orthosteric agonist and increase affinity and/or efficiency of the orthosteric agonist, potentially providing more 'physiological' regulation (Bridges & Lindsley, 2008). Recently, two small molecule agonists, compound 2 and compound B, have been described as ago-allosteric agonists of the GLP-1R, which act not only as allosteric modulators but also as agonists (Knudsen et al, 2007; Sloop et al, 2010). This has provided optimism in the development of high affinity, orally active compounds, which are clinically applicable for the treatment of type 2 diabetes.

In this study, both small molecule agonists of the hGLP-1R induced cAMP production but not intracellular Ca^{2+} accumulation or ERK phosphorylation and as a result did not induce hGLP-1R internalisation. Studying compound 2 and compound B induced GLP-1R internalisation is useful in assessing the effectiveness of these compounds with longer half-life. This is because internalisation of the receptor can lead to dampening of its biological response (Hanyaloglu & von Zastrow, 2008). Other allosteric agonists bind to GPCRs and activate different signalling pathways to that of the orthosteric agonist. For example, the μ-opioid receptor allosteric agonist, herkinorin, induces ERK1/2 phosphorylation but not internalisation of the receptor (Groer et al, 2007). Additionally, allosteric agonist AC-42 (4-n-butyl-1-[4-(2-methylphenyl)-4-oxo-1-butyl] piperidine), binds to the M_1 muscarinic acetylcholine receptor resulting in ERK phosphorylation and intracellular Ca^{2+} accumulation but not internalisation of the receptor (Ma et al, 2009; Thomas et al, 2009). This

suggests orthosteric and allosteric agonists cause subtle differences in the conformation of the receptor, activating separate signalling pathways. Additionally, this further supports the idea that the GLP-1R does not require cAMP for internalisation of the receptor, but instead intracellular Ca^{2+} accumulation and ERK phosphorylation are essential.

In this study, antagonists Ex(9-39) (Goke et al, 1993; Thorens et al, 1993) and JANT-4 (Patterson et al, 2011) inhibited GLP-1 induced GLP-1R internalisation and signalling. However, Ex(9-39) and JANT-4 did not inhibit compound 2 or compound B induced signalling, suggesting a second agonist binding site on the hGLP-1R that is distinct from the orthosteric binding site. These findings are consistent with results obtained in previous studies for compound 2 (Knudsen et al, 2007) and compound B (Knudsen et al, 2007; Sloop et al, 2010), which showed the antagonist, Ex(9-39), had no effect on cAMP signalling. This was further confirmed with the use of two mutants of the hGLP-1R (V36A and K334A). The V36A mutation in the GLP-1R has previously been shown to affect GLP-1 binding to the orthosteric binding site (Underwood et al, 2010). In this study, HEK293 cells expressing the V36A mutant did not show GLP-1 stimulated cAMP. In contrast, the V36A mutant expressing cells did show compound 2 and compound B stimulated cAMP production to the same levels produced in the hGLP-1R WT expressing cells. These results demonstrated that the V36A mutation in the hGLP-1R only affects the orthosteric binding site and, compounds 2 and B interact with the hGLP-1R at a site different to the orthosteric binding site. Additionally, the K334A mutation in the GLP-1R has previously been shown to reduce coupling of the receptor to the $G\alpha_s$ subunit (Mathi, 1997; Takhar et al, 1996). In this study the K334A mutant reduced cAMP production stimulated by GLP-1, compound 2 and compound B. This demonstrates that these small molecule agonists and GLP-1 induce similar conformational changes in the hGLP-1R, which are required for $G\alpha_s$ coupling, although they bind at different sites on the hGLP-1R. In future studies, it would be interesting to assess where on the hGLP-1R compounds 2 and B bind using internal deletions to the extracellular loops in the GLP-1R.

In this study, preincubation of the hGLP-1R with small molecule agonists prior to GLP-1 addition inhibited hGLP-1R internalisation, intracellular Ca^{2+} accumulation and ERK phosphorylation. This is interesting because compounds 2 and B reduced hGLP-1R internalisation induced by GLP-1, which would prevent dampening of the receptor's activity (Hanyaloglu & von Zastrow, 2008). Therefore, these small molecule agonists may strengthen GLP-1 potency by allowing the orthosteric agonist to act on the receptor for a prolonged period before it is desensitised. As a result, compounds based on this ability may provide insight into the mechanisms of agonist directed GLP-1R regulation and may represent a step further in the development of effective orally active insulinotropic agents with limited adverse effects. This result is in contrast to allosteric agonists of the cannabinoid CB_1 receptor, because their binding to the receptor results in a conformational change that increases the affinity of the orthosteric agonist to the receptor (Price et al, 2005). Similar to compounds 2 and B, allosteric agonist alcuronium inhibits, in a concentration dependent manner, the actions of orthosteric agonist pilocarpine on the M_2 muscarinic acetylcholine receptor (Zahn et al, 2002). It would be interesting to determine, for example using biotin conjugated GLP-1, whether compounds 2 and B cause a conformational change that reduces access of GLP-1 to the orthosteric binding site in a non-competitive manner or whether they prevent GLP-1 bound hGLP-1R coupling to the $G\alpha_q$ pathway, thereby inhibiting intracellular Ca^{2+} accumulation and ERK phosphorylation required for internalisation of the receptor.

The identification of allosteric modulators of the hGLP-1R that have a longer half-life and the potential to be orally active is highly beneficial in the treatment of type 2 diabetes. In this study, small molecule agonists, compound 2 and compound B, were analysed for their effects on hGLP-1R cAMP production, intracellular Ca^{2+} accumulation, ERK phosphorylation and internalisation. Although small molecule agonists induced cAMP production with a similar maximal response to GLP-1, unlike GLP-1 they did not induce intracellular Ca^{2+} accumulation and ERK phosphorylation, and as a result did not induce hGLP-1R internalisation. With the use of antagonists and the V36A mutant of the hGLP-

1R, this study demonstrated that compounds 2 and B act on a region of the hGLP-1R independent to the orthosteric agonist site. However, the use of the K334A mutant of the hGLP-1R demonstrated that compounds 2 and B induce a conformational change in the GLP-1R, which is required for $G\alpha_s$ coupling, similar to that induced by the orthosteric agonist binding to the receptor. Additionally, compounds 2 and B inhibit GLP-1 induced hGLP-1R internalisation, intracellular Ca^{2+} accumulation and ERK phosphorylation. Therefore, although this data suggests a potential advantage in the selective activation of specific signalling pathways, allosteric agonists may cause GPCR conformations that are less favourable to the internalisation of the receptor than orthosteric agonists.

5. Agonist Induced Internalisation of the Human Glucagon Like Peptide-1 Receptor is Mediated by the $G\alpha_q$ Pathway

5.1. Introduction

One of the main physiological roles of glucagon like peptide-1 (GLP-1) is to increase insulin secretion from pancreatic β-cells in a glucose dependent manner (Doyle & Egan, 2007; Holz et al, 1999; Thompson & Kanamarlapudi, 2013). This hormone is secreted by the intestinal L-cells after food intake (Thompson & Kanamarlapudi, 2013). GLP-1 exerts its physiological effects by binding to its G-protein coupled receptor (GPCR), the GLP-1 receptor (GLP-1R). Therefore, human GLP-1R (hGLP-1R) is an important target in the treatment of type 2 diabetes (Gallwitz, 2010; Thompson & Kanamarlapudi, 2013).

Upon agonist binding, GPCRs undergo a conformational change and transmit extracellular signals through heterotrimeric G-proteins, which consist of Gα and Gβγ subunits (Cabrera-Vera et al, 2003). The agonist occupied GLP-1R activates both $G\alpha_s$ and $G\alpha_q$ subunits (Montrose-Rafizadeh et al, 1999). The $G\alpha_s$ subunit activates adenylyl cyclase (AC), increasing cyclic adenosine monophosphate (cAMP) levels, which in turn activates protein kinase A (PKA) (Bos, 2003). The $G\alpha_q$ subunit activates phospholipase C (PLC), which in turn hydrolyses phosphatidylinositol-4,5-bisphophate (PIP_2) to inositol-1,4,5-triphosphate (IP_3) and diacylglycerol (DAG). IP_3 binds to its receptor, the IP_3 receptor (IP_3R), on the endoplasmic reticulum (ER), which causes cytosolic calcium (Ca^{2+}) accumulation (Werry et al, 2003). DAG together with intracellular Ca^{2+} activates protein kinase C (PKC), which then induces extracellular signal-regulated kinase (ERK) phosphorylation (Budd et al, 2001; Hawes et al, 1995). ERKs are one class of mitogen-activated protein kinases (MAPKs) and their activity is regulated by phosphorylation (Cobb & Goldsmith, 1995). The GLP-1R has previously been

shown to activate ERK (Jolivalt et al, 2011; Koole et al, 2010; Quoyer et al, 2010; Syme et al, 2006). Further, the activation of ERK by a number of GPCRs including the M_3-muscarinic receptor (Budd et al, 1999; Budd et al, 2001; Kim et al, 1999; Wylie et al, 1999), prostaglandin F2α receptor (Watanabe et al, 1995), angiotensin II receptor (Zou et al, 1996), cholecystokinin type A receptor (Tapia et al, 1999), chemokine CXCR-2 receptor (Venkatakrishnan et al, 2000) and purinergic P_2Y_2 receptor (Soltoff et al, 1998) has been shown to be mediated by PKC. These receptors mediated ERK phosphorylation which was either abolished or significantly reduced upon PKC inhibition, demonstrating PKC acts upstream of ERK and provides the primary signal that links activation of the receptor to ERK phosphorylation. The agonist bound GLP-1R has been shown to induce both cAMP production by coupling to the $G\alpha_s$ pathway and intracellular Ca^{2+} accumulation by coupling to the $G\alpha_q$ pathway (Montrose-Rafizadeh et al, 1999). In β-cells, the increase in intracellular Ca^{2+} through the $G\alpha_q$ pathway causes secretory vesicles containing insulin to fuse to the plasma membrane and thereby increases insulin exocytosis (De Vos et al, 1995; Holz, 2004). The exocytotic insulin response caused by increased intracellular Ca^{2+} accumulation is potentiated by elevated cAMP production by coupling to the $G\alpha_s$ pathway (Holst & Gromada, 2004).

After activation by agonist, most GPCRs internalise from the cell surface to dampen the biological response, to resensitise the desensitised receptor by recycling, or to propagate signals through novel transduction pathways (Hanyaloglu & von Zastrow, 2008). For example, the δ-opioid receptor requires the activation of PKC to allow phosphorylation of the receptor for internalisation (Xiang et al, 2001). Here, the activation of ERK is required for the desensitisation and sequestration of the δ-opioid receptor (Daaka et al, 1998; Eisinger & Schulz, 2004). The importance of GPCR internalisation in switching off the signal has been shown by the discovery of acquired mutations in the G-CSF receptor (G-CSFR) in leukaemia patients. These mutations result in impaired agonist induced internalisation of the G-CSFR (Hunter & Avalos, 1999; Ward et al, 1999). The agonist bound serotonin 5-hydroxytryptamine 2a (5-$HT2_A$) receptor undergoes desensitisation and internalisation. The 5-$HT2_A$

receptor recycles back to the plasma membrane after 5-HT stimulated internalisation, suggesting that the desensitised 5-$HT2_A$ receptor undergoes internalisation for resensitisation (Bhattacharyya et al, 2002).

GPCR kinases (GRKs), arrestins and clathrin coated pits predominantly regulate agonist induced GPCR internalisation. The agonist activated GPCR is phosphorylated by GRKs, which facilitates the recruitment of arrestin and targets the GPCR to clathrin-coated pits for rapid internalisation (Gurevich & Gurevich, 2006). However, some GPCRs such as the endothelin A receptor, somatostatin receptor and angiotensin II type 1 receptor internalise in a caveolae dependent manner (Chini & Parenti, 2004). The dynamin family of GTPases play an important role in agonist induced GPCR internalisation, by fission of clathrin-coated vesicles or caveolae membranes (Kanamarlapudi et al, 2012). Currently, there is some confusion whether the GLP-1R uses clathrin or caveolin mediated endocytosis for its agonist induced internalisation. It has been reported that clathrin coated endocytosis mediates GLP-1R internalisation and three PKC phosphorylation sites within the C-terminal domain are important for this to occur (Widmann, 1997). However, the GLP-1R has also been shown to interact and co-localise with caveolin-1 for internalisation of the receptor by caveolae mediated endocytosis (Syme et al, 2006; Williams & Lisanti, 2004).

In agonist stimulated pancreatic β-cells, the internalised GLP-1R colocalises with AC within endosomes and stimulates insulin secretion (Kuna et al, 2013). Therefore, a better understanding of GLP-1R internalisation is essential for introducing novel agonists that activate the GLP-1R in the treatment of type 2 diabetes. Although, the GLP-1R is known to activate both $G\alpha_s$ and $G\alpha_q$ coupled pathways, it is unknown which pathway is required for agonist induced internalisation of the hGLP-1R. Currently, it is suggested that the GLP-1R acts through the $G\alpha_s$ pathway to potentiate insulin secretion in β-cells (Willard & Sloop, 2012). Further, it has been suggested that agonist induced GLP-1R internalisation may be arrestin dependent (Jorgensen et al, 2007; Sonoda et al, 2008; Willard & Sloop, 2012). Apparent variations can be seen in these studies

and at present the molecular mechanism regulating GLP-1R function remains unclear.

In this study, it was determined that agonist induced hGLP-1R internalisation is caveolin-1 and dynamin dependent. Furthermore, this study revealed that the $G\alpha_q$ pathway mediates agonist induced hGLP-1R internalisation. Consistent with this, the hGLP-1R T149M mutant and small molecule agonists (compounds 2 and B) not only failed to activate the $G\alpha_q$ pathway but also prevented agonist induced internalisation of the hGLP-1R. Additionally, the $G\alpha_q$ signalling pathway inhibitors PBP10 (a membrane permeable PIP_2 sequestering peptide), U73122 (a PLC inhibitor), 2-APB (an IP_3R inhibitor), BAPTA-AM (a membrane permeable Ca^{2+} chelator), Go6976 and Ro318820 (PKC inhibitors) and PD98059 (an inhibitor for ERK phosphorylation by MAPK) reduced agonist induced hGLP-1R internalisation. These inhibitors also suppressed ERK phosphorylation induced by hGLP-1R activation, demonstrating that phosphorylated ERK acts downstream of the $G\alpha_q$ pathway in hGLP-1R internalisation.

5.2. Materials and methods

5.2.1. Materials

The primary antibodies used were rabbit anti-vesicular stomatitis virus glycoprotein (VSVG) and rabbit anti-red fluorescent protein (RFP) (Abcam Biochemicals), mouse anti-green fluorescent protein (GFP) (Roche), mouse anti-hGLP-1R (R&D Systems), mouse anti-CAV-1 (Santa Cruz Biotechnology), rabbit anti-phospho ERK1/2 (pERK1/2) and rabbit anti-ERK1/2 (New England Biolabs). The Cy3-conjugated anti-mouse immunoglobulin G (IgG) secondary antibody (Jackson Laboratories) was used for immunofluorescence. The horseradish peroxidase (HRP)-conjugated anti-mouse and anti-rabbit IgG (GE Healthcare) secondary antibodies were used for immunoblotting. Enhanced chemiluminescence (ECL) select reagent was obtained from GE Healthcare. The cAMP polyclonal antibody and cAMP-HRP were obtained from Genscript. GLP-1 (Liraglutide) was from Novo Nordisk. Compound 2 and compound B were

purchased from Calbiochem. The chemical inhibitors used were 2-APB, BAPTA-AM, chlorpromazine hydrochloride, filipin complex, genistein, monodansylcadaverine (MDC), tunicamycin (Sigma), dynasore (Abcam Biochemicals), Go6976, PD98059, Ro318820, U73122, U73343 (Tocris), PBP10 (Millipore) and pentratin peptide (Thermo Scientific). All other chemicals were from Sigma unless otherwise stated.

5.2.2. Plasmids

The full-length hGLP-1RΔN23 cDNA was amplified from mammalian gene collection (MGC) clone 142053 (Source Bioscience) by polymerase chain reaction (PCR) using High Fidelity Taq DNA polymerase (Roche Applied Science) and sequence specific primers containing *Eco*RI restriction site and VSVG-tag coding sequence (5' primer), and *Sal*I restriction site and no stop codon (3' primer). SP-VSVG-hGLP-1RΔN23 cDNA was amplified by overlap PCR using VSVG-hGLP-1RΔN23 cDNA as the template, the sense primer, containing *Eco*RI restriction site, the signal peptide (SP, 1-23 amino acids) coding sequence followed by VSVG coding sequence and 3' primer. The cDNA was digested with *Eco*RI and *Sal*I, and cloned in frame into the same sites of pEGFP-N1 vector (Clontech) for expression as the N-terminus VSVG-tagged (after the SP) and the C-terminus GFP-tagged fusion protein in mammalian cells (SP-VSVG-hGLP-1RΔN23-GFP). The T149M (SP-VSVG-hGLP-1RΔN23 T149M-GFP) point mutation within the hGLP-1R was generated using Quickchange II XL site-directed mutagenesis kit (Stratagene) and SP-VSVG-hGLP-1RΔN23-GFP plasmid as the template. The dominant negative (DN) mutant of dynamin K44A, β-arrestin1 Δ319-418 and clathrin EPS15 Δ95-295 used in this study have been described previously (Kanamarlapudi et al, 2012; Mundell et al, 2001). The caveolae DN (CAV-1-P132L) described previously (Holst et al, 2009) was obtained from Addgene. The $G\alpha_q$ G188S DN plasmid was kindly provided by Prof. Karnam S. Murthy (Virginia Commonwealth University, USA) (Huang et al, 2007). Luciferase pGL4.29-Luc-CRE, pGL4.30-Luc-NFAT and pGL4.33-Luc-SRE reporter plasmids were from Promega.

5.2.3. Cell culture and transfection

Human embryonic kidney 293 (HEK293) cells were maintained at 37°C in a 5% CO_2 humidified environment in Dulbecco's modified Eagle medium (DMEM; serum free medium [SFM]) supplemented with 10% fetal calf serum, 2 mM glutamine, 100 U/ml penicillin and 0.1 mg/ml streptomycin (full serum medium [FSM]). Cells were transiently transfected for 48 h using JetPrime transfection reagent (Polyplus; 2 µl/µg DNA) according to the manufacturer's instructions.

5.2.4. Enzyme linked immunosorbent assay (ELISA)

This is carried out as described previously with unpermeabilised cells to quantify cell surface expression (Kanamarlapudi et al, 2012). Briefly, HEK293 cells expressing the hGLP-1R were serum starved for 1 h and then stimulated without or with agonist at 37°C/5% CO_2. Where indicated, cells were incubated without or with inhibitors for 30 min prior and during stimulation with agonist at 37°C/5% CO_2. Cells were then fixed with 4% paraformaldehyde (PFA) for 5 min and non-specific binding sites blocked with 1% bovine serum albumin (BSA) made in Tris buffered saline (TBS) (1% BSA/TBS) for 45 min. Cells were incubated with the anti-hGLP-1R mouse antibody (diluted 1:15000) in 1% BSA/TBS for 1 h, washed with TBS and then incubated with the HRP-conjugated anti-mouse IgG (diluted 1:5000) in 1% BSA/TBS for 1 h. Cells were washed and developed using 1-step Ultra TMB-ELISA substrate (Bio-Rad) for 15 min and the reaction stopped by adding an equal volume of 2 M sulphuric acid. The optical density was read at 450 nm using a plate reader.

5.2.5. Immunofluorescence

Intracellular localisation of hGLP-1R expression was assessed by immunofluorescence as described previously (Kanamarlapudi et al, 2012). Briefly, cells were serum starved for 1 h and where indicated cells were preincubated without or with inhibitors at the indicated concentration for 30 min. Cells were then incubated with the anti-hGLP-1R mouse antibody (diluted 1:5000) in 1% BSA/SFM for 1 h at 4°C and then stimulated without or with agonist in the presence of inhibitor at 37°C/5% CO_2. Cells were then fixed with

4% PFA for 30 min. Cells were permeabilised with 0.2% Triton X-100 made in phosphate buffered saline (PBS) for 10 min, blocked in blocking buffer (1% BSA made in wash buffer [0.1% Triton X-100 in PBS]) for 30 min and then incubated with the Cy3-conjugated anti-mouse antibody (diluted 1:200 in blocking buffer) for 1 h. Cells were then washed 3 times with wash buffer and incubated with DAPI (4′,6-diamidino-2-phenylindole dihydrochloride, 1 mg/ml) diluted 1:2000 in PBS to stain nucleus. Coverslips were mounted on glass microscopic slides using mounting solution (0.1 M Tris-hydrochloric acid [HCl], pH 8.5, 10% Mowiol 50% glycerol) containing 2.5% DABCO (1,4 diazabicyclo (2.2.2) octane). Immunofluorescence staining was visualised using a Zeiss LSM710 confocal microscope fitted with a 63x oil immersion lens.

5.2.6. cAMP assay

Cells were serum starved for 1 h and then stimulated without or with 100 nM GLP-1 for 1 h at 37°C/5% CO_2 in the presence of 0.25 mM phosphodiesterase inhibitor Ro201724. Cells were lysed and cAMP levels in the cell lysates were estimated using the cAMP direct immunoassay kit (Abcam).

5.2.7. cAMP, Ca^{2+} and ERK luciferase assay

HEK293 cells cotransfected with the hGLP-1R plasmid and luciferase reporter plasmid for cAMP (pGL4.29-Luc-CRE) or intracellular Ca^{2+} (pGL4.30-Luc-NFAT) or ERK phosphorylation (pGL4.33-Luc-SRE) were treated with increasing concentrations of agonist for 4 h (cAMP and ERK) or 8 h (Ca^{2+}) at 37°C/5% CO_2. After incubation, an equal volume of ONE-Glo™ lysis buffer containing luciferase substrate (Promega) was then added to each well and luminescence (relative light units [RLU]) measured using a plate reader in accordance with the manufacturer's instructions.

5.2.8. Cell lysates

To make cell lysates, HEK293 cells expressing the hGLP-1R were washed 3 times with ice cold PBS and lysed in ice cold modified RIPA lysis buffer (10 mM

Tris HCl, pH 7.5 containing 10 mM ethylenediaminetetraacetic acid [EDTA], 1% nonyl phenoxypolyethoxylethanol [NP40], 0.1% sodium dodecyl sulphate [SDS], 0.5% sodium deoxycholate and 150 mM sodium chloride [NaCl]) with 1% mammalian protease inhibitors. Cell lysates were incubated at 4°C for 15 min and then centrifuged at 22000 xg for 10 min at 4°C. The supernatant was collected and ½ volume of 3x SDS-polyacrylamide gel electrophoresis (PAGE) sample loading buffer (75 mM Tris HCl, pH 6.8 containing 3% SDS, 30% glycerol, 0.003% bromophenol blue and 0.3 M dithiothreitol [DTT]) was added and left at room temperature for 1 h. These cell lysates were used to detect hGLP-1R expression by immunoblotting using the anti-GFP and anti-VSVG antibodies.

For assessing ERK1/2 phosphorylation, HEK293 cells expressing the hGLP-1R were lysed in ice cold modified RIPA lysis buffer (50 mM Tris HCl, pH 7.5, containing 0.2 M NaCl; 10 mM $MgCl_2$; 0.1% SDS; 0.5% sodium deoxycholate; 1% TritonX-100; 5% Glycerol) with 1% mammalian protease inhibitors. Cell lysates were incubated at 4°C for 15 min and centrifuged at 22000 xg for 10 min at 4°C. The supernatant was collected and ¼ volume of 5x SDS-PAGE sample loading buffer (125 mM Tris HCl, pH 6.8 containing 5% SDS, 50% glycerol, 0.005% bromophenol blue and 5% β-mercaptoethanol) was added and heated at 100°C for 5 min. These cell lysates were used to detect phosphorylated ERK and total ERK by immunoblotting using the anti-pERK1/2 and anti-ERK1/2 antibodies.

5.2.9. Coimmunoprecipitation

This was performed as described previously (Syme et al, 2006). Cells were washed 3 times with ice cold PBS and lysed in ice cold lysis buffer containing 1 mM $CaCl_2$, 1% TritonX-100, 0.5% SDS in PBS with 1% mammalian protease inhibitors. Cell lysates were incubated with protein G Dynabeads® (Life technology) bound to 0.5 µg of either the anti-GFP mouse, anti-RFP rabbit or anti-CAV-1 antibody at 4°C for 2 h. Beads were washed 3 times with lysis buffer and the bound protein eluted in 1x SDS-PAGE sample loading buffer (25 mM Tris HCl, pH 6.8, containing 1% SDS, 10% glycerol, 0.001% bromophenol blue

and 0.1 M DTT). The lysate not incubated with beads was mixed with ½ volume of 3x SDS PAGE sample loading buffer and used to assess total hGLP-1R. Total and coimmunoprecipitated receptors were detected by immunoblotting using the anti-GFP mouse antibody.

5.2.10. Immunoblotting

Proteins were separated in a SDS-PAGE gel by electrophoresis and transferred onto polyvinylidene fluoride (PDVF) membrane. Membranes were blocked with TBST (TBS with 0.1% tween 20) containing 5% milk powder (blocking buffer) for 1 h at room temperature or overnight at 4°C. Membranes were immunoblotted with the anti-GFP mouse antibody (diluted 1:500 in blocking buffer) to assess protein expression levels or the anti-pERK1/2 rabbit antibody (diluted 1:1000 in blocking buffer) to assess ERK1/2 phosphorylation for 1 h at room temperature or overnight at 4°C. Membranes were washed and then incubated with the HRP-conjugated anti-mouse or anti-rabbit secondary antibody (diluted 1:2500 in blocking buffer) for 1 h at room temperature. Membranes were then incubated in ECL select substrate and bands visualised using the ChemiDoc™ XRS system (Bio-Rad). Blots probed with the anti-GFP mouse antibody were stripped with western blot stripping buffer (Thermo Scientific) and reprobed with the anti-VSVG rabbit antibody (diluted 1:1000 in blocking buffer) to assess protein expression levels. Blots probed with the anti-pERK1/2 rabbit antibody were stripped and reprobed with the anti-ERK1/2 rabbit antibody (diluted 1:1000 in blocking buffer) to assess ERK1/2 phosphorylation. The HRP-conjugated anti-rabbit secondary antibody (diluted 1:2500 in blocking buffer) was used as described above.

5.2.11. Data analysis

Data were analysed using the GraphPad Prism program. All data are presented as means ± standard error of the mean (SEM) of three independent experiments. Statistical comparisons between the control and test value was made by a two-tailed unpaired student t-test. Statistical analysis between multiple groups were determined by the Bonferroni's post test after one-way or

two-way analysis of variance (ANOVA), where $p>0.05$ was considered as statistically not significant (n.s.), and $p<0.05$, $p<0.01$ and $p<0.001$ shown as *, ** and *** respectively, was considered statistically significant. Concentration response curves were also fitted using Prism, according to a standard logistic equation. Scale bar in confocal images represents 10 μm. Confocal images shown in the figures are representative of 190-200 transfected cells from three different experiments. Similarly, immunoblotting data shown in the figures are representative of three independent experiments.

5.3. Results

5.3.1. HGLP-1R internalises by caveolae mediated endocytosis

Firstly, the role of clathrin, caveolin and dynamin in agonist induced internalisation of the hGLP-1R was analysed. Most GPCRs internalise in either a clathrin or caveolae dependent manner (Chini & Parenti, 2004; Luttrell & Lefkowitz, 2002). Dynamin regulates both clathrin and caveolae mediated endocytosis through fission of the endocytosed vesicles (Le & Nabi, 2003). To determine whether agonist induced hGLP-1R internalisation is mediated by clathrin or caveolae and dynamin, HEK293 cells expressing the hGLP-1R were either cotransfected with DN mutants (Figure 5.1A) or treated with inhibitors (Figure 5.1B) of clathrin, caveolae or dynamin and stimulated with agonist and analysed by ELISA and immunofluorescence. GLP-1R internalisation in the presence of inhibitors or DN mutants is shown as percentage of that in absence of the treatment.

The DN mutant of dynamin (dynamin K44A), which affects both clathrin and caveolae mediated endocytosis, significantly reduced (33.7 ± 3.8%, $p<0.001$) agonist induced hGLP-1R internalisation (Figure 5.1A). However, clathrin DN mutants, β-arrestin1 Δ319-418 (93.1 ± 4.6%, $p>0.05$) and EPS15 Δ95-295 (90.3 ± 5.2%, $p>0.05$), had little effect on the internalisation of the receptor. In

contrast, the DN mutant of caveolin-1 (CAV-1-P132L) completely abolished hGLP-1R internalisation (0.1 ± 0.0%, $p<0.001$). Immunofluorescence analysis confirmed the inhibition of hGLP-1R internalisation by dynamin and caveolin-1 DN mutants (Figure 5.1A).

Inhibitors of clathrin mediated endocytosis, chlorpromazine (95.5 ± 2.8%, $p>0.05$) and MDC (94.7 ± 3.4%, $p>0.05$), had no significant effect on hGLP-1R internalisation. However, inhibitors of dynamin, dynasore (40.6 ± 3.4%, $p<0.001$), and caveolae mediated endocytosis, genistein (55.3 ± 1.8%, $p<0.001$) and filipin (29.7 ± 5.1%, $p<0.001$), inhibited agonist induced hGLP-1R internalisation (Figure 5.1B). These observations were supported by immunofluorescence analysis where a reduction in agonist induced intracellular accumulation of hGLP-1R in endosomes was observed in cells treated with caveolae inhibitors. The concentration dependent inhibition of agonist induced hGLP-1R internalisation by dynasore (Figure 5.2A), filipin (Figure 5.2B) and genistein (Figure 5.2C) was used to assess maximal inhibition of each inhibitor. These observations were confirmed by immunofluorescence where inhibition of agonist induced internalisation was evident. Taken together, these results demonstrate that agonist induced hGLP-1R internalisation is caveolae and dynamin dependent.

Coimmunoprecipitation of hGLP-1R with caveolin-1 was performed to study whether caveolin-1 regulated hGLP-1R internalisation by interacting with the receptor (Figure 5.3). HEK293 cells coexpressing GFP or hGLP-1R-GFP and RFP or CAV-1-RFP were immunoprecipitated with the GFP, RFP and CAV-1 antibodies and immunoblotted with GFP antibody. As shown in Figure 5.3, hGLP-1R immunoprecipitated with CAV-1-RFP by the anti-RFP and anti-CAV-1 antibodies, indicating the *in vivo* interaction between hGLP-1R and caveolin-1. Additionally, a small fraction of the hGLP-1R was immunoprecipitated with the anti-CAV-1 antibody from the cells coexpressing hGLP-1R-GFP and RFP, demonstrating the interaction between endogenous caveolin-1 and exogenously expressed hGLP-1R-GFP.

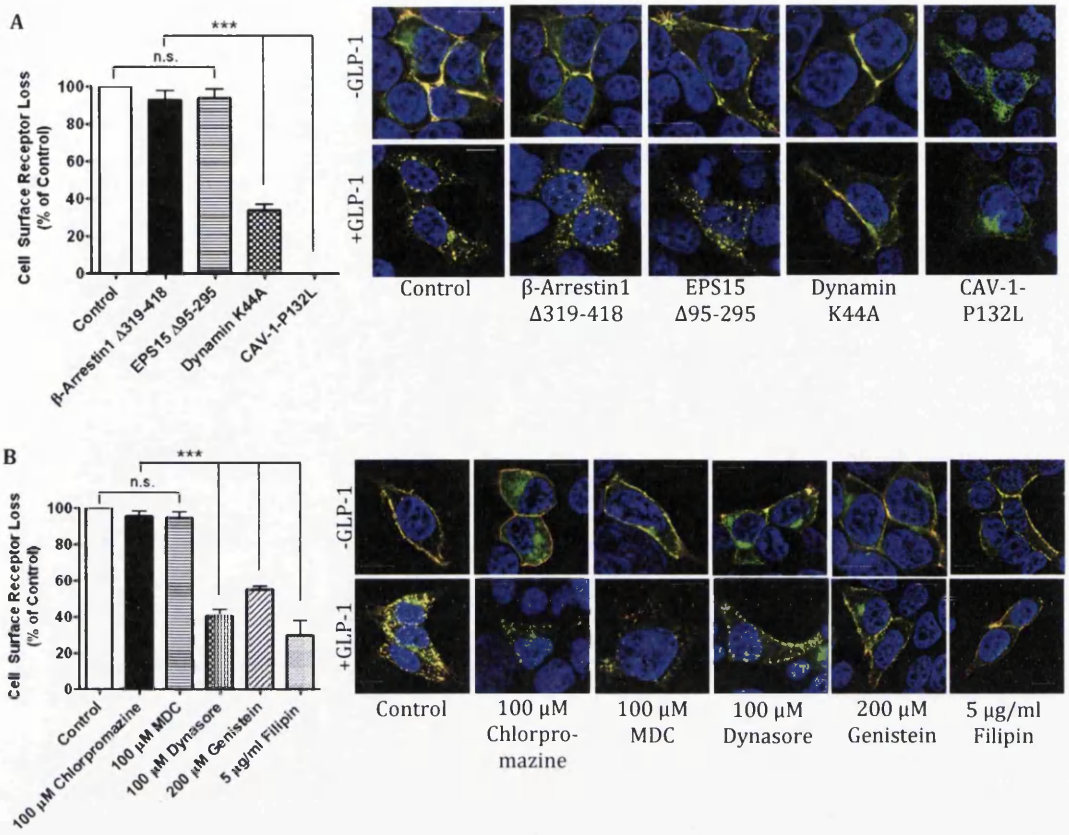

Figure 5.1. HGLP-1R is internalised by caveolae mediated endocytosis. HEK293 cells expressing the hGLP-1R were either cotransfected with DN mutants (A) or treated with inhibitors (B) as indicated. Cells were stimulated with 100 nM GLP-1 for 60 min and hGLP-1R internalisation assessed by ELISA (left panel) and immunofluorescence (right panel) using the anti-hGLP-1R antibody. In immunofluorescence, EGFP (green) and the anti-hGLP-1R antibody (red) overlay shown in yellow and nuclear staining with DAPI in blue. Data are mean ± SEM, n=3. Data were analysed by Bonferroni's post test after one-way ANOVA; values differ from control, n.s. $p>0.05$, *** $p<0.001$.

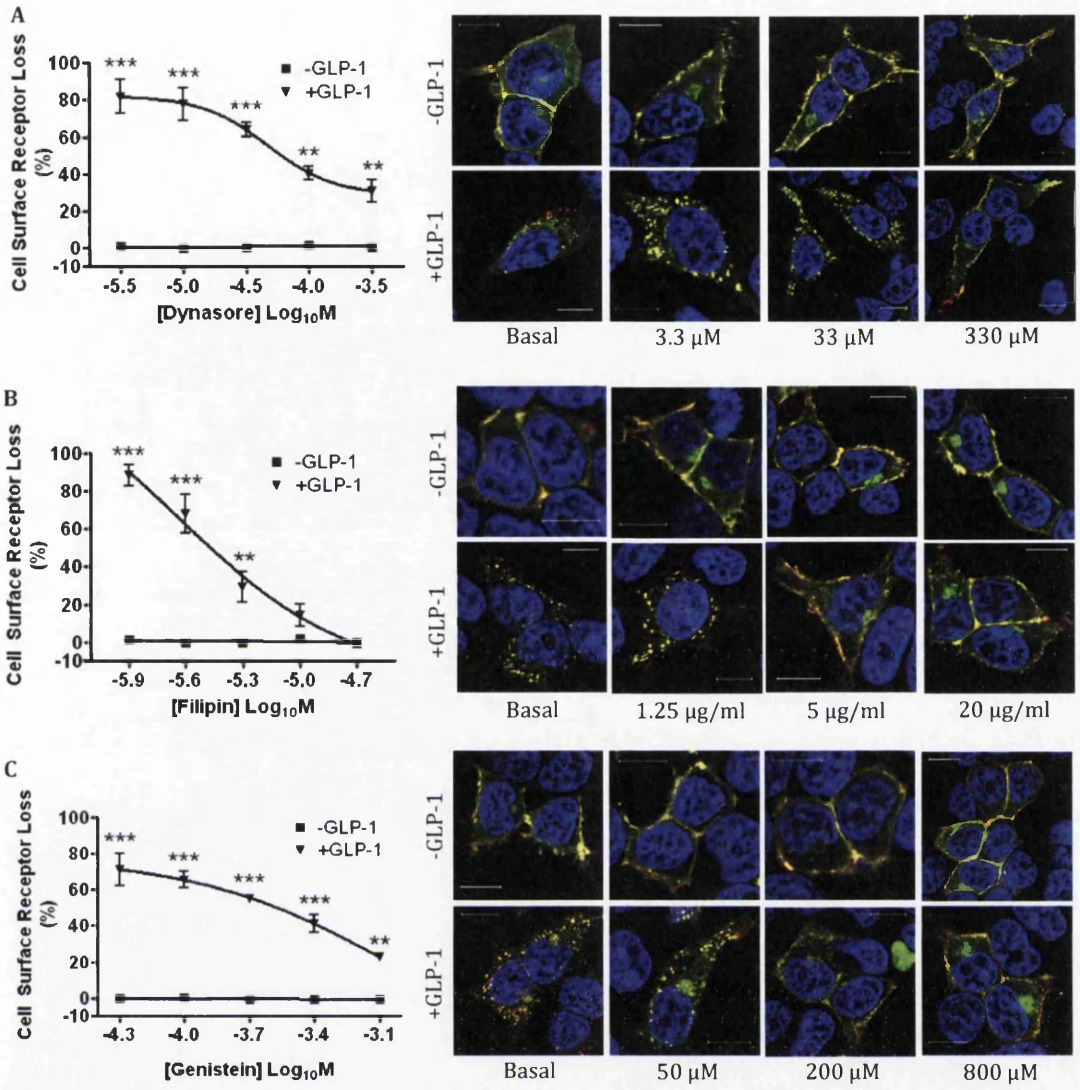

Figure 5.2. Concentration dependent effect of caveolae inhibitors on agonist induced hGLP-1R internalisation. HGLP-1R internalisation in HEK293 cells treated with 100 nM GLP-1 for 60 min in the presence of various concentrations of dynasore (A), filipin (B) and genistein (C) was assessed by ELISA (left panel) and immunofluorescence (right panel) using the anti-hGLP-1R antibody. In immunofluorescence, EGFP (green) and the anti-hGLP-1R antibody (red) overlay shown in yellow and nuclear staining with DAPI in blue. Data are percentage of total cell surface receptors and are mean ± SEM, n=3. Data were analysed by Bonferroni's post test after two-way ANOVA; values differ from control, ** $p<0.01$, *** $p<0.001$.

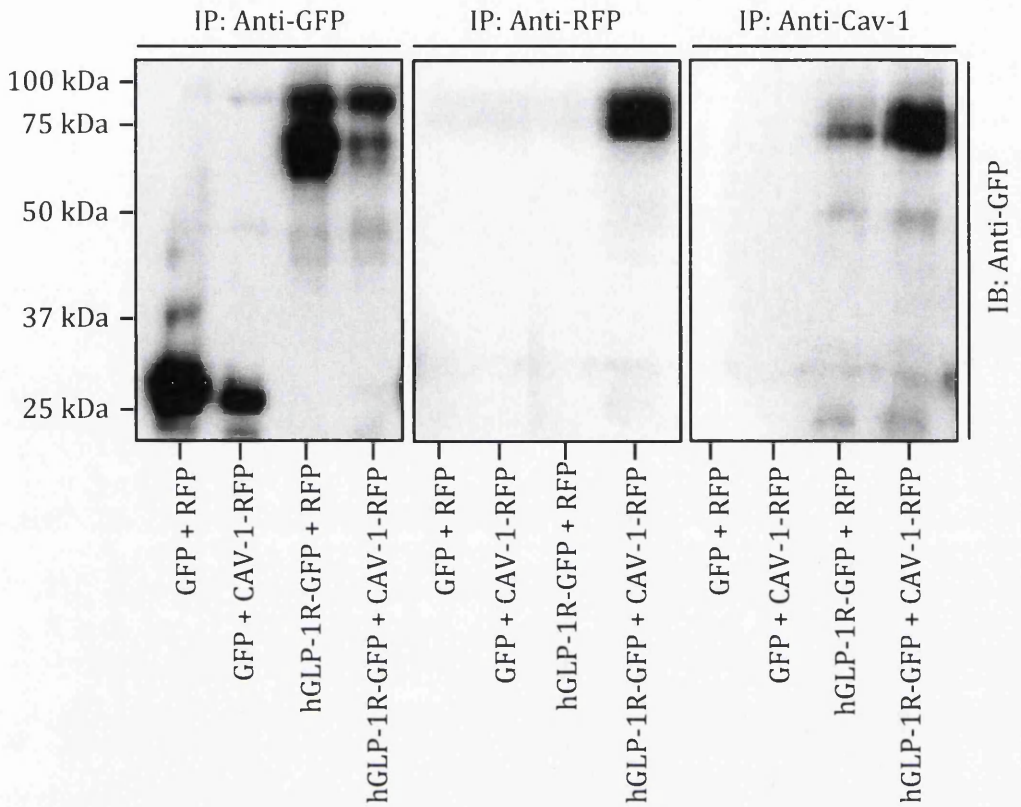

Figure 5.3. HGLP-1R coimmunoprecipitation with caveolin-1. HEK293 cells cotransfected with GFP or hGLP-1R-GFP and RFP or CAV-1-RFP were lysed and immunoprecipitated (IP) with the anti-GFP, anti-RFP and anti-CAV-1 antibodies and immunoblotted (IB) with the anti-GFP antibody.

5.3.2. Agonist induced hGLP-1R internalisation is dependent on the $G\alpha_q$ pathway

Following agonist binding, the hGLP-1R acts through the $G\alpha_s$ coupled pathway to stimulate cAMP production and the $G\alpha_q$ coupled pathway to increase intracellular Ca^{2+} levels (Montrose-Rafizadeh et al, 1999). However, the involvement of these two pathways in agonist induced hGLP-1R internalisation is unknown. Therefore, whether agonist induced internalisation of the hGLP-1R was dependent on the $G\alpha_s$ or $G\alpha_q$ pathway was determined using a number of activators and inhibitors of both pathways (Figure 5.4A). The $G\alpha_s$ pathway

activator forskolin (99.6 ± 1.0%, p>0.05) and inhibitors, SQ22536 (98.4 ± 2.9%, p>0.05) and H89 (104.3 ± 5.6%, p>0.05), had no effect on hGLP-1R agonist induced internalisation (Figure 5.4B). In contrast, the $G\alpha_q$ (G188S) DN mutant inhibited agonist induced hGLP-1R internalisation (66.0 ± 2.9%, p<0.001). This was further confirmed by immunofluorescence (Figure 5.4C). These results strongly suggest hGLP-1R internalisation requires the $G\alpha_q$ pathway.

The requirement of the $G\alpha_q$ pathway for agonist induced hGLP-1R internalisation was then further assessed using the hGLP-1R T149M mutant (Beinborn et al, 2005) and small molecule agonists (compounds 2 and B) of the hGLP-1R that are known to activate only the $G\alpha_s$ pathway (Coopman et al, 2010; Irwin et al, 2010; Knudsen et al, 2007; Sloop et al, 2010; Wootten et al, 2013). The T149M mutants total protein expression (determined by immunoblotting [Figure 5.5A]), cell surface expression (assessed by ELISA [Figure 5.5B; 106.9 ± 4.3%, p>0.05] and immunofluorescence [Figure 5.5E]); receptor activity (assessed by cAMP response [Figure 5.5C; 107.5 ± 0.4%, p>0.05]) were similar to that of the hGLP-1R WT. However, agonist induced hGLP-1R internalisation was abolished by the T149M mutation (assessed by ELISA [Figure 5.5D; 1.5 ± 0.8%, p<0.001] and immunofluorescence [Figure 5.5E]). These results demonstrate that the T149M mutation had no effect on expression of the receptor, which confirmed previous findings (Beinborn et al, 2005), but abolished agonist induced hGLP-1R internalisation. HEK293 cells expressing either the wild type (WT) or T149M mutation were treated with increasing concentrations of GLP-1 and assessed for the mutation's effect on cAMP production (Figure 5.6A), intracellular Ca^{2+} accumulation (Figure 5.6B) and ERK phosphorylation (Figure 5.6C). GLP-1 stimulated a concentration dependent increase of cAMP production in HEK293 cells expressing the hGLP-1R WT and T149M constructs with an EC_{50} of 1.7 ± 0.2 pM and 1.2 ± 0.6 pM respectively, demonstrating both constructs act through the $G\alpha_s$ with similar potency. GLP-1 also activated Ca^{2+} accumulation (EC_{50} 79.6 ± 0.1 nM) and ERK phosphorylation (EC_{50} 52.1 ± 0.3 nM) in a concentration dependent manner in WT expressing cells. In contrast, intracellular Ca^{2+} accumulation (EC_{50} 110.2 ± 0.6 nM) and ERK phosphorylation (EC_{50} 75.9 ± 0.8 nM) in agonist stimulated cells expressing the T149M mutant

were significantly reduced. Taken together, these results suggest that the T149M mutation of hGLP-1R affects agonist induced internalisation of the receptor and the activation of the $G\alpha_q$ coupled pathway, indicating the importance of the $G\alpha_q$ pathway for agonist induced hGLP-1R internalisation.

The small molecule agonists, compound 2 and compound B, were also assessed for their effects on agonist induced hGLP-1R internalisation (assessed by ELISA [Figure 5.7A] and immunofluorescence [Figure 5.7B]), cAMP production (Figure 5.7C), intracellular Ca^{2+} accumulation (Figure 5.7D) and ERK phosphorylation (Figure 5.7E). No hGLP-1R internalisation was observed in cells stimulated with compound 2 (0.3 ± 0.2%, $p<0.001$) or compound B (0.1 ± 0.0%, $p<0.001$). Immunofluorescence supported these observations by demonstrating the reduction in hGLP-1R internalisation in cells treated with the small molecule agonists, compounds 2 and B. As observed previously by other studies (Coopman et al, 2010; Irwin et al, 2010; Knudsen et al, 2007; Sloop et al, 2010; Wootten et al, 2013), both small molecule agonists have induced cAMP production but intracellular Ca^{2+} accumulation and ERK phosphorylation was not present. Stimulation with optimal concentrations of compound 2 resulted in only 7.3 ± 7.3% ($p<0.001$) intracellular Ca^{2+} accumulation and 20.0 ± 8.5% ($p<0.001$) ERK phosphorylation when compared to that of GLP-1 stimulation. Compound B caused only 16.8 ± 9.0% ($p<0.001$) intracellular Ca^{2+} accumulation and 13.6 ± 7.8% ($p<0.001$) ERK phosphorylation. These results show that small molecule agonists, compounds 2 and B, are unable to internalise the hGLP-1R because of their inability to induce sufficient levels of intracellular Ca^{2+} accumulation and ERK phosphorylation, demonstrating the importance of the $G\alpha_q$ pathway and ERK phosphorylation for agonist induced hGLP-1R internalisation.

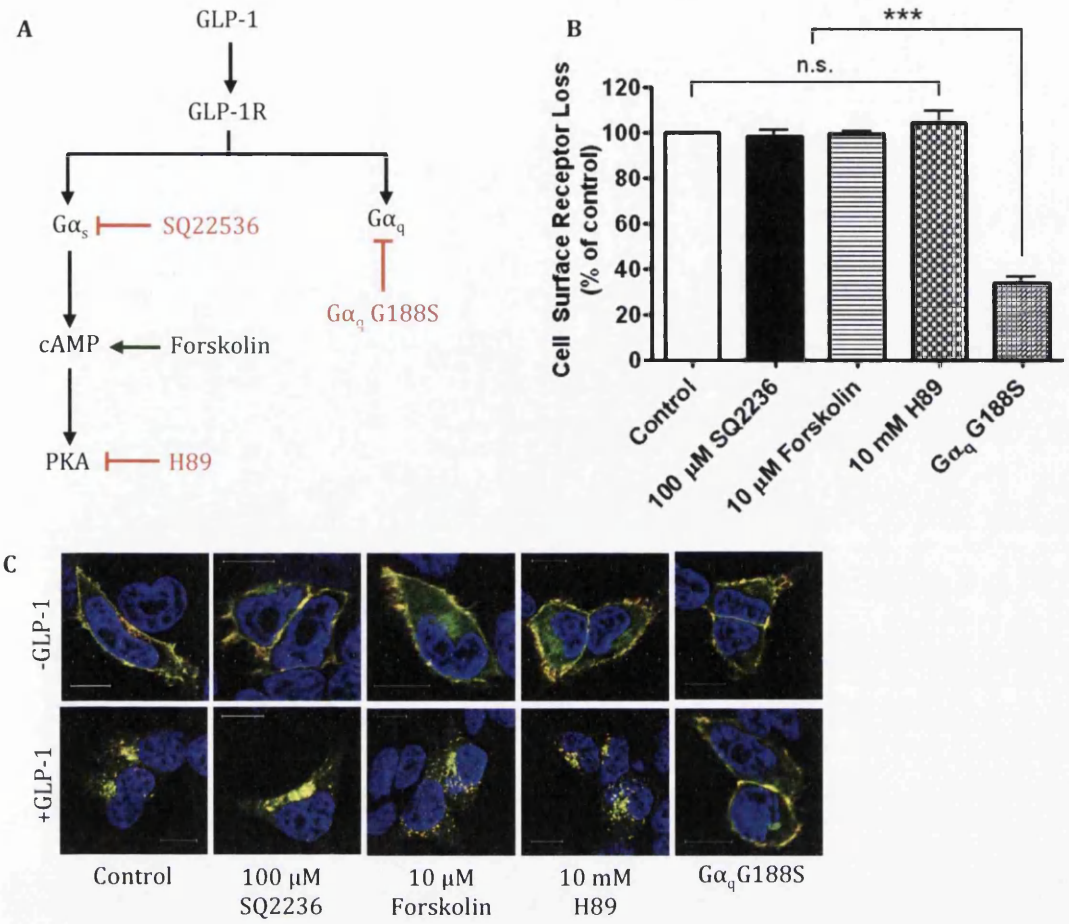

Figure 5.4. HGLP-1R internalisation is dependent on the $G\alpha_q$ pathway. (A) Simplified schematic representation of agonist bound activation of the $G\alpha_s$ pathway to activate cAMP signalling or activation of $G\alpha_q$. (B) HGLP-1R internalisation in HEK293 cells treated with the inhibitors as indicated and stimulated with 100 nM GLP-1 for 60 min was assessed using the anti-hGLP-1R antibody by ELISA. (C) Immunofluorescence showing hGLP-1R internalisation, EGFP (green) and the anti-hGLP-1R antibody (red) overlay shown in yellow and nuclear staining with DAPI in blue. Data are mean ± SEM, n=3. Data were analysed by Bonferroni's post test after one-way ANOVA; values differ from control, n.s. $p>0.05$, *** $p<0.001$.

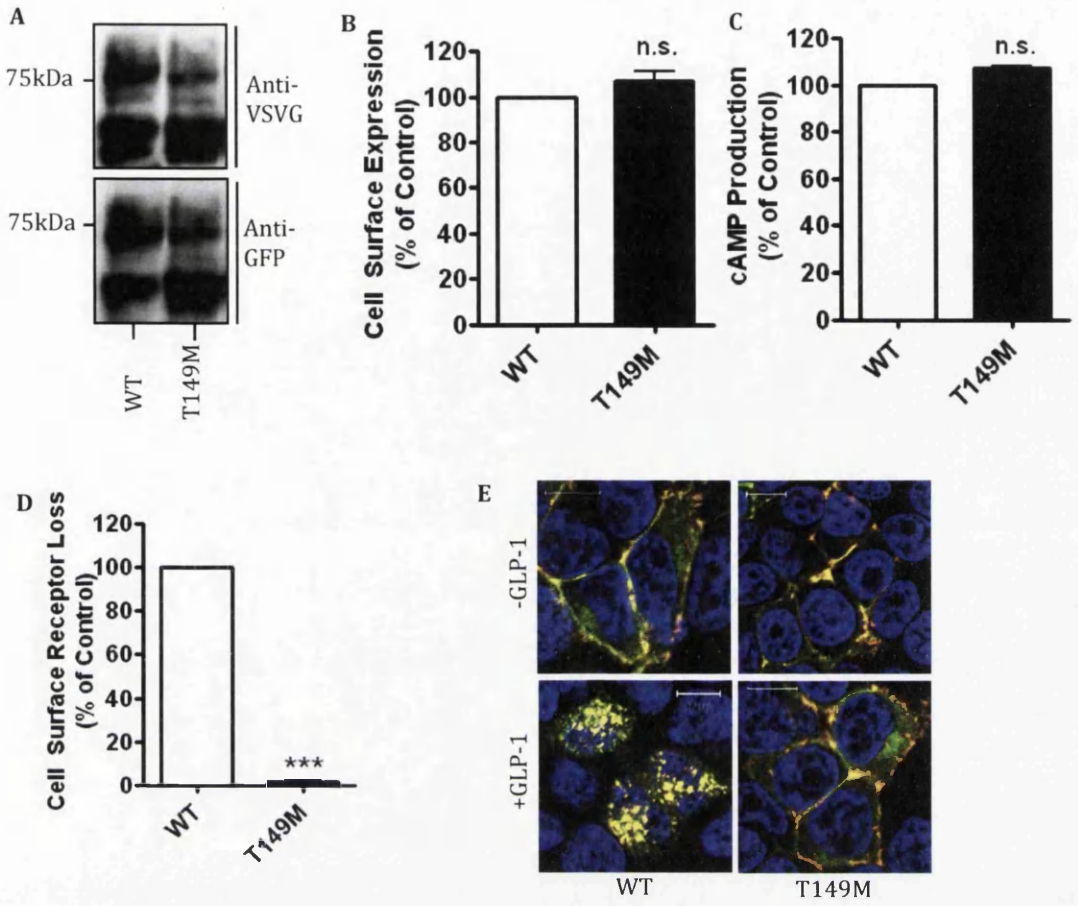

Figure 5.5. The T149M mutation inhibits agonist induced hGLP-1R internalisation. HEK293 cells were transfected with the WT hGLP-1R or the T149M mutant for 48 h. (A) Total protein expression was assessed by immunoblotting using the anti-GFP and anti-VSVG antibodies. (B) Cell surface expression of the WT or mutant hGLP-1R was assessed by ELISA using the anti-hGLP-1R antibody. (C) cAMP production in the WT or mutant hGLP-1R stimulated with 100 nM GLP-1 for 60 min was measured to assess the activity of the receptor. (D) Internalisation of the WT or mutant hGLP-1R stimulated with 100 nM GLP-1 for 60 min was assessed by ELISA using the anti-hGLP-1R antibody. (E) Immunofluorescence showing hGLP-1R internalisation, EGFP (green) and the anti-hGLP-1R antibody (red) overlay shown in yellow and nuclear staining with DAPI in blue. Data are mean ± SEM, n=3. Data were analysed by two-tailed unpaired t-test; values differ from control, n.s. $p>0.05$, *** $p<0.001$.

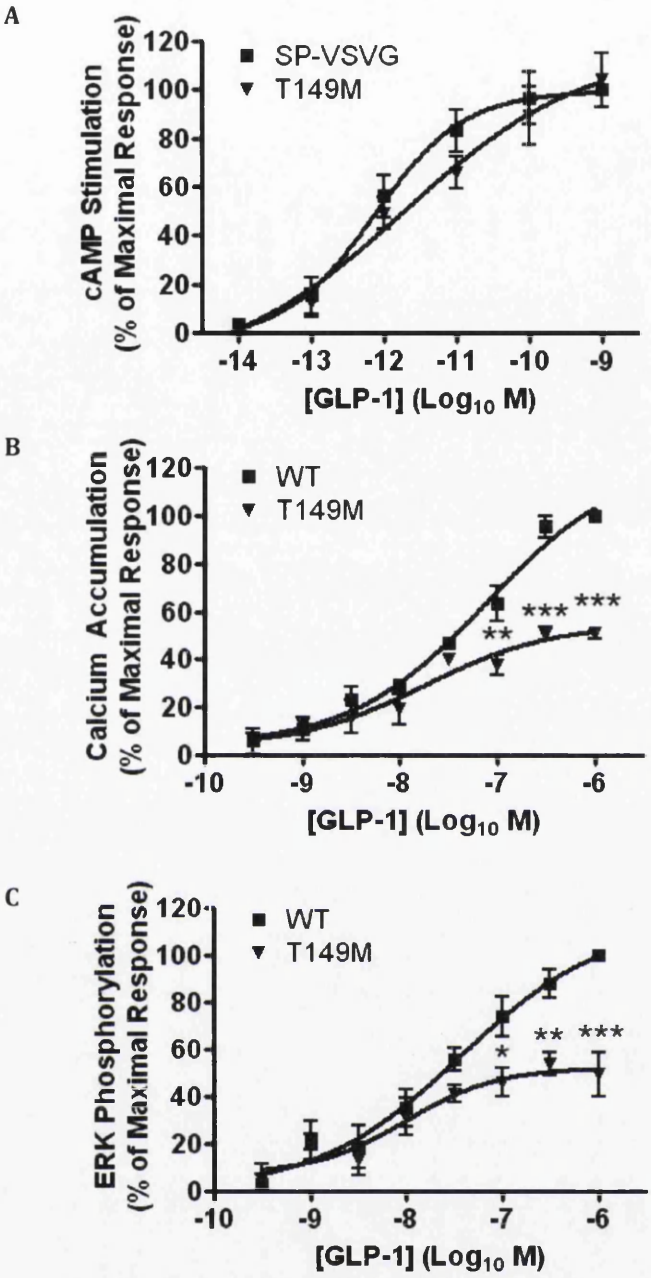

Figure 5.6. The T149M mutation inhibits agonist induced intracellular Ca^{2+} accumulation and ERK phosphorylation but not cAMP production. HEK293 cells cotransfected with the hGLP-1R plasmid and the luciferase reporter plasmid for cAMP (pGL4.29-Luc-CRE), intracellular Ca^{2+} (pGL4.30-Luc-NFAT) or ERK phosphorylation (pGL4.33-Luc-SRE) were stimulated with GLP-1 as indicated for 4 h (cAMP and ERK phosphorylation) or 8 h (intracellular Ca^{2+} accumulation) to assess cAMP production (A), intracellular Ca^{2+} accumulation (B) and ERK phosphorylation (C). Data are mean ± SEM, n=3. Data were analysed by Bonferroni's post test after two-way ANOVA; values differ from control, n.s. $p>0.05$, * $p<0.05$, ** $p<0.01$, *** $p<0.001$.

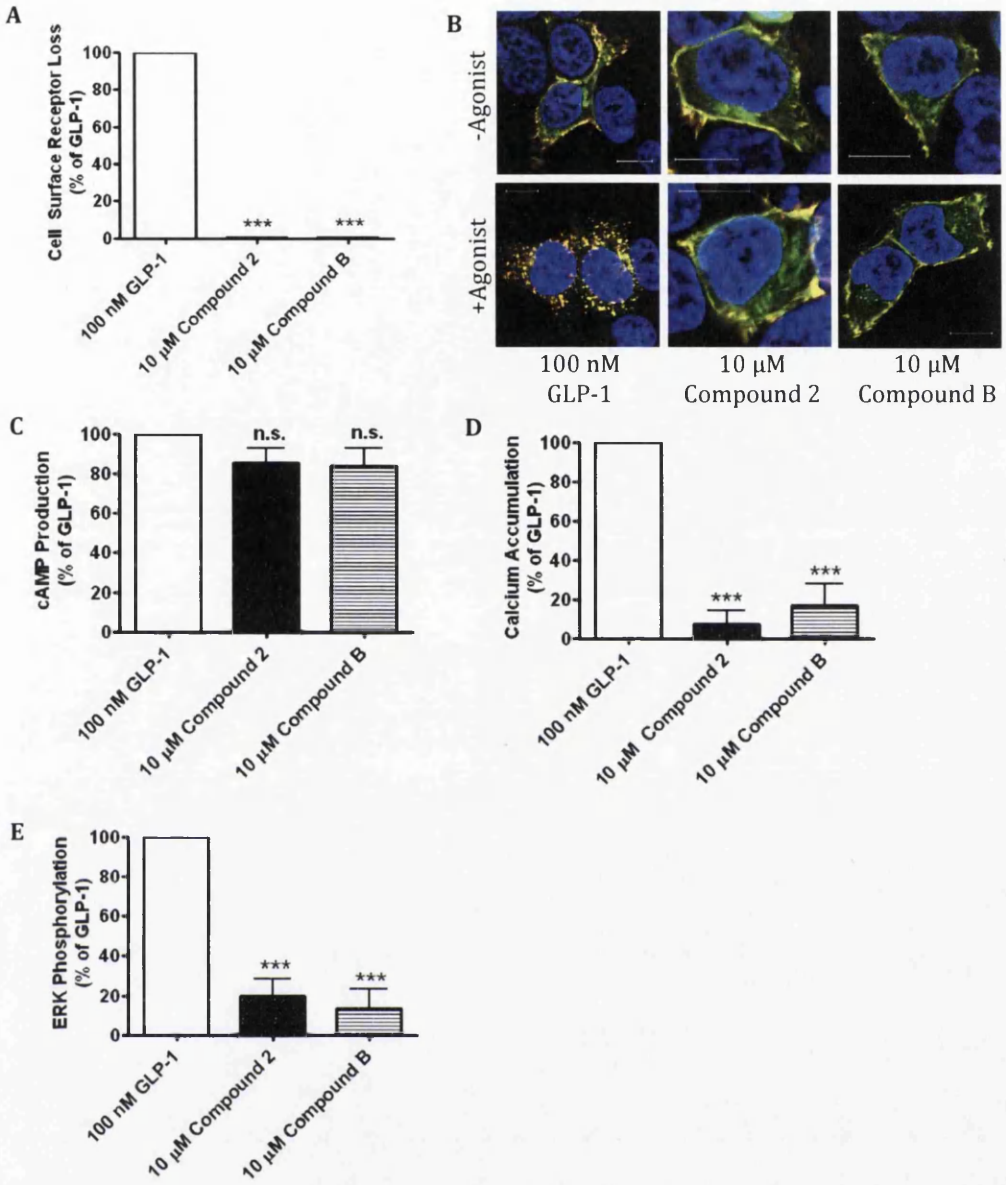

Figure 5.7. Small molecule agonists activate the $G\alpha_s$ pathway and inhibit hGLP-1R internalisation. HEK293 cells cotransfected with the hGLP-1R plasmid and the luciferase reporter plasmid for cAMP (pGL4.29-Luc-CRE), intracellular Ca^{2+} (pGL4.30-Luc-NFAT) or ERK phosphorylation (pGL4.33-Luc-SRE) were stimulated with GLP-1, compound 2 and compound B for 60 min as indicated to assess hGLP-1R internalisation by ELISA (A) and immunofluorescence (B), for 4 h to assess cAMP production (C), for 8 h to assess intracellular Ca^{2+} accumulation (D) and for 4 h to assess ERK phosphorylation (E). In immunofluorescence, EGFP (green) and the anti-hGLP-1R antibody (red) overlay shown in yellow and nuclear staining with DAPI in blue. Data are mean ± SEM, n=3. Data were analysed by Bonferroni's post test after one-way ANOVA; values differ from control, n.s. $p>0.05$, *** $p<0.001$.

5.3.3. Inhibition of the $G\alpha_q$ pathway prevents agonist induced hGLP-1R internalisation

The $G\alpha_q$ pathway causes intracellular Ca^{2+} accumulation by activating PLC, which hydrolyses PIP_2 to IP_3 and DAG. IP_3 binds to the IP_3R on the ER and increases cytosolic Ca^{2+} levels. An increase in intracellular Ca^{2+} levels leads to PKC activation, which then regulates many signalling pathways including ERK phosphorylation (Cobb & Goldsmith, 1995; Hawes et al, 1995; Werry et al, 2003). To study the importance of the $G\alpha_q$ pathway in agonist stimulated hGLP-1R internalisation, several activators and inhibitors were used to determine whether the $G\alpha_q$ pathway is critical for agonist induced internalisation of the hGLP-1R or not (Figure 5.8A). A number of controls such as membrane permeable penetratin (as a negative control to PBP10, a membrane permeable PIP_2 sequestering peptide), U73343 (negative control to U73122, a PLC inhibitor) and BAPTA-AM saturated with Ca^{2+} (BAPTA-AM+Ca^{2+}, a negative control to BAPTA-AM-Ca^{2+}, a membrane permeable chelator for intracellular calcium) was also used to authenticate the specificity of the $G\alpha_q$ pathway inhibitors. As expected all negative controls used in this study showed no effect on agonist induced hGLP-1R internalisation (penetratin 89.0 ± 9.0%, U73343 93.9 ± 4.1% and BAPTA-AM+Ca^{2+} 91.7 ± 6.3%, $p>0.05$, to that of the untreated control, Figure 5.8B). In contrast agonist induced hGLP-1R internalisation was reduced to 21.2 ± 9.8% ($p<0.001$) by the PIP_2 sequestering peptide, PBP10, and was almost abolished to 3.8 ± 3.8% ($p<0.001$) by the PLC inhibitor, U73122. The IP_3R inhibitor, 2-APB, reduced agonist induced internalisation to 24.4 ± 3.8% ($p<0.001$) whereas BAPTA-AM-Ca^{2+}, a chelator of intracellular Ca^{2+}, significantly reduced agonist induced internalisation of the hGLP-1R (9.9 ± 3.9%, $p<0.001$). The PKC inhibitors, Go6976 and Ro318820, also inhibited agonist induced hGLP-1R internalisation to 48.0 ± 5.5% ($p<0.01$) and 30.9 ± 5.6% ($p<0.001$) respectively. Lastly, the ERK inhibitor, PD98059, also prevented agonist induced hGLP-1R internalisation to 37.5 ± 4.3%, ($p<0.001$). Immunofluorescence analysis supported these observations by demonstrating the inhibition of agonist induced hGLP-1R internalisation by PBP10, U73122, 2-APB, BAPTA-AM-Ca^{2+}, Go6976, Ro318220 and PD98059 (Figure 5.8C). However, the negative

control inhibitors (penetratin peptide, U73343 and BAPTA-AM+Ca^{2+}) showed no effect on hGLP-1R internalisation.

The concentration dependent effect of various inhibitors on the $G\alpha_q$ pathway and ERK phosphorylation was also analysed (Figure 5.9A-G). PBP10 inhibited internalisation of the receptor in a concentration dependent manner and maximal inhibition was observed in the presence of 30 μM PBP10 (8.1 ± 2.6%, $p<0.001$). U73122 treatment also resulted in the concentration dependent inhibition of hGLP-1R internalisation with maximal inhibition at 100 μM (1.9 ± 1.8%, $p<0.001$). In cells treated with the IP_3R inhibitor, 2-APB, the inhibition of internalisation was also concentration dependent and resulted in maximal inhibition at 4 mM (4.8 ± 1.2%, $p<0.001$). BAPTA-AM-Ca^{2+} also inhibited hGLP-1R internalisation in a concentration dependent manner and had maximal inhibition at 1 mM (8.9 ± 2.4%, $p<0.001$). In cells treated with either PKC inhibitors, Go6976 and Ro318220, ranging from 1 μM to 100 μM agonist induced internalisation was inhibited in a concentration dependent manner, with maximal inhibition at 46.0 ± 4.3% and 24.1 ± 5.4% ($p<0.001$) respectively. The ERK inhibitor, PD98059, inhibited hGLP-1R internalisation in concentrations from 6.25 μM to 100 μM, with maximal inhibition at 100 μM (9.3 ± 2.9%, $p<0.001$). These observations were confirmed by immunofluorescence where inhibition of agonist induced internalisation was evident. Taken together, these results demonstrated that the $G\alpha_q$ pathway regulates agonist induced hGLP-1R internalisation.

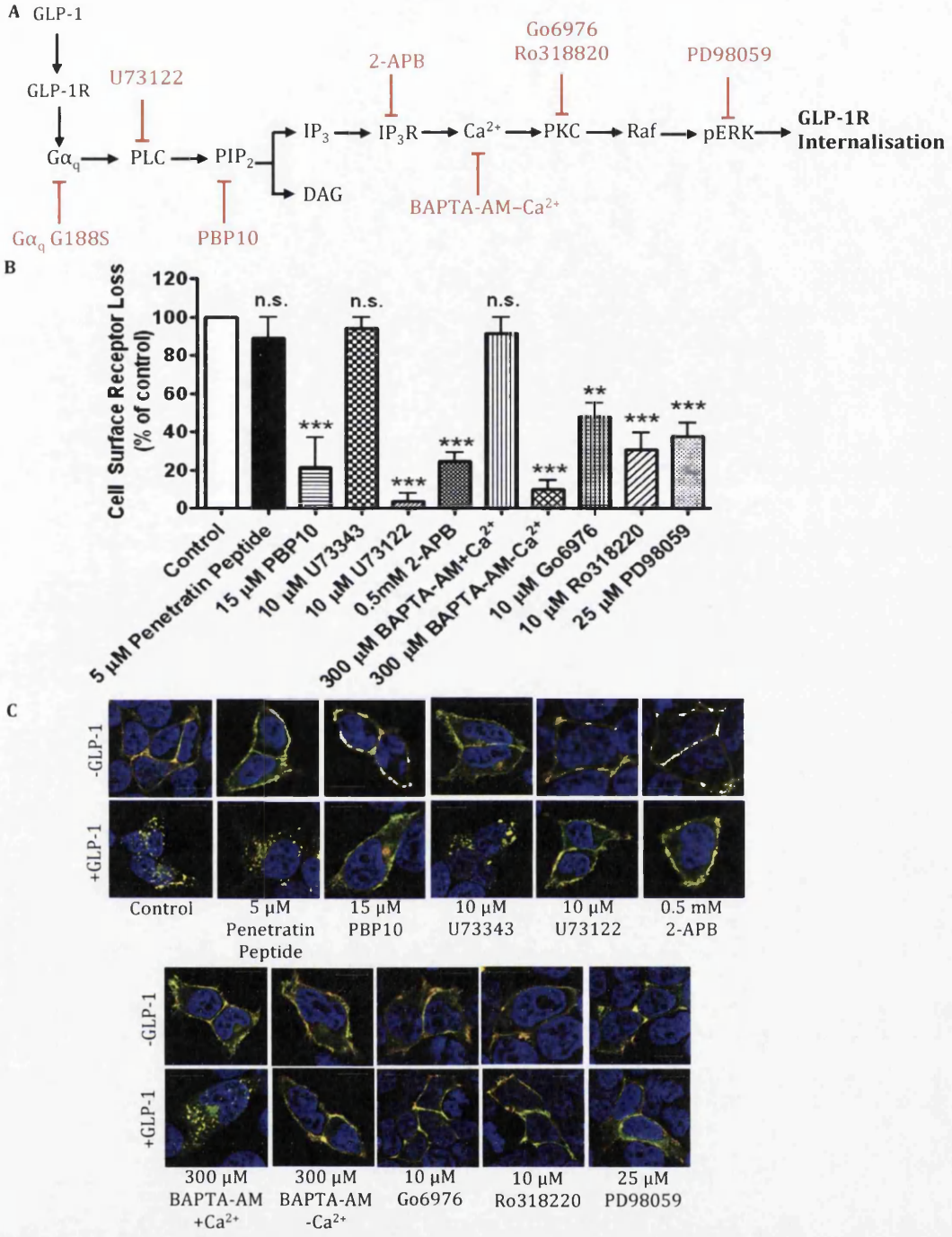

Figure 5.8. Inhibiting the $G\alpha_q$ pathway prevents agonist induced hGLP-1R internalisation. (A) Schematic representation of the pathway of agonist induced hGLP-1R internalisation. (B) HGLP-1R internalisation in HEK293 cells treated with inhibitors of the $G\alpha_q$ pathway as indicated and stimulated with 100 nM GLP-1 for 60 min was assessed by ELISA using the anti-hGLP-1R antibody. (C) Immunofluorescence showing hGLP-1R internalisation, EGFP (green) and the anti-hGLP-1R antibody (red) overlay shown in yellow and nuclear staining with DAPI in blue. Data are mean ± SEM, n=3. Data were analysed by Bonferroni's post test after one-way ANOVA; values differ from control, n.s. $p>0.05$, ** $p<0.01$, *** $p<0.001$.

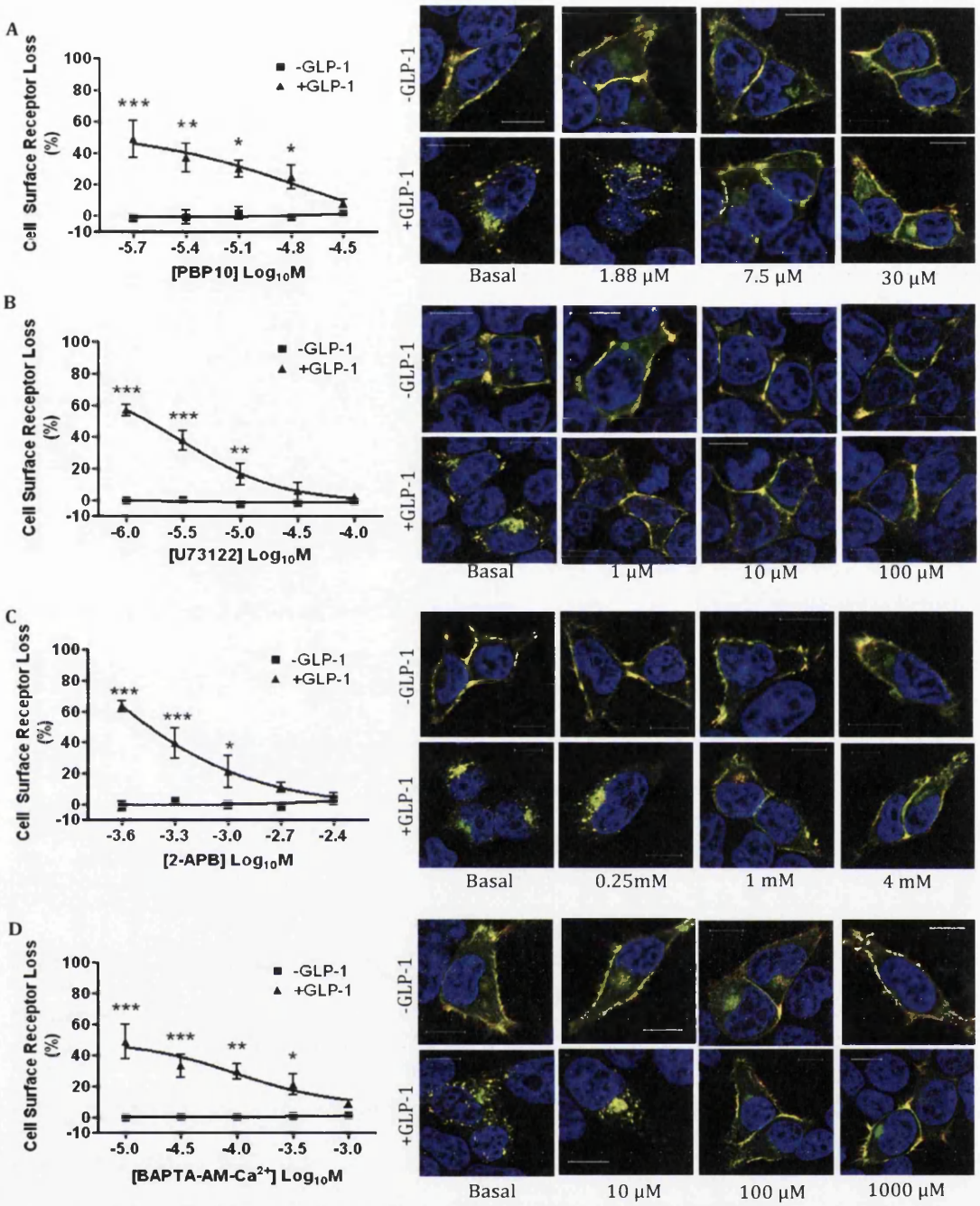

Figure 5.9. Concentration dependent effect of inhibitors of the $G\alpha_q$ pathway on agonist induced hGLP-1R internalisation. Agonist induced hGLP-1R internalisation in HEK293 cells treated with inhibitors PBP10 (A), U73122 (B), 2-APB (C), BAPTA-AM–Ca^{2+} (D), Go6976 (E), Ro318220 (F) and PD98059 (G) as indicated and stimulated with 100 nM GLP-1 for 60 min was assessed by ELISA (left panel) and immunofluorescence (right panel) using the anti-hGLP-1R antibody. In immunofluorescence, EGFP (green) and the anti-hGLP-1R antibody (red) overlay shown in yellow and nuclear staining with DAPI in blue. Data are mean ± SEM, n=3. Data were analysed by Bonferroni's post test after two-way ANOVA; values differ from control, * $p<0.05$, ** $p<0.01$, *** $p<0.001$.

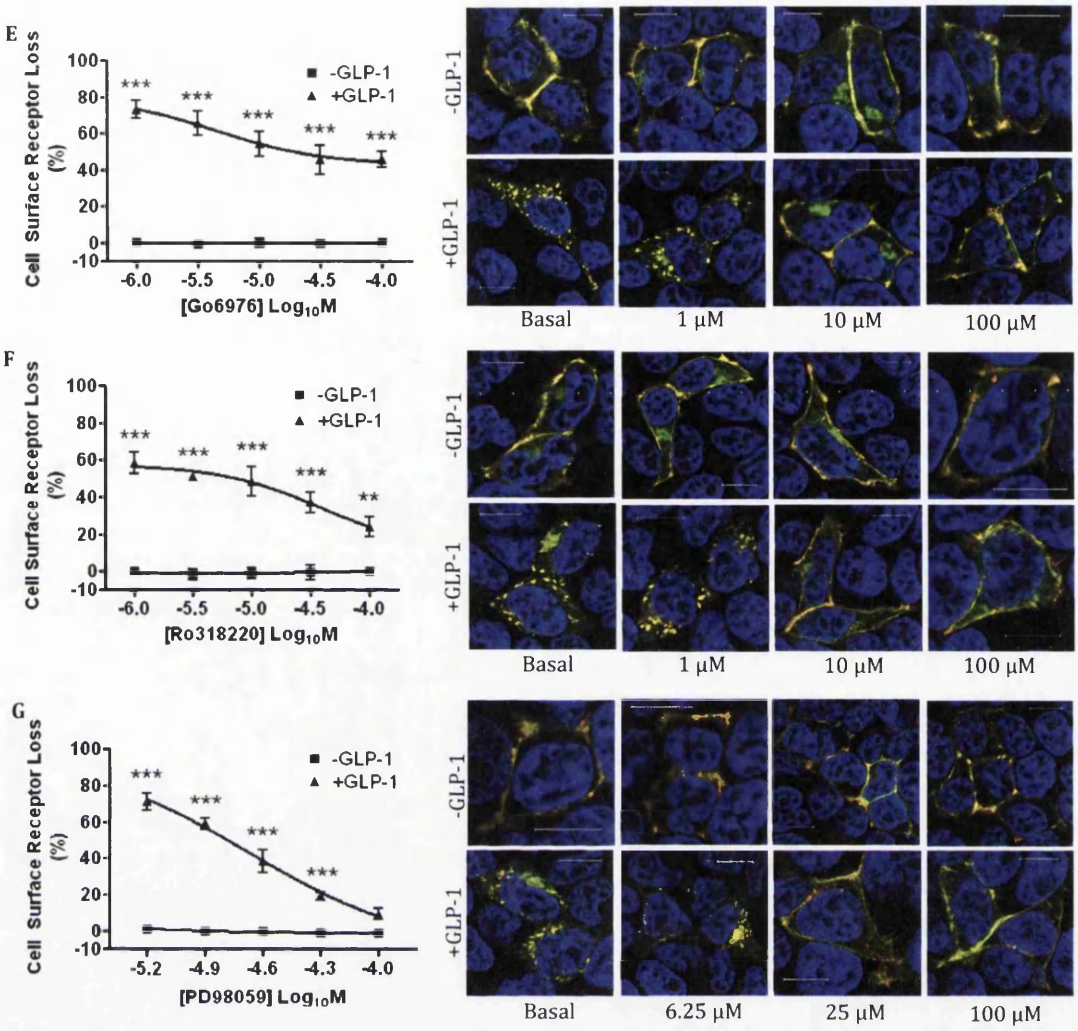

Figure 5.9 cont. Concentration dependent effect of inhibitors of the $G\alpha_q$ pathway on agonist induced hGLP-1R internalisation. Agonist induced hGLP-1R internalisation in HEK293 cells treated with inhibitors PBP10 (A), U73122 (B), 2-APB (C), BAPTA-AM–Ca^{2+} (D), Go6976 (E), Ro318220 (F) and PD98059 (G) as indicated and stimulated with 100 nM GLP-1 for 60 min was assessed by ELISA (left panel) and immunofluorescence (right panel) using the anti-hGLP-1R antibody. In immunofluorescence, EGFP (green) and the anti-hGLP-1R antibody (red) overlay shown in yellow and nuclear staining with DAPI in blue. Data are mean ± SEM, n=3. Data were analysed by Bonferroni's post test after two-way ANOVA; values differ from control, * $p<0.05$, ** $p<0.01$, *** $p<0.001$.

5.3.4. Effect of the $G\alpha_q$ pathway inhibitors on GLP-1 induced ERK phosphorylation and cAMP production

Since the activation of Ca^{2+} dependent PKC and ERK is required for agonist induced hGLP-1R internalisation and the activation of the $G\alpha_q$ pathway leads to an increase in intracellular Ca^{2+} levels, it was determined whether the $G\alpha_q$ pathway regulates internalisation of the receptor through ERK phosphorylation. For this purpose, the effect of inhibitors of the $G\alpha_q$ pathway on agonist induced ERK phosphorylation was assessed (Figure 5.10A-B). The negative controls, penetratin (for PBP10), U73343 (for U73122) and BAPTA-AM+Ca^{2+} (for BAPTA-AM-Ca^{2+}) showed no effect on ERK phosphorylation (107.9 ± 3.6%, 99.6 ± 9.9%, 96.0 ± 12.7%, $p>0.05$, respectively). In contrast, the PIP_2 inhibitor, PBP10, significantly reduced ERK phosphorylation to 36.8 ± 8.2% ($p<0.001$). U73122, the inhibitor of PLC, almost abolished ERK phosphorylation to 4.8 ± 0.7% ($p<0.001$). The IP_3R inhibitor, 2-APB, significantly inhibited ERK phosphorylation (46.6 ± 8.0%, $p<0.001$). Only 22.3 ± 8.8% ($p<0.001$) ERK phosphorylation was shown in the presence of BAPTA-AM-Ca^{2+}, the chelator of intracellular Ca^{2+}. The PKC inhibitors, Go6976 and Ro318820, almost abolished agonist induced ERK phosphorylation to 9.3 ± 1.8% ($p<0.001$) and 14.9 ± 2.2% ($p<0.001$) respectively. Lastly, the MAPK inhibitor, PD98059, also inhibited ERK phosphorylation (16.0 ± 8.1%, $p<0.001$), as expected. Since the $G\alpha_s$ pathway mediates cAMP generation, the $G\alpha_q$ pathway specific inhibitors should not affect its production. As expected, the $G\alpha_q$ pathway inhibitors had no effect ($p>0.05$) on agonist induced cAMP production (Figure 5.11). Taking these results together with the effect of the inhibitors of the $G\alpha_q$ pathway on hGLP-1R internalisation further indicates that the $G\alpha_q$ pathway regulates agonist induced hGLP-1R internalisation via ERK phosphorylation.

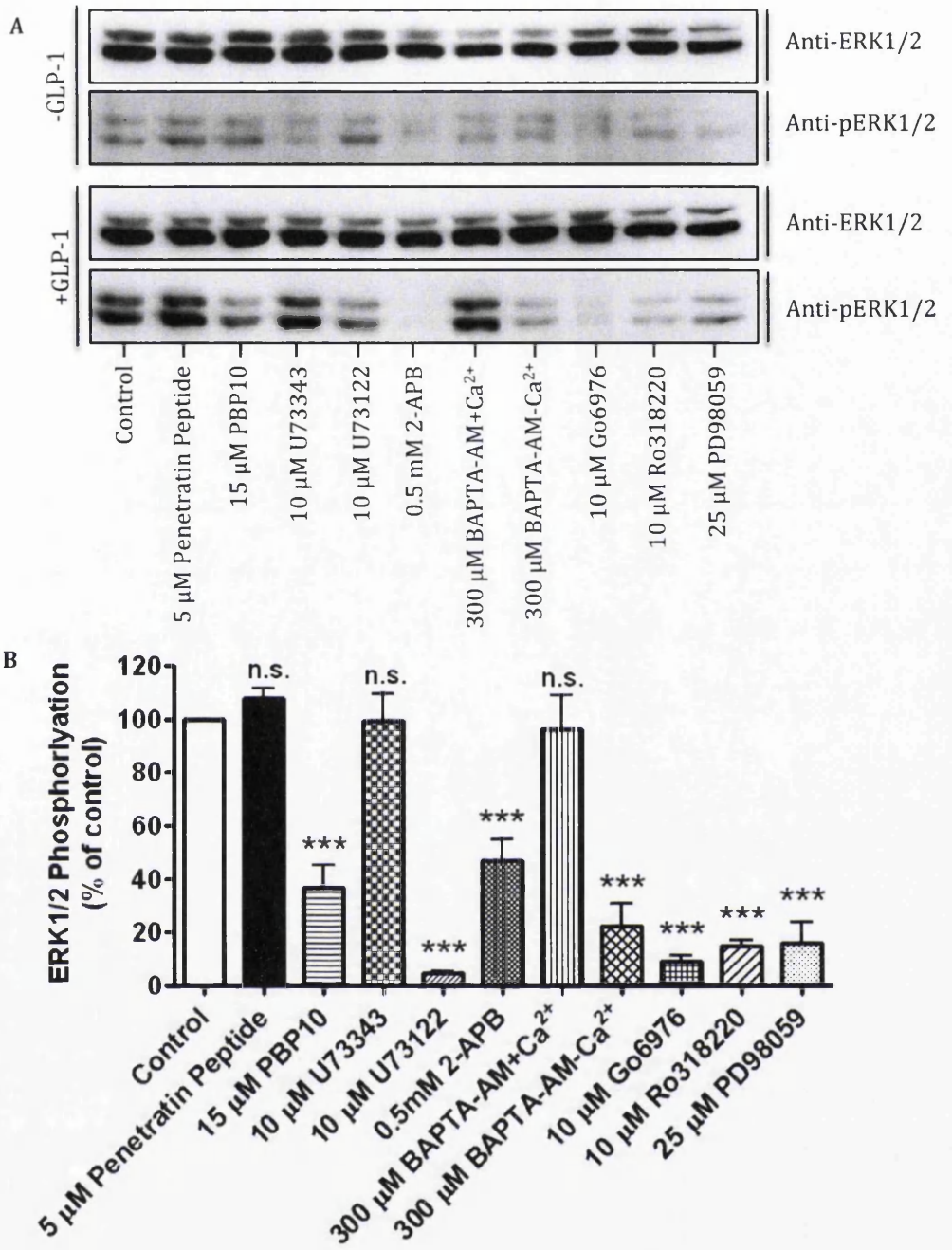

Figure 5.10. Effect of the $G\alpha_q$ pathway inhibition on agonist stimulated ERK phosphorylation. HEK293 cells transfected with the hGLP-1R were stimulated with 100 nM GLP-1 for 5 min, lysed and ERK1/2 phosphorylation in the presence of $G\alpha_q$ pathway inhibitors was measured by immunoblotting (A) and quantified by densitometry and normalised to total ERK1/2 levels (B). The densitometry data is presented as percentage phosphorylation and are shown as mean ± SEM, n=3. Data were analysed by Bonferroni's post test after one-way ANOVA; values differ from control, n.s. $p>0.05$, *** $p<0.001$.

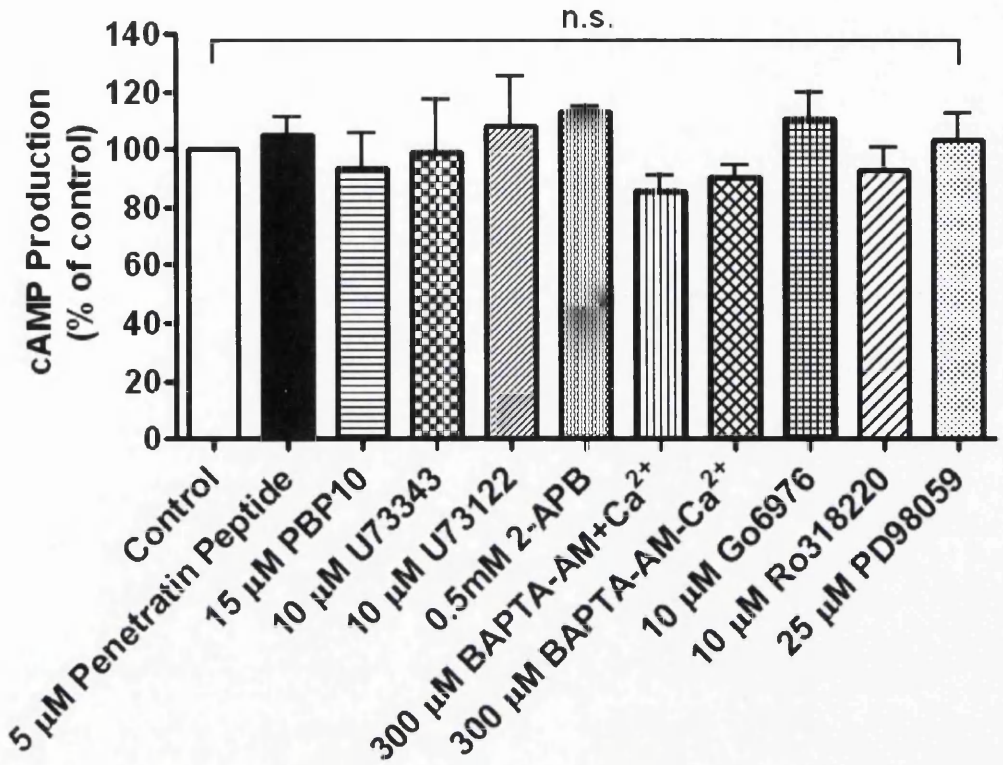

Figure 5.11. Effect of the $G\alpha_q$ pathway inhibition on agonist stimulated cAMP production. HEK293 cells expressing the hGLP-1R were stimulated with 100 nM GLP-1 for 60 min in the presence of $G\alpha_q$ pathway inhibitors and measured cAMP production to assess hGLP-1R activity. Data are mean ± SEM, n=3. Data were analysed by Bonferroni's post test after one-way ANOVA; values differ from control, n.s. $p>0.05$.

5.4. Discussion

Upon activation by agonist binding, many GPCRs are internalised to reduce the activity of the receptor. The internalised GPCRs are subjected to one of two sorting fates. They are either recycled back to the plasma membrane resulting in resensitisation of the receptor or transported to lysosomes and proteolysed leading to long-term attenuation of signalling (down-regulation) (Marchese et al, 2003). Currently, it is unknown which pathway the GLP-1R undergoes and how cells respond to drugs after the initial internalisation phase. With the

possibility of drugs being produced which are administered once a week or once a month rather than once daily. The effects these drugs have on GLP-1R activity and cell surface expression needs to be understood for the half-life of these compounds to be prolonged further and for the effect of 'long-acting-release' drugs to be successful (Gedulin et al, 2005). In pancreatic β-cells, an increase in cytosolic Ca^{2+} causes the release of insulin by exocytosis (De Vos et al, 1995; Holz, 2004). The increase in intracellular Ca^{2+} mediated insulin secretion is potentiated by elevated cAMP levels (Holst & Gromada, 2004). Upon agonist stimulation, the internalised GLP-1R has been shown to colocalise with AC on endosomes and stimulate insulin secretion from pancreatic β-cells demonstrating the importance of hGLP-1R internalisation for insulin secretion (Kuna et al, 2013). Therefore, agonist induced internalisation of the hGLP-1R into intracellular compartments of the cell is important for regulation of the receptor's activity (Bhaskaran & Ascoli, 2005; Kanamarlapudi et al, 2012). This study systematically analysed the involvement of the $G\alpha_q$ pathway in agonist induced GLP-1R internalisation.

The trafficking of GPCRs in caveolae has several functions including: receptor signalling, internalisation and stability (Chini & Parenti, 2004). In this study, the hGLP-1R was demonstrated by various approaches to internalise by caveolae mediated endocytosis. Additionally, the hGLP-1R was found to interact with caveolin-1 and interference of this interaction by the DN mutant of caveolin-1 abolished cell surface expression of the receptor. This is consistent with previous findings where caveolin-1 has been shown to interact with the hGLP-1R and be important for targeting, internalisation and recycling of the receptor (Syme et al, 2006). These findings strongly suggest that caveolin-1 functions as a molecular chaperone for the hGLP-1R, which is consistent with it acting as a molecular chaperone for a number of other GPCRs, including the endothelin A receptor (Chini & Parenti, 2004).

The GLP-1R has been shown to activate both the $G\alpha_s$ coupled pathway to generate cAMP and the $G\alpha_q$ coupled pathway to cause accumulation of intracellular Ca^{2+} (Montrose-Rafizadeh et al, 1999). In this study, inhibition of

the $G\alpha_q$, but not the $G\alpha_s$, signalling pathway markedly reduced agonist induced internalisation of the hGLP-1R, indicating a critical role for the $G\alpha_q$ pathway in hGLP-1R internalisation. The 5-$HT2_A$ receptor and the gonadotropin-releasing hormone receptor also couples and internalises through the $G\alpha_q$ pathway (Bhattacharyya et al, 2002; Kramer et al, 1997; McArdle et al, 2002; Nash et al, 1997). The T149M mutation in the hGLP-1R, which was originally identified in a type 2 diabetic patient with impaired insulin secretion (Tokuyama et al, 2004), has been shown to reduce agonist responsiveness (Beinborn et al, 2005). In this study, HEK293 cells expressing either the WT hGLP-1R or T149M mutant demonstrated similar EC_{50} values for cAMP generation when stimulated with GLP-1, indicating the mutation had no effect on either agonist binding to the receptor or its activity. This study also demonstrates that the mutation, instead, significantly reduces agonist induced hGLP-1R internalisation by affecting intracellular Ca^{2+} accumulation and ERK phosphorylation, which strongly suggests this as a possible cause for the patient's reduced insulin secretion found in the type 2 diabetic patient with the T149M mutation in the Tokuyama et al study. Like the T149M mutant, small molecule agonists, compounds 2 and B, neither activated the $G\alpha_q$ pathway nor induced hGLP-1R internalisation. This is consistent with previous studies that demonstrated compounds 2 and B activate only the $G\alpha_s$ pathway (Coopman et al, 2010; Irwin et al, 2010; Knudsen et al, 2007; Sloop et al, 2010; Wootten et al, 2013). Further, cAMP produced in response to hGLP-1R stimulation is important for glucose stimulated insulin secretion (Lee & Jun, 2014). It has recently been shown that pharmacological inhibition of GLP-1R internalisation attenuates agonist mediated insulin secretion (Kuna et al, 2013). This is because the internalised GLP-1R associates with AC on endosomes to generate cAMP required for insulin secretion. It is therefore a possibility that the T149M mutation and small molecule agonists (compounds 2 and B) affect insulin secretion by inhibiting GLP-1R internalisation and thereby endosomal cAMP generation. Future studies should be undertaken to assess whether or not inhibition of GLP-1R internalisation alters agonist induced insulin secretion from β-cells.

In this study, inhibition of PLC activation and intracellular Ca^{2+} accumulation affected agonist induced internalisation of the hGLP-1R, further demonstrating the GLP-1R couples and internalises through the $G\alpha_q$ pathway (Werry et al, 2003). Since the increase in intracellular Ca^{2+} levels downstream of agonist stimulated GLP-1R activates PKC (Werry et al, 2003), the effect of two PKC inhibitors, Go6976 and Ro318220, on the agonist induced internalisation of the GLP-1R was determined. The PKC family consists of several isoforms in humans that are activated in either a Ca^{2+} dependent or independent manner. The inhibitor Go6976 is selective for Ca^{2+} dependent PKC isoforms (Martiny-Baron et al, 1993) whereas Ro318220 is a broad spectrum PKC inhibitor, which inhibits both Ca^{2+} dependent and Ca^{2+} independent PKC isoforms (Davies et al, 2000). The inhibition of agonist induced GLP-1R by both the PKC inhibitors demonstrate the importance of Ca^{2+} dependent PKC isoforms for internalisation of the hGLP-1R. It is also important to note that the GLP-1R contains three PKC phosphorylation sites within the C-terminal domain, which are also important for internalisation (Widmann, 1997). Removal of these phosphorylation sites has been shown to prevent agonist induced GLP-1R internalisation demonstrating the importance of PKC phosphorylation of the receptor in GLP-1R internalisation. The δ-opioid receptor also requires the activation of PKC to allow phosphorylation of the receptor for internalisation (Xiang et al, 2001). In this study, the inhibition of PKC not only prevented agonist induced internalisation but also ERK phosphorylation, indicating that PKC may play a role in GLP-1R internalisation by phosphorylating the receptor as well as regulating the phosphorylation of ERK.

ERK is phosphorylated by receptor tyrosine kinases in Src and Ras dependent manners (Budd et al, 2001; Crespo et al, 1994; Hawes et al, 1995; Lopez-Ilasaca et al, 1997; Luttrell et al, 1996). However, GPCRs phosphorylate ERK through $G\alpha_s$, $G\alpha_i$ and $G\alpha_q$ pathways depending on receptor type and environment (Gutkind, 1998). ERK phosphorylation that occurs through the $G\alpha_q$ pathway is highly dependent on both intracellular Ca^{2+} accumulation and PKC activation (Budd et al, 2001). The inhibition of PKC in the α_{1B} adrenergic receptor (Della Rocca et al, 1997), bradykinin receptor, lysophospholipid receptors (Dikic et al,

1996) and thyrotropin-releasing hormone receptor (Hinkle et al, 2012) either abolished or significantly reduced these receptors mediated ERK phosphorylation, demonstrating PKC acts upstream of ERK. The results obtained in this study strongly suggest GLP-1 mediated ERK phosphorylation occurs downstream of PKC activation. This suggests that the accumulation of intracellular Ca^{2+} and thereby activation of PKC is able to induce ERK phosphorylation, linking activation of the receptor to ERK phosphorylation. ERK phosphorylation has also been shown to play an important role in the internalisation, desensitisation and sequestration of GPCRs such as the δ-opioid receptor, G-CSFR and 5-$HT2_A$ receptor (Bhattacharyya et al, 2002; Daaka et al, 1998; Eisinger & Schulz, 2004; Hunter & Avalos, 1999; Ward et al, 1999). It is possible that ERK phosphorylation may also play a role in receptor desensitisation and sequestration of the hGLP-1R but requires further investigation.

In conclusion, these results demonstrate that caveolin-1 plays an important role in hGLP-1R trafficking to the cell surface and its internalisation. Upon agonist activation, the hGLP-1R signals through the $G\alpha_q$ pathway to hydrolyse PIP_2 by PLC to generate IP_3. IP_3 binds the IP_3R and increases cytosolic Ca^{2+} accumulation, which causes the activation of PKC. In turn, this leads to the phosphorylation of ERK via the MAPK pathway (Werry et al, 2003). In this study, the inhibition of the $G\alpha_q$ pathway affected not only hGLP-1R internalisation but also ERK phosphorylation, indicating that together they play a vital role in the agonist induced internalisation of the receptor (Figure 5.8). In this study, the T149M mutation, which was previously found in a Japanese patient with type 2 diabetes with impaired insulin secretion, and small molecule agonists (compound 2 and B) of the GLP-1R also inhibited agonist induced hGLP-1R internalisation. This suggests an important role for hGLP-1R internalisation in insulin secretion. These findings also suggest that new targets in the treatment of type 2 diabetes should be assessed for their effects on GLP-1R internalisation.

6. Identification of Distinct Regions Within the C-Terminal Domain Required for Human Glucagon Like Peptide-1 Receptor Cell Surface Expression, Activity and Internalisation

6.1. Introduction

Glucagon like peptide-1 (GLP-1) mediates insulin secretion by acting on the GLP-1 receptor (GLP-1R), making the receptor an important target and of high therapeutic potential in the treatment of type 2 diabetes (Gallwitz, 2010; Thompson & Kanamarlapudi, 2013). The GLP-1R is a member of the family B G-protein coupled receptors (GPCRs) (Thompson & Kanamarlapudi, 2013; Thorens et al, 1993). The C-terminal domain of GPCRs plays a critical role in agonist induced internalisation, desensitisation, down regulation and arrestin signalling (Kuramasu et al, 2006; McArdle et al, 2002). Further, the C-terminal region is also required for GPCR trafficking to the plasma membrane (Ohno et al, 1995; Sandoval & Bakke, 1994; Trowbridge et al, 1993). The C-terminal domain of GPCRs is also known to interact with intracellular proteins involved in the internalisation of the receptor to activate intracellular signalling pathways. Many GPCRs, including the GLP-1R, regulate the activity of intracellular effector proteins such as phospholipase C (PLC) and adenylyl cyclase (AC) via heterotrimeric G-proteins (Bohm et al, 1997a; Ferguson, 2001).

The C-terminal domain of GPCRs is required for targeting to endosomes, the Golgi and the plasma membrane (Ohno et al, 1995; Sandoval & Bakke, 1994; Trowbridge et al, 1993). Using mutagenesis studies, motifs such as E(X)3LL, FN(X)2LL(X)3L and F(X)3F(X)3F within the C-terminus have been identified for GPCR targeting to the plasma membrane (Dong et al, 2007). Additionally, motifs within the C-terminus that are four to six amino acids (aa) long and contain a critical tyrosine residue and follow a general consensus of YXXΦ (where Y is a

tyrosine residue, X denotes any amino acid and Φ is a hydrophobic residue) have also been shown to be required for the trafficking of some GPCRs (Ohno et al, 1995; Sandoval & Bakke, 1994; Trowbridge et al, 1993). Some GPCRs possess a helix-8 motif located just downstream of transmembrane (TM) 7 that associates with a number of intracellular proteins (Kuramasu et al, 2006). The dopamine receptor interacting protein 78 binds to a conserved sequence located in the helix-8 domain of the dopamine D1 receptor (D1R) and is responsible for trafficking the receptor to the plasma membrane (Bermak et al, 2001). Additionally, many GPCRs possess a PDZ binding site at the very end of the C-terminal domain that interacts with PDZ domain containing proteins required for trafficking of the receptor. For example, Tctex-1 interacts with the C-terminal end of the rhodopsin receptor through its PDZ domain. A mutation in the C-terminal domain of the receptor not only inhibits this interaction but also prevents the transport of rhodopsin within the rod cells (Tai et al, 1999). The region between helix-8 and the very end of the C-terminus is referred to as 'binding sites with GPCR interacting proteins' (Kuramasu et al, 2006). The metabotropic glutamate receptor (mGluR, types 1a, 5a and 5b) contains a PPXXFR motif within this region of the C-terminus that interacts with homer proteins 1, 2 and 3 to target and regulate the receptor's trafficking to dendritic synapse sites (Ango et al, 2000; Ango et al, 2001; Ango et al, 2002).

In addition to its role in targeting and trafficking of GPCRs, the C-terminal domain is known to interact with intracellular proteins involved in the internalisation of the receptor (Kuramasu et al, 2006). The tyrosine motif (YXXΦ) within the C-terminus has also been shown to associate with clathrin (Chang et al, 1993; Glickman et al, 1989; Pearse, 1988; Sorkin & Carpenter, 1993; Sorkin et al, 1995). However, a common binding motif within clathrin for the YXXΦ motif has not yet been identified. In the mGluR7a and mGluR7b, the βγ subunit of heterotrimeric G-proteins and calcium (Ca^{2+})/calmodulin bind to this domain and regulate P and Q type Ca^{2+} channels (O'Connor et al, 1999). The β_3-adrenergic receptor (AR) contains a PXXP motif within the C-terminal domain that interacts with Src, which results in the activation of extracellular signal-regulated kinase (ERK) (Cao et al, 2000). Further, a NPXXY motif at the C-

terminal domain closest to TM7 within the serotonin 5-hydroxytryptamine 2a ($5\text{-}HT_{2a}$) receptor interacts with ADP-ribosylation factor 1 (ARF1) and couples to phospholipase D (PLD) in a heterotrimeric G-protein independent manner (Robertson et al, 2003).

Single transmembrane receptors such as the epidermal growth factor receptor, insulin receptor and transferrin receptor, contain a tyrosine residue within a tight-turn-forming motif in the C-terminal domain, which is required for their internalisation (Trowbridge et al, 1993). The dileucine (LL) motif within the C-terminal domain is required for internalisation of the T-lymphocyte cluster of differentiation 3 (CD3) and glucose transporter, GLUT4 (Letourneur & Klausner, 1992; Verhey & Birnbaum, 1994). The LL motif has also been shown to promote GPCRs internalisation by binding to adapter proteins (Ferguson, 2001). Although, the mutation of specific amino acids within the LL motif may prevent GPCR internalisation in some instances, this is not a common motif required for GPCR internalisation (Widmann, 1997). GPCRs, such as the neurokinin 1 and the angiotensin II receptor (AT_2R), require conserved aromatic residue tyrosine in the C-terminal domain for their internalisation (Bohm et al, 1997b; Thomas et al, 1995). The M_3 muscarinic receptor (M_3R) requires three tyrosine residues within the C-terminal domain for its internalisation (Yang et al, 1995). For some GPCRs such as the β_2-AR, gastrin-releasing peptide receptor (GRPR) and the GLP-1R, serine and threonine rich amino acid sequences in TM3 and the C-terminal domain are required for their internalisation (Benya et al, 1993; Hausdorff et al, 1991; Widmann, 1997). Internalisation of the β_2-AR is supressed with a mutation to Tyr^{326} (Barak et al, 1994). A mutation of Ser^{344} within the C-terminal domain of the δ-opioid receptor prevents protein kinase C (PKC) phosphorylation required for internalisation of the receptor (Xiang et al, 2001). The GLP-1R contains three serine doublets at positions $Ser^{441,442}$, $Ser^{444,445}$ and $Ser^{451,452}$ and their phosphorylation is also important for internalisation of the receptor. Additionally, intermediate rates of internalisation was demonstrated with the GLP-1R mutants containing one or two of these phosphorylation sites (Widmann, 1997).

GPCR internalisation occurs after agonist binding, which is required for receptor desensitisation (Harden, 1983; Lefkowitz et al, 1983). Typically, GPCRs are phosphorylated at specific sites within the C-terminal domain in response to agonist binding (Tobin, 2008). This sterically hinders heterotrimeric G-protein association and thereby prevents its activation (Ferguson, 2001; Zhang et al, 1997). Interestingly, removing GPCR kinase (GRK) phosphorylation sites from the β_2-AR still allowed internalisation of the receptor but supressed desensitisation, demonstrating the importance of these phosphorylation sites for desensitisation (Bouvier et al, 1988; Strader et al, 1987). However, overexpression of GRK2 has been shown to induce internalisation of the internalisation resistant β_2-AR mutant by phosphorylating the receptor (Ferguson et al, 1995). This demonstrated the importance of receptor phosphorylation for both GPCR internalisation and desensitisation. However, GLP-1 induced phosphorylation of serine doublets at positions $Ser^{431,432}$, $Ser^{441,442}$, $Ser^{444,445}$ and $Ser^{451,452}$ within the GLP-1R is important not only for internalisation but also desensitisation of the receptor (Widmann, 1997). Further, phosphorylation of some serine doublets within the C-terminal domain of the GLP-1R is mediated by PKC (Widmann et al, 1996a).

Most GPCRs, including the GLP-1R, contain a conserved cysteine residue within the C-terminal domain that is important for palmitoylation of the receptor (Bouvier et al, 1995a; Bouvier et al, 1995b; Morello & Bouvier, 1996; Vazquez et al, 2005b). This palmitoylation causes the C-terminal domain to anchor to the cell surface and therefore creates a fourth intracellular loop (Bouvier et al, 1995a). A mutation to the palmitoylation site (Cys^{438}) of the GLP-1R has previously been shown not to affect cell surface expression or internalisation of the receptor. However, a 3-fold decrease in the activity of the receptor (assessed by cyclic adenosine monophosphate [cAMP] production) has been demonstrated for the GLP-1R C438A mutant (Vazquez et al, 2005b). This decrease in the activity of the GLP-1R by mutating the palmitoylation site is also consistent with that shown for other GPCRs including the β_2-AR (O'Dowd et al, 1989) and D1R (Jensen et al, 1995). Further, mutation of Glu^{408}, Val^{409}, Gln^{410}, which are conserved among family B GPCRs, showed reduced agonist binding

and cAMP production (Vazquez et al, 2005a). However, it is unknown whether this triple mutation affects agonist binding and cAMP production by altering cell surface expression of the GLP-1R.

Although some GPCRs require E(X)3LL, FN(X)2LL(X)3L, F(X)3F(X)3F, tyrosine YXXΦ, PPXXFR, PXXP, NPXXY and LL motifs within the C-terminal domain for trafficking, interactions with intracellular proteins and internalisation of the receptor, these motifs are not present within the GLP-1R. Therefore this study established the importance of other residues and regions within the C-terminal domain of the human GLP-1R (hGLP-1R) for cell surface expression, activity and internalisation using a number of C-terminal deletions and site-directed mutants. It was determined that residues 411-418 of the hGLP-1R C-terminus are critical in targeting the receptor to the plasma membrane. Residues 419-430 within the C-terminal domain are important for the activity of the receptor (as assessed by cAMP production), most likely for coupling to $G\alpha_s$. Further, residues 431-450 within the C-terminus are essential for hGLP-1R internalisation.

6.2. Materials and methods

6.2.1. Materials

The primary antibodies used were rabbit anti-vesicular stomatitis virus glycoprotein (VSVG) (Abcam Biochemicals), mouse anti-green fluorescent protein (GFP) (Roche), mouse anti-hGLP-1R (ELISA, R&D Systems), mouse anti-hGLP-1R (Immunoblotting, Santa Cruz), rabbit anti-phospho ERK1/2 (pERK1/2) and rabbit anti-ERK1/2 (New England Biolabs). The Cy3-conjugated anti-mouse immunoglobulin G (IgG) secondary antibody (Jackson Laboratories) was used for immunofluorescence. The horseradish peroxidase (HRP)-conjugated anti-mouse and anti-rabbit IgG (GE Healthcare) secondary antibodies were used for immunoblotting. Enhanced chemiluminescence (ECL) select reagent was obtained from GE Healthcare. The cAMP polyclonal antibody

and cAMP-HRP were obtained from Genscript. GLP-1 (Liraglutide) was from Novo Nordisk. All other chemicals were from Sigma unless otherwise stated.

6.2.2. Plasmids

The full-length hGLP-1RΔN23 cDNA was amplified from mammalian gene collection (MGC) clone 142053 (Source Bioscience) by polymerase chain reaction (PCR) using High Fidelity Taq DNA polymerase (Roche Applied Science) and sequence specific primers containing *Eco*RI restriction site and VSVG-tag coding sequence (5' primer), and *Sal*I restriction site and no stop codon (3' primer). SP-VSVG-hGLP-1RΔN23 cDNA was amplified by overlap PCR using VSVG-hGLP-1RΔN23 cDNA as the template, the sense primer, containing *Eco*RI restriction site, the signal peptide (SP, 1-23aa) coding sequence followed by VSVG coding sequence and 3' primer. The cDNA was digested with *Eco*RI and *Sal*I, and cloned in frame into the same sites of pEGFP-N1 vector (Clontech) for expression as the N-terminus VSVG-tagged (after the SP) and the C-terminus GFP-tagged fusion protein in mammalian cells (SP-VSVG-hGLP-1RΔN23-GFP). The SP-VSVG-hGLP-1RΔN23 with no GFP-tag and its C-terminal deletion constructs were generated by PCR using sequence specific primers containing *Eco*RI restriction site (5' primer), *Sal*I restriction site and stop codon (3' primer), which prevents GFP-tagging at the C-terminus and SP-VSVG-hGLP-1RΔN23-GFP plasmid as the template. The E408A,V409A,Q410A mutation within the hGLP-1R was generated using Quickchange II XL site-directed mutagenesis kit (Stratagene) and SP-VSVG-hGLP-1RΔN23-GFP plasmid as the template. The mutants with internal deletions (Δ) within the C-terminus of hGLP-1R were generated using Q5 site-directed mutagenesis kit (New England Biolabs) and SP-VSVG-hGLP-1RΔN23-GFP plasmid as the template. See Table 6.1 for constructs used in this study.

Table 6.1. Series of hGLP-1R constructs used in this study.

	Construct Name	Abbreviation	Epitope Tags
1	SP-VSVG-hGLP-1RΔN23	SP-VSVG	VSVG
2	SP-VSVG-hGLP-1RΔN23 N450	N450	VSVG
3	SP-VSVG-hGLP-1RΔN23 N443	N443	VSVG
4	SP-VSVG-hGLP-1RΔN23 N440	N440	VSVG
5	SP-VSVG-hGLP-1RΔN23 N430	N430	VSVG
6	SP-VSVG-hGLP-1RΔN23 N410	N410	VSVG
7	SP-VSVG-hGLP-1RΔN23-GFP	SP-VSVG-GFP	VSVG GFP
8	SP-VSVG-hGLP-1RΔN23 E408A,V409A,Q410A-GFP	E408A,V409A,Q410A	VSVG GFP
9	SP-VSVG-hGLP-1RΔN23 Δ411-418-GFP	Δ411-418	VSVG GFP
10	SP-VSVG-hGLP-1RΔN23 Δ419-430-GFP	Δ419-430	VSVG GFP
11	SP-VSVG-hGLP-1RΔN23 Δ431-450-GFP	Δ431-450	VSVG GFP

The table shows the hGLP-1R constructs full name, abbreviated name and epitope tags.

6.2.3. Cell culture and transfection

Human embryonic kidney 293 (HEK293) cells were maintained at 37°C in a 5% CO_2 humidified environment in Dulbecco's modified Eagle medium (DMEM; serum free medium [SFM]) supplemented with 10% fetal calf serum, 2 mM glutamine, 100 U/ml penicillin and 0.1 mg/ml streptomycin (full serum medium [FSM]). Cells were transiently transfected for 48 h using JetPrime transfection reagent (Polyplus; 2 µl/µg DNA) according to the manufacturer's instructions.

6.2.4. Enzyme linked immunosorbent assay (ELISA)

This is carried out as described previously with unpermeabilised cells to quantify cell surface expression (Kanamarlapudi et al, 2012). Briefly, HEK293 cells expressing the hGLP-1R were serum starved for 1 h and then stimulated without or with GLP-1 at 37°C/5% CO_2. Cells were then fixed with 4% paraformaldehyde (PFA) for 5 min and non-specific binding sites blocked with 1% bovine serum albumin (BSA) made in Tris buffered saline (TBS) (1% BSA/TBS) for 45 min. Cells were incubated with the anti-hGLP-1R mouse antibody (diluted 1:15000) in 1% BSA/TBS for 1 h, washed with TBS and then incubated with the HRP-conjugated anti-mouse IgG (diluted 1:5000) in 1% BSA/TBS for 1 h. Cells were washed and developed using 1-step Ultra TMB-ELISA substrate (Bio-Rad) for 15 min and the reaction stopped by adding an equal volume of 2 M sulphuric acid. The optical density was read at 450 nm using a plate reader.

6.2.5. Immunofluorescence

Intracellular localisation of hGLP-1R expression was assessed by immunofluorescence as described previously (Kanamarlapudi et al, 2012). Briefly, cells were serum starved for 1 h, incubated with the anti-hGLP-1R mouse antibody (diluted 1:5000) in 1% BSA/SFM for 1 h at 4°C and then stimulated without or with GLP-1 at 37°C/5% CO_2. Cells were then fixed with 4% PFA for 30 min. Cells were permeabilised with 0.2% Triton X-100 made in phosphate buffered saline (PBS) for 10 min, blocked in blocking buffer (1% BSA made in wash buffer [0.1% Triton X-100 in PBS]) for 30 min and then incubated

with the Cy3-conjugated anti-mouse antibody (diluted 1:200 in blocking buffer) for 1 h. Cells were then washed 3 times with wash buffer and incubated with DAPI (4′,6-diamidino-2-phenylindole dihydrochloride, 1 mg/ml) diluted 1:2000 in PBS to stain nucleus. Coverslips were mounted on glass microscopic slides using mounting solution (0.1 M Tris-hydrochloric acid [HCl], pH 8.5, 10% Mowiol 50% glycerol) containing 2.5% DABCO (1,4 diazabicyclo (2.2.2) octane). Immunofluorescence staining was visualised using a Zeiss LSM710 confocal microscope fitted with a 63x oil immersion lens.

6.2.6. cAMP assay

Cells were serum starved for 1 h and then stimulated without or with 100 nM GLP-1 for 1 h at 37°C/5% CO_2 in the presence of 0.25 mM phosphodiesterase inhibitor Ro201724. Cells were lysed and cAMP levels in the cell lysates were estimated using the cAMP direct immunoassay kit (Abcam).

6.2.7. Cell lysates

To make cell lysates, HEK293 cells expressing the hGLP-1R were washed 3 times with ice cold PBS and lysed in ice cold modified RIPA lysis buffer (10 mM Tris HCl, pH 7.5 containing 10 mM ethylenediaminetetraacetic acid [EDTA], 1% nonyl phenoxypolyethoxylethanol [NP40], 0.1% sodium dodecyl sulphate [SDS], 0.5% sodium deoxycholate and 150 mM sodium chloride [NaCl]) with 1% mammalian protease inhibitors. Cell lysates were incubated at 4°C for 15 min and then centrifuged at 22000 xg for 10 min at 4°C. The supernatant was collected and ½ volume of 3x SDS-polyacrylamide gel electrophoresis (PAGE) sample loading buffer (75 mM Tris HCl, pH 6.8 containing 3% SDS, 30% glycerol, 0.003% bromophenol blue and 0.3 M dithiothreitol [DTT]) was added and left at room temperature for 1 h. These cell lysates were used to detect hGLP-1R expression by immunoblotting using the anti-GFP and anti-VSVG antibodies.

For assessing ERK1/2 phosphorylation, HEK293 cells expressing the hGLP-1R were lysed in ice cold modified RIPA lysis buffer (50 mM Tris HCl, pH 7.5,

containing 0.2 M NaCl; 10 mM $MgCl_2$; 0.1% SDS; 0.5% sodium deoxycholate; 1% TritonX-100; 5% Glycerol) with 1% mammalian protease inhibitors. Cell lysates were incubated at 4°C for 15 min and centrifuged at 22000 xg for 10 min at 4°C. The supernatant was collected and ¼ volume of 5x SDS-PAGE sample loading buffer (125 mM Tris HCl, pH 6.8 containing 5% SDS, 50% glycerol, 0.005% bromophenol blue and 5% β-mercaptoethanol) was added and heated at 100°C for 5 min. These cell lysates were used to detect phosphorylated ERK and total ERK by immunoblotting using the anti-pERK1/2 and anti-ERK1/2 antibodies.

6.2.8. Immunoblotting

Proteins were separated in a SDS-PAGE gel by electrophoresis and transferred onto polyvinylidene fluoride (PDVF) membrane. Membranes were blocked with TBST (TBS with 0.1% tween 20) containing 5% milk powder (blocking buffer) for 1 h at room temperature or overnight at 4°C. Membranes were immunoblotted with either the anti-hGLP-1R mouse antibody or anti-GFP mouse antibody (diluted 1:500 in blocking buffer) to assess protein expression levels or the anti-pERK1/2 rabbit antibody (diluted 1:1000 in blocking buffer) to assess ERK1/2 phosphorylation for 1 h at room temperature or overnight at 4°C. Membranes were washed and then incubated with the HRP-conjugated anti-mouse or anti-rabbit secondary antibody (diluted 1:2500 in blocking buffer) for 1 h at room temperature. Membranes were then incubated in ECL select substrate and bands visualised using the ChemiDoc™ XRS system (Bio-Rad). Blots probed with either the anti-hGLP-1R mouse antibody or anti-GFP mouse antibody were stripped with western blot stripping buffer (Thermo Scientific) and reprobed with the anti-VSVG rabbit antibody (diluted 1:1000 in blocking buffer) to assess protein expression levels. Blots probed with the anti-pERK1/2 rabbit antibody were stripped and reprobed with the anti-ERK1/2 rabbit antibody (diluted 1:1000 in blocking buffer) to assess ERK1/2 phosphorylation. The HRP-conjugated anti-rabbit secondary antibody (diluted 1:2500 in blocking buffer) was used as described above.

6.2.9. Tunicamycin treatment

This was carried out as described previously (Whitaker et al, 2012). Briefly, cells were treated with 5 μg/ml tunicamycin at the time of transfection. After 48 h of transfection, cells were lysed and subjected to immunoblotting.

6.2.10. Data analysis

Data were analysed using the GraphPad Prism program. All data are presented as means ± standard error of the mean (SEM) of three independent experiments. Statistical comparisons between the control and test value was made by a two-tailed unpaired student t-test. Statistical analysis between multiple groups were determined by the Bonferroni's post test after one-way or two-way analysis of variance (ANOVA), where $p>0.05$ was considered as statistically not significant (n.s.), and $p<0.05$, $p<0.01$ and $p<0.001$ shown as *, ** and *** respectively, was considered statistically significant. Concentration response curves were also fitted using Prism, according to a standard logistic equation. Scale bar in confocal images represents 10 μm. Confocal images shown in the figures are representative of 190-200 transfected cells from three different experiments. Similarly, immunoblotting data shown in the figures are representative of three independent experiments.

6.3. Results

6.3.1. Effect of the C-terminal mutants on hGLP-1R cell surface expression and *N*-linked glycosylation

The importance of the C-terminus for hGLP-1R cell surface expression was determined using a number of C-terminal deletion constructs, which contained the VSVG-epitope tag at the N-terminus after the SP (Figure 6.1). The first deletion removed 13aa from the end of the C-terminal domain (N450). The second deletion removed the last 20aa from the C-terminus (N443). In the N440 deletion, 23aa were removed from the end. The fourth deletion (N430) removed

the last 33aa from the C-terminal domain. The final deletion (N410) removed the entire C-terminal domain (53aa). Three more deletion constructs were made by deleting different regions within the C-terminal domain, Δ411-418, Δ419-430 and Δ431-450, which contained the GFP-tag at the C-terminus in addition to the VSVG-tag at the N-terminus after the SP. These internal deletions were used to assess the effect of distinct regions within the C-terminal domain on hGLP-1R cell surface expression. Lastly, the effect of the E408A,V409A,Q410A mutation, which has previously been shown to affect agonist binding to the hGLP-1R (Vazquez et al, 2005a), on cell surface expression of the receptor was also determined.

Lysates of HEK293 cells transfected with the C-terminal deleted constructs showed a doublet in immunoblotting (~55 kDa and ~35 kDa in size) with both the anti-hGLP-1R and anti-VSVG antibodies, demonstrating similar protein expression levels. The high molecular weight band in the doublet has previously been shown as the mature form of the receptor whereas the low molecular weight band represents the immature form of the receptor (see Chapter 3, Figure 3.1B). However, the N410 construct only showed a single band at the lower molecular weight (~35 kDa) with both antibodies demonstrating it existing as the immature form of the receptor (Figure 6.2). It is important to note that immunoblotting with the anti-VSVG antibody produced a non-specific band at ~37 kDa and the anti-hGLP-1R antibody produced a non-specific band at ~55 kDa, which were also present in lanes loaded with the lysate of untransfected HEK293 cells (Figure 6.2). Additionally, the SP-VSVG-GFP (wild type, WT), Δ419-430 and Δ431-450 constructs all showed a doublet (~65 kDa and ~85 kDa in size) when the lysates of HEK293 cells transfected with these constructs were immunoblotted with the anti-VSVG and anti-GFP antibodies (Figure 6.2). In contrast, the Δ411-419 and E408A,V409A,Q410A constructs only showed a single band at the lower molecular weight (~65 kDa) with both the anti-VSVG and anti-GFP antibodies demonstrating them as the immature form of the receptor (Figure 6.2). All constructs showed similar protein expression levels.

To determine the effect of the C-terminal deleted and site-directed mutants on hGLP-1R cell surface expression, HEK293 cells transfected with the C-terminal deletion and mutation constructs were analysed for their cell surface expression by ELISA (Figure 6.3A) and immunofluorescence (Figure 6.3B). The SP-VSVG full length (FL, 463aa) control construct and the N450, N443, N440 and N430 deletion constructs all showed similar cell surface expression when assessed by ELISA (96.6 ± 2.2%, 97.1 ± 1.7%, 93.5 ± 3.7%, 97.0 ± 1.5%, $p>0.05$, respectively, Figure 6.3A). However, the mutant with the entire C-terminal domain deletion (N410) does not express at the cell surface (0.1 ± 0.1%, $p<0.001$), demonstrating that the C-terminal domain is required for hGLP-1R trafficking to the cell surface. These results demonstrate that the last 33aa within the C-terminus are not required for cell surface expression of the hGLP-1R, but residues 411-430 are most likely involved in the receptor's cell surface expression, possibly by binding to a chaperone protein. Next, the mutants with internal deletions within the C-terminus, Δ411-418, Δ419-430 and Δ431-450, were used to assess the exact region within the C-terminus that is required for targeting the hGLP-1R to the cell surface. The Δ411-418 deletion abolished hGLP-1R cell surface expression (0.7 ± 0.7%, $p<0.001$). However, the Δ419-430 and Δ431-450 deletion mutants cell surface expressions were similar to that of the SP-VSVG-GFP WT control (81.6 ± 6.1% and 97.9 ± 3.7%, $p>0.05$, respectively). These results demonstrate that the 411-418 region of the hGLP-1R is critical for cell surface expression of the receptor. The E408A,V409A,Q410A mutation also abolished hGLP-1R cell surface expression (9.7 ± 9.7%, $p<0.001$). The ELISA results were also confirmed by immunofluorescence (Figure 6.3B) where cell surface expression was seen for the N450, N443, N440, N430, Δ419-430 and Δ431-450 deletion mutants, which was assessed by colocalisation of GFP tagged to the receptor and cell surface staining of the receptor with the anti-hGLP-1R antibody. However, N410, Δ411-418 and E408A,V409A,Q410A mutants only showed intracellular expression of GFP and no cell surface expression when assessed with the anti-hGLP-1R antibody staining. (Figure 6.3B). Immunofluorescence analysis also confirmed the immunoblotting data (Figure 6.2), demonstrating the reduction in cell

surface expression of these mutants was not due to altered protein expression levels of the receptor.

The mature hGLP-1R that is targeted to the cell surface is *N*-linked glycosylated (Chen et al, 2010; Huang et al, 2010; Whitaker et al, 2012). To establish whether the hGLP-1R C-terminal deletion or site-directed mutants were unable to target to the cell surface because they are not *N*-linked glycosylated, the deletion and site-directed mutants were assessed for their *N*-linked glycosylation. For this purpose, cells expressing the C-terminal deleted constructs or E408A,V409A,Q410A mutant were treated without or with tunicamycin, an *N*-linked glycosylation inhibitor, and their band pattern analysed by immunoblotting using either the anti-VSVG or anti-GFP antibodies. Immunoblotting of the SP-VSVG FL control construct showed the characteristic doublet at ~55 kDa and ~35 kDa (Figure 6.4). Treatment with tunicamycin, altered this pattern and instead a single band at ~30 kDa was seen instead. This shift is used as a readout assay to assess hGLP-1R *N*-linked glycosylation. The C-terminal deletion mutants (N450, N443, N440 and N430) of the hGLP-1R that express at the cell surface also showed a shift in the band pattern when treated with tunicamycin, demonstrating these deletions were also glycosylated like the SP-VSVG FL control. However, the N410 deletion mutant that did not show cell surface expression ran as a single band at ~35 kDa in immunoblotting and a shift in the bands mobility was seen when treated with tunicamycin. This suggested that the loss of this mutants cell surface expression is not due to impaired *N*-linked glycosylation. Immunoblotting of the SP-VSVG-GFP WT control showed the doublet at ~65 kDa and ~85 kDa (Figure 6.4). Treatment with tunicamycin altered this band pattern and instead, two bands at ~60 kDa and ~65 kDa were observed. Like the SP-VSVG-GFP WT control, the Δ419-430 and Δ431-450 deletion constructs showed the double band pattern that shifted to ~60 kDa and ~65 kDa when treated with tunicamycin, demonstrating that the deletions have no effect on *N*-linked glycosylation. The E408A,V409A,Q410A and Δ411-418 mutants that did not target to the cell surface only showed a single band at ~65 kDa and a shift in the band mobility was seen when treated with tunicamycin, indicating that these mutants also have no effect on *N*-linked

glycosylation of the receptor. Taken together, these results demonstrate that all hGLP-1R C-terminal mutants are *N*-linked glycosylated and any reduction in cell surface expression is not a result of impaired *N*-linked glycosylation.

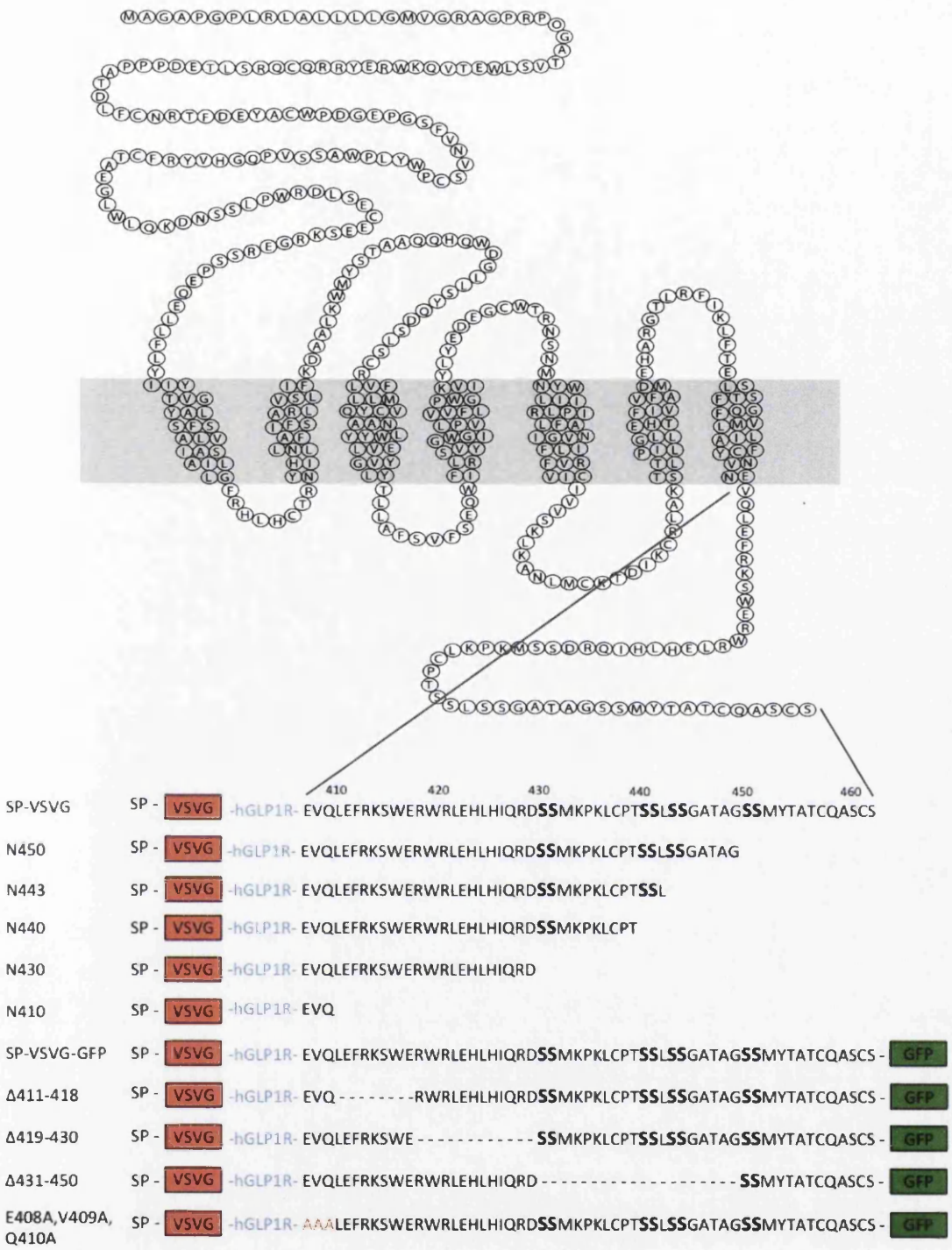

Figure 6.1. HGLP-1R constructs used to characterise the C-terminal domain for cell surface expression, internalisation and activity of the receptor. A representation of the C-terminal domain showing deleted and site-directed mutants of the hGLP-1R used in this study.

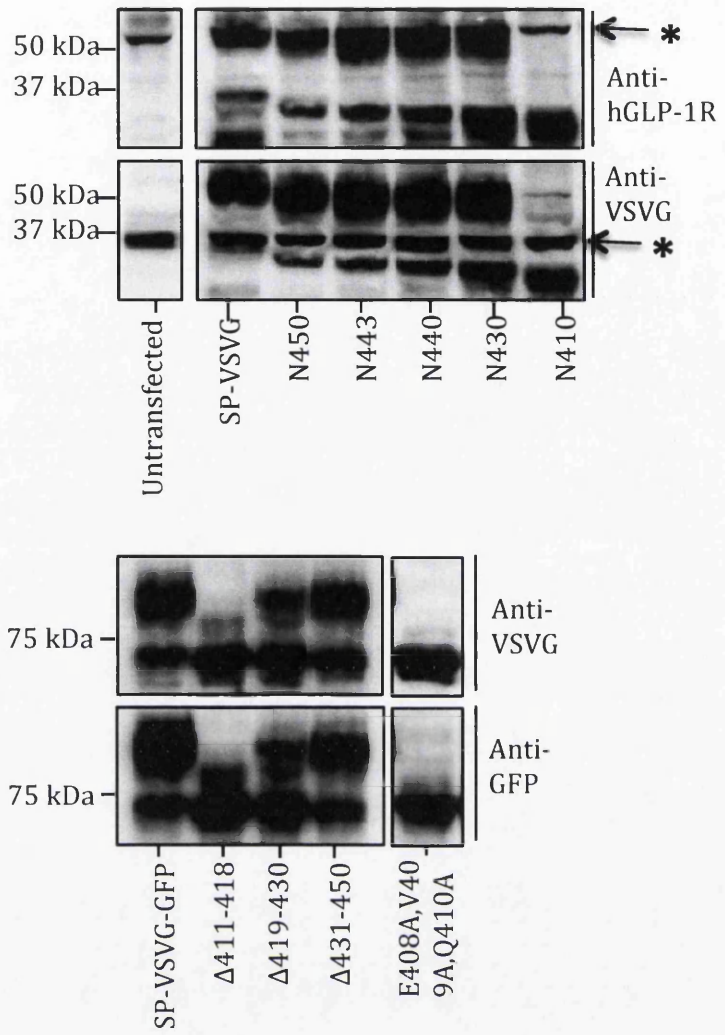

Figure 6.2. Total protein expression of hGLP-1R C-terminal domain mutants. HEK293 cells were transfected with the C-terminal deleted and site-directed mutants and total protein expression was assessed by immunoblotting using the anti-VSVG and anti-GFP antibodies. * denotes the non-specific band.

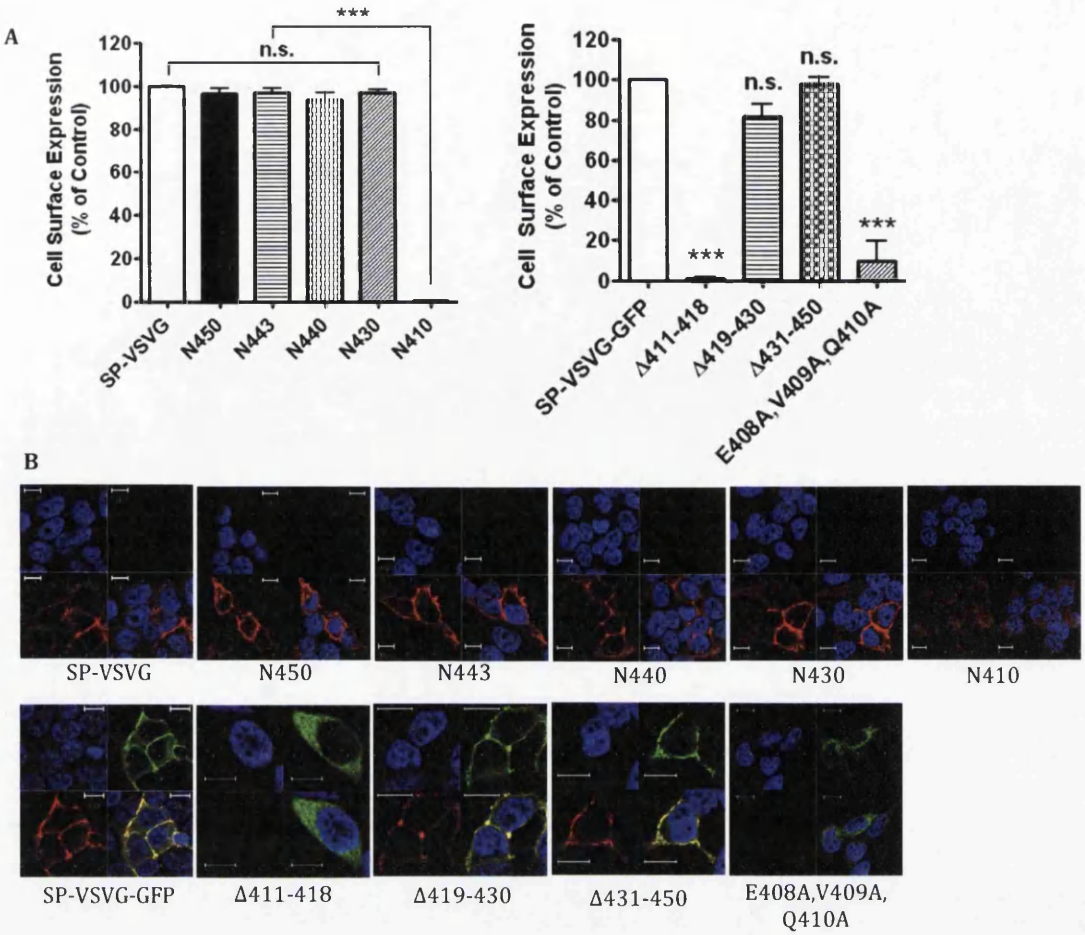

Figure 6.3. Cell surface expression of hGLP-1R C-terminal domain mutants. Cell surface expression of hGLP-1R mutants in HEK293 cells was assessed by ELISA (A) and immunofluorescence (B) using the anti-hGLP-1R antibody. In immunofluorescence, EGFP (green) and the anti-hGLP-1R antibody (red) overlay shown in yellow and nuclear staining with DAPI in blue. Data are mean ± SEM, n=3. Data were analysed by Bonferroni's post test after one-way ANOVA; values differ from control, n.s. $p>0.05$, *** $p<0.001$.

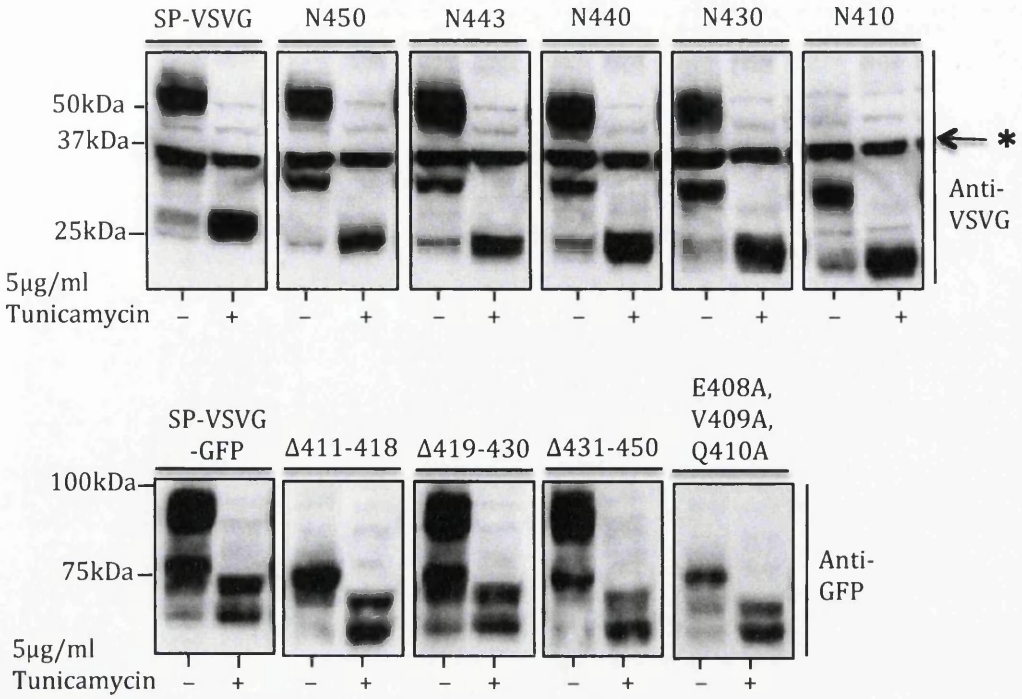

Figure 6.4. Effect of hGLP-1R C-terminal domain mutants on *N*-linked glycosylation. HEK293 cells transfected with the C-terminal deletion and site-directed mutants were treated without or with 5 μg/ml tunicamycin for 48 h. The cells were lysed and the cell lysates were immunoblotted with the anti-GFP or anti-VSVG antibodies. * denotes the non-specific band.

6.3.2. Effect of the C-terminal mutants on hGLP-1R activity

The GLP-1R is a $G\alpha_s$ coupled GPCR and therefore the receptor's activity was assessed by measuring cAMP production in the hGLP-1R mutants stimulated with 100 nM GLP-1 (Figure 6.5). Deleting up to 33aa from the end of the C-terminal domain (450, N443, N440 and N430) of the hGLP-1R had no significant effect on cAMP production (100.7 ± 1.0%, 95.0 ± 5.0%, 99.2 ± 5.2% and 98.6 ± 6.0%, $p>0.05$, respectively). However, deleting the entire C-terminal domain (N410) almost completely abolished agonist induced cAMP production (6.8 ± 2.8%, $p<0.001$). This demonstrated that residues 411-430 are most likely involved in $G\alpha_s$ coupling of the receptor. Further, the effect of internal deletions

made in this region (Δ411-418 and Δ419-430) on agonist stimulated cAMP production was assessed. The hGLP-1R deletion construct Δ411-418 does not express at the cell surface and therefore as expected no agonist stimulated cAMP production was observed in cells transfected with this mutant (9.2 ± 3.5%, $p<0.001$). However, the 419-430 deletion within the C-terminal domain of the hGLP-1R had also almost completely abolished cAMP production (8.6 ± 5.3%, $p<0.001$) even though this deletion mutant still targeted to the cell surface. The Δ431-450 mutant showed cAMP production (97.7 ± 3.0%, $p>0.05$) similar to that of the SP-VSVG-GFP WT control. Additionally, the E408A,V409A,Q410A mutant of the hGLP-1R showed very low cAMP production (10.0 ± 4.3%, $p<0.001$), which is expected as this construct did not target to the cell surface. Taken together, these results indicate residues 419-430 of the hGLP-1R are involved in coupling the receptor to $G\alpha_s$ to stimulate cAMP production.

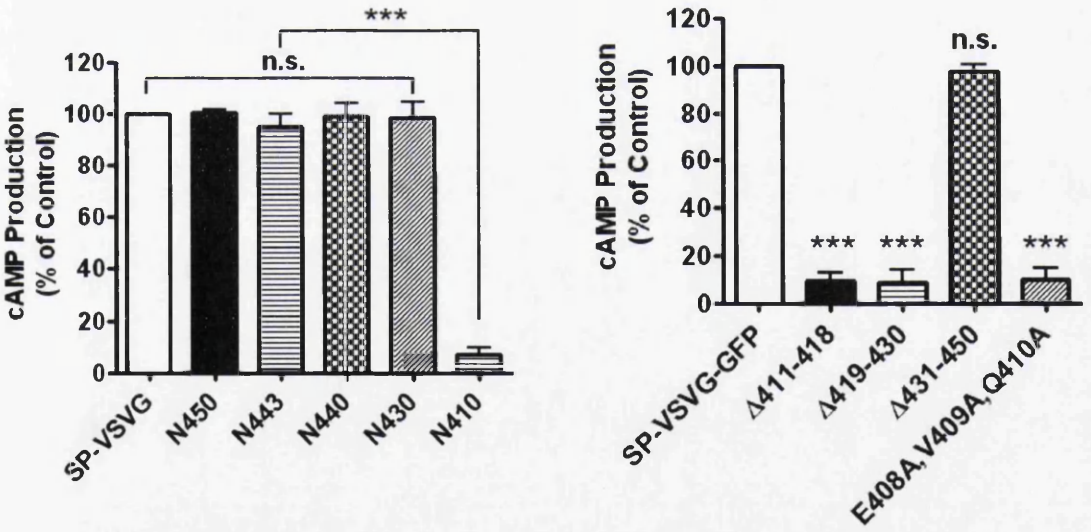

Figure 6.5. Effect of the C-terminal domain mutants on hGLP-1R activity. HEK293 cells expressing the C-terminal deletion and site-directed mutants were stimulated with 100 nM GLP-1 for 60 min and the agonist stimulated cAMP production measured to determine hGLP-1R activity. Data are mean ± SEM, n=3. Data were analysed by Bonferroni's post test after one-way ANOVA; values differ from control, n.s. $p>0.05$, *** $p<0.001$.

6.3.3. Effect of the C-terminal mutants on agonist induced hGLP-1R internalisation and ERK1/2 phosphorylation

The C-terminal deleted and site-directed mutants of the hGLP-1R that showed cell surface expression were assessed for their effect on agonist induced hGLP-1R internalisation by ELISA (Figure 6.6A) and immunofluorescence (Figure 6.6B). Deleting 13aa (N450) from the end of the C-terminal domain had no effect on agonist induced internalisation (100.0 ± 1.0%, $p>0.05$). However, the N443, N440 and N430 mutants all showed a significant reduction in agonist induced internalisation compared to the control (79.5 ± 4.7% [$p<0.01$], 57.1 ± 2.4% and 31.5 ± 5.8% [$p<0.001$], respectively). This demonstrated that residues 430-450 are most likely to be involved in hGLP-1R internalisation. This was confirmed by using the hGLP-1R internal deletion mutants, Δ419-430 and Δ431-450. The Δ431-450 deletion mutant significantly reduced agonist induced internalisation of the hGLP-1R, as only 22.9 ± 5.3% ($p<0.001$) of the receptor, expressed at the cell surface was internalised. The Δ419-430 deletion mutant showed no significant change in agonist induced hGLP-1R internalisation (111.9 ± 7.1%, $p>0.05$). These results were confirmed by immunofluorescence (Figure 6.6B).

Upon activation by agonist binding, the GLP-1R is known to cause ERK1/2 phosphorylation (Jolivalt et al, 2011; Koole et al, 2010; Quoyer et al, 2010; Syme et al, 2006). Therefore, the C-terminal deletion mutants were assessed for their effect on ERK1/2 phosphorylation (Figure 6.7A-B). The N410, Δ411-418 and E408A,V409A,Q410A mutants, which show no cell surface expression, did not induce ERK1/2 phosphorylation (4.0 ± 1.5%, 6.7 ± 2.7% and 10.3 ± 0.6%, $p<0.001$, respectively). The hGLP-1R C-terminal deletion mutants, N450, N443, N440 and N430, showed ERK1/2 phosphorylation, which correlated with their agonist induced internalisation. The hGLP-1R mediated ERK1/2 phosphorylation was reduced, as internalisation of the receptor was also reduced, with these deletions (103.6 ± 2.4%, 90.0 ± 5.5% [$p>0.05$], 28.5 ± 8.6% and 8.5 ± 5.8% [$p<0.001$], respectively). Lastly, the Δ419-430 mutant showed no significant change in ERK1/2 phosphorylation compared to the WT control (103.9 ± 7.5%, $p>0.05$). Further, as residues 431-450 of the hGLP-1R are

essential for internalisation of the receptor, it is expected that ERK1/2 phosphorylation mediated by the hGLP-1R would also be reduced with this deletion. Indeed this was observed, only 20.7 ± 3.1% ($p<0.001$) agonist stimulated ERK1/2 phosphorylation was produced in HEK293 cells transfected with the Δ431-450 hGLP-1R mutant. Taken together, these results demonstrate that residues 431-450 are essential for hGLP-1R internalisation.

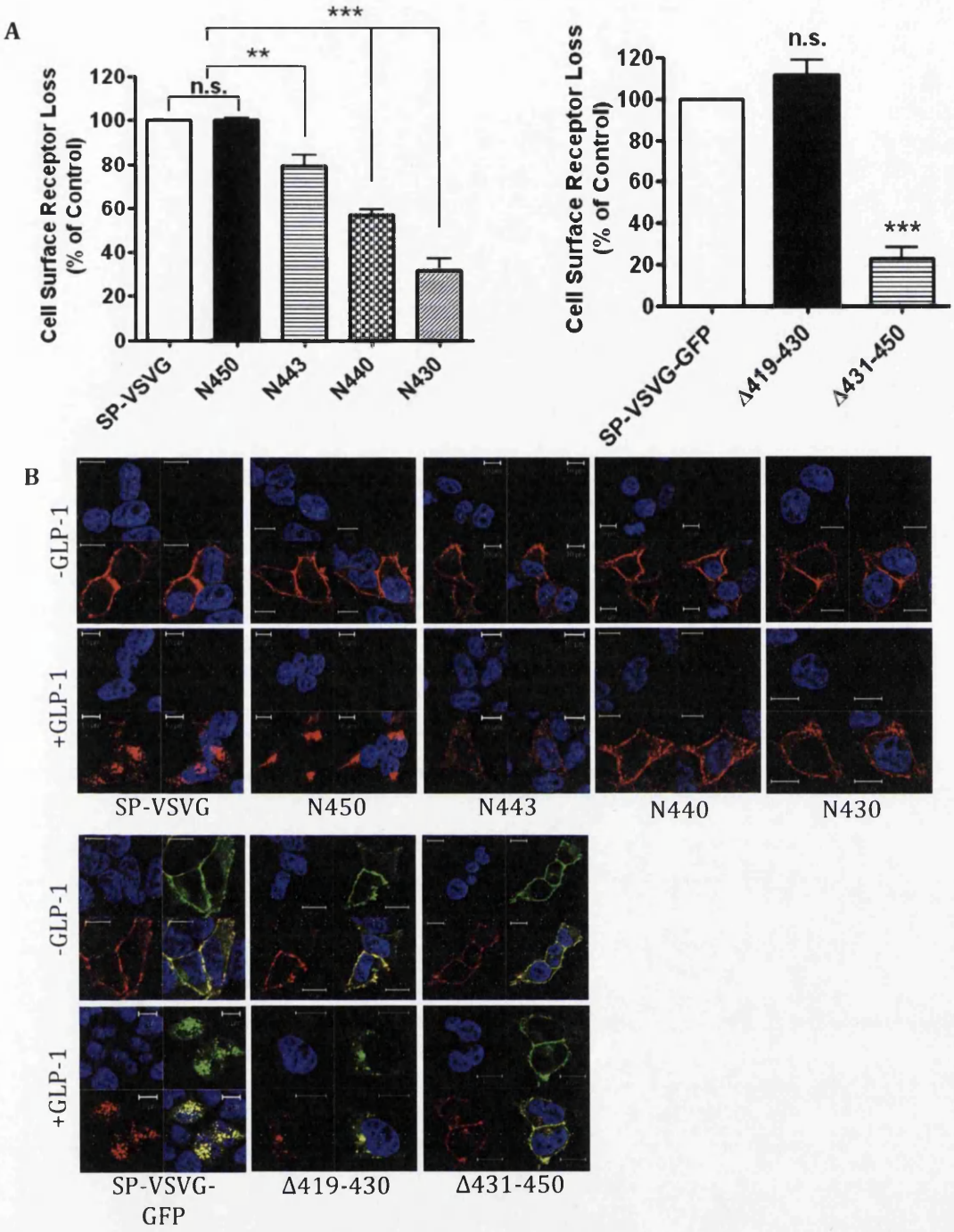

Figure 6.6. Effect of the C-terminal domain mutants on hGLP-1R internalisation. HEK293 cells expressing the C-terminal deletion and site-directed mutants were stimulated with 100 nM GLP-1 for 60 min and assessed for hGLP-1R internalisation by ELISA (A) and immunofluorescence (B) using the anti-hGLP-1R antibody. In immunofluorescence, EGFP (green) and the anti-hGLP-1R antibody (red) overlay shown in yellow and nuclear staining with DAPI in blue. Data are mean ± SEM, n=3. Data were analysed by Bonferroni's post test after one-way ANOVA; values differ from control, n.s. $p>0.05$, *** $p<0.001$, ** $p<0.01$.

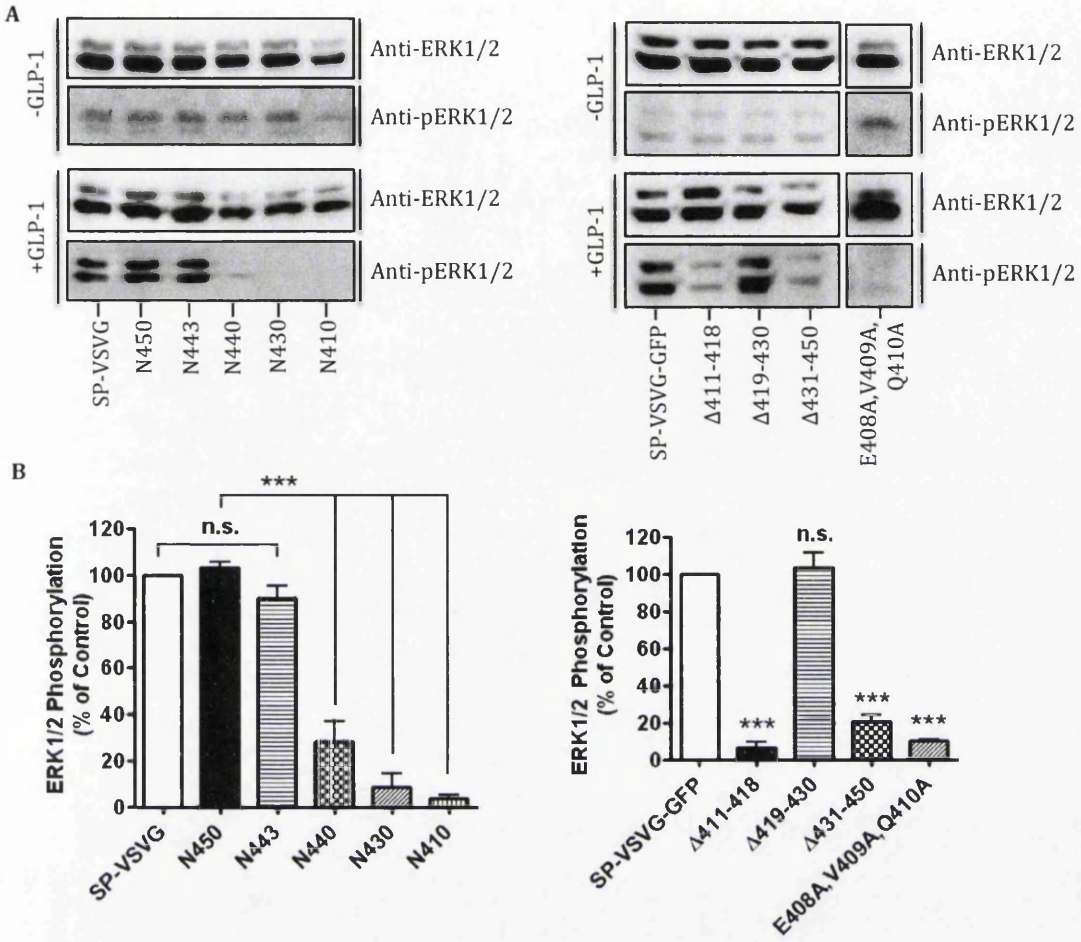

Figure 6.7. Effect of hGLP-1R C-terminal domain mutants on ERK1/2 phosphorylation. HEK293 cells transfected with the C-terminal deletion and site-directed mutant constructs were stimulated with 100 nM GLP-1 for 5 min, lysed and ERK1/2 phosphorylation was measured by immunoblotting (A) and quantified by densitometry and normalised to total ERK1/2 levels (B). The densitometry data is presented as percentage phosphorylation and are ± SEM, n=3. Data were analysed by Bonferroni's post test after one-way ANOVA; values differ from control, n.s. $p>0.05$, *** $p<0.001$.

6.4. Discussion

The C-terminal domain of GPCRs play a critical role in trafficking, agonist induced internalisation, desensitisation, down regulation and arrestin signalling (Kuramasu et al, 2006; McArdle et al, 2002). In this study, several deletion and site-directed mutants of the hGLP-1R were generated to identify the distinct regions within the C-terminal domain required for hGLP-1R trafficking, its $G\alpha_s$ coupled activity (cAMP producing activity) and internalisation. Additionally, an E408A,V409A,Q410A mutant was generated and assessed for its effect on hGLP-1R cell surface expression, as this mutation had previously been shown to inhibit internalisation and cAMP production of the hGLP-1R (Vazquez et al, 2005a).

The expression of GPCRs at the cell surface is essential for the functional response of the receptor. Therefore, the mechanisms underlying GPCR targeting to the cell surface is of high importance. GPCRs are synthesised in the endoplasmic reticulum (ER) and transported to the Golgi before being trafficked to the plasma membrane, which is tightly regulated (Dong et al, 2007). Some GPCRs require specific motifs within the C-terminal domain to target to endosomes, the Golgi and plasma membrane, but this specificity is not clear for all GPCRs (Kuramasu et al, 2006; McArdle et al, 2002; Ohno et al, 1995; Sandoval & Bakke, 1994; Trowbridge et al, 1993). Using a number of C-terminal deletion mutants of the hGLP-1R, this study determined residues 411-418 are critical for hGLP-1R cell surface expression. The membrane proximal region of the C-terminal domain is important for the trafficking of many GPCRs (Li et al, 2012). This region is required by the α_{2B}-AR (Duvernay et al, 2004; Gaborik et al, 1998), AT_2R type 1A (Duvernay et al, 2004), bradykinin B2 receptor (Feierler et al, 2011), D1R (Bermak et al, 2001) and hydroxycarboxylic acid receptor (HCAR) (Li et al, 2012) for trafficking to the plasma membrane. Using deletion mutations and alanine scanning mutagenesis, residues within the membrane proximal region of the C-terminal domain of the α_{2B}-AR, AT_2R type 1A (Duvernay et al, 2004) and HCAR (Li et al, 2012) have been shown to be essential for exportation of the receptor from the ER. This study and others

have shown that the *N*-linked glycosylation is critical for GLP-1R targeting to the cell surface (Chen et al, 2010; Huang et al, 2010; Whitaker et al, 2012). However, the hGLP-1R with the 411-418 deletion is still glycosylated but not targeted to the cell surface. It is therefore possible that this deletion prevents trafficking of the glycosylated hGLP-1R to the plasma membrane, which requires further investigation.

In this study, the mutation of Glu^{408}, Val^{409}, Gln^{410} to alanine within TM7 (closest to the C-terminal domain) of the GLP-1R has been shown to affect cell surface expression of the receptor. This triple mutation has previously been shown to abolish agonist binding and cAMP production (Vazquez et al, 2005a). This study demonstrates that the triple mutant did not bind the agonist or induce cAMP production because it is not expressed at the cell surface. Since Glu^{408}, Val^{409} and Gln^{410} in hGLP-1R are adjacent to the membrane proximal region of the C-terminus their mutation most likely causes a conformational change within the C-terminus and thereby reduces access to residues 411-418, which are required for targeting of the receptor to the plasma membrane.

The C-terminal domain is also known to interact with intracellular proteins to activate intracellular signalling pathways (Bohm et al, 1997a; Ferguson, 2001). The C-terminal domain of the β_3-AR interacts with Src, which results in the activation of ERK (Cao et al, 2000). Additionally, the $\beta\gamma$ subunit of the heterotrimeric G-protein and Ca^{2+}/calmodulin bind to the C-terminal domain of the mGluR7a and 7b and regulate P and Q type Ca^{2+} channels (O'Connor et al, 1999). In this study, residues 419-430 of the hGLP-1R have been shown to be important for agonist induced cAMP production. This is similar to a previous study, which showed deleting residues 419-435 of the hGLP-1R decreases the cAMP production (Vazquez et al, 2005a). Like the GLP-1R, a mutant of mGluR1α lacking the C-terminus has been shown to be defective in stimulating cAMP production through the $G\alpha_s$ pathway (Tateyama & Kubo, 2007).

The internalisation of GPCRs from the cell surface after agonist stimulation is required to dampen the biological response (Hanyaloglu & von Zastrow, 2008).

The phosphorylation of serine/threonine residues within the C-terminal domain is critical for the internalisation and desensitisation of many GPCRs (Benya et al, 1993; Hausdorff et al, 1991; Widmann, 1997). The hGLP-1R has previously been shown to require four serine phosphorylation sites at positions $Ser^{431,432}$, $Ser^{441,442}$, $Ser^{444,445}$ and $Ser^{451,452}$ for internalisation and desensitisation of the receptor (Widmann, 1997; Widmann et al, 1996a; Widmann et al, 1996b). Here, a series of deletion mutants were used to identify the distinct region required for hGLP-1R internalisation. This study showed, the region between 431-450, which contains serine doublets $Ser^{431,432}$, $Ser^{441,442}$ and $Ser^{444,445}$ of the hGLP-1R are required for internalisation of the receptor. This is consistent with a previous report, which demonstrated the mutation of the serine doublet, $Ser^{451,452}$, had little effect on hGLP-1R internalisation (Widmann, 1997). Additionally, a separate study reported a mutation of the serine doublet, $Ser^{431,432}$, had little effect on hGLP-1R internalisation (Vazquez et al, 2005b). Therefore, the phosphorylation of serine doublets $Ser^{441,442}$ and $Ser^{444,445}$ are likely to be essential for hGLP-1R internalisation. The bradykinin B2 receptor with alanine mutations to serine/threonine residues within the C-terminal domain has been shown to be deficient in arrestin binding and internalisation of the receptor (Zimmerman et al, 2011). Further, mutations of Ser^{355}, Ser^{356} and Ser^{366} to alanine within the C-terminal domain of the β_2-AR prevented GRK2 phosphorylation and almost abolished internalisation of the receptor (Seibold et al, 2000). Additionally, phosphorylation of Ser^{326}, Thr^{327} and Ser^{328} by GRK2 has shown to be required by the HCAR for its internalisation (Li et al, 2012). In this study, ERK1/2 phosphorylation was also used as a readout assay to confirm hGLP-1R internalisation because the GLP-1R is known to phosphorylate ERK1/2 upon agonist activation and internalisation of the receptor (Jolivalt et al, 2011; Koole et al, 2010; Quoyer et al, 2010; Syme et al, 2006). Interestingly, residues 419-430 of the hGLP-1R were important for stimulation of cAMP production with no negative effect on its internalisation, which supports the idea that the GLP-1R does not require cAMP for internalisation of the receptor.

Overall, this study identified distinct regions within the C-terminal domain of the hGLP-1R that are critical for cell surface expression (411-418), cAMP

production (419-430) and agonist induced internalisation (431-450) of the receptor (Figure 6.8). These findings provide a better understanding of the C-terminal domains role in regulating hGLP-1R cell surface expression, activity and internalisation.

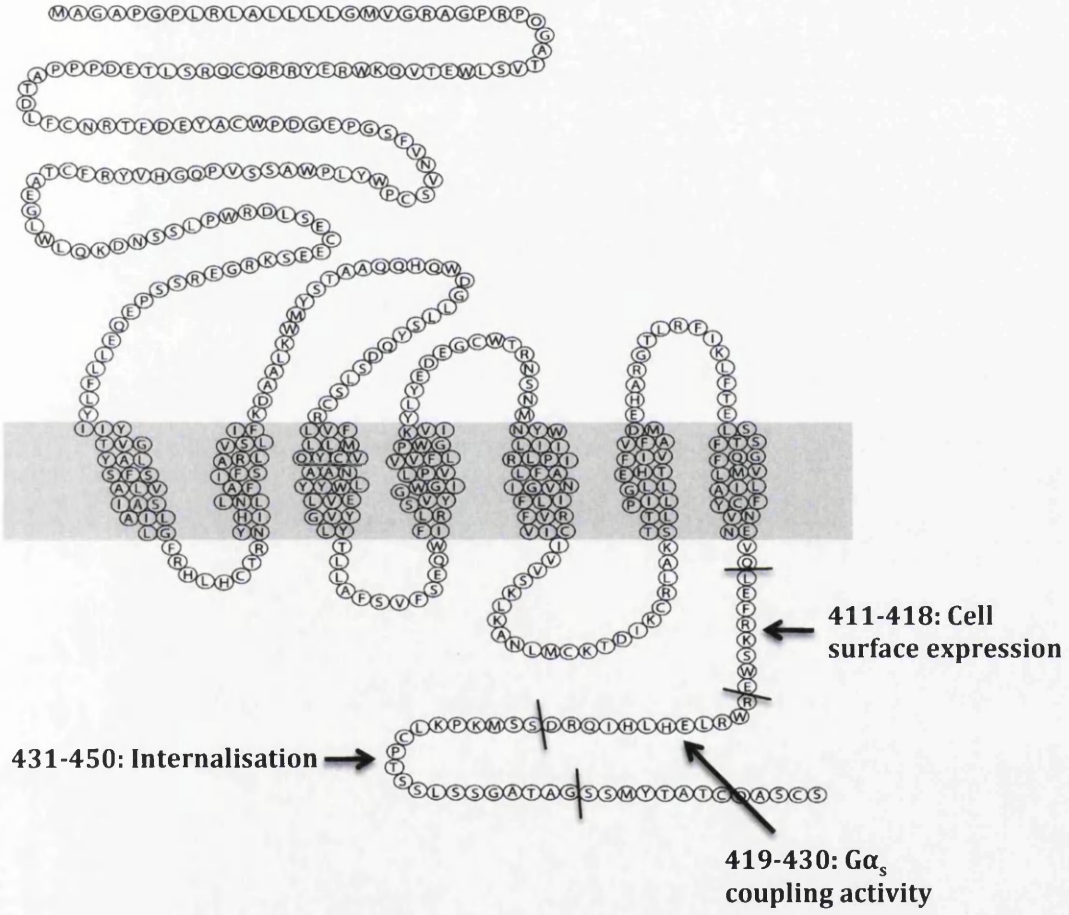

Figure 6.8. Overview of the hGLP-1R showing the distinct regions within the C-terminal domain required for hGLP-1R cell surface expression, activity and internalisation as deduced in the present study. The hGLP-1R with the distinct regions within the C-terminal domain identified for cell surface expression (411-418), activity (419-430) and internalisation (431-450) in this study.

7. Final Discussion

The ability of glucagon like peptide-1 (GLP-1) to lower postprandial hyperglycaemia by increasing insulin secretion and thereby reducing blood glucose levels makes this peptide an ideal candidate for the treatment of type 2 diabetes (Doyle & Egan, 2007; Holz et al, 1999). Additionally, as GLP-1 is able to reduce blood glucose levels in patients with type 2 diabetes, it is also of significant clinical relevance (Haluzik, 2014; Thompson & Kanamarlapudi, 2013). GLP-1 has a very short half-life, which is the main limitation for its clinical use and as a result therapeutic strategies that activate the GLP-1 receptor (GLP-1R) and improve GLP-1 stability have been extensively studied and developed. GLP-1R stimulation by GLP-1 has many beneficial effects, which is most likely due to the activation of a number of downstream signalling pathways upon agonist binding to the receptor. The GLP-1R is a member of the family B G-protein coupled receptors (GPCRs). Studying GPCR agonist binding is important because it is an early signal transduction event (Bhaskaran & Ascoli, 2005; Kanamarlapudi et al, 2012). GPCR internalisation as a result of agonist binding and subsequent desensitisation is vital for correct cell signalling, dampening of the biological response and re-sensitising the desensitised receptor (Hanyaloglu & von Zastrow, 2008). Although a generalised transduction pathway exists for GPCRs (Claing, 2004), it has become clear that the GLP-1R activated signalling pathways and the receptor agonist interactions are more complex than was previously thought. A clear understanding of GLP-1R activation and internalisation by agonist binding will lead to much better drug targeting of the receptor and its downstream signalling transduction pathway. A better understanding of the internalisation pathway is also essential for introducing new strategies, such as small molecule agonists, which target the human GLP-1R (hGLP-1R) in the treatment of type 2 diabetes. To further enhance this understanding, this study has:

1. Assessed the importance of the N-terminal domain for cell surface expression of the hGLP-1R.
2. Examined the effect of two small molecule agonists on hGLP-1R internalisation and activation.
3. Determined the downstream signalling pathway for internalisation of the hGLP-1R after agonist activation.
4. Identified distinct regions within the C-terminal domain required for hGLP-1R cell surface expression, agonist induced cyclic adenosine monophosphate (cAMP) activity and internalisation.

Family B GPCRs contain a signal peptide (SP) sequence within the N-terminal domain, which is often critical for synthesis and processing of the receptor (Kochl et al, 2002). In addition, several GPCRs have been shown to require the hydrophobic region after the SP (HRASP) and post-translational modifications such as glycosylation for their cell surface expression (Alken et al, 2009; Hatsuzawa et al, 1997; Huang et al, 2010; Whitaker et al, 2012; Widmann et al, 1995). This study showed that the SP sequence of the hGLP-1R is cleaved during processing of the receptor. Additionally, cleavage of the receptor was essential for *N*-linked glycosylation and trafficking of the hGLP-1R to the cell surface, which is consistent with previous findings (Huang et al, 2010). In this study, the hGLP-1R with the SP deleted (ΔSP) functioned in exactly the same way as the receptor with the SP present and expressed at the cell surface. This contradicts a previous study, which showed the hGLP-1R with the SP deleted is synthesised but does not express at the cell surface (Huang et al, 2010). The reason for the variation in results is unclear. In this study, the hGLP-1RΔSP was expressed with the VSVG-epitope tag at the N-terminus whereas Huang et al (2010) expressed the same deletion construct with a HA-epitope tag. However, it has been observed that the hGLP-1R wild type and hGLP-1RΔSP without any epitope tag at the N-terminus still targets to the cell surface (see Chapter 4), indicating that the difference in the N-terminal tag between studies may not be the reason for variation in the results. Interestingly, this study revealed that prevention of SP cleavage inhibited hGLP-1R cell surface expression by preventing access to the Asn^{63}, Asn^{82} and Asn^{115} glycosylation sites. After the SP

is cleaved, the receptor undergoes *N*-linked glycosylation. The glycosylated receptor translocates to the Golgi and then onto the plasma membrane. Although the role of the SP in family B GPCR trafficking is well established (Huang et al, 2010), the significance of the HRASP in trafficking of the receptor is not well studied. This study demonstrated that the HRASP (Ser^{31}-Glu^{40}) of the hGLP-1R is necessary for its efficient trafficking to the cell surface. Similar to the endothelin B receptor, it is likely that this region may be important for translocation of the hGLP-1R across the endoplasmic reticulum (ER) membrane but requires further experimentation to confirm this. Extending on these findings, the importance of Trp^{39}, Tyr^{69} and Tyr^{88}, three conserved residues across family B GPCRs within the N-terminal domain, which has previously been shown to be important for agonist binding, was studied (Runge et al, 2008; Underwood et al, 2010; Van Eyll et al, 1996). The Trp^{39}, Tyr^{69} and Tyr^{88} mutations caused a significant loss in hGLP-1R cell surface expression. The exact reason for these mutations affecting hGLP-1R cell surface expression is still unclear, but they did not interfere with either cleavage of the SP or *N*-linked glycosylation of the receptor and therefore it is unlikely that these mutations had any effect on the stability of the receptor. However, it is possible that these mutations may affect trafficking of the *N*-linked glycosylated hGLP-1R to the Golgi or interfere with further processing within the ER and Golgi. This is an area requiring further investigation.

Some GPCRs, such as the gonadotropin-releasing hormone receptor, are not efficiently exported from the ER to the plasma membrane and a large proportion of the synthesised receptor is retained in the ER and then subjected to degradation (Armstrong et al, 2011; Conn & Ulloa-Aguirre, 2010). Therefore, pharmacoperone (chemical chaperone) drugs can be used to increase cell surface expression of the receptor and thereby its activity (Conn & Ulloa-Aguirre, 2010; Zhao et al, 2008). This study clearly shows the hGLP-1R is primarily localised at the cell surface but with some intracellular expression. However, this study made use of the hGLP-1R overexpressed in the HEK293 model cell line. Nevertheless, there is evidence demonstrating the down regulation of GLP-1R expression in β-cells contributes to the impaired incretin

effect in type 2 diabetes (Shu et al, 2009; Xu et al, 2007). This is consistent with observations of reduced GLP-1 responses on β-cells in type 2 diabetes (Fritsche et al, 2000; Kjems et al, 2003). Therefore, there is a need to investigate the expression and localisation of the GLP-1R in the β-cells of type 2 diabetes. However, it is unknown if pharmacoperone drugs may enhance GLP-1 based therapies for type 2 diabetes by increasing GLP-1R expression at the plasma membrane. To study the localisation of hGLP-1R and the effect of pharmacoperone drugs on the location, *in vitro,* human β-cell samples of type 2 diabetic patients would be required.

Liraglutide and Exenatide are two commercially available injectable drugs currently used in the treatment of type 2 diabetes but are very expensive and have difficulties associated with long-term administration including pancreatitis and papillary thyroid cancer (Drucker et al, 2010). This has driven the need for relatively less expensive and orally active small molecule agonists of the GLP-1R. Allosteric small molecule drugs not only have oral bioactivity but also have the potential benefit of binding to a site on the receptor distinct from that used by the orthosteric agonist (Bridges & Lindsley, 2008). Compound 2 and compound B are two small molecule agonists that have been shown to stimulate insulin secretion (Knudsen et al, 2007; Sloop et al, 2010). At the start of this study, very little was published about the effects of compound 2 and compound B on the hGLP-1R. This study confirmed that compound 2 and compound B are ago-allosteric modulators because antagonists Ex(9-39) and JANT-4 inhibited GLP-1 induced GLP-1R internalisation and signalling but had no effect on compound 2 or compound B signalling. Additionally, the V36A mutation of hGLP-1R, which has previously been shown to affect GLP-1 binding to the orthosteric binding site of the receptor (Underwood et al, 2010), abolished GLP-1 stimulated cAMP production but had no effect on cAMP production induced by compound 2 and B. However, the K334A mutation of hGLP-1R, which has previously been shown to prevent efficient coupling to adenylyl cyclase (AC) (Mathi, 1997), reduced cAMP production by GLP-1, compound 2 and compound B, demonstrating GLP-1R couples to the $G\alpha_s$ pathway in the same way when stimulated with either the orthosteric or allosteric agonists. Unlike GLP-1, no

hGLP-1R internalisation was demonstrated when treated with compound 2 and compound B. It is possible that the binding of these small molecule agonists to the GLP-1R causes a conformational change, which prevents internalisation of the receptor but not coupling to the $G\alpha_s$ pathway, but this needs to be confirmed using molecular modelling. Both small molecule agonists induce cAMP production with a maximal response similar to GLP-1. However, unlike GLP-1, compound 2 and compound B are unable to induce intracellular calcium (Ca^{2+}) accumulation and extracellular signal-regulated kinases (ERK) phosphorylation. Since intracellular Ca^{2+} accumulation and ERK phosphorylation are required for GLP-1 induced hGLP-1R internalisation (see Chapter 5), the reason why compounds 2 and B do not induce hGLP-1R internalisation is most likely linked to their inability to stimulate intracellular Ca^{2+} accumulation and ERK phosphorylation. The exact location where compound 2 and compound B interact and bind to the hGLP-1R has not been explored in this study but that information may help with the development of new small molecule agonists. In previous studies, compound 2 and compound B were unable to stimulate insulin secretion as effectively as GLP-1 (Irwin et al, 2010; Knudsen et al, 2007; Sloop et al, 2010). This suggests that binding of the orthosteric and allosteric agonists to the hGLP-1R cause subtle differences in the receptor's conformation, thereby activating downstream signalling pathways. This study suggests a potential advantage in the selectivity of specific signalling pathways activated by allosteric agonist binding. Interestingly, this study found, preincubation with either compounds 2 and B prior to GLP-1 stimulation, inhibited GLP-1 induced intracellular Ca^{2+} accumulation, ERK phosphorylation and internalisation of the receptor, but not cAMP production. It would be interesting to determine, for example using biotin conjugated GLP-1, whether compounds 2 and B cause a conformational change that reduces access of GLP-1 to the orthosteric binding site in a non-competitive manner or whether they prevent GLP-1 bound hGLP-1R coupling to the $G\alpha_q$ pathway, thereby inhibiting intracellular Ca^{2+} accumulation and ERK phosphorylation required for internalisation of the receptor. Therefore, allosteric agonists may cause GPCR conformations, which are less favourable in the internalisation of the receptor than orthosteric agonists. Although these small molecule agonists may result in a longer half-life,

the significance of this effect is unknown and the adverse effects associated with increasing the half-life of drugs that target the hGLP-1R needs to be explored further. Overall, compounds based on this structure may provide insight into the mechanisms of agonist directed GLP-1R regulation and may represent a step in the development of effective insulinotropic agents with limited adverse effects.

This study determined the downstream signalling pathway required for GLP-1 induced hGLP-1R internalisation. After agonist stimulation, most GPCRs internalise in a clathrin dependent fashion via β-arrestins (Luttrell & Lefkowitz, 2002). However, some GPCRs use alternative pathways such as the caveolin dependent pathway for endocytosis (Chini & Parenti, 2004). Using chemical inhibitors, dominant negative mutants and coimmunoprecipitation, this study clearly showed the hGLP-1R to interact with caveolin-1 for its internalisation. Although, the agonist occupied GLP-1R signals through the $G\alpha_s$ and $G\alpha_q$ pathways, this study showed that the agonist induced hGLP-1R internalises through the $G\alpha_q$ pathway and not through the $G\alpha_s$ pathway. Binding of the orthosteric agonist to the hGLP-1R results in the $G\alpha_q$ activation, which then leads to hydrolysis of phosphatidylinositol-4,5-bisphophate (PIP_2) by phospholipase C (PLC) to inositol-1,4,5-triphosphate (IP_3). IP_3 activates the IP_3 receptor to increase cytosolic Ca^{2+} levels. The increase in cytosolic Ca^{2+} levels activates protein kinase C (PKC), which in turn phosphorylates ERK (Werry et al, 2003). The involvement of the $G\alpha_q$ pathway in agonist induced internalisation has been deduced using chemical inhibitors. This study illustrates the importance of analysing the downstream signalling pathway in agonist induced GLP-1R internalisation. This is because orthosteric agonist stimulation of the GLP-1R results in cAMP production, intracellular Ca^{2+} accumulation and ERK phosphorylation, but it is only intracellular Ca^{2+} accumulation and ERK phosphorylation that are linked directly with the internalisation of the receptor. This suggests that new targets for the treatment of type 2 diabetes should be assessed for their effects on intracellular Ca^{2+} accumulation and ERK phosphorylation and not just cAMP activity. The molecular pathways identified in this study are likely to be shared by other

GPCRs and be of relevance to their trafficking and signalling. In future studies, it would be interesting to assess whether or not inhibition of GLP-1R internalisation alters agonist induced insulin secretion from β-cells.

The T149M mutation within the GLP-1R has been shown to reduce glucose effectiveness, insulin secretion and sensitivity within a Japanese patient with type 2 diabetes (Tokuyama et al, 2004). Interestingly, in this study the T149M mutation was found to inhibit agonist induced hGLP-1R internalisation, intracellular Ca^{2+} accumulation and ERK phosphorylation with no effect on cAMP production. This suggests impaired hGLP-1R internalisation due to reduced intracellular Ca^{2+} accumulation and ERK phosphorylation may possibly be the cause for the patients reduced glucose effectiveness, insulin secretion and sensitivity. Therefore, the T149M mutation inhibits insulin secretion without affecting cAMP production demonstrating the importance of hGLP-1R intracellular Ca^{2+} accumulation, ERK phosphorylation and internalisation for GLP-1 mediated insulin secretion. Recently, the internalised GLP-1R in agonist stimulated pancreatic β-cells has been shown to colocalise with AC within endosomes and stimulate insulin secretion (Kuna et al, 2013). This also demonstrates the importance of hGLP-1R internalisation for insulin secretion because inhibiting internalisation would prevent the endosomal cAMP production required for insulin secretion. As the T149M mutant is defective in the internalisation of the receptor, it may prevent insulin secretion by affecting endosomal cAMP activity. It would be interesting to look at other point mutations within type 2 diabetic patients and determine whether they may also inhibit hGLP-1R internalisation.

Some GPCRs have been shown to require E(X)3LL, FN(X)2LL(X)3L, F(X)3F(X)3F (Dong et al, 2007), tyrosine YXXΦ (Ohno et al, 1995; Sandoval & Bakke, 1994; Trowbridge et al, 1993), PPXXFR (Ango et al, 2000; Ango et al, 2001; Ango et al, 2002), PXXP (Cao et al, 2000), NPXXY (Robertson et al, 2003) and LL (Ferguson, 2001; Letourneur & Klausner, 1992; Verhey & Birnbaum, 1994) motifs within the C-terminal domain for cell surface expression, interactions with intracellular proteins and internalisation of the receptor. However, these conserved motifs

are not present within the GLP-1R. Therefore, in this study, the regions important for hGLP-1R cell surface expression, its activity (using cAMP production as readout) and internalisation were determined using a number of C-terminal deletion and site-directed mutants. The membrane proximal region of the C-terminal domain is important for the trafficking of many GPCRs to the plasma membrane (Li et al, 2012). Similar to other GPCRs, this study determined that residues 411-418 are critical for hGLP-1R cell surface expression. This region within the C-terminus of the hGLP-1R is most likely important in exporting the receptor from the ER to the cell surface as the mutant with these residues deleted is still glycosylated within the ER but not targeted to the cell surface. Additionally, the C-terminal domain of GPCRs is also known to interact with intracellular proteins to activate intracellular signalling pathways (Bohm et al, 1997a; Ferguson, 2001). This study showed residues 419-430 within the C-terminus of the hGLP-1R are important for cAMP production. It would be interesting to determine if the C-terminal domain of the hGLP-1R contains other regions important for Ca^{2+} accumulation and ERK phosphorylation because the importance of the $G\alpha_q$ pathway has already been demonstrated in this study (see Chapter 5). Further, the phosphorylation of serine/threonine residues within the C-terminal domain of GPCRs is critical for internalisation and desensitisation of the receptor (Benya et al, 1993; Hausdorff et al, 1991; Widmann, 1997). Therefore, this study used a series of deletion mutants to identify the distinct region required for agonist induced internalisation of the hGLP-1R. The region between 431-450, which contains serine doublets, $Ser^{431,432}$, $Ser^{441,442}$ and $Ser^{444,445}$, of the hGLP-1R is required for internalisation of the receptor. However, taking previous literature into account, the phosphorylation of serine doublets, $Ser^{441,442}$ and $Ser^{444,445}$, are more likely to be essential for hGLP-1R internalisation (Vazquez et al, 2005b; Widmann, 1997). As residues 419-430 of the hGLP-1R are important for cAMP production with no negative effect on the internalisation of the receptor, this supports the idea that the GLP-1R does not require the production of cAMP for its internalisation. These findings demonstrate a better structural and mechanistic understanding of GPCR regulation within the C-terminal domain.

The C-terminal domain sequences of some GPCRs (mentioned in Chapter 6) including the GLP-1R, adenosine A2b receptor, angiotensin II receptor type 1, bradykinin B2 receptor, dopamine D1 receptor, hydroxycarboxylic acid receptor and metabotropic glutamate receptor type 7 were aligned using Cluster Omega (Goujon et al, 2010; McWilliam et al, 2013; Sievers et al, 2011), but no conserved sequences were identified. Therefore, the C-terminal domain sequence of the family B GPCRs were aligned and showed some conservation in the region closest to transmembrane (TM) 7 (Figure 7.1). The ^{408}EVQ^{410} motif in the hGLP-1R is highly conserved across family B GPCRs, the alignment results showed E^{408} and V^{409} to be fully conserved (*) and the Q^{410} to be highly conserved (:). Additionally, residues F^{413}, K^{415} and W^{417} within the C-terminal domain of the hGLP-1R showed conservation with other family B GPCRs. The F^{413} is less conserved (.), whereas K^{415} is highly conserved and W^{417} is fully conserved (*). These conserved residues were critical for hGLP-1R cell surface expression, therefore it would be interesting in future to determine if this region may be a common protein binding motif and also required by the other family B GPCRs for cell surface expression of the receptor.

In conclusion, this study has provided a foundation to further expand the knowledge of cellular trafficking and functional characterisation of the hGLP-1R (summarised in Figure 7.2). All experiments performed in this study were assessed in a model cell line expressing recombinant hGLP-1R. Therefore, further work should investigate whether these results could be replicated in a human pancreatic β-cell line or patient samples. Overall, a lot remains to be determined in GLP-1R characterisation, pharmacology and drug development in the treatment of type 2 diabetes.

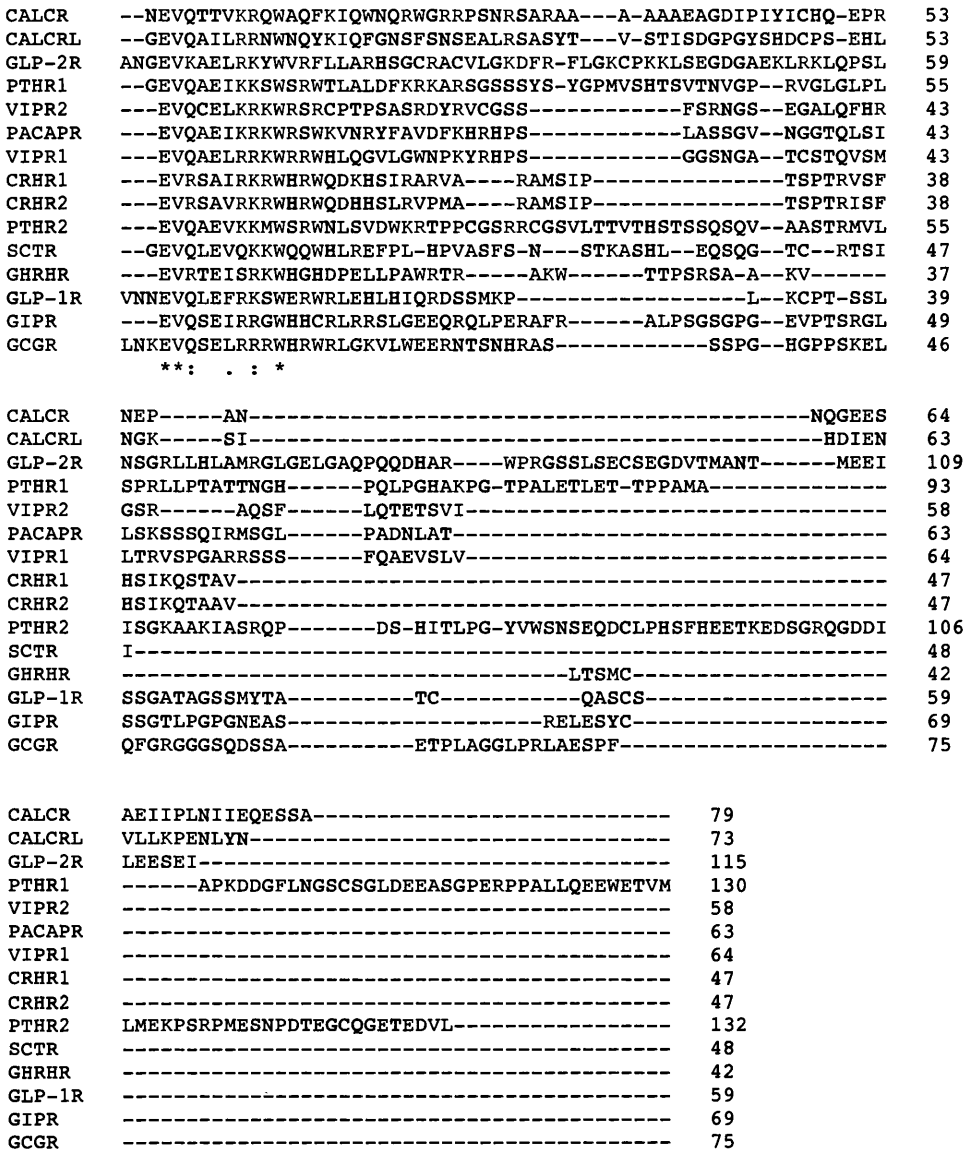

Figure 7.1. Sequence alignment of the C-terminal domain of family B GPCRs. Multiple sequence alignment of family B GPCRs with numbering using Cluster Omega (1.2.1). An asterisk (*) indicates fully conserved residues; a colon (:) indicates high conservation; and a full stop (.) indicates low conservation. Amino acids are coloured according to their properties, where red residues are small and hydrophobic excluding Y (AVFPMILW); blue residues are acidic (DE); magenta residues are basic excluding H (RK) and green are hydroxyl, sulfhydryl and amine residues including G (STYHCNGQ). Abbreviations of receptors are GLP-2R, glucagon-like peptide 2 receptor; PACAPR, pituitary adenylate cyclase-activating polypeptide receptor; CALCR, calcitonin receptor; CALCRL, calcitonin receptor-like protein; CRHR, corticotropin-releasing hormone receptor; GIPR, glucose-dependent insulinotropic polypeptide receptor; GCGR, glucagon receptor; GHRHR, growth hormone releasing hormone receptor; PTHR, parathyroid hormone receptor; SCTR, secretin receptor; VIPR1, vasoactive intestinal peptide receptor.

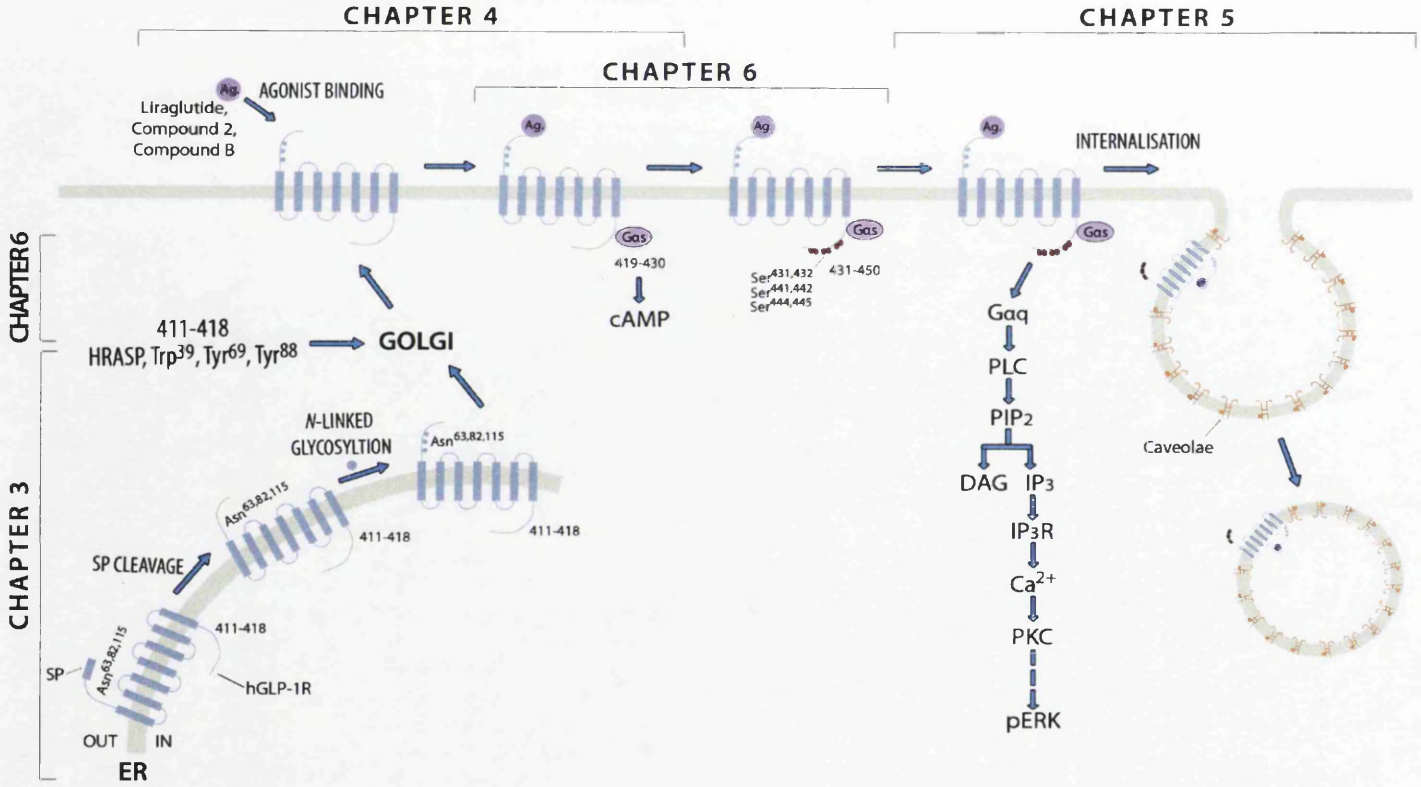

Figure 7.2. Proposed schematic model of hGLP-1R trafficking, agonist induced internalisation and downstream signalling pathway as deduced from the present study. Simplified scheme of the key findings from this study. This study reveals the importance of the N-terminal domain for cell surface expression of the receptor (Chapter 3), the effect of small molecule agonists on hGLP-1R internalisation and activation (Chapter 4), the downstream signalling pathway for agonist induced internalisation of the hGLP-1R (Chapter 5) and distinct regions within the C-terminal domain required for hGLP-1R cell surface expression, agonist induced cAMP production and internalisation (Chapter 6).

Bibliography

Abu-Hamdah R, Rabiee A, Meneilly GS, Shannon RP, Andersen DK, Elahi D (2009) Clinical review: The extrapancreatic effects of glucagon-like peptide-1 and related peptides. *J Clin Endocrinol Metab* **94:** 1843-1852

Achour L, Labbe-Jullie C, Scott MG, Marullo S (2008) An escort for GPCRs: implications for regulation of receptor density at the cell surface. *Trends Pharmacol Sci* **29:** 528-535

Akamizu T, Kosugi S, Kohn LD (1990) Thyrotropin receptor processing and interaction with thyrotropin. *Biochem Biophys Res Commun* **169:** 947-952

Al-Sabah S (2003) The positive charge at Lys-288 of the glucagon-like peptide-1 (GLP-1) receptor is important for binding the N-terminus of peptide agonists. *FEBS Letters* **553:** 342-346

Alba-Loureiro TC, Munhoz CD, Martins JO, Cerchiaro GA, Scavone C, Curi R, Sannomiya P (2007) Neutrophil function and metabolism in individuals with diabetes mellitus. *Braz J Med Biol Res* **40:** 1037-1044

Alberti KG, Zimmet PZ (1998) Definition, diagnosis and classification of diabetes mellitus and its complications. Part 1: diagnosis and classification of diabetes mellitus provisional report of a WHO consultation. *Diabet Med* **15:** 539-553

Alken M, Rutz C, Kochl R, Donalies U, Oueslati M, Furkert J, Wietfeld D, Hermosilla R, Scholz A, Beyermann M, Rosenthal W, Schulein R (2005) The signal peptide of the rat corticotropin-releasing factor receptor 1 promotes receptor expression but is not essential for establishing a functional receptor. *Biochem J* **390:** 455-464

Alken M, Schmidt A, Rutz C, Furkert J, Kleinau G, Rosenthal W, Schulein R (2009) The sequence after the signal peptide of the G protein-coupled endothelin B receptor is required for efficient translocon gating at the endoplasmic reticulum membrane. *Mol Pharmacol* **75:** 801-811

Alvarez DF, Helm K, Degregori J, Roederer M, Majka S (2010) Publishing flow cytometry data. *Am J Physiol Lung Cell Mol Physiol* **298:** L127-130

An HJ, Froehlich JW, Lebrilla CB (2009) Determination of glycosylation sites and site-specific heterogeneity in glycoproteins. *Curr Opin Chem Biol* **13:** 421-426

Anderson JW, Kendall CW, Jenkins DJ (2003) Importance of weight management in type 2 diabetes: review with meta-analysis of clinical studies. *J Am Coll Nutr* **22:** 331-339

Angeli FS, Shannon RP (2014) Incretin-based therapies: can we achieve glycemic control and cardioprotection? *J Endocrinol* **221:** T17-30

Ango F, Pin JP, Tu JC, Xiao B, Worley PF, Bockaert J, Fagni L (2000) Dendritic and axonal targeting of type 5 metabotropic glutamate receptor is regulated by homer1 proteins and neuronal excitation. *J Neurosci* **20:** 8710-8716

Ango F, Prezeau L, Muller T, Tu JC, Xiao B, Worley PF, Pin JP, Bockaert J, Fagni L (2001) Agonist-independent activation of metabotropic glutamate receptors by the intracellular protein Homer. *Nature* **411:** 962-965

Ango F, Robbe D, Tu JC, Xiao B, Worley PF, Pin JP, Bockaert J, Fagni L (2002) Homer-dependent cell surface expression of metabotropic glutamate receptor type 5 in neurons. *Mol Cell Neurosci* **20:** 323-329

Armstrong SP, Caunt CJ, Finch AR, McArdle CA (2011) Using automated imaging to interrogate gonadotrophin-releasing hormone receptor trafficking and function. *Mol Cell Endocrinol* **331:** 194-204

Baggio LL, Drucker DJ (2004) Clinical endocrinology and metabolism. Glucagon-like peptide-1 and glucagon-like peptide-2. *Best Pract Res Clin Endocrinol Metab* **18:** 531-554

Baggio LL, Drucker DJ (2007) Biology of incretins: GLP-1 and GIP. *Gastroenterology* **132:** 2131-2157

Balzarini J (2007) Targeting the glycans of glycoproteins: a novel paradigm for antiviral therapy. *Nat Rev Microbiol* **5:** 583-597

Ban T, Kosugi S, Kohn LD (1992) Specific antibody to the thyrotropin receptor identifies multiple receptor forms in membranes of cells transfected with wild-type receptor complementary deoxyribonucleic acid: characterization of their relevance to receptor synthesis, processing, structure, and function. *Endocrinology* **131:** 815-829

Bansal P, Wang QH (2008) Insulin as a physiological modulator of glucagon secretion. *Am J Physiol-Endoc M* **295:** E751-E761

Barak LS, Tiberi M, Freedman NJ, Kwatra MM, Lefkowitz RJ, Caron MG (1994) A highly conserved tyrosine residue in G protein-coupled receptors is required for agonist-mediated beta 2-adrenergic receptor sequestration. *J Biol Chem* **269:** 2790-2795

Barnard ND, Katcher HI, Jenkins DJ, Cohen J, Turner-McGrievy G (2009) Vegetarian and vegan diets in type 2 diabetes management. *Nutr Rev* **67:** 255-263

Bavec A (2003) Different role of intracellular loops of glucagon-like peptide-1 receptor in G-protein coupling. *Regul Pept* **111:** 137-144

Bazarsuren A, Grauschopf U, Wozny M, Reusch D, Hoffmann E, Schaefer W, Panzner S, Rudolph R (2002) In vitro folding, functional characterization, and disulfide pattern of the extracellular domain of human GLP-1 receptor. *Biophysical Chemistry* **96:** 305-318

Bazzano LA, Serdula M, Liu S (2005) Prevention of type 2 diabetes by diet and lifestyle modification. *J Am Coll Nutr* **24:** 310-319

Beinborn M (2006) Class B GPCRs: a hidden agonist within? *Mol Pharmacol* **70:** 1-4

Beinborn M, Worrall CI, McBride EW, Kopin AS (2005) A human glucagon-like peptide-1 receptor polymorphism results in reduced agonist responsiveness. *Regul Pept* **130:** 1-6

Benovic JL, Pike LJ, Cerione RA, Staniszewski C, Yoshimasa T, Codina J, Caron MG, Lefkowitz RJ (1985) Phosphorylation of the mammalian beta-adrenergic receptor by cyclic AMP-dependent protein kinase. Regulation of the rate of receptor phosphorylation and dephosphorylation by agonist occupancy and effects on coupling of the receptor to the stimulatory guanine nucleotide regulatory protein. *J Biol Chem* **260:** 7094-7101

Benya RV, Fathi Z, Battey JF, Jensen RT (1993) Serines and threonines in the gastrin-releasing peptide receptor carboxyl terminus mediate internalization. *J Biol Chem* **268:** 20285-20290

Benya RV, Kusui T, Katsuno T, Tsuda T, Mantey SA, Battey JF, Jensen RT (2000) Glycosylation of the gastrin-releasing peptide receptor and its effect on expression, G protein coupling, and receptor modulatory processes. *Mol Pharmacol* **58:** 1490-1501

Berg JM, Tymoczko JL, Stryer L (2002) *Biochemistry*, 5 edn. New York: W. H. Freeman.

Bermak JC, Li M, Bullock C, Zhou QY (2001) Regulation of transport of the dopamine D1 receptor by a new membrane-associated ER protein. *Nat Cell Biol* **3:** 492-498

Bhaskaran RS, Ascoli M (2005) The post-endocytotic fate of the gonadotropin receptors is an important determinant of the desensitization of gonadotropin responses. *Journal of molecular endocrinology* **34:** 447-457

Bhattacharyya S, Puri S, Miledi R, Panicker MM (2002) Internalization and recycling of 5-HT2A receptors activated by serotonin and protein kinase C-mediated mechanisms. *Proc Natl Acad Sci U S A* **99:** 14470-14475

Bisello A, Adams AE, Mierke DF, Pellegrini M, Rosenblatt M, Suva LJ, Chorev M (1998) Parathyroid hormone-receptor interactions identified directly by photocross-linking and molecular modeling studies. *J Biol Chem* **273:** 22498-22505

Blonde L (2009) Current antihyperglycemic treatment strategies for patients with type 2 diabetes mellitus. *Cleve Clin J Med* **76 Suppl 5:** S4-11

Bockaert J, Marin P, Dumuis A, Fagni L (2003) The 'magic tail' of G protein-coupled receptors: an anchorage for functional protein networks. *FEBS Letters* **546:** 65-72

Bohm SK, Grady EF, Bunnett NW (1997a) Regulatory mechanisms that modulate signalling by G-protein-coupled receptors. *Biochem J* **322 (Pt 1):** 1-18

Bohm SK, Khitin LM, Smeekens SP, Grady EF, Payan DG, Bunnett NW (1997b) Identification of potential tyrosine-containing endocytic motifs in the carboxyl-tail and seventh transmembrane domain of the neurokinin 1 receptor. *J Biol Chem* **272:** 2363-2372

Bond A (2006) Exenatide (Byetta) as a novel treatment option for T2DM. *Proceedings (Baylor University, Medical Center)* **19:** 281-284

Bos JL (2003) Epac: a new cAMP target and new avenues in cAMP research. *Nat Rev Mol Cell Biol* **4:** 733-738

Bouvier M, Hausdorff WP, De Blasi A, O'Dowd BF, Kobilka BK, Caron MG, Lefkowitz RJ (1988) Removal of phosphorylation sites from the beta 2-adrenergic receptor delays onset of agonist-promoted desensitization. *Nature* **333:** 370-373

Bouvier M, Loisel TP, Hebert T (1995a) Dynamic regulation of G-protein coupled receptor palmitoylation: potential role in receptor function. *Biochemical Society Transactions* **23:** 577-581

Bouvier M, Moffett S, Loisel TP, Mouillac B, Hebert T, Chidiac P (1995b) Palmitoylation of G-protein-coupled receptors: a dynamic modification with functional consequences. *Biochemical Society Transactions* **23:** 116-120

Bratanova-Tochkova TK, Cheng H, Daniel S, Gunawardana S, Liu YJ, Mulvaney-Musa J, Schermerhorn T, Straub SG, Yajima H, Sharp GW (2002) Triggering and augmentation mechanisms, granule pools, and biphasic insulin secretion. *Diabetes* **51 Suppl 1:** S83-90

Brauner-Osborne H, Wellendorph P, Jensen AA (2007) Structure, pharmacology and therapeutic prospects of family C G-protein coupled receptors. *Curr Drug Targets* **8:** 169-184

Bridges TM, Lindsley CW (2008) G-protein-coupled receptors: from classical modes of modulation to allosteric mechanisms. *ACS Chem Biol* **3:** 530-541

Brodsky JL (1998) Translocation of proteins across the endoplasmic reticulum membrane. *Int Rev Cytol* **178:** 277-328

Bromberg L, Alakhov V (2003) Effects of polyether-modified poly(acrylic acid) microgels on doxorubicin transport in human intestinal epithelial Caco-2 cell layers. *J Control Release* **88:** 11-22

Brooks SA (2009) Strategies for analysis of the glycosylation of proteins: current status and future perspectives. *Mol Biotechnol* **43:** 76-88

Brubaker PL, Drucker DJ (2002) Structure-function of the glucagon receptor family of G protein-coupled receptors: the glucagon, GIP, GLP-1, and GLP-2 receptors. *Receptors & Channels* **8:** 179-188

Budd DC, Rae A, Tobin AB (1999) Activation of the mitogen-activated protein kinase pathway by a Gq/11-coupled muscarinic receptor is independent of receptor internalization. *J Biol Chem* **274:** 12355-12360

Budd DC, Willars GB, McDonald JE, Tobin AB (2001) Phosphorylation of the G(q/11)-coupled M-3-muscarinic receptor is involved in receptor activation of the ERK-1/2 mitogen-activated protein kinase pathway. *Journal of Biological Chemistry* **276:** 4581-4587

Bullock BP, Heller RS, Habener JF (1996) Tissue distribution of messenger ribonucleic acid encoding the rat glucagon-like peptide-1 receptor. *Endocrinology* **137:** 2968-2978

Burcelin R, Serino M, Cabou C (2009) A role for the gut-to-brain GLP-1-dependent axis in the control of metabolism. *Curr Opin Pharmacol* **9:** 744-752

Buse JB, Rosenstock J, Sesti G, Schmidt WE, Montanya E, Brett JH, Zychma M, Blonde L (2009) Liraglutide once a day versus exenatide twice a day for type 2 diabetes: a 26-week randomised, parallel-group, multinational, open-label trial (LEAD-6). *Lancet* **374:** 39-47

Cabrera-Vera TM, Vanhauwe J, Thomas TO, Medkova M, Preininger A, Mazzoni MR, Hamm HE (2003) Insights into G protein structure, function, and regulation. *Endocr Rev* **24:** 765-781

Campbell JE, Drucker DJ (2013) Pharmacology, physiology, and mechanisms of incretin hormone action. *Cell Metab* **17:** 819-837

Cao W, Luttrell LM, Medvedev AV, Pierce KL, Daniel KW, Dixon TM, Lefkowitz RJ, Collins S (2000) Direct binding of activated c-Src to the beta 3-adrenergic receptor is required for MAP kinase activation. *J Biol Chem* **275:** 38131-38134

Casado V, Cortes A, Mallol J, Perez-Capote K, Ferre S, Lluis C, Franco R, Canela EI (2009) GPCR homomers and heteromers: a better choice as targets for drug development than GPCR monomers? *Pharmacol Ther* **124:** 248-257

Cassano PA, Rosner B, Vokonas PS, Weiss ST (1992) Obesity and body fat distribution in relation to the incidence of non-insulin-dependent diabetes mellitus. A prospective cohort study of men in the normative aging study. *Am J Epidemiol* **136:** 1474-1486

Chang MP, Mallet WG, Mostov KE, Brodsky FM (1993) Adaptor self-aggregation, adaptor-receptor recognition and binding of alpha-adaptin subunits to the plasma membrane contribute to recruitment of adaptor (AP2) components of clathrin-coated pits. *Embo J* **12:** 2169-2180

Charbonnel B, Karasik A, Liu J, Wu M, Meininger G (2006) Efficacy and safety of the dipeptidyl peptidase-4 inhibitor sitagliptin added to ongoing metformin therapy in patients with type 2 diabetes inadequately controlled with metformin alone. *Diabetes Care* **29:** 2638-2643

Chen Q, Miller LJ, Dong M (2010) Role of N-linked glycosylation in biosynthesis, trafficking, and function of the human glucagon-like peptide 1 receptor. *Am J Physiol Endocrinol Metab* **299:** E62-68

Cheong YH, Kim MK, Son MH, Kaang BK (2012) Two small molecule agonists of glucagon-like peptide-1 receptor modulate the receptor activation response differently. *Biochem Biophys Res Commun* **417:** 558-563

Chiasson J-L (2009) Early Insulin Use in Type 2 Diabetes: What are the cons? *Diabetes Care* **32:** S270-S274

Chini B, Parenti M (2004) G-protein coupled receptors in lipid rafts and caveolae: how, when and why do they go there? *Journal of molecular endocrinology* **32:** 325-338

Chun M, Liyanage UK, Lisanti MP, Lodish HF (1994) Signal transduction of a G protein-coupled receptor in caveolae: colocalization of endothelin and its receptor with caveolin. *Proc Natl Acad Sci U S A* **91:** 11728-11732

Clague MJ (1998) Molecular aspects of the endocytic pathway. *Biochem J* **336 (Pt 2):** 271-282

Claing A (2004) Regulation of G protein-coupled receptor endocytosis by ARF6 GTP-binding proteins. *Biochem Cell Biol* **82:** 610-617

Claing A, Laporte SA, Caron MG, Lefkowitz RJ (2002) Endocytosis of G protein-coupled receptors- roles of G protein-coupled receptor kinases and ß-arrestin proteins. *Progress in neurobiology* **66:** 61-79

Clark SD, Tran HT, Zeng J, Reinscheid RK (2010) Importance of extracellular loop one of the neuropeptide S receptor for biogenesis and function. *Peptides* **31:** 130-138

Cobb MH, Goldsmith EJ (1995) How MAP kinases are regulated. *J Biol Chem* **270:** 14843-14846

Conn PM, Ulloa-Aguirre A (2010) Trafficking of G-protein-coupled receptors to the plasma membrane: insights for pharmacoperone drugs. *Trends Endocrinol Metab* **21:** 190-197

Cooke DW, Plotnick L (2008) Type 1 diabetes mellitus in pediatrics. *Pediatr Rev* **29:** 374-384; quiz 385

Coopman K, Huang Y, Johnston N, Bradley SJ, Wilkinson GF, Willars GB (2010) Comparative effects of the endogenous agonist glucagon-like peptide-1 (GLP-1)-(7-36) amide and the small-molecule ago-allosteric agent "compound 2" at the GLP-1 receptor. *J Pharmacol Exp Ther* **334:** 795-808

Couet J, Li S, Okamoto T, Ikezu T, Lisanti MP (1997) Identification of peptide and protein ligands for the caveolin-scaffolding domain. Implications for the interaction of caveolin with caveolae-associated proteins. *J Biol Chem* **272:** 6525-6533

Couvineau A, Rouyer-Fessard C, Darmoul D, Maoret JJ, Carrero I, Ogier-Denis E, Laburthe M (1994) Human intestinal VIP receptor: cloning and functional expression of two cDNA encoding proteins with different N-terminal domains. *Biochem Biophys Res Commun* **200:** 769-776

Couvineau A, Rouyer-Fessard C, Laburthe M (2004) Presence of a N-terminal signal peptide in class II G protein-coupled receptors: crucial role for expression of the human VPAC1 receptor. *Regul Pept* **123:** 181-185

Crespo P, Xu N, Simonds WF, Gutkind JS (1994) Ras-dependent activation of MAP kinase pathway mediated by G-protein beta gamma subunits. *Nature* **369:** 418-420

Creutzfeldt W, Ebert R (1985) New developments in the incretin concept. *Diabetologia* **28:** 565-573

Cunha DA, Ladriere L, Ortis F, Igoillo-Esteve M, Gurzov EN, Lupi R, Marchetti P, Eizirik DL, Cnop M (2009) Glucagon-like peptide-1 agonists protect pancreatic beta-cells from lipotoxic endoplasmic reticulum stress through upregulation of BiP and JunB. *Diabetes* **58:** 2851-2862

Daaka Y, Luttrell LM, Ahn S, Della Rocca GJ, Ferguson SS, Caron MG, Lefkowitz RJ (1998) Essential role for G protein-coupled receptor endocytosis in the activation of mitogen-activated protein kinase. *J Biol Chem* **273:** 685-688

Daaka Y, Pitcher JA, Richardson M, Stoffel RH, Robishaw JD, Lefkowitz RJ (1997) Receptor and Gβγ isoform-specific interactions with G protein-coupled receptor kinases. *Proc Natl Acad Sci U S A* **94:** 2180-2185

Daunt DA, Hurt C, Hein L, Kallio J, Feng F, Kobilka BK (1997) Subtype-specific intracellular trafficking of alpha2-adrenergic receptors. *Mol Pharmacol* **51:** 711-720

Davies SP, Reddy H, Caivano M, Cohen P (2000) Specificity and mechanism of action of some commonly used protein kinase inhibitors. *Biochem J* **351:** 95-105

Davis D, Liu X, Segaloff DL (1995) Identification of the sites of N-linked glycosylation on the follicle-stimulating hormone (FSH) receptor and assessment of their role in FSH receptor function. *Mol Endocrinol* **9:** 159-170

De Amici M, Dallanoce C, Holzgrabe U, Trankle C, Mohr K (2010) Allosteric ligands for G protein-coupled receptors: a novel strategy with attractive therapeutic opportunities. *Med Res Rev* **30:** 463-549

De Leon DD, Crutchlow MF, Ham JY, Stoffers DA (2006) Role of glucagon-like peptide-1 in the pathogenesis and treatment of diabetes mellitus. *Int J Biochem Cell Biol* **38:** 845-859

De Marinis YZ, Salehi A, Ward CE, Zhang Q, Abdulkader F, Bengtsson M, Braha O, Braun M, Ramracheya R, Amisten S, Habib AM, Moritoh Y, Zhang E, Reimann F, Rosengren AH, Shibasaki T, Gribble F, Renstrom E, Seino S, Eliasson L, Rorsman P (2010) GLP-1 inhibits and adrenaline stimulates glucagon release by differential modulation of N- and L-type Ca2+ channel-dependent exocytosis. *Cell Metab* **11:** 543-553

De Vos A, Heimberg H, Quartier E, Huypens P, Bouwens l, Pipeleers D, Schuit F (1995) Human and rat beta cells differ in glucose transporter but not in glucokinase gene expression. *Journal of Clinical Investigation* **96:** 2489-2495

Deacon CF, Holst JJ (2006) Dipeptidyl peptidase IV inhibitors: a promising new therapeutic approach for the management of type 2 diabetes. *Int J Biochem Cell Biol* **38:** 831-844

Deacon CF, Knudsen LB, Madsen K, Wiberg FC, Jacobsen O, Holst JJ (1998) Dipeptidyl peptidase IV resistant analogues of glucagon-like peptide-1 which have extended metabolic stability and improved biological activity. *Diabetologia* **41:** 271-278

Della Rocca GJ, van Biesen T, Daaka Y, Luttrell DK, Luttrell LM, Lefkowitz RJ (1997) Ras-dependent mitogen-activated protein kinase activation by G protein-coupled receptors. Convergence of Gi- and Gq-mediated pathways on calcium/calmodulin, Pyk2, and Src kinase. *J Biol Chem* **272:** 19125-19132

Deretic D, Williams AH, Ransom N, Morel V, Hargrave PA, Arendt A (2005) Rhodopsin C terminus, the site of mutations causing retinal disease, regulates trafficking by binding to ADP-ribosylation factor 4 (ARF4). *Proc Natl Acad Sci U S A* **102:** 3301-3306

Deslauriers B, Ponce C, Lombard C, Larguier R, Bonnafous JC, Marie J (1999) N-glycosylation requirements for the AT1a angiotensin II receptor delivery to the plasma membrane. *Biochem J* **339 (Pt 2):** 397-405

Dhanvantari S, Izzo A, Jansen E, Brubaker PL (2001) Coregulation of Glucagon-Like Peptide-1 Synthesis with Proglucagon and Prohormone Convertase 1 Gene Expression in Enteroendocrine GLUTag Cells. *Endocrinology* **142:** 37-42

Diabetes UK. (2014) What is diabetes? Available at http://www.diabetes.org.uk/Guide-to-diabetes/What-is-diabetes/ (Accessed on 02 September, 2014).

Dikic I, Tokiwa G, Lev S, Courtneidge SA, Schlessinger J (1996) A role for Pyk2 and Src in linking G-protein-coupled receptors with MAP kinase activation. *Nature* **383:** 547-550

Doherty GJ, McMahon HT (2009) Mechanisms of endocytosis. *Annual review of biochemistry* **78:** 857-902

Dong C, Filipeanu CM, Duvernay MT, Wu G (2007) Regulation of G protein-coupled receptor export trafficking. *Biochim Biophys Acta* **1768:** 853-870

Dong M, Lam PC, Pinon DI, Orry A, Sexton PM, Abagyan R, Miller LJ (2010) Secretin occupies a single protomer of the homodimeric secretin receptor complex: insights from photoaffinity labeling studies using dual sites of covalent attachment. *J Biol Chem* **285:** 9919-9931

Dong M, Li Z, Pinon DI, Lybrand TP, Miller LJ (2004a) Spatial approximation between the amino terminus of a peptide agonist and the top of the sixth transmembrane segment of the secretin receptor. *J Biol Chem* **279:** 2894-2903

Dong M, Pinon DI, Miller LJ (2012) Site of action of a pentapeptide agonist at the glucagon-like peptide-1 receptor. Insight into a small molecule agonist-binding pocket. *Bioorg Med Chem Lett* **22:** 638-641

Dong MQ, Gao F, Pinon DI, Miller LJ (2008) Insights into the structural basis of endogenous agonist activation of family B G protein-coupled receptors. *Mol Endocrinol* **22:** 1489-1499

Dong MQ, Pinon DI, Asmann YW, Miller LJ (2006) Possible endogenous agonist mechanism for the activation of secretin family G protein-coupled receptors. *Mol Pharmacol* **70:** 206-213

Dong MQ, Pinon DI, Cox RF, Miller LJ (2004b) Molecular approximation between a residue in the amino-terminal region of calcitonin and the third extracellular loop of the class B G protein-coupled calcitonin receptor. *Journal of Biological Chemistry* **279:** 31177-31182

Dong MQ, Pinon DI, Miller LJ (2005) Insights into the structure and molecular basis of ligand docking to the G protein-coupled secretin receptor using charge-modified amino-terminal agonist probes. *Mol Endocrinol* **19:** 1821-1836

Doyle ME, Egan JM (2007) Mechanisms of action of glucagon-like peptide 1 in the pancreas. *Pharmacol Ther* **113:** 546-593

Drucker DJ, Philippe J, Mojsov S, Chick WL, Habener JF (1987) Glucagon-like peptide I stimulates insulin gene expression and increases cyclic AMP levels in a rat islet cell line. *Proc Natl Acad Sci U S A* **84:** 3434-3438

Drucker DJ, Sherman SI, Gorelick FS, Bergenstal RM, Sherwin RS, Buse JB (2010) Incretin-based therapies for the treatment of type 2 diabetes: evaluation of the risks and benefits. *Diabetes Care* **33:** 428-433

Duvernay MT, Filipeanu CM, Wu G (2005) The regulatory mechanisms of export trafficking of G protein-coupled receptors. *Cell Signal* **17:** 1457-1465

Duvernay MT, Zhou F, Wu G (2004) A conserved motif for the transport of G protein-coupled receptors from the endoplasmic reticulum to the cell surface. *J Biol Chem* **279:** 30741-30750

Edavalath M, Stephens JW (2010) Liraglutide in the treatment of type 2 diabetes mellitus: clinical utility and patient perspectives. *Patient Prefer Adherence* **4:** 61-68

Eisinger DA, Schulz R (2004) Extracellular signal-regulated kinase/mitogen-activated protein kinases block internalization of delta-opioid receptors. *J Pharmacol Exp Ther* **309:** 776-785

Eknoyan G (2008) Adolphe Quetelet (1796-1874)--the average man and indices of obesity. *Nephrol Dial Transplant* **23:** 47-51

Elbein AD (1987) Inhibitors of the biosynthesis and processing of N-linked oligosaccharide chains. *Annual review of biochemistry* **56:** 497-534

Eng J, Kleinman WA, Singh L, Singh G, Raufman JP (1992) Isolation and characterization of exendin-4, an exendin-3 analogue, from Heloderma suspectum venom. Further evidence for an exendin receptor on dispersed acini from guinea pig pancreas. *J Biol Chem* **267:** 7402-7405

Feierler J, Wirth M, Welte B, Schussler S, Jochum M, Faussner A (2011) Helix 8 plays a crucial role in bradykinin B(2) receptor trafficking and signaling. *J Biol Chem* **286:** 43282-43293

Ferguson GG (2001) Evolving Concepts in G Protein-Coupled Receptor Endocytosis- The Role in Receptor Desensitization and Signaling. *Pharmacol Rev* **53:** 1-24

Ferguson SS, Menard L, Barak LS, Koch WJ, Colapietro AM, Caron MG (1995) Role of phosphorylation in agonist-promoted beta 2-adrenergic receptor

sequestration. Rescue of a sequestration-defective mutant receptor by beta ARK1. *J Biol Chem* **270:** 24782-24789

Fritsche A, Stefan N, Hardt E, Haring H, Stumvoll M (2000) Characterisation of beta-cell dysfunction of impaired glucose tolerance: evidence for impairment of incretin-induced insulin secretion. *Diabetologia* **43:** 852-858

Fukushima Y, Oka Y, Saitoh T, Katagiri H, Asano T, Matsuhashi N, Takata K, van Breda E, Yazaki Y, Sugano K (1995) Structural and functional analysis of the canine histamine H2 receptor by site-directed mutagenesis: N-glycosylation is not vital for its action. *Biochem J* **310 (Pt 2):** 553-558

Gaborik Z, Mihalik B, Jayadev S, Jagadeesh G, Catt KJ, Hunyady L (1998) Requirement of membrane-proximal amino acids in the carboxyl-terminal tail for expression of the rat AT1a angiotensin receptor. *FEBS Letters* **428:** 147-151

Gallwitz B (2006) Exenatide in type 2 diabetes: treatment effects in clinical studies and animal study data. *Int J Clin Pract* **60:** 1654-1661

Gallwitz B (2010) The evolving place of incretin-based therapies in type 2 diabetes. *Pediatr Nephrol* **25:** 1207-1217

Ge X, Loh HH, Law PY (2009) mu-Opioid receptor cell surface expression is regulated by its direct interaction with Ribophorin I. *Mol Pharmacol* **75:** 1307-1316

Gedulin BR, Smith P, Prickett KS, Tryon M, Barnhill S, Reynolds J, Nielsen LL, Parkes DG, Young AA (2005) Dose-response for glycaemic and metabolic changes 28 days after single injection of long-acting release exenatide in diabetic fatty Zucker rats. *Diabetologia* **48:** 1380-1385

George SR, O'Dowd BF, Lee SR (2002) G-protein-coupled receptor oligomerization and its potential for drug discovery. *Nature Reviews Drug Discovery* **1:** 808-820

Gether U (2000) Uncovering molecular mechanisms involved in activation of G protein-coupled receptors. *Endocr Rev* **21:** 90-113

Gilbert MP, Pratley RE (2009) Efficacy and safety of incretin-based therapies in patients with type 2 diabetes mellitus. *Am J Med* **122:** S11-24

Glickman JN, Conibear E, Pearse BM (1989) Specificity of binding of clathrin adaptors to signals on the mannose-6-phosphate/insulin-like growth factor II receptor. *Embo J* **8:** 1041-1047

Goke R, Fehmann HC, Linn T, Schmidt H, Krause M, Eng J, Goke B (1993) Exendin-4 is a high potency agonist and truncated exendin-(9-39)-amide an antagonist at the glucagon-like peptide 1-(7-36)-amide receptor of insulin-secreting beta-cells. *J Biol Chem* **268:** 19650-19655

Goke R, Just R, Lankatbuttgereit B, Goke B (1994) Glycosylation of the Glp-1 Receptor Is a Prerequisite for Regular Receptor Function. *Peptides* **15:** 675-681

Gonzalez C, Beruto V, Keller G, Santoro S, Di Girolamo G (2006) Investigational treatments for Type 2 diabetes mellitus: exenatide and liraglutide. *Expert Opin Investig Drugs* **15:** 887-895

Goodman OB, Krupnick JG, Santini F, Gurevich VV, Penn RB, Gagnon AW, Keen JH, Benovic JL (1996) beta-arrestin acts as a clathrin adaptor in endocytosis of the beta(2)-adrenergic receptor. *Nature* **383:** 447-450

Goujon M, McWilliam H, Li W, Valentin F, Squizzato S, Paern J, Lopez R (2010) A new bioinformatics analysis tools framework at EMBL-EBI. *Nucleic Acids Res* **38:** W695-699

Grace CRR, Perrin MH, DiGruccio MR, Miller CL, Rivier JE, Vale WW, Riek R (2004) NMR structure and peptide hormone binding site of the first extracellular domain of a type B1 G protein-coupled receptor. *Proc Natl Acad Sci U S A* **101:** 12836-12841

Gray JA, Roth BL (2002) Cell biology. A last GASP for GPCRs? *Science* **297:** 529-531

Graziano MP, Hey PJ, Borkowski D, Chicchi GG, Strader CD (1993) Cloning and Functional Expression of a Human Glucagon-Like Peptide-1-Receptor. *Biochem Biophys Res Commun* **196:** 141-146

Green BD, Irwin N, Duffy NA, Gault VA, O'Harte FPM, Flatt PR (2006) Inhibition of dipeptidyl peptidase-IV activity by metformin enhances the antidiabetic effects of glucagon-like peptide-1. *Eur J Pharmacol* **547:** 192-199

Grieve DJ, Cassidy RS, Green BD (2009) Emerging cardiovascular actions of the incretin hormone glucagon-like peptide-1: potential therapeutic benefits beyond glycaemic control? *Br J Pharmacol* **157:** 1340-1351

Groer CE, Tidgewell K, Moyer RA, Harding WW, Rothman RB, Prisinzano TE, Bohn LM (2007) An opioid agonist that does not induce μ-opioid receptor--arrestin interactions or receptor internalization. *Mol Pharmacol* **71:** 549-557

Guan XM, Kobilka TS, Kobilka BK (1992) Enhancement of membrane insertion and function in a type IIIb membrane protein following introduction of a cleavable signal peptide. *J Biol Chem* **267:** 21995-21998

Guariguata L, Whiting DR, Hambleton I, Beagley J, Linnenkamp U, Shaw JE (2014) Global estimates of diabetes prevalence for 2013 and projections for 2035. *Diabetes Res Clin Pract* **103:** 137-149

Gupta NA, Mells J, Dunham RM, Grakoui A, Handy J, Saxena NK, Anania FA (2010) Glucagon-like peptide-1 receptor is present on human hepatocytes and has a direct role in decreasing hepatic steatosis in vitro by modulating elements of the insulin signaling pathway. *Hepatology* **51:** 1584-1592

Gurevich VV, Gurevich EV (2006) The structural basis of arrestin-mediated regulation of G-protein-coupled receptors. *Pharmacol Ther* **110:** 465-502

Gutkind JS (1998) The pathways connecting G protein-coupled receptors to the nucleus through divergent mitogen-activated protein kinase cascades. *J Biol Chem* **273:** 1839-1842

Hall RA, Lefkowitz RJ (2002) Regulation of G protein-coupled receptor signaling by scaffold proteins. *Circ Res* **91:** 672-680

Hallbrink M, Holmqvist T, Olsson M, Ostenson CG, Efendic S, Langel U (2001) Different domains in the third intracellular loop of the GLP-1 receptor are responsible for Gαs and Gαi/Gαo activation. *Biochim Biophys Acta* **1546:** 79-86

Haluzik M (2014) The expanding role of incretin-based therapies: how much should we expect? *J Endocrinol* **221:** E1-2

Hamnvik OP, McMahon GT (2009) Balancing risk and benefit with oral hypoglycemic drugs. *Mt Sinai J Med* **76:** 234-243

Hansen L, Deacon CF, Orskov C, Holst JJ (1999) Glucagon-like peptide-1-(7-36)amide is transformed to glucagon-like peptide-1-(9-36)amide by dipeptidyl peptidase IV in the capillaries supplying the L cells of the porcine intestine. *Endocrinology* **140:** 5356-5363

Hanson MA, Stevens RC (2009) Discovery of New GPCR Biology: One Receptor Structure at a Time. *Structure* **17:** 8-14

Hanyaloglu AC, von Zastrow M (2008) Regulation of GPCRs by endocytic membrane trafficking and its potential implications. *Annu Rev Pharmacol Toxicol* **48:** 537-568

Haque TS, Lee VG, Riexinger D, Lei M, Malmstrom S, Xin L, Han S, Mapelli C, Cooper CB, Zhang G, Ewing WR, Krupinski J (2010) Identification of potent 11mer glucagon-like peptide-1 receptor agonist peptides with novel C-terminal amino acids: Homohomophenylalanine analogs. *Peptides* **31:** 950-955

Harden TK (1983) Agonist-induced desensitization of the beta-adrenergic receptor-linked adenylate cyclase. *Pharmacol Rev* **35:** 5-32

Harikumar KG, Ball AM, Sexton PM, Miller LJ (2010) Importance of lipid-exposed residues in transmembrane segment four for family B calcitonin receptor homo-dimerization. *Regul Pept* **164:** 113-119

Harikumar KG, Pinon DI, Miller LJ (2007) Transmembrane segment IV contributes a functionally important interface for oligomerization of the Class II G protein-coupled secretin receptor. *J Biol Chem* **282:** 30363-30372

Harikumar KG, Wootten D, Pinon DI, Koole C, Ball AM, Furness SG, Graham B, Dong M, Christopoulos A, Miller LJ, Sexton PM (2012) Glucagon-like peptide-1 receptor dimerization differentially regulates agonist signaling but does not affect small molecule allostery. *Proc Natl Acad Sci U S A* **109:** 18607-18612

Harris BZ, Lim WA (2001) Mechanism and role of PDZ domains in signaling complex assembly. *Journal of Cell Science* **114:** 3219-3231

Hatsuzawa K, Tagaya M, Mizushima S (1997) The hydrophobic region of signal peptides is a determinant for SRP recognition and protein translocation across the ER membrane. *J Biochem* **121:** 270-277

Hausdorff WP, Campbell PT, Ostrowski J, Yu SS, Caron MG, Lefkowitz RJ (1991) A small region of the beta-adrenergic receptor is selectively involved in its rapid regulation. *Proc Natl Acad Sci U S A* **88:** 2979-2983

Hawes BE, van Biesen T, Koch WJ, Luttrell LM, Lefkowitz RJ (1995) Distinct pathways of Gi- and Gq-mediated mitogen-activated protein kinase activation. *J Biol Chem* **270:** 17148-17153

Hayes MR (2012) Neuronal and intracellular signaling pathways mediating GLP-1 energy balance and glycemic effects. *Physiol Behav* **106:** 413-416

Hayes MR, Bradley L, Grill HJ (2009) Endogenous hindbrain glucagon-like peptide-1 receptor activation contributes to the control of food intake by mediating gastric satiation signaling. *Endocrinology* **150:** 2654-2659

Heasman SJ, Ridley AJ (2008) Mammalian Rho GTPases: new insights into their functions from in vivo studies. *Nat Rev Mol Cell Bio* **9:** 690-701

Hegde RS, Lingappa VR (1997) Membrane protein biogenesis: regulated complexity at the endoplasmic reticulum. *Cell* **91:** 575-582

Heilker R, Wolff M, Tautermann CS, Bieler M (2009) G-protein-coupled receptor-focused drug discovery using a target class platform approach. *Drug Discov Today* **14:** 231-240

Helenius A, Aebi M (2001) Intracellular functions of N-linked glycans. *Science* **291:** 2364-2369

Heller RS, Kieffer TJ, Habener JF (1996) Point Mutations in the First and Third Intracellular Loops of the Glucagon-like Peptide-1 Receptor Alter Intracellular Signaling. *Biochem Biophys Res Commun* **223:** 624-632

Hinkle PM, Gehret AU, Jones BW (2012) Desensitization, trafficking, and resensitization of the pituitary thyrotropin-releasing hormone receptor. *Front Neurosci* **6:** 180

Hoare SR (2007) Allosteric modulators of class B G-protein-coupled receptors. *Curr Neuropharmacol* **5:** 168-179

Hoare SRJ (2005) Mechanisms of peptide and nonpeptide ligand binding to class B G-protein coupled receptors. *Drug Discov Today* **10:** 417-427

Hojberg PV, Vilsboll T, Rabol R, Knop FK, Bache M, Krarup T, Holst JJ, Madsbad S (2009) Four weeks of near-normalisation of blood glucose improves the insulin response to glucagon-like peptide-1 and glucose-dependent insulinotropic polypeptide in patients with type 2 diabetes. *Diabetologia* **52:** 199-207

Hollander P (2007) Anti-Diabetes and Anti-Obesity Medications: Effects on Weight in People With Diabetes. *Diabetes Spectrum* **20:** 159-165

Holscher C (2014) Central effects of GLP-1: new opportunities for treatments of neurodegenerative diseases. *J Endocrinol* **221:** T31-41

Holst JJ (2007) The physiology of glucagon-like peptide 1. *Physiol Rev* **87:** 1409-1439

Holst JJ, Deacon CF, Vilsboll T, Krarup T, Madsbad S (2008) Glucagon-like peptide-1, glucose homeostasis and diabetes. *Trends Mol Med* **14:** 161-168

Holst JJ, Gromada J (2004) Role of incretin hormones in the regulation of insulin secretion in diabetic and nondiabetic humans. *Am J Physiol Endocrinol Metab* **287:** E199-206

Holst JJ, Vilsboll T, Deacon CF (2009) The incretin system and its role in type 2 diabetes mellitus. *Mol Cell Endocrinol* **297:** 127-136

Holz GG (2004) Epac: A new cAMP-binding protein in support of glucagon-like peptide-1 receptor-mediated signal transduction in the pancreatic beta-cell. *Diabetes* **53:** 5-13

Holz GG, Leech CA, Heller RS, Castonguay M, Habener JF (1999) cAMP-dependent Mobilization of Intracellular Ca Stores by Activation of Ryanodine Receptors in Pancreatic β-Cells. *J Biol Chem* **274:** 14147-14156

Holz GGt, Kuhtreiber WM, Habener JF (1993) Pancreatic beta-cells are rendered glucose-competent by the insulinotropic hormone glucagon-like peptide-1(7-37). *Nature* **361:** 362-365

Hu FB (2011) Globalization of diabetes: the role of diet, lifestyle, and genes. *Diabetes Care* **34:** 1249-1257

Huang J, Zhou H, Mahavadi S, Sriwai W, Murthy KS (2007) Inhibition of Galphaq-dependent PLC-beta1 activity by PKG and PKA is mediated by phosphorylation of RGS4 and GRK2. *Am J Physiol Cell Physiol* **292:** C200-208

Huang Y, Wilkinson GF, Willars GB (2010) Role of the signal peptide in the synthesis and processing of the glucagon-like peptide-1 receptor. *Br J Pharmacol* **159:** 237-251

Hung AY, Sheng M (2002) PDZ domains: structural modules for protein complex assembly. *J Biol Chem* **277:** 5699-5702

Hunter K, Holscher C (2012) Drugs developed to treat diabetes, liraglutide and lixisenatide, cross the blood brain barrier and enhance neurogenesis. *BMC Neurosci* **13:** 33

Hunter MG, Avalos BR (1999) Deletion of a critical internalization domain in the G-CSFR in acute myelogenous leukemia preceded by severe congenital neutropenia. *Blood* **93:** 440-446

Irwin N, Flatt PR, Patterson S, Green BD (2010) Insulin-releasing and metabolic effects of small molecule GLP-1 receptor agonist 6,7-dichloro-2-methylsulfonyl-3-N-tert-butylaminoquinoxaline. *Eur J Pharmacol* **628:** 268-273

Jacoby E, Bouhelal R, Gerspacher M, Seuwen K (2006) The 7 TM G-protein-coupled receptor target family. *ChemMedChem* **1:** 761-782

Jalink K, Moolenaar WH (2010) G protein-coupled receptors: the inside story. *Bioessays* **32:** 13-16

Jensen AA, Pedersen UB, Kiemer A, Din N, Andersen PH (1995) Functional importance of the carboxyl tail cysteine residues in the human D1 dopamine receptor. *J Neurochem* **65:** 1325-1331

Jhala US, Canettieri G, Screaton RA, Kulkarni RN, Krajewski S, Reed J, Walker J, Lin X, White M, Montminy M (2003) cAMP promotes pancreatic beta-cell survival via CREB-mediated induction of IRS2. *Genes Dev* **17:** 1575-1580

Jolivalt CG, Fineman M, Deacon CF, Carr RD, Calcutt NA (2011) GLP-1 signals via ERK in peripheral nerve and prevents nerve dysfunction in diabetic mice. *Diabetes Obes Metab*: DOI: 10.1111/j.1463-1326.2011.01431.x

Jorgensen R, Kubale V, Vrecl M, Schwartz TW, Elling CE (2007) Oxyntomodulin differentially affects glucagon-like peptide-1 receptor beta-arrestin recruitment and signaling through Galpha(s). *J Pharmacol Exp Ther* **322:** 148-154

Kanamarlapudi V, Thompson A, Kelly E, Lopez Bernal A (2012) ARF6 activated by the LHCG receptor through the cytohesin family of guanine nucleotide

exchange factors mediates the receptor internalization and signaling. *J Biol Chem* **287:** 20443-20455

Kang G, Joseph JW, Chepurny OG, Monaco M, Wheeler MB, Bos JL, Schwede F, Genieser HG, Holz GG (2003) Epac-selective cAMP analog 8-pCPT-2'-O-Me-cAMP as a stimulus for Ca2+-induced Ca2+ release and exocytosis in pancreatic β-cells. *J Biol Chem* **278:** 8279-8285

Kang ZF, Deng Y, Zhou Y, Fan RR, Chan JCN, Laybutt DR, Luzuriaga J, Xu G (2013) Pharmacological reduction of NEFA restores the efficacy of incretin-based therapies through GLP-1 receptor signalling in the beta cell in mouse models of diabetes. *Diabetologia* **56:** 423-433

Kasai K (2005) Rab27a mediates the tight docking of insulin granules onto the plasma membrane during glucose stimulation. *Journal of Clinical Investigation* **115:** 388-396

Kashima Y, Miki T, Shibasaki T, Ozaki N, Miyazaki M, Yano H, Seino S (2001) Critical role of cAMP-GEFII.Rim2 complex in incretin-potentiated insulin secretion. *Journal of Biological Chemistry* **276:** 46046-46053

Kenakin TP (2009) '7TM Receptor Allostery: Putting Numbers to Shapeshifting Proteins. *Trends Pharmacol Sci* **30:** 460-469

Kern A, Agoulnik AI, Bryant-Greenwood GD (2007) The low-density lipoprotein class A module of the relaxin receptor (leucine-rich repeat containing G-protein coupled receptor 7): its role in signaling and trafficking to the cell membrane. *Endocrinology* **148:** 1181-1194

Khunti K, Davies M (2010) Glycaemic goals in patients with type 2 diabetes: current status, challenges and recent advances. *Diabetes Obes Metab* **12:** 474-484

Kieffer TJ, McIntosh CH, Pederson RA (1995) Degradation of glucose-dependent insulinotropic polypeptide and truncated glucagon-like peptide 1 in vitro and in vivo by dipeptidyl peptidase IV. *Endocrinology* **136:** 3585-3596

Kim Chung le T, Hosaka T, Yoshida M, Harada N, Sakaue H, Sakai T, Nakaya Y (2009) Exendin-4, a GLP-1 receptor agonist, directly induces adiponectin expression through protein kinase A pathway and prevents inflammatory adipokine expression. *Biochem Biophys Res Commun* **390:** 613-618

Kim DH, D'Alessio DA, Woods SC, Seeley RJ (2009) The effects of GLP-1 infusion in the hepatic portal region on food intake. *Regul Pept* **155:** 110-114

Kim JY, Yang MS, Oh CD, Kim KT, Ha MJ, Kang SS, Chun JS (1999) Signalling pathway leading to an activation of mitogen-activated protein kinase by stimulating M3 muscarinic receptor. *Biochem J* **337 (Pt 2):** 275-280

Kim W, Egan JM (2008) The role of incretins in glucose homeostasis and diabetes treatment. *Pharmacol Rev* **60:** 470-512

Kitabchi AE, Nyenwe EA (2006) Hyperglycemic crises in diabetes mellitus: diabetic ketoacidosis and hyperglycemic hyperosmolar state. *Endocrinol Metab Clin North Am* **35:** 725-751, viii

Kjems LL, Holst JJ, Vølund A, Madsbad S (2003) The influence of GLP-1 on glucose-stimulated insulin secretion- effects on β-cell sensitivity in type 2 and nondiabetic subjects. *Diabetes* **52:** 380-386

Knop FK, Vilsboll T, Hojberg PV, Larsen S, Madsbad S, Volund A, Holst JJ, Krarup T (2007) Reduced incretin effect in type 2 diabetes: cause or consequence of the diabetic state? *Diabetes* **56:** 1951-1959

Knudsen LB, Kiel D, Teng M, Behrens C, Bhumralkar D, Kodra JT, Holst JJ, Jeppesen CB, Johnson MD, de Jong JC, Jorgensen AS, Kercher T, Kostrowicki J,

Madsen P, Olesen PH, Petersen JS, Poulsen F, Sidelmann UG, Sturis J, Truesdale L, May J, Lau J (2007) Small-molecule agonists for the glucagon-like peptide 1 receptor. *Proc Natl Acad Sci U S A* **104:** 937-942

Kochl R, Alken M, Rutz C, Krause G, Oksche A, Rosenthal W, Schulein R (2002) The signal peptide of the G protein-coupled human endothelin B receptor is necessary for translocation of the N-terminal tail across the endoplasmic reticulum membrane. *J Biol Chem* **277:** 16131-16138

Koole C, Wootten D, Simms J, Miller LJ, Christopoulos A, Sexton PM (2012a) Second extracellular loop of human glucagon-like peptide-1 receptor (GLP-1R) has a critical role in GLP-1 peptide binding and receptor activation. *J Biol Chem* **287:** 3642-3658

Koole C, Wootten D, Simms J, Savage EE, Miller LJ, Christopoulos A, Sexton PM (2012b) Second extracellular loop of human glucagon-like peptide-1 receptor (GLP-1R) differentially regulates orthosteric but not allosteric agonist binding and function. *J Biol Chem* **287:** 3659-3673

Koole C, Wootten D, Simms J, Valant C, Sridhar R, Woodman OL, Miller LJ, Summers RJ, Christopoulos A, Sexton PM (2010) Allosteric ligands of the glucagon-like peptide 1 receptor (GLP-1R) differentially modulate endogenous and exogenous peptide responses in a pathway-selective manner: implications for drug screening. *Mol Pharmacol* **78:** 456-465

Kramer HK, Poblete JC, Azmitia EC (1997) Activation of protein kinase C (PKC) by 3,4-methylenedioxymethamphetamine (MDMA) occurs through the stimulation of serotonin receptors and transporter. *Neuropsychopharmacol* **17:** 117-129

Kristiansen K (2004) Molecular mechanisms of ligand binding, signaling, and regulation within the superfamily of G-protein-coupled receptors: molecular

modeling and mutagenesis approaches to receptor structure and function. *Pharmacol Ther* **103:** 21-80

Kuna RS, Girada SB, Asalla S, Vallentyne J, Maddika S, Patterson JT, Smiley DL, DiMarchi RD, Mitra P (2013) Glucagon-like peptide-1 receptor-mediated endosomal cAMP generation promotes glucose-stimulated insulin secretion in pancreatic beta-cells. *Am J Physiol Endocrinol Metab* **305:** E161-170

Kuramasu A, Sukegawa J, Yanagisawa T, Yanai K (2006) Recent advances in molecular pharmacology of the histamine systems: roles of C-terminal tails of histamine receptors. *J Pharmacol Sci* **101:** 7-11

Kuzuya T, Matsuda A (1997) Classification of diabetes on the basis of etiologies versus degree of insulin deficiency. *Diabetes Care* **20:** 219-220

Lamont BJ, Andrikopoulos S (2014) Hope and fear for new classes of type 2 diabetes drugs: is there preclinical evidence that incretin-based therapies alter pancreatic morphology? *J Endocrinol* **221:** T43-61

Larsen J, Hylleberg B, Ng K, Damsbo P (2001) Glucagon-like peptide-1 infusion must be maintained for 24 h/day to obtain acceptable glycemia in type 2 diabetic patients who are poorly controlled on sulphonylurea treatment. *Diabetes Care* **24:** 1416-1421

Le PU, Nabi IR (2003) Distinct caveolae-mediated endocytic pathways target the Golgi apparatus and the endoplasmic reticulum. *Journal of Cell Science* **116:** 1059-1071

Lee YS, Jun HS (2014) Anti-diabetic actions of glucagon-like peptide-1 on pancreatic beta-cells. *Metabolism* **63:** 9-19

Lefkowitz RJ, Stadel JM, Caron MG (1983) Adenylate cyclase-coupled beta-adrenergic receptors: structure and mechanisms of activation and desensitization. *Annual review of biochemistry* **52:** 159-186

Letourneur F, Klausner RD (1992) A novel di-leucine motif and a tyrosine-based motif independently mediate lysosomal targeting and endocytosis of CD3 chains. *Cell* **69:** 1143-1157

Li G, Zhou Q, Yu Y, Chen L, Shi Y, Luo J, Benovic J, Lu J, Zhou N (2012) Identification and characterization of distinct C-terminal domains of the human hydroxycarboxylic acid receptor-2 that are essential for receptor export, constitutive activity, desensitization, and internalization. *Mol Pharmacol* **82:** 1150-1161

Li L, El-Kholy W, Rhodes CJ, Brubaker PL (2005) Glucagon-like peptide-1 protects beta cells from cytokine-induced apoptosis and necrosis: role of protein kinase B. *Diabetologia* **48:** 1339-1349

López de Maturana R, Donnelly D (2002) The glucagon-like peptide-1 receptor binding site for the N-terminus of GLP-1 requires polarity at Asp198 rather than negative charge. *FEBS Letters* **530:** 244-248

Lopez de Maturana R, Treece-Birch J, Abidi F, Findlay JB, Donnelly D (2004) Met-204 and Tyr-205 are together important for binding GLP-1 receptor agonists but not their N-terminally truncated analogues. *Protein Pept Lett* **11:** 15-22

Lopez-Ilasaca M, Crespo P, Pellici PG, Gutkind JS, Wetzker R (1997) Linkage of G protein-coupled receptors to the MAPK signaling pathway through PI 3-kinase gamma. *Science* **275:** 394-397

Luttrell LM, Hawes BE, van Biesen T, Luttrell DK, Lansing TJ, Lefkowitz RJ (1996) Role of c-Src tyrosine kinase in G protein-coupled receptor- and

Gbetagamma subunit-mediated activation of mitogen-activated protein kinases. *J Biol Chem* **271:** 19443-19450

Luttrell LM, Lefkowitz RJ (2002) The role of beta-arrestins in the termination and transduction of G-protein-coupled receptor signals. *Journal of Cell Science* **115:** 455-465

Ma L, Seager MA, Wittmann M, Jacobson M, Bickel D, Burno M, Jones K, Graufelds VK, Xu G, Pearson M, McCampbell A, Gaspar R, Shughrue P, Danziger A, Regan C, Flick R, Pascarella D, Garson S, Doran S, Kreatsoulas C, Veng L, Lindsley CW, Shipe W, Kuduk S, Sur C, Kinney G, Seabrook GR, Ray WJ (2009) Selective activation of the M1 muscarinic acetylcholine receptor achieved by allosteric potentiation. *Proc Natl Acad Sci U S A* **106:** 15950-15955

Maley F, Trimble RB, Tarentino AL, Plummer TH (1989) Characterization of Glycoproteins and Their Associated Oligosaccharides through the Use of Endoglycosidases. *Anal Biochem* **180:** 195-204

Mapelli C, Natarajan SI, Meyer JP, Bastos MM, Bernatowicz MS, Lee VG, Pluscec J, Riexinger DJ, Sieber-McMaster ES, Constantine KL, Smith-Monroy CA, Golla R, Ma ZP, Longhi DA, Shi D, Xin L, Taylor JR, Koplowitz B, Chi CL, Khanna A, Robinson GW, Seethala R, Anatal-Zimanyi IA, Stoffel RH, Han SP, Whaley JM, Huang CS, Krupinski J, Ewing WR (2009) Eleven Amino Acid Glucagon-like Peptide-1 Receptor Agonists with Antidiabetic Activity. *J Med Chem* **52:** 7788-7799

Marchese A, Chen C, Kim YM, Benovic JL (2003) The ins and outs of G protein-coupled receptor trafficking. *Trends in Biochemical Sciences* **28:** 369-376

Marchese A, Paing MM, Temple BR, Trejo J (2008) G protein-coupled receptor sorting to endosomes and lysosomes. *Annu Rev Pharmacol Toxicol* **48:** 601-629

Marshall RD (1974) The nature and metabolism of the carbohydrate-peptide linkages of glycoproteins. *Biochem Soc Symp*: 17-26

Martiny-Baron G, Kazanietz MG, Mischak H, Blumberg PM, Kochs G, Hug H, Marme D, Schachtele C (1993) Selective inhibition of protein kinase C isozymes by the indolocarbazole Go 6976. *J Biol Chem* **268:** 9194-9197

Mathi SK (1997) Scanning of the Glucagon-Like Peptide-1 Receptor Localizes G Protein-Activating Determinants Primarily to the N Terminus of the Third Intracellular Loop. *Mol Endocrinol* **11:** 424-432

Matschinsky FM (2002) Regulation of Pancreatic β-Cell Glucokinase: from basics to therapeutics. *Diabetes* **51:** S394-404

McArdle CA, Franklin J, Green L, Hislop JN (2002) The gonadotrophin-releasing hormone receptor: signalling, cycling and desensitisation. *Arch Physiol Biochem* **110:** 113-122

McWilliam H, Li W, Uludag M, Squizzato S, Park YM, Buso N, Cowley AP, Lopez R (2013) Analysis Tool Web Services from the EMBL-EBI. *Nucleic Acids Res* **41:** W597-600

Meier JJ, Nauck MA (2010) Is the Diminished Incretin Effect in Type 2 Diabetes Just an Epi-Phenomenon of Impaired beta-Cell Function? *Diabetes* **59:** 1117-1125

Meneghini LF (2009) Early insulin treatment in type 2 diabetes: what are the pros? *Diabetes Care* **32 Suppl 2:** S266-269

Mentlein R (2009) Mechanisms underlying the rapid degradation and elimination of the incretin hormones GLP-1 and GIP. *Best Pract Res Clin Endocrinol Metab* **23:** 443-452

Millar RP, Newton CL (2010) The Year In G Protein-Coupled Receptor Research. *Mol Endocrinol* **24:** 261-274

Milligan G (2009) G protein-coupled receptor hetero-dimerization: contribution to pharmacology and function. *Br J Pharmacol* **158:** 5-14

Mojsov S, Heinrich G, Wilson IB, Ravazzola M, Orci L, Habener JF (1986) Preproglucagon gene expression in pancreas and intestine diversifies at the level of post-translational processing. *J Biol Chem* **261:** 11880-11889

Montrose-Rafizadeh C, Avdonin P, Garant MJ, Rodgers BD, Kole S, Yang H, Levine MA, Schwindinger W, Bernier M (1999) Pancreatic glucagon-like peptide-1 receptor couples to multiple G proteins and activates mitogen-activated protein kinase pathways in Chinese hamster ovary cells. *Endocrinology* **140:** 1132-1140

Montrose-Rafizadeh C, Egan JM, Roth J (1994) Incretin Hormones Regulate Glucose-Dependent Insulin-Secretion in Rin-1046-38 Cells - Mechanisms of Action. *Endocrinology* **135:** 589-594

Montrose-Rafizadeh C, Yang H, Rodgers BD, Beday A, Pritchette LA, Eng J (1997) High potency antagonists of the pancreatic glucagon-like peptide-1 receptor. *J Biol Chem* **272:** 21201-21206

Moore CA, Milano SK, Benovic JL (2007) Regulation of receptor trafficking by GRKs and arrestins. *Annu Rev Physiol* **69:** 451-482

Morello JP, Bouvier M (1996) Palmitoylation: a post-translational modification that regulates signalling from G-protein coupled receptors. *Biochem Cell Biol* **74:** 449-457

Mozaffarian D, Kamineni A, Carnethon M, Djousse L, Mukamal KJ, Siscovick D (2009) Lifestyle risk factors and new-onset diabetes mellitus in older adults: the cardiovascular health study. *Arch Intern Med* **169:** 798-807

Mundell SJ, Matharu AL, Pula G, Roberts PJ, Kelly E (2001) Agonist-induced internalization of the metabotropic glutamate receptor 1a is arrestin- and dynamin-dependent. *J Neurochem* **78:** 546-551

Muoio DM, Newgard CB (2008) Mechanisms of disease: molecular and metabolic mechanisms of insulin resistance and beta-cell failure in type 2 diabetes. *Nat Rev Mol Cell Biol* **9:** 193-205

Muscelli E, Mari A, Casolaro A, Camastra S, Seghieri G, Gastaldelli A, Holst JJ, Ferrannini E (2008) Separate impact of obesity and glucose tolerance on the incretin effect in normal subjects and type 2 diabetic patients. *Diabetes* **57:** 1340-1348

Nabi IR, Le PU (2003) Caveolae/raft-dependent endocytosis. *J Cell Biol* **161:** 673-677

Nash MS, Wood JPM, Osborne NN (1997) Protein kinase C activation by serotonin potentiates agonist-induced stimulation of cAMP production in cultured rat retinal pigment epithelial cells. *Exp Eye Res* **64:** 249-255

Nathan DM, Buse JB, Davidson MB, Ferrannini E, Holman RR, Sherwin R, Zinman B (2008) Management of hyperglycemia in type 2 diabetes: a consensus algorithm for the initiation and adjustment of therapy: update regarding thiazolidinediones: a consensus statement from the American Diabetes Association and the European Association for the Study of Diabetes. *Diabetes Care* **31:** 173-175

Nathan DM, Buse JB, Davidson MB, Ferrannini E, Holman RR, Sherwin R, Zinman B (2009) Medical management of hyperglycemia in type 2 diabetes: a consensus algorithm for the initiation and adjustment of therapy: a consensus statement of the American Diabetes Association and the European Association for the Study of Diabetes. *Diabetes Care* **32:** 193-203

Nauck M, Stöckmann F, Ebert R, Creutzfeldt W (1986) Reduced incretin effect in Type 2 (non-insulin-dependent) diabetes. *Diabetologia* **29:** 46-52

Nauck MA, El-Ouaghlidi A, Gabrys B, Hucking K, Holst JJ, Deacon CF, Gallwitz B, Schmidt WE, Meier JJ (2004) Secretion of incretin hormones (GIP and GLP-1) and incretin effect after oral glucose in first-degree relatives of patients with type 2 diabetes. *Regul Pept* **122:** 209-217

Nauck MA, Heimesaat MM, Orskov C, Holst JJ, Ebert R, Creutzfeldt W (1993) Preserved incretin activity of glucagon-like peptide 1 [7-36 amide] but not of synthetic human gastric inhibitory polypeptide in patients with type-2 diabetes mellitus. *J Clin Invest* **91:** 301-307

Nauck MA, Ratner RE, Kapitza C, Berria R, Boldrin M, Balena R (2009) Treatment with the human once-weekly glucagon-like peptide-1 analog taspoglutide in combination with metformin improves glycemic control and lowers body weight in patients with type 2 diabetes inadequately controlled with metformin alone: a double-blind placebo-controlled study. *Diabetes Care* **32:** 1237-1243

Nauck MA, Vardarli I, Deacon CF, Holst JJ, Meier JJ (2011) Secretion of glucagon-like peptide-1 (GLP-1) in type 2 diabetes: what is up, what is down? *Diabetologia* **54:** 10-18

Nelson DL, Lehninger AL, Cox MM (2008) *Lehninger principles of biochemistry*, 5thedn edn. New York: W. H. Freeman.

Nyholm B, Walker M, Gravholt CH, Shearing PA, Sturis J, Alberti KG, Holst JJ, Schmitz O (1999) Twenty-four-hour insulin secretion rates, circulating concentrations of fuel substrates and gut incretin hormones in healthy offspring of Type II (non-insulin-dependent) diabetic parents: evidence of several aberrations. *Diabetologia* **42:** 1314-1323

Nystrom T (2008) The potential beneficial role of glucagon-like peptide-1 in endothelial dysfunction and heart failure associated with insulin resistance. *Horm Metab Res* **40:** 593-606

O'Connor V, El Far O, Bofill-Cardona E, Nanoff C, Freissmuth M, Karschin A, Airas JM, Betz H, Boehm S (1999) Calmodulin dependence of presynaptic metabotropic glutamate receptor signaling. *Science* **286:** 1180-1184

O'Dowd BF, Hnatowich M, Caron MG, Lefkowitz RJ, Bouvier M (1989) Palmitoylation of the human beta 2-adrenergic receptor. Mutation of Cys341 in the carboxyl tail leads to an uncoupled nonpalmitoylated form of the receptor. *J Biol Chem* **264:** 7564-7569

Ohno H, Stewart J, Fournier MC, Bosshart H, Rhee I, Miyatake S, Saito T, Gallusser A, Kirchhausen T, Bonifacino JS (1995) Interaction of tyrosine-based sorting signals with clathrin-associated proteins. *Science* **269:** 1872-1875

Okamoto T, Schlegel A, Scherer PE, Lisanti MP (1998) Caveolins, a family of scaffolding proteins for organizing "preassembled signaling complexes" at the plasma membrane". *Journal of Biological Chemistry* **273:** 5419-5422

Okamoto Y, Ninomiya H, Miwa S, Masaki T (2000) Cholesterol oxidation switches the internalization pathway of endothelin receptor type A from caveolae to clathrin-coated pits in Chinese hamster ovary cells. *J Biol Chem* **275:** 6439-6446

Orskov C, Bersani M, Johnsen AH, Hojrup P, Holst JJ (1989) Complete sequences of glucagon-like peptide-1 from human and pig small intestine. *J Biol Chem* **264:** 12826-12829

Orskov C, Holst JJ, Knuhtsen S, Baldissera FG, Poulsen SS, Nielsen OV (1986) Glucagon-like peptides GLP-1 and GLP-2, predicted products of the glucagon

gene, are secreted separately from pig small intestine but not pancreas. *Endocrinology* **119:** 1467-1475

Orskov C, Holst JJ, Poulsen SS, Kirkegaard P (1987) Pancreatic and intestinal processing of proglucagon in man. *Diabetologia* **30:** 874-881

Orskov C, Wettergren A, Holst JJ (1993) Biological effects and metabolic rates of glucagonlike peptide-1 7-36 amide and glucagonlike peptide-1 7-37 in healthy subjects are indistinguishable. *Diabetes* **42:** 658-661

Ozaki N, Shibasaki T, Kashima Y, Miki T, Takahashi K, Ueno H, Sunaga Y, Yano H, Matsuura Y, Iwanaga T, Takai Y, Seino S (2000) cAMP-GEFII is a direct target of cAMP in regulated exocytosis. *Nat Cell Biol* **2:** 805-811

Palczewski K (2000) Crystal Structure of Rhodopsin: A G Protein-Coupled Receptor. *Science* **289:** 739-745

Parthier C, Kleinschmidt M, Neumann P, Rudolph R, Manhart S, Schlenzig D, Fanghanel J, Rahfeld JU, Demuth HU, Stubbs MT (2007) Crystal structure of the incretin-bound extracellular domain of a G protein-coupled receptor. *Proc Natl Acad Sci U S A* **104:** 13942-13947

Parthier C, Reedtz-Runge S, Rudolph R, Stubbs MT (2009) Passing the baton in class B GPCRs: peptide hormone activation via helix induction? *Trends in Biochemical Sciences* **34:** 303-310

Parton RG, Richards AA (2003) Lipid rafts and caveolae as portals for endocytosis- new insights and common mechanisms. *Traffic (Copenhagen, Denmark)* **4:** 724-738

Patterson JT, Ottaway N, Gelfanov VM, Smiley DL, Perez-Tilve D, Pfluger PT, Tschop MH, Dimarchi RD (2011) A novel human-based receptor antagonist of

sustained action reveals body weight control by endogenous GLP-1. *ACS Chem Biol* **6:** 135-145

Pearse BM (1988) Receptors compete for adaptors found in plasma membrane coated pits. *Embo J* **7:** 3331-3336

Pelkmans L, Kartenbeck J, Helenius A (2001) Caveolar endocytosis of simian virus 40 reveals a new two-step vesicular-transport pathway to the ER. *Nat Cell Biol* **3:** 473-483

Perley MJ, Kipnis DM (1967) Plasma insulin responses to oral and intravenous glucose: studies in normal and diabetic sujbjects. *J Clin Invest* **46:** 1954-1962

Petaja-Repo UE, Hogue M, Laperriere A, Walker P, Bouvier M (2000) Export from the endoplasmic reticulum represents the limiting step in the maturation and cell surface expression of the human delta opioid receptor. *J Biol Chem* **275:** 13727-13736

Pinkney J, Fox T, Lakshiminarayan R (2010) Selecting GLP-1 agonists in the management of type 2 diabetes: differential pharmacology and therapeutic benefits of liraglutide and exenatide. *Therapeutics and Clinical Risk Management*: 401

Pioszak AA, Harikumar KG, Parker NR, Miller LJ, Xu HE (2010) Dimeric arrangement of the parathyroid hormone receptor and a structural mechanism for ligand-induced dissociation. *J Biol Chem* **285:** 12435-12444

Poitout V (2013) Lipotoxicity impairs incretin signalling. *Diabetologia* **56:** 231-233

Premont RT, Inglese J, Lefkowitz RJ (1995) Protein kinases that phosphorylate activated G protein-coupled receptors. *The FASEB Journal* **9:** 175-182

Prentki M, Nolan CJ (2006) Islet beta cell failure in type 2 diabetes. *J Clin Invest* **116:** 1802-1812

Price MR, Baillie GL, Thomas A, Stevenson LA, Easson M, Goodwin R, McLean A, McIntosh L, Goodwin G, Walker G, Westwood P, Marrs J, Thomson F, Cowley P, Christopoulos A, Pertwee RG, Ross RA (2005) Allosteric modulation of the cannabinoid CB1 receptor. *Mol Pharmacol* **68:** 1484-1495

Quoyer J, Longuet C, Broca C, Linck N, Costes S, Varin E, Bockaert J, Bertrand G, Dalle S (2010) GLP-1 mediates antiapoptotic effect by phosphorylating Bad through a beta-arrestin 1-mediated ERK1/2 activation in pancreatic beta-cells. *J Biol Chem* **285:** 1989-2002

Radcliff G, Jaroszeski MJ (1998) Basics of flow cytometry. *Methods Mol Biol* **91:** 1-24

Rahbar S, Blumenfeld O, Ranney HM (1969) Studies of an unusual hemoglobin in patients with diabetes mellitus. *Biochem Biophys Res Commun* **36:** 838-843

Rapacciuolo A, Suvarna S, Barki-Harrington L, Luttrell LM, Cong M, Lefkowitz RJ, Rockman HA (2003) Protein kinase A and G protein-coupled receptor kinase phosphorylation mediates β-1 adrenergic receptor endocytosis through different pathways. *J Biol Chem* **278:** 35403-35411

Ratner R, Nauck M, Kapitza C, Asnaghi V, Boldrin M, Balena R (2010) Safety and tolerability of high doses of taspoglutide, a once-weekly human GLP-1 analogue, in diabetic patients treated with metformin: a randomized double-blind placebo-controlled study. *Diabet Med* **27:** 556-562

Rayner CK, Samsom M, Jones KL, Horowitz M (2001) Relationships of upper gastrointestinal motor and sensory function with glycemic control. *Diabetes Care* **24:** 371-381

Reimann F (2010) Molecular mechanisms underlying nutrient detection by incretin-secreting cells. *Int Dairy J* **20:** 236-242

Rhodes CJ, White MF (2002) Molecular insights into insulin action and secretion. *European Journal of Clinical Investigation* **32:** 3-13

Riserus U, Willett WC, Hu FB (2009) Dietary fats and prevention of type 2 diabetes. *Prog Lipid Res* **48:** 44-51

Robertson DN, Johnson MS, Moggach LO, Holland PJ, Lutz EM, Mitchell R (2003) Selective interaction of ARF1 with the carboxy-terminal tail domain of the 5-HT2A receptor. *Mol Pharmacol* **64:** 1239-1250

Rouille Y, Westermark G, Martin SK, Steiner DF (1994) Proglucagon is processed to glucagon by prohormone convertase PC2 in alpha TC1-6 cells. *Proc Natl Acad Sci U S A* **91:** 3242-3246

Roy S, Perron B, Gallo-Payet N (2010) Role of asparagine-linked glycosylation in cell surface expression and function of the human adrenocorticotropin receptor (melanocortin 2 receptor) in 293/FRT cells. *Endocrinology* **151:** 660-670

Rung J, Cauchi S, Albrechtsen A, Shen L, Rocheleau G, Cavalcanti-Proenca C, Bacot F, Balkau B, Belisle A, Borch-Johnsen K, Charpentier G, Dina C, Durand E, Elliott P, Hadjadj S, Jarvelin MR, Laitinen J, Lauritzen T, Marre M, Mazur A, Meyre D, Montpetit A, Pisinger C, Posner B, Poulsen P, Pouta A, Prentki M, Ribel-Madsen R, Ruokonen A, Sandbaek A, Serre D, Tichet J, Vaxillaire M, Wojtaszewski JF, Vaag A, Hansen T, Polychronakos C, Pedersen O, Froguel P, Sladek R (2009) Genetic variant near IRS1 is associated with type 2 diabetes, insulin resistance and hyperinsulinemia. *Nat Genet* **41:** 1110-1115

Runge S, Thogersen H, Madsen K, Lau J, Rudolph R (2008) Crystal structure of the ligand-bound glucagon-like peptide-1 receptor extracellular domain. *J Biol Chem* **283:** 11340-11347

Rutz C, Renner A, Alken M, Schulz K, Beyermann M, Wiesner B, Rosenthal W, Schulein R (2006) The corticotropin-releasing factor receptor type 2a contains an N-terminal pseudo signal peptide. *J Biol Chem* **281:** 24910-24921

Ruvinsky I, Sharon N, Lerer T, Cohen H, Stolovich-Rain M, Nir T, Dor Y, Zisman P, Meyuhas O (2005) Ribosomal protein S6 phosphorylation is a determinant of cell size and glucose homeostasis. *Genes Dev* **19:** 2199-2211

Rybin VO, Xu XH, Lisanti MP, Steinberg SF (2000) Differential targeting of beta-adrenergic receptor subtypes and adenylyl cyclase to cardiomyocyte caveolae - A mechanism to functionally regulate the cAMP signaling pathway. *Journal of Biological Chemistry* **275:** 41447-41457

Sadava D, Heller HC, Orians GH, Purves WK, Hillis DM (2006) *Life: The Science of Biology*, 8thedn edn. New York: W. H. Freeman.

Sadeghi H, Birnbaumer M (1999) O-Glycosylation of the V2 vasopressin receptor. *Glycobiology* **9:** 731-737

Salapatek AMF (1999) Mutations to the Third Cytoplasmic Domain of the Glucagon-Like Peptide 1 (GLP-1) Receptor Can Functionally Uncouple GLP-1-Stimulated Insulin Secretion in HIT-T15 Cells. *Mol Endocrinol* **13:** 1305-1317

Salehi M, Aulinger B, Prigeon RL, D'Alessio DA (2010) Effect of endogenous GLP-1 on insulin secretion in type 2 diabetes. *Diabetes* **59:** 1330-1337

Sandoval IV, Bakke O (1994) Targeting of membrane proteins to endosomes and lysosomes. *Trends Cell Biol* **4:** 292-297

Schirra J, Katschinski M, Weidmann C, Schafer T, Wank U, Arnold R, Goke B (1996) Gastric emptying and release of incretin hormones after glucose ingestion in humans. *J Clin Invest* **97:** 92-103

Schlondorff J, Del Camino D, Carrasquillo R, Lacey V, Pollak MR (2009) TRPC6 mutations associated with focal segmental glomerulosclerosis cause constitutive activation of NFAT-dependent transcription. *Am J Physiol Cell Physiol* **296:** C558-569

Schulz K, Rutz C, Westendorf C, Ridelis I, Vogelbein S, Furkert J, Schmidt A, Wiesner B, Schulein R (2010) The pseudo signal peptide of the corticotropin-releasing factor receptor type 2a decreases receptor expression and prevents Gi-mediated inhibition of adenylyl cyclase activity. *J Biol Chem* **285:** 32878-32887

Schwartz TW, Holst B (2007) Allosteric enhancers, allosteric agonists and ago-allosteric modulators: where do they bind and how do they act? *Trends Pharmacol Sci* **28:** 366-373

Schwarz PE, Reimann M, Li J, Bergmann A, Licinio J, Wong ML, Bornstein SR (2007) The Metabolic Syndrome - a global challenge for prevention. *Horm Metab Res* **39:** 777-780

Schwencke C, Okumura S, Yamamoto M, Geng YJ, Ishikawa Y (1999) Colocalization of beta-adrenergic receptors and caveolin within the plasma membrane. *J Cell Biochem* **75:** 64-72

Seibold A, Williams B, Huang ZF, Friedman J, Moore RH, Knoll BJ, Clark RB (2000) Localization of the sites mediating desensitization of the beta(2)-adrenergic receptor by the GRK pathway. *Mol Pharmacol* **58:** 1162-1173

Serre V, Dolci W, Schaerer E, Scrocchi L, Drucker D, Efrat S, Thorens B (1998) Exendin-(9-39) is an inverse agonist of the murine glucagon-like peptide-1 receptor: implications for basal intracellular cyclic adenosine 3',5'-monophosphate levels and beta-cell glucose competence. *Endocrinology* **139:** 4448-4454

Shu L, Matveyenko AV, Kerr-Conte J, Cho JH, McIntosh CH, Maedler K (2009) Decreased TCF7L2 protein levels in type 2 diabetes mellitus correlate with downregulation of GIP- and GLP-1 receptors and impaired beta-cell function. *Hum Mol Genet* **18:** 2388-2399

Sievers F, Wilm A, Dineen D, Gibson TJ, Karplus K, Li W, Lopez R, McWilliam H, Remmert M, Soding J, Thompson JD, Higgins DG (2011) Fast, scalable generation of high-quality protein multiple sequence alignments using Clustal Omega. *Mol Syst Biol* **7:** 539

Sloop KW, Willard FS, Brenner MB, Ficorilli J, Valasek K, Showalter AD, Farb TB, Cao JX, Cox AL, Michael MD, Gutierrez Sanfeliciano SM, Tebbe MJ, Coghlan MJ (2010) Novel small molecule glucagon-like peptide-1 receptor agonist stimulates insulin secretion in rodents and from human islets. *Diabetes* **59:** 3099-3107

Soltoff SP, Avraham H, Avraham S, Cantley LC (1998) Activation of P2Y2 receptors by UTP and ATP stimulates mitogen-activated kinase activity through a pathway that involves related adhesion focal tyrosine kinase and protein kinase C. *J Biol Chem* **273:** 2653-2660

Sonoda N, Imamura T, Yoshizaki T, Babendure JL, Lu JC, Olefsky JM (2008) β-Arrestin-1 mediates glucagon-like peptide-1 signaling to insulin secretion in cultured pancreatic β cells. *Proc Natl Acad Sci U S A* **105:** 6614-6619

Sorkin A, Carpenter G (1993) Interaction of activated EGF receptors with coated pit adaptins. *Science* **261:** 612-615

Sorkin A, McKinsey T, Shih W, Kirchhausen T, Carpenter G (1995) Stoichiometric interaction of the epidermal growth factor receptor with the clathrin-associated protein complex AP-2. *J Biol Chem* **270:** 619-625

Stoffel M, Espinosa R, 3rd, Le Beau MM, Bell GI (1993) Human glucagon-like peptide-1 receptor gene. Localization to chromosome band 6p21 by fluorescence in situ hybridization and linkage of a highly polymorphic simple tandem repeat DNA polymorphism to other markers on chromosome 6. *Diabetes* **42:** 1215-1218

Stoner GD (2005) Hyperosmolar hyperglycemic state. *Am Fam Physician* **71:** 1723-1730

Strader CD, Fong TM, Graziano MP, Tota MR (1995) The family of G-protein-coupled receptors. *Faseb J* **9:** 745-754

Strader CD, Sigal IS, Blake AD, Cheung AH, Register RB, Rands E, Zemcik BA, Candelore MR, Dixon RA (1987) The carboxyl terminus of the hamster beta-adrenergic receptor expressed in mouse L cells is not required for receptor sequestration. *Cell* **49:** 855-863

Stulc T, Sedo A (2010) Inhibition of multifunctional dipeptidyl peptidase-IV: is there a risk of oncological and immunological adverse effects? *Diabetes Res Clin Pract* **88:** 125-131

Swinnen SG, Hoekstra JB, DeVries JH (2009) Insulin therapy for type 2 diabetes. *Diabetes Care* **32 Suppl 2:** S253-259

Syme CA, Zhang L, Bisello A (2006) Caveolin-1 regulates cellular trafficking and function of the glucagon-like Peptide 1 receptor. *Mol Endocrinol* **20:** 3400-3411

Tai AW, Chuang JZ, Bode C, Wolfrum U, Sung CH (1999) Rhodopsin's carboxy-terminal cytoplasmic tail acts as a membrane receptor for cytoplasmic dynein by binding to the dynein light chain Tctex-1. *Cell* **97:** 877-887

Takhar S, Gyomorey S, Su RC, Mathi SK, Li X, Wheeler MB (1996) The third cytoplasmic domain of the GLP-1[7-36 amide] receptor is required for coupling to the adenylyl cyclase system. *Endocrinology* **137:** 2175-2178

Tapia JA, Ferris HA, Jensen RT, Garcia LJ (1999) Cholecystokinin activates PYK2/CAKbeta by a phospholipase C-dependent mechanism and its association with the mitogen-activated protein kinase signaling pathway in pancreatic acinar cells. *J Biol Chem* **274:** 31261-31271

Tateyama M, Kubo Y (2007) Coupling profile of the metabotropic glutamate receptor 1alpha is regulated by the C-terminal domain. *Mol Cell Neurosci* **34:** 445-452

Thomas L, Leduc R, Thorne BA, Smeekens SP, Steiner DF, Thomas G (1991) Kex2-like endoproteases PC2 and PC3 accurately cleave a model prohormone in mammalian cells: evidence for a common core of neuroendocrine processing enzymes. *Proc Natl Acad Sci U S A* **88:** 5297-5301

Thomas RL, Langmead CJ, Wood MD, Challiss RA (2009) Contrasting effects of allosteric and orthosteric agonists on m1 muscarinic acetylcholine receptor internalization and down-regulation. *J Pharmacol Exp Ther* **331:** 1086-1095

Thomas WG, Baker KM, Motel TJ, Thekkumkara TJ (1995) Angiotensin II receptor endocytosis involves two distinct regions of the cytoplasmic tail. A role for residues on the hydrophobic face of a putative amphipathic helix. *J Biol Chem* **270:** 22153-22159

Thompson A, Kanamarlapudi V (2013) Type 2 Diabetes Mellitus and Glucagon Like Peptide-1 Receptor Signalling. *Clin Exp Pharmacol* **3:** DOI: 2161-1459.1000138

Thorens B (1992) Expression cloning of the pancreatic β cell receptor for the gluco-incretin hormone glucagon-like peptide 1. *Proc Natl Acad Sci U S A* **89:** 8641-8645

Thorens B, Porret A, Buhler L, Deng SP, Morel P, Widmann C (1993) Cloning and functional expression of the human islet GLP-1 receptor. Demonstration that exendin-4 is an agonist and exendin-(9-39) an antagonist of the receptor. *Diabetes* **42:** 1678-1682

Tobin AB (2008) G-protein-coupled receptor phosphorylation: where, when and by whom. *Br J Pharmacol* **153 Suppl 1:** S167-176

Toft-Nielsen MB (2001) Determinants of the Impaired Secretion of Glucagon-Like Peptide-1 in Type 2 Diabetic Patients. *Journal of Clinical Endocrinology & Metabolism* **86:** 3717-3723

Tokuyama Y, Matsui K, Egashira T, Nozaki O, Ishizuka T, Kanatsuka A (2004) Five missense mutations in glucagon-like peptide 1 receptor gene in Japanese population. *Diabetes Res Clin Pract* **66:** 63-69

Tomas E, Habener JF (2010) Insulin-like actions of glucagon-like peptide-1: a dual receptor hypothesis. *Trends Endocrinol Metab* **21:** 59-67

Trowbridge IS, Collawn JF, Hopkins CR (1993) Signal-dependent membrane protein trafficking in the endocytic pathway. *Annu Rev Cell Biol* **9:** 129-161

Tsuboi T, da Silva Xavier G, Holz GG, Jouaville LS, Thomas AP, Rutter GA (2003) Glucagon-like peptide-1 mobilizes intracellular Ca2+ and stimulates mitochondrial ATP synthesis in pancreatic MIN6 β-cells. *Biochemical Journal* **369:** 287-299

Tuomilehto J, Schwarz P, Lindstrom J (2011) Long-term benefits from lifestyle interventions for type 2 diabetes prevention: time to expand the efforts. *Diabetes Care* **34 Suppl 2:** S210-214

Tuteja N (2009) Signaling through G protein coupled receptors. *Plant Signal Behav* **4:** 942-947

Underwood CR, Garibay P, Knudsen LB, Hastrup S, Peters GH, Rudolph R, Reedtz-Runge S (2010) Crystal Structure of Glucagon-like Peptide-1 in Complex with the Extracellular Domain of the Glucagon-like Peptide-1 Receptor. *Journal of Biological Chemistry* **285:** 723-730

Uniprot. P43220 Human GLP1R. Available at http://expasy.org/uniprot/P43220 (Accessed on 02 September, 2014).

Urban JD, Clarke WP, von Zastrow M, Nichols DE, Kobilka B, Weinstein H, Javitch JA, Roth BL, Christopoulos A, Sexton PM, Miller KJ, Spedding M, Mailman RB (2007) Functional selectivity and classical concepts of quantitative pharmacology. *J Pharmacol Exp Ther* **320:** 1-13

Urwyler S (2011) Allosteric modulation of family C G-protein-coupled receptors: from molecular insights to therapeutic perspectives. *Pharmacol Rev* **63:** 59-126

Vahl TP, Paty BW, Fuller BD, Prigeon RL, D'Alessio DA (2003) Effects of GLP-1-(7-36)NH2, GLP-1-(7-37), and GLP-1- (9-36)NH2 on intravenous glucose tolerance and glucose-induced insulin secretion in healthy humans. *J Clin Endocrinol Metab* **88:** 1772-1779

van Bloemendaal L, Ten Kulve JS, la Fleur SE, Ijzerman RG, Diamant M (2014) Effects of glucagon-like peptide 1 on appetite and body weight: focus on the CNS. *J Endocrinol* **221:** T1-16

Van Eyll B, Goke B, Wilmen A, Goke R (1996) Exchange of W39 by A within the N-terminal extracellular domain of the GLP-1 receptor results in a loss of receptor function. *Peptides* **17:** 565-570

van Eyll B, Lankat-Buttgereit B, Bode HP, Goke R, Goke B (1994) Signal transduction of the GLP-1-receptor cloned from a human insulinoma. *FEBS Letters* **348:** 7-13

van Koppen CJ, Nathanson NM (1990) Site-directed mutagenesis of the m2 muscarinic acetylcholine receptor. Analysis of the role of N-glycosylation in receptor expression and function. *J Biol Chem* **265:** 20887-20892

Varki A, Cummings RD, Esko JD, Freeze HH, Stanley P, Bertozzi CR, Hart GW, Etzler ME, editors (2009) *Essentials of Glycobiology. 2nd Edition*, New York: Cold Spring Harbour Laboratory Press.

Vazquez P, Roncero I, Blazquez E, Alvarez E (2005a) The cytoplasmic domain close to the transmembrane region of the glucagon-like peptide-1 receptor contains sequence elements that regulate agonist-dependent internalisation. *J Endocrinol* **186:** 221-231

Vazquez P, Roncero I, Blazquez E, Alvarez E (2005b) Substitution of the cysteine 438 residue in the cytoplasmic tail of the glucagon-like peptide-1 receptor alters signal transduction activity. *J Endocrinol* **185:** 35-44

Venables MC, Jeukendrup AE (2009) Physical inactivity and obesity: links with insulin resistance and type 2 diabetes mellitus. *Diabetes Metab Res Rev* **25 Suppl 1:** S18-23

Venkatakrishnan G, Salgia R, Groopman JE (2000) Chemokine receptors CXCR-1/2 activate mitogen-activated protein kinase via the epidermal growth factor receptor in ovarian cancer cells. *J Biol Chem* **275:** 6868-6875

Verhey KJ, Birnbaum MJ (1994) A Leu-Leu sequence is essential for COOH-terminal targeting signal of GLUT4 glucose transporter in fibroblasts. *J Biol Chem* **269:** 2353-2356

Vezzosi D, Bennet A, Fauvel J, Caron P (2007) Insulin, C-peptide and proinsulin for the biochemical diagnosis of hypoglycaemia related to endogenous hyperinsulinism. *Eur J Endocrinol* **157:** 75-83

Vilardaga JP, Bunemann M, Feinstein TN, Lambert N, Nikolaev VO, Engelhardt S, Lohse MJ, Hoffmann C (2009) GPCR and G proteins: drug efficacy and activation in live cells. *Mol Endocrinol* **23:** 590-599

Vilsboll T, Agerso H, Krarup T, Holst JJ (2003) Similar elimination rates of glucagon-like peptide-1 in obese type 2 diabetic patients and healthy subjects. *J Clin Endocrinol Metab* **88:** 220-224

Vilsboll T, Krarup T, Madsbad S, Holst JJ (2002) Defective amplification of the late phase insulin response to glucose by GIP in obese Type II diabetic patients. *Diabetologia* **45:** 1111-1119

Wallin E, Vonheijne G (1995) Properties of N-Terminal Tails in G-Protein Coupled Receptors - a Statistical Study. *Protein Eng* **8:** 693-698

Wang LY, Martin B, Brenneman R, Luttrell LM, Maudsley S (2009) Allosteric Modulators of G Protein-Coupled Receptors: Future Therapeutics for Complex Physiological Disorders. *Journal of Pharmacology and Experimental Therapeutics* **331:** 340-348

Wang Q, Li L, Xu E, Wong V, Rhodes C, Brubaker PL (2004) Glucagon-like peptide-1 regulates proliferation and apoptosis via activation of protein kinase B in pancreatic INS-1 beta cells. *Diabetologia* **47:** 478-487

Ward AC, van Aesch YM, Schelen AM, Touw IP (1999) Defective internalization and sustained activation of truncated granulocyte colony-stimulating factor receptor found in severe congenital neutropenia/acute myeloid leukemia. *Blood* **93:** 447-458

Watanabe T, Waga I, Honda Z, Kurokawa K, Shimizu T (1995) Prostaglandin F2 alpha stimulates formation of p21ras-GTP complex and mitogen-activated protein kinase in NIH-3T3 cells via Gq-protein-coupled pathway. *J Biol Chem* **270:** 8984-8990

Wei Y, Mojsov S (1995) Tissue-specific expression of the human receptor for glucagon-like peptide-I: brain, heart and pancreatic forms have the same deduced amino acid sequences. *FEBS Letters* **358:** 219-224

Werry TD, Wilkinson GF, Willars GB (2003) Mechanisms of cross-talk between G-protein-coupled receptors resulting in enhanced release of intracellular Ca2+. *Biochemical Journal* **374:** 281-296

Whitaker GM, Lynn FC, McIntosh CH, Accili EA (2012) Regulation of GIP and GLP1 receptor cell surface expression by N-glycosylation and receptor heteromerization. *Plos One* **7:** e32675

Whiting DR, Guariguata L, Weil C, Shaw J (2011) IDF diabetes atlas: global estimates of the prevalence of diabetes for 2011 and 2030. *Diabetes Res Clin Pract* **94:** 311-321

Wideman RD, Covey SD, Webb GC, Drucker DJ, Kieffer TJ (2007) A switch from prohormone convertase (PC)-2 to PC1/3 expression in transplanted alpha-cells is accompanied by differential processing of proglucagon and improved glucose homeostasis in mice. *Diabetes* **56:** 2744-2752

Wideman RD, Gray SL, Covey SD, Webb GC, Kieffer TJ (2009) Transplantation of PC1/3-Expressing alpha-cells improves glucose handling and cold tolerance in leptin-resistant mice. *Mol Ther* **17:** 191-198

Wideman RD, Yu IL, Webber TD, Verchere CB, Johnson JD, Cheung AT, Kieffer TJ (2006) Improving function and survival of pancreatic islets by endogenous production of glucagon-like peptide 1 (GLP-1). *Proc Natl Acad Sci U S A* **103:** 13468-13473

Widmann C (1997) Internalization and Homologous Desensitization of the GLP-1 Receptor Depend on Phosphorylation of the Receptor Carboxyl Tail at the Same Three Sites. *Mol Endocrinol* **11:** 1094-1102

Widmann C, Dolci W, Thorens B (1995) Agonist-induced internalization and recycling of the glucagon-like peptide-1 receptor in transfected fibroblasts and in insulinomas. *Biochemical Journal* **310:** 203-214

Widmann C, Dolci W, Thorens B (1996a) Desensitization and phosphorylation of the glucagon-like peptide-1 (GLP-1) receptor by GLP-1 and 4-phorbol 12-myristate 13-acetate. *Mol Endocrinol* **10:** 62-75

Widmann C, Dolci W, Thorens B (1996b) Heterologous desensitization of the glucagon-like peptide-1 receptor by phorbol esters requires phosphorylation of the cytoplasmic tail at four different sites. *Journal of Biological Chemistry* **271:** 19957-19963

Willard FS, Sloop KW (2012) Physiology and emerging biochemistry of the glucagon-like peptide-1 receptor. *Exp Diabetes Res* **2012:** 470851

Williams TM, Lisanti MP (2004) The caveolin proteins. *Genome Biol* **5:** 214

Wilmen A, Van Eyll B, Göke B, Göke R (1997) Five Out of Six Tryptophan Residues in the N-Terminal Extracellular Domain of the Rat GLP-1 Receptor Are Essential for its Ability to Bind GLP-1. *Peptides* **18:** 301-305

Wolfe BL, Trejo J (2007) Clathrin-dependent mechanisms of G protein-coupled receptor endocytosis. *Traffic* **8:** 462-470

Wootten D, Savage EE, Willard FS, Bueno AB, Sloop KW, Christopoulos A, Sexton PM (2013) Differential activation and modulation of the glucagon-like peptide-1 receptor by small molecule ligands. *Mol Pharmacol* **83:** 822-834

World Health Organisation (1999) Definition, diagnosis and classification of diabetes mellitus and its complications: Report of a WHO Consultation. Part 1. Diagnosis and classification of diabetes mellitus. **WHO/NCD/NCS/99.2**

World Health Organisation (2011) Use of glycated haemoglobin (HbA1c) in the diagnosis of diabetes mellitus. **WHO/NMH/CHP/CPM/11.1**

Wright EE, Jr. (2009) Overview of insulin replacement therapy. *J Fam Pract* **58:** S3-9

Wylie PG, Challiss RA, Blank JL (1999) Regulation of extracellular-signal regulated kinase and c-Jun N-terminal kinase by G-protein-linked muscarinic acetylcholine receptors. *Biochem J* **338 (Pt 3):** 619-628

Xiang B, Yu GH, Guo J, Chen L, Hu W, Pei G, Ma L (2001) Heterologous activation of protein kinase C stimulates phosphorylation of delta-opioid receptor at serine 344, resulting in beta-arrestin- and clathrin-mediated receptor internalization. *J Biol Chem* **276:** 4709-4716

Xiao Q, Jeng W, Wheeler MB (2000) Characterization of glucagon-like peptide-1 receptor-binding determinants. *Journal of molecular endocrinology* **25:** 321-335

Xu G, Kaneto H, Laybutt DR, Duvivier-Kali VF, Trivedi N, Suzuma K, King GL, Weir GC, Bonner-Weir S (2007) Downregulation of GLP-1 and GIP receptor expression by hyperglycemia: possible contribution to impaired incretin effects in diabetes. *Diabetes* **56:** 1551-1558

Yang J, Williams JA, Yule DI, Logsdon CD (1995) Mutation of carboxyl-terminal threonine residues in human m3 muscarinic acetylcholine receptor modulates the extent of sequestration and desensitization. *Mol Pharmacol* **48:** 477-485

Yoon JW, Jun HS (2005) Autoimmune destruction of pancreatic beta cells. *Am J Ther* **12:** 580-591

Young AA, Gedulin BR, Bhavsar S, Bodkin N, Jodka C, Hansen B, Denaro M (1999) Glucose-lowering and insulin-sensitizing actions of exendin-4 - Studies in obese diabetic (ob/ob, db/db) mice, diabetic fatty Zucker rats, and diabetic rhesus monkeys (Macaca mulatta). *Diabetes* **48:** 1026-1034

Yu DM, Yao TW, Chowdhury S, Nadvi NA, Osborne B, Church WB, McCaughan GW, Gorrell MD (2010) The dipeptidyl peptidase IV family in cancer and cell biology. *Febs J* **277:** 1126-1144

Zahn K, Eckstein N, Trankle C, Sadee W, Mohr K (2002) Allosteric modulation of muscarinic receptor signaling: alcuronium-induced conversion of pilocarpine from an agonist into an antagonist. *J Pharmacol Exp Ther* **301:** 720-728

Zander M, Madsbad S, Madsen JL, Holst JJ (2002) Effect of 6-week course of glucagon-like peptide 1 on glycaemic control, insulin sensitivity, and β-cell function in type 2 diabetes: a parallel-group study. *The Lancet* **359:** 824-830

Zhang J, Ferguson SS, Barak LS, Aber MJ, Giros B, Lefkowitz RJ, Caron MG (1997) Molecular mechanisms of G protein-coupled receptor signaling: role of G protein-coupled receptor kinases and arrestins in receptor desensitization and resensitization. *Receptors & Channels* **5:** 193-199

Zhang Z, Henzel WJ (2004) Signal peptide prediction based on analysis of experimentally verified cleavage sites. *Protein Sci* **13:** 2819-2824

Zhao JH, Liu HL, Lin HY, Huang CH, Fang HW, Chen SS, Ho Y, Tsai WB, Chen WY (2008) Chemical chaperone and inhibitor discovery: potential treatments for protein conformational diseases. *Perspect Medicin Chem* **1:** 39-48

Zimmerman B, Simaan M, Akoume MY, Houri N, Chevallier S, Seguela P, Laporte SA (2011) Role of ssarrestins in bradykinin B2 receptor-mediated signalling. *Cell Signal* **23:** 648-659

Zimmet P, Alberti KG, Shaw J (2001) Global and societal implications of the diabetes epidemic. *Nature* **414:** 782-787

Zou Y, Komuro I, Yamazaki T, Aikawa R, Kudoh S, Shiojima I, Hiroi Y, Mizuno T, Yazaki Y (1996) Protein kinase C, but not tyrosine kinases or Ras, plays a critical role in angiotensin II-induced activation of Raf-1 kinase and extracellular signal-regulated protein kinases in cardiac myocytes. *J Biol Chem* **271:** 33592-33597